JAI MAHAVIR

ELECTRON MICROSCOPIC AND INTERFEROMETRIC STUDIES OF DIAMOND CRYSTALS

THESIS

SUBMITTED TO THE UNIVERSITY OF LONDON FOR

THE DEGREE OF DOCTOR OF PHILOSOPHY

BY

JAYA (KHEMSARA) PUNGLIA

March, 1972.

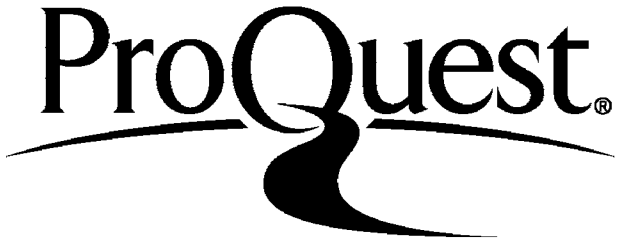

A B S T R A C T

Early chapters review the structure and physical properties of diamond, the theories of crystal growth and dissolution and the methods for synthesizing diamond. Chapter 5 describes surface topographical studies on diamonds by previous workers and chapter 6 presents a survey of previous experiments on diamond etching.

Chapter 7 describes the techniques used and these include interferometry and electron microscopy. A single-stage replica technique developed during the present investigation for studying the surfaces of micro-crystals only a few microns in size and a two-stage technique for crystals more than 100 microns in size are described in detail. The former was used for studying the surfaces of Du-Pont synthetic diamonds.

De Beers synthetic diamonds are for the first time studied in detail. Electron microscopic studies reveal many new surface details. A notable change of orientation of etch pits on the cubic faces was discovered at about 600 to 650°C. To investigate this phenomenon, an etching apparatus was designed which

agitated the specimen during etching. Results indicate that the by-products of the etching reaction at sites of fast etching are responsible for the change in etch-pit orientation.

The change in etch-pit orientation was observed also on the cube faces of cubo-octahedral diamonds and on polished (100) faces which indicated that the phenomenon is probably an intrinsic property of all cubic faces.

Detailed studies on the etching of naturally smooth cubic faces are here being reported for the first time. Optical and electron optical studies indicate that the cube faces of these cubo-octahedral crystals probably arise from a dissolution mechanism.

Electron-microscopic studies on the natural cubic diamonds suggest that 'quadrons' are growth features.

In addition, octahedral faces of the Premier Mine micro-diamonds are studied in detail. They show various features in addition to the usual ones. A mechanism for their formation is suggested.

C O N T E N T S

CHAPTER 1

PHYSICAL PROPERTIES OF DIAMOND

1.1 Introduction

Diamond is a remarkable material and its unique properties have made it valued for many purposes. It is the hardest natural material known to mankind and it is this hardness which places it in the utmost important position in modern technology.

Diamond has been prized for many centuries as a gem stone. This it owes to its special qualities, e.g. high refractive index and high dispersion and hardness. The refractive index of diamond for wavelength 5890A^{o} is 2·42 as compared to 1·5 for glass and thus it has the high reflectivity of 18% compared to 4% for glass. High dispersion in diamond makes it the most beautiful of the 'gemstones'; diamond has its pre-eminent place among precious stones, not only because of beauty and rarity but also due to its extreme hardness and permanance. Its hardness is 10

on Mho's scale and it has a Vickers hardness number in excess of 10,000. The permanance of diamond is partly due to its resistance to abrasion, and partly to its extreme resistance to chemical attack.

Because of the said qualities diamond plays a key role in modern industry as a cutting and shaping tool. Nearly six tons of the yearly output of the diamond mines is used in industry, while only one ton is used as decorative gems (Tolansky 1968).

1.2 Structure and Related Properties

Diamond is one of the crystalline forms of carbon. It crystallizes in the cubic system, while its other allotrope graphite crystallizes in the hexagonal form. Initially the structure of diamond was determined by W.H. Bragg and W.L. Bragg in (1913) by means of X-ray diffraction studies. They showed that there are 8 atoms in the unit cell, arranged on two interpenetrating face centred lattices, one of which is displaced with respect to the other by one quarter of the length of the cube diagonal. From general measurements the structure belongs to the space group Fd3m and has centre of symmetry. The length

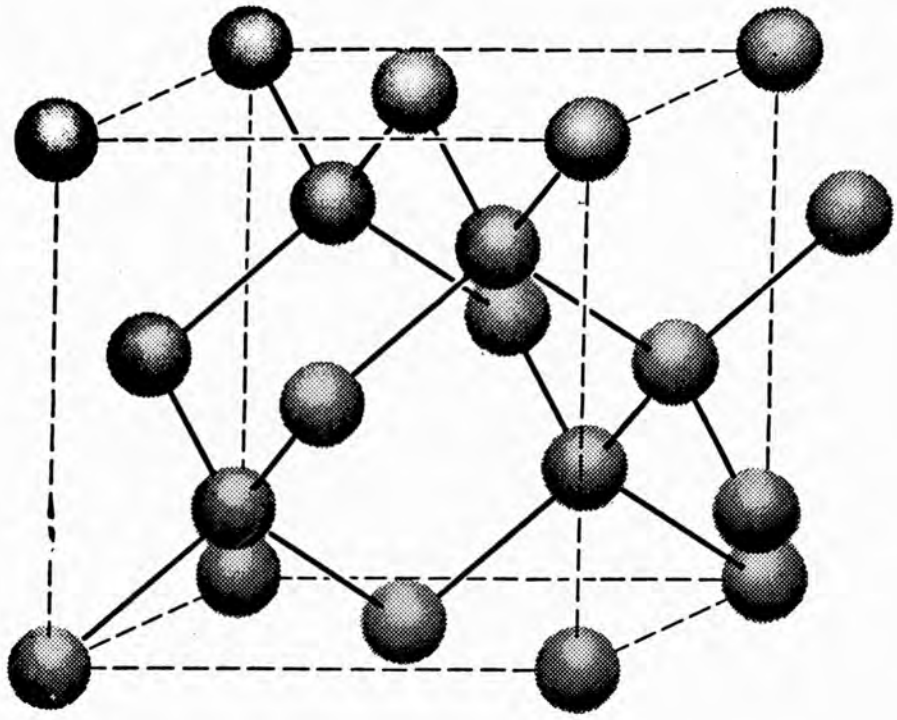

Figure 1.1.

Unit cell of diamond crystal lattice

(After Bragg, 1937)

of the edge of the unit cell of diamond is 3·56Å. The figure 1.1 shows the arrangement of atoms in diamond. The atoms are located at the positions

$$(000),\ \tfrac{1}{2}\cdot\tfrac{1}{2}\cdot 0),\ (0\cdot\tfrac{1}{2}\cdot\tfrac{1}{2}) \text{ and } (\tfrac{1}{2}\cdot 0\ \tfrac{1}{2})$$

$$(\tfrac{3}{4}\cdot\tfrac{3}{4}\cdot\tfrac{1}{4}),\ (\tfrac{1}{4}\cdot\tfrac{3}{4}\cdot\tfrac{3}{4}),\ (\tfrac{3}{4}\cdot\tfrac{1}{4}\cdot\tfrac{3}{4}) \text{ and } (\tfrac{1}{4}\cdot\tfrac{1}{4}\cdot\tfrac{1}{4})$$

Thus the arrangement is such that each carbon atom is situated at one corner of a regular tetrahedron with four nearest neighbours symmetrically placed at equal distances of 1·54Å. The bonds between the atoms make an angle of 109°, 28'. A similar arrangement is found in various other elements like, silicon, germanium, zinc sulphide, grey tin etc. The carbon atoms in the case of diamond are joined to each other by co-valent homopolar bonds. Thus the electrons are shared between the outermost orbit of the adjacent atoms as shown in figure (1.2).

The six electrons surrounding the carbon nucleus arrange themselves with the 2 K electrons remaining relatively undisturbed in the normal K-shell. The L electrons pair up in the overlapping orbitals which arrange themselves along the bond directions.

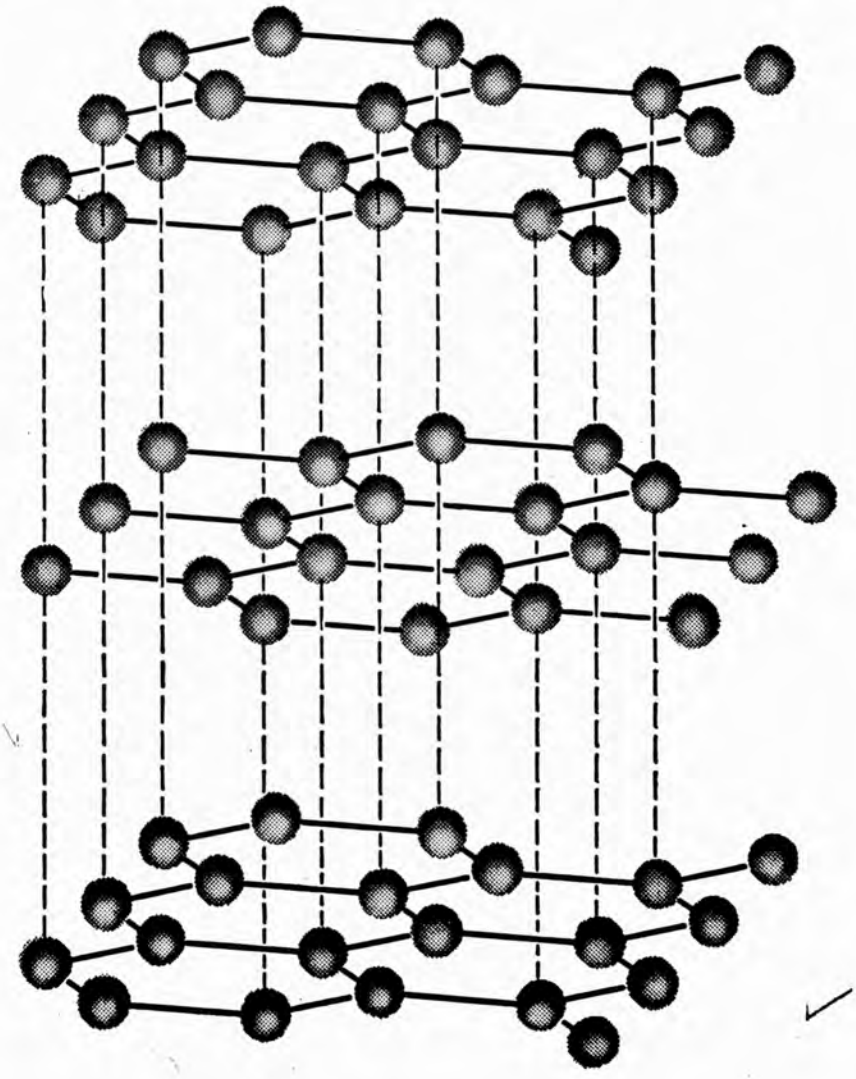

Figure 1.2.

Structure of Graphite

(After Bragg, 1937)

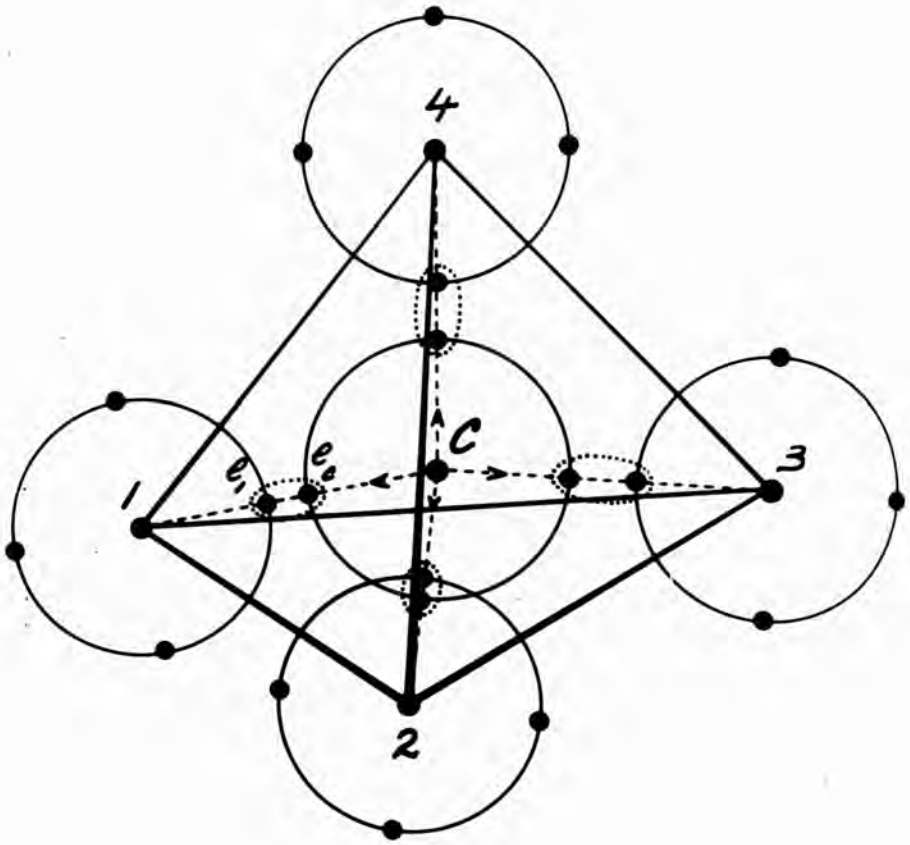

Figure 1.3.

(After Custers, 1956)

The figure 1.2 represents the carbon atoms situated at the corners of a tetrahedron. Only the outermost orbitals are shown. The four valency electrons are shown as lying on a common orbit. The possibility of finding e_1 near c would be the same as finding it near atom 1. The same would apply to the electron e_c. Thus the two electrons are shared between the two atoms 1 and c. Hence the carbon atoms having 4 electrons in the outermost orbit can share 4 with other four of its nearest neighbours and thus have a stable configuration of 8 electrons.

The arrangement of carbon atoms in the case of graphite is shown in figure 1.3. Here the atoms are arranged in clearly separated layers, showing hexagonal symmetry. Each carbon atom is surrounded by the nearest three neighbours and thus the fourth valency is not satisfied. This accounts for the electrical conductivity of graphite. The bond length is 1·42A^{o} in one layer and hence this bond is stronger than the bonds between two carbon atoms in diamond. Thus in case of graphite there are various layers of carbon atoms which are attracted by relatively

weaker Van der Waals forces. The distance between the consecutive layers of carbon atoms in graphite is 3·42Å. This accounts for the easy cleavage of graphite.

1.3 Habit

Diamond is found in various crystal forms. These, in many cases, are far from ideal, very often the faces may be markedly curved. However, diamond crystallizes most commonly as octahedra or dodecahedra. The simple cube is less commonly found. Tetrahexahedra and hexaoctahedra have been reported by Sutton (1928). Tetrahedra are extremely rare. Recently after an extensive study of 13,000 Premier Mine micro diamonds from South Africa Tolansky (1970) discovered 4 tetrahedral crystals. During the present work on Premier Mine micro crystals 1% of the micro crystals exhibited the unusual cubo-octahedral form.

As mentioned above the crystal shape is not perfect, for example the dodecahedra have rounded faces. Octahedra may develop as twin plates (macles). The various common crystal forms of natural diamond are shown in figure (1.4), while the figure (1.5) shows the crystal

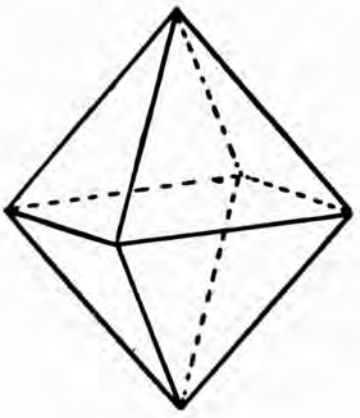

The octahedron

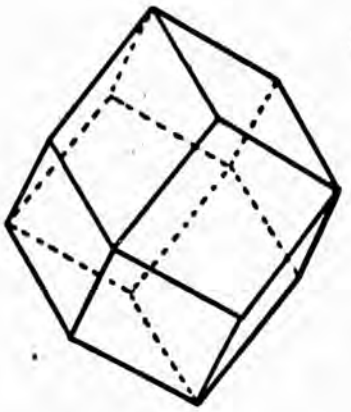

The dodecahedron

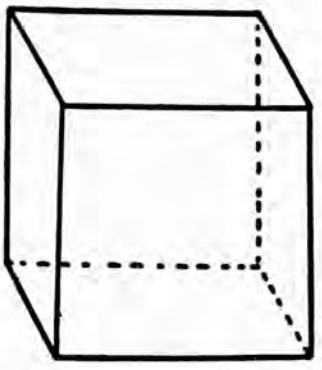

The cube

Figure 1.4.

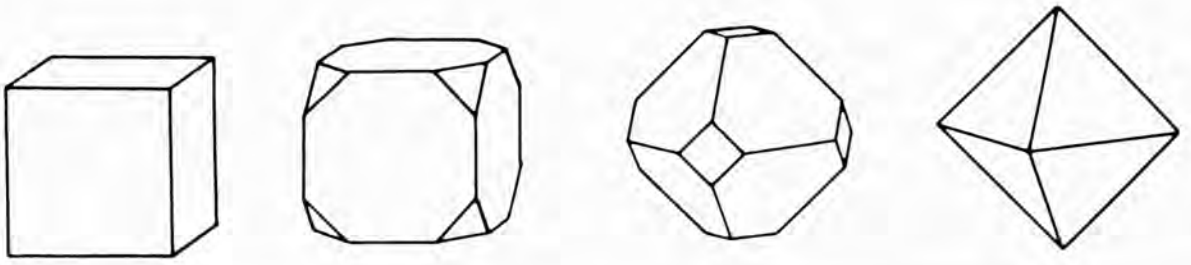

Figure 1.5.

forms of the synthetic diamonds.

Diamond ranges in colour from clear white to yellow, brown, grey and black. The colouration may be the result of impurities. Even the best gem diamonds contain impurities, with concentration of the order of 1 part in 10^5.

Quantitative spectroscopic analysis confirms the presence of impurities such as, silicon, aluminium, copper, nitrogen and a variety of other elements. Diamond has a cleavage direction along the $\{111\}$ planes, this is used in dividing large stones during the shaping process (Raal 1957).

1.4 Thermal Properties

Diamond has a much higher thermal conductivity at room temperature than other material and this plays an important part in the industrial use of the stone. The extreme hardness and high thermal conductivity make it unique material for cutting and engraving tools. A good gem quality type IIa diamond conducts heat five times better than copper. In addition to this, diamond has an unusually low coefficient of expansion. It

is 35 x 10^{-6} per degree centigrade compared to 397 x 10^{-6} per degree centigrade in the case of steel (Sutton 1928).

1.5 Optical Properties

Diamond has a high refractive index (2·417 at = 5890Å). The fire of the gemstone depends, firstly on the high refractive index, which implies a low angle of total reflection, and secondly on its high dispersion which makes the light reflected in a given direction change in colour as the stone is moved slightly. Being a cubic crystal diamond is isotropic and one would expect it to show no birefringence. But nearly all diamonds are birefringent (Tolansky 1966) probably caused by strain. Brewsterim 1815 was the first to recognize the existence of birefringence in diamond. Friedel (1924) after examining nearly 200 diamond crystals and 150 cleavages, concluded that nearly all of them show this property upto some extent. According to Friedel and Ribaud (1924), all diamonds are isotropic at formation and they pass through a plastic state at higher temperature sufficient for causing permanent deformation, which gives rise to birefringence.

Raman and Rendall (1944) observed parallel striations between crossed polarizers. Ramachandran (1946) also observed 'lamination' in diamonds in polarized light. These laminae were found to be parallel to $\{111\}$ planes. They interpreted this as due to alternate compression and tension between two varieties of diamond layers having slightly different lattice spacing. Tolansky (1966) made an extensive study of 3,000 micro-diamonds and 2,000 large crystals and found that without exception all those diamonds showed birefringence.

Harrison and Tolansky (1964) etched the sections of an octahedron. The stratigraphic etch pattern so obtained corresponded to the birefringence pattern. They suggested that the stratigraphic pattern produced is the result of the different types of layers which are susceptible to an etch to a different extent. They suggested further that the co-relation between the etch pattern and birefringence pattern may be due to the small difference in either the thermal expansion property or the elastic strength or the lattice dimension of the two types of layers. This produces invariably the strain leading to ubiquitous birefringence of crystals.

1.6 Types of Diamond

Diamonds have been classified as type I and type II according to their absorption in the ultraviolet, visible and infrared regions (Robertson, Fox and Martin 1934; Sutherland, Blackwell and Simeral 1954 and Clark, Ditchburn and Dyer 1956). Type II diamonds transmit well in the ultraviolet down to the absorption edge at 2200A^{o} but type I diamonds show absorption starting at 3300A^{o} and increasing fairly rapidly at shorter wavelengths. Thus the type II diamonds are ultraviolet transparent and display fluorescence, but the type I diamonds absorb ultraviolet light.

The difference in the absorption spectra indicates that type II diamonds are more nearly perfect crystals than type I diamonds, i.e. they are relatively free from some kind of defect or impurity which produces an additional absorption in type I class. The existence of this additional absorption in type I diamonds indicates the presence of crystal defects or impurity which lowers the symmetry of the structure.

Type I diamonds show absorption in the region 7 - 8μ and this absorption is absent in the case of type II. They also absorb in the visible region and

have continuous absorption starting at 1·7 ev below the energy gap 5·6 ev between the conduction and valance bands of diamonds (Champion 1953).

Raman and Nilakantan (1940) discovered that type I diamonds show anomalous 'spikes' projecting from certain spots in Laue Pattern obtained with X-rays. Hoerni and Wooster (1955) suggested that these spikes indicated the presence of defects in the cube planes, they assumed that planes of carbon atoms occurred with an abnormal electron distribution. Frank (1956) also suggested that spikes could be produced by the occurrence of occasionaly abnormal spacing in the $\langle 100 \rangle$ direction and postulated, as a possible origin of such abnormal spacing, the segregation in $\{100\}$ planes of silicon atoms as an impurity. Caticha-Ellis and Cochram (1958) considered this theory in terms of actual intensity of the effect and amount of silicon known to be present, and found the latter to be too small by an order of magnitude.

Kaiser and Bond (1959) showed experimentally that the strongest absorption bands in the infrared at 7·8 microns and ultraviolet 3036Å are proportional to N_2 impurity concentration. They showed that a considerable

amount of N_2 upto 0·23% is present. From their studies they concluded that nitrogen is present in substitutional position in diamond lattice and it is obviously the cause of 'spikes'. Elliot (1960) reviewed evidence relevant to the state of aggregation of nitrogen impurity in type I diamonds and proposed models for layers of substitutional nitrogen parallel to {100} planes.

Evans and Phaal (1962) were able to obtain transmission electron micrographs of thin plates of diamonds and showed the presence of platelet defects in type I diamonds. They showed that platelets are present in {100} planes and they were able to calculate their number and extent. Lang (1964) proposed a structure for the nitrogen impurity platelets. He suggested that N_2 is not present in purely substitutional form. He stressed that nitrogen is in platelet form. Latter, Moore and Lang (1972), studied platelet distribution by X-ray topographical methods. According to them the platelets are 150A°-200A° in diameter.

Recently Sobolev, Lisoivan et al. (1968) compared the optical properties of 100 natural diamonds

from Yakutia with their Laue patterns. They concluded that nitrogen is present not only in platelet form but also in other disordered forms.

Tolansky and Rawle-Cope (1970) after studying nearly 6,000 perfect micro crystals out of thousands of crystals from Premier Mine, found that nearly 90% of the micro crystals are ultraviolet transparent (2536A°). According to them, as diamonds grow bigger they progressively become type I due to the incorporation of type I layers. They showed that diamonds are formed by the deposition of type I and type II layers. Thus all diamonds are the mixture of the two types, the predominent type determines the ultimate classification.

Tolansky (1955) suggested that type II diamonds cleave better than type I diamonds.

No X-ray spikes have yet been observed in any synthetic diamond (Milledge and Meyer 1962).

Most diamonds are very good electric insulators but Custers (1952, 1955) showed that a small proportion of type II diamonds are semi-conducting. He classified non-conducting as type IIa diamonds and semi-conducting as type IIb diamonds. The type IIb property is present to a varying extent and there is

probably a range from insulating diamonds, whose resistivity is about 5×10^{14} Ohms-cm, to a semiconductor of resistivity 100 Ohms-cm at room temperature.

CHAPTER 2

THEORIES OF CRYSTAL GROWTH

The theories of crystal growth can be conveniently divided in two parts:

1 - Growth of ideally perfect crystals.

2 - Growth of real crystals.

2.1 Introduction

The first quantitative theory of crystal growth was given by Gibbs (1878) on thermodynamical grounds. Gibbs made use of the analogy of the liquid drop and applied conditions for the stability of an isolated drop of liquid. For a crystal in equilibrium with its surroundings at constant temperature and pressure, this condition implies that for a given volume, Gibbs free energy must be a minimum. It therefore follows that, for a given volume, those faces which lead to minimum surface free energy will develop. However, whereas the atoms or molecules in a liquid are randomly arranged, the structural units in a crystal have a regular arrangement.

Curie (1885) proposed that there was an intimate connection between the crystalline form and the surface energy of solids. He calculated the shape and the end form of a crystal. Curie's theory of crystal growth was not based on the actual atomic arrangement of the crystal surfaces, and was extended further by Wolff (1901). He calculated the velocities of growth of different faces in the direction of face normals and suggested that these are proportional to the surface free energy of that particular face. A crystal will therefore form a polyhedron in which the distances of the faces from the centre of the crystal are proportional to the surface free energy per unit area for that particular face.

All these theories ignored the atomic arrangement of the crystal surfaces.

According to Buckley (1951) crystals generally grow by following three methods:

1 - Crystallization from solution.

2 - Crystallization from melt.

3 - Growth from vapour.

2.2 Atomic Theories of Crystal Growth

Atomic theories of crystal growth were put

forward by Volmer (1922) and by Kossel (1927), Stranski (1928), Becker, Doring, Frenkel (1946) and Burbon, Cabrera and Frank (1951). These theories were developed for the growth of crystals from vapour, but are also applicable to the growth from solution.

Volmer (1922) was the first to introduce the idea of adsorption. He suggested that when a crystallising particle arrives at a surface, it only loses a part of its energy and binds itself to the surface. Because of the residual energy, the particle can still move laterally. Thus these adsorbed particles constitute a layer which interposes between the solution and the crystal surface and it attains equilibrium with the crystal surface immediately. As a result of inelastic collision between these adsorbed molecules the germ of a two dimensional crystal will be formed, which will attach itself to the lattice plane below. Volmer deduced that velocity of spread of the layers is approximately proportional to the square of the density of particles in it.

In 1866 Bravais had advanced the view that the velocities of growth of different faces of a crystal are dependent upon the density of atoms in the planes.

According to him planes of maximum density will move normally to themselves at the slowest rate, and consequently should extend laterally, to the exclusion of more rapidly depositing planes.

2.3 Atomic Theories for Perfect Crystals

An atomic theory for perfect crystals was given by Kossel (1927) and Stranski (1928). According to Kossel and Stranski, in the simplest case, molecules can be represented as simple cubes. These cubes are stacked face to face, and each cube is attracted equally by all its six neighbours. The energy required to separate two cubes is called the binding energy and is different for different materials. According to them, once the layer has been initiated by a single atom, the planes will spread rapidly to completion. Figure (2.1) shows the simple crystal growth process conceived by them near to absolute zero.

If the temperature is increased from near absolute zero, the molecules on the layer start vibrating. These vibrations become stronger as the temperature is raised, and some of the molecules have sufficient energy to break away from the body of the crystal. These are

generally the most loosely bound ones. Two processes will occur simultaneously: some molecules will arrive while others will depart. When the rates of the two opposing processes are equal, equilibrium is attained. Under these conditions the surface will appear as in figure (2.2).

There are some 'kinks' (a kink is a re-entrant corner where the step shifts through one lattice spacing), adsorbed atoms and surface vacancies on the surface. The kinks serve the purpose of exchange sites for the molecules, because the molecules leave and enter the crystal surface at kinks, where they are loosely bound to the surface. The number of kinks that will exist in a molecular step at a finite temperature has been calculated on simple thermodynamical consideration by Frenkel (1945, 1946). Burton, Cabrera and Frank (1951), deduced the concentration of kinks to be even higher than that suggested by Frenkel. They suggested that the number of kinks is dependent upon temperature and is practically unchanged by supersaturation of vapour. Thus at a temperature T, the distance between the kinks is given by the equation $no = \frac{1}{2} a e^{\phi/KT}$ where a is the distance between the two molecules in the lattice, and ϕ is the nearest neighbour interaction energy. At temperatures

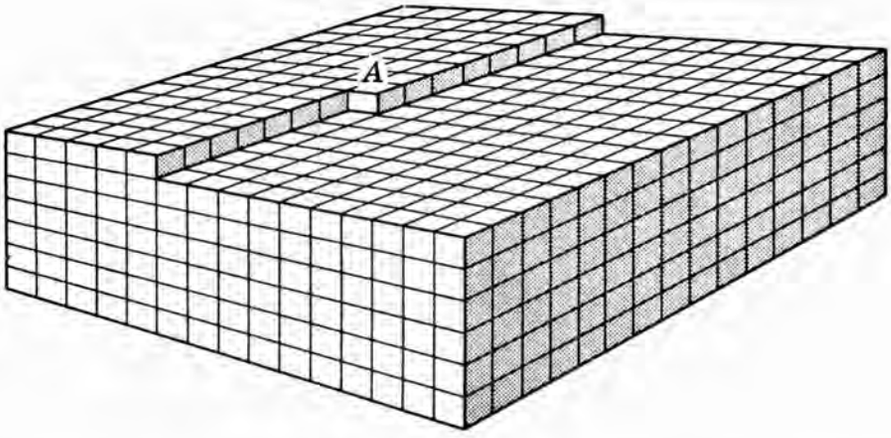

Figure 2.1.

Structure of a low-index face (001) for a perfect crystal on Kossel - Stranski model at low temperature (From Verma & Krishna)

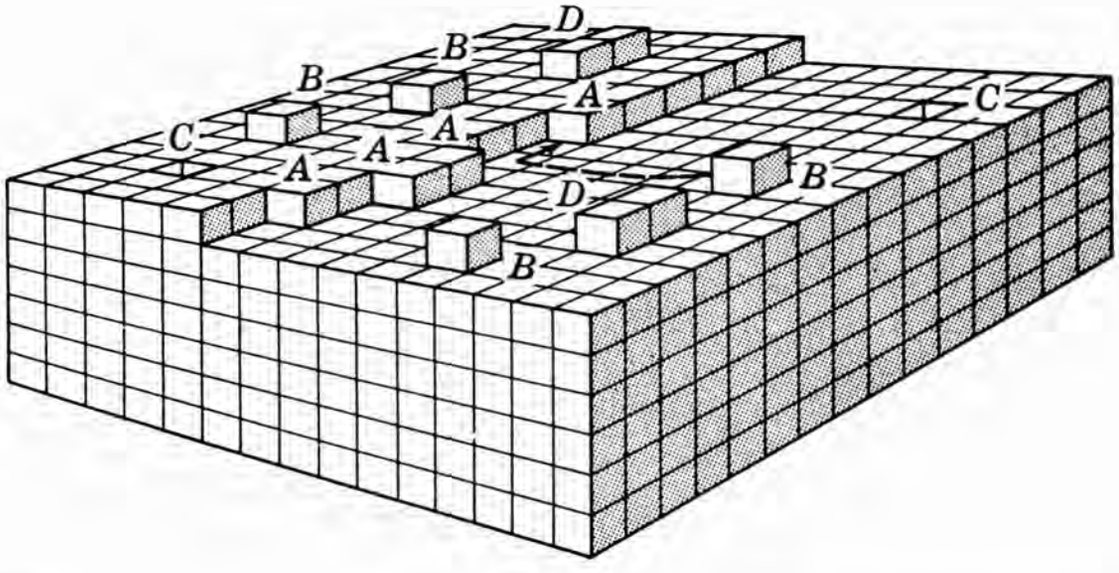

Figure 2.2.

Crystal surface at temperature higher than in figure 2.1.

nearly 0·5 to 0·8 times the boiling point n = 4a, and therefore there are kinks, every four molecules on the surface. The rate of arrival is proportional to the vapour concentration, while the rate of departure depends upon the temperature.

Experiments indicate (Verma and Krishna 1966) that the arrival of molecules at any particular point is more due to surface migration rather than direct arrival. During the growth of a crystal from the vapour, the molecules arrive at the surface and then diffuse through a considerable distance before evaporating again. Growth rate can only be explained if diffusion is taken into account (Volmer 1922). According to Burton, Cabrera and Frank (1951) a molecule diffuses through a considerable distance before re-evaporation.

Therefore the process of growth on a perfect crystal whose surface has steps will be the result of three processes:

1 - The arrival of molecules from the vapour phase on the crystal surface.

2 - Surface diffusion of the molecules until they meet a step.

3 - The diffusion of molecules along the edge of the

step until they reach a kink.

Thus at a particular temperature, the step will go on receiving more molecules at the kinks than they lose from the kinks, so long as the supersaturation of the vapour prevails. Again Burton, Cabrera and Frank (1951) have suggested that the rate of advance of an incomplete layer is proportional to the supersaturation. This means that all steps initially present, will travel during the growth process, towards the edges of the crystal, leaving few vacancies and adsorbed molecules. Thus all the high index stepped planes will be eliminated during the process of growth and only the low index surfaces will be left. Therefore the further growth of the crystal depends on the formation of steps.

Evidence in support of the layered growth of a crystal was presented by Anderson (1932).

Bunn and Emmett (1949) made a careful study of the phenomenon of layer formation on a variety of crystals. Their results can be summarized as follows:

1 - Layers very often start from the centres, rather than the edges of the face and spread outwards. As they approach the edges the layers become thicker.

2 - In the case of rapid growth of crystals the boundaries

of the layers are often irregular. When the growth is slow, there is tendency towards regularity and conformity to the symmetry of the crystal face.

3 - The thickness and shape of the layers can be strongly influenced by dissolved impurities.

4 - Thick layers are often seen on polar crystals. Thinner layers have higher velocity because of the high energy at the steps.

Seager (1953) examined crystals of several species for evidence of the mechanism of growth and arrived at the conclusion that layer spreading seems to offer the only satisfactory explanation for the origin of the structures observed. He suggested that the velocity of spread for the layers not only depends on the supersaturation but it also depends on the form of the face and is structure sensitive. After studying the structures on large numbers of crystals he has arrived at the following conclusions:

1 - The growth velocity is a function of supersaturation, but it also depends on the index of the surface. Increase in supersaturation increases the growth velocity and high index faces grow rapidly.

2 - Each form has a critical value of supersaturation

below which the growth will not take place on the perfect face.

3 - This value of supersaturation bears an inverse relation to the index of the form.

4 - Deposition is confined to high index faces.

2.4 Layered Growth in Diamond

Tolansky made an extensive study using precision optical techniques on various crystals. He has shown clearly that many crystals grow by layer deposition. Pandya and Tolansky (1954), during their etch studied on sections of octahedral and dodecahedral diamonds, have concluded that diamond grows by layer deposition on {111} faces. It was proved further by etch and ultraviolet studies by Harrison and Tolansky (1964). By sectioning the octahedra and dodecahedra and slightly etching them, they observed lamination inside the body of the crystal. They suggested that diamond can be formed by the deposition of type I and type II layers which etch at different rates. Similar growth laminae were observed by Seal (1962 c, d).

Seal (1965) extended this method to natural as well as synthetic diamonds. He suggested that natural

diamond grows by layer deposition on the octahedral planes, while in synthetic diamonds the growth takes place on other planes as well.

During the present investigation strong evidence of layered growth on various planes in the case of synthetic diamonds have been observed.

Ramachandran (1946) suggested that the birefringence in diamond is the result of juxta position of layers of diamond whose lattice spacing is slightly different.

Tolansky (1966) after studying nearly 5000 crystals concluded that birefringence which is ubiquitous in all diamonds can be attributed to the different elastic strength and thermal expansion properties of the layers composing the crystals.

Tolansky and Rawle-Cope (1968) studied micro-diamonds from Premier and Finsch Mines. It was found that the majority of Premier Mine micro-crystals were type II, but as they grow bigger, they incorporate few ultraviolet absorbing layers and become type I. This confirms the layered growth of diamonds. Further evidence for layered growth was obtained by Varma (1967 b).

2.5 Growth of Real Crystals

As discussed, crystal growth will not continue unless there are steps present. Detailed thermodynamical calculations by Burton, Cabrera and Frank (1951) showed that steps will not be created on a low index face until the temperature of the crystal is raised almost to its melting point. Gibbs (1928) first realized, that continuous crystal growth requires the initiation of new layers, i.e. a step formation. A group of molecules can form an island and this may provide the necessary steps and growth layers can spread until the new nucleus is formed again. It turns out however that when the nucleus is less than a certain critical size, the changes of molecules being added are smaller than being removed. The radius of critical nucleus is given by $\rho_c = \frac{a\phi}{2\ kT \log \alpha}$ (Burton, Cabrera and Frank 1951), where ϕ is the nearest neighbour interaction, and α is the supersaturation ratio. Burton, Cabrera and Frank (1951) suggested that the rate of formation of nuclei is given by $Z\left(\frac{S}{So}\right)\ e^{-\phi^2/k^2T^2}\ \log \alpha$. Where Z is the rate of arrival of fresh molecules at a single site, S is the area of the crystal face under consideration and S_o is the area per molecule in the layer.

The expression suggests that the probability of formation of the critical nucleus is negligible under the super-saturation of the order of 50%.

Experiments suggest, however that real crystals do grow, even at supersaturation as low as 1% (Frank 1949).

Volmer and Schultze (1931) have studied the growth rate of individual iodine crystals in slightly supersaturated vapour at $0^{\circ}C$. They suggested that growth rate is proportional to supersaturation down to the value of 1% or even lower.

Thus the growth of a real crystal is a complex phenomenon. In order to explain this discrepency, Frank (1949) considered the influence on the nucleation of the presence of dislocations, in the growing crystals. The idea of dislocation was first proposed by Taylor (1934) to explain the theoretical and experimentally observed discrepency on the yield strengths of metal crystals.

2.6 Dislocations

Dislocations are geometrical faults in an otherwise perfect lattice. There are mainly two types of dislocation:

1 - Edge dislocation.

2 - Screw dislocation.

(i) Edge Dislocation

This type of dislocation was proposed by Orowan (1934), Polanyi (1934) and Taylor (1934). In this type of dislocation the slip vector is at right angles to the dislocation. A dislocation here is a line imperfection forming the boundary of the slipped area within the crystal. A diagram of an edge dislocation is shown in figure (2.3). The slip has occurred over the area ABCD. AD is the boundary of the slipped area and along it the atoms have no counterpart in the lower half of the crystal figure (2.4). AD is called the dislocation edge.

The number of atomic planes above and below the slip planes differs by one. This necessitates one vertical plane of atoms to terminate on the slip plane and hence the name edge dislocation. It is clear that the lattice is under compression above the slip plane and tension below it. An edge dislocation can move in the slip plane along the direction parallel to the slip vector, under the action of a stress, since no transformation of material is needed.

(ii) Screw Dislocation

Burgers (1939) introduced the idea of a screw

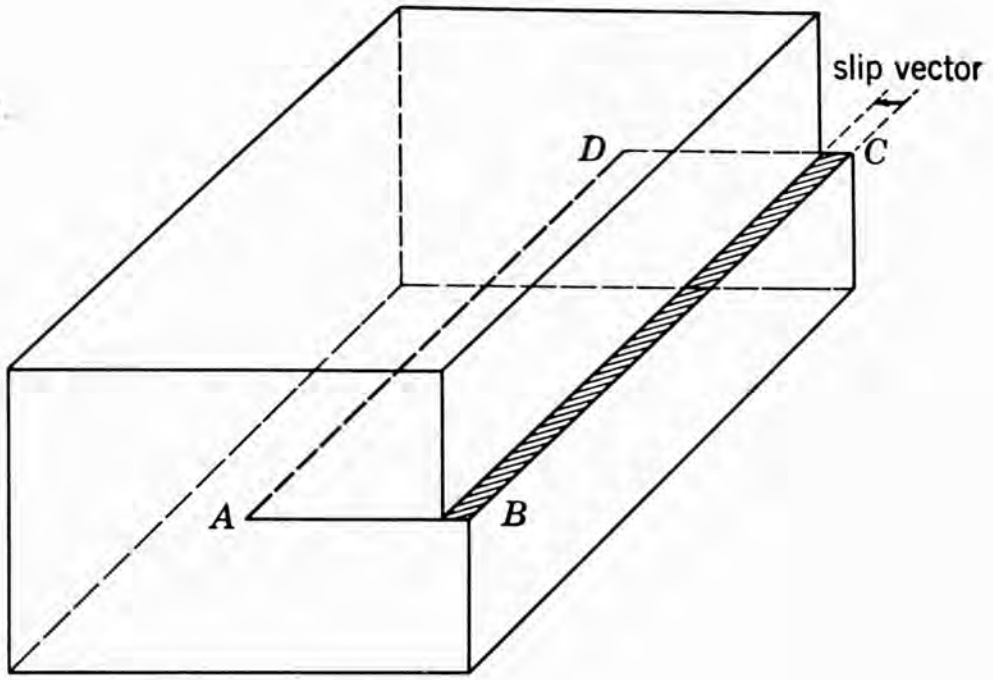

Figure 2.3.

The creation of an edge dislocation

(From Verma & Krishna)

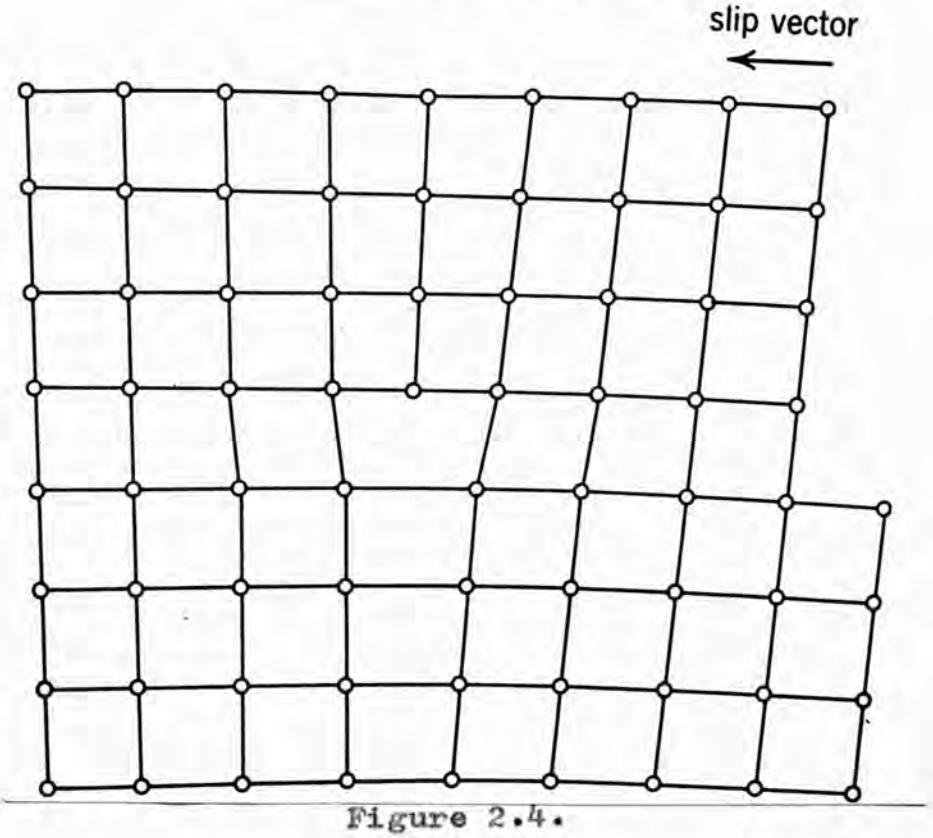

Figure 2.4.

The structure of an edge dislocation
(From Verma & Krishna)

dislocation. In this type of dislocation the dislocation line is parallel to the slip vector. Figure (2.5) shows how screw dislocation forms by slip. The dislocation FE is the boundary within the crystal of slipped area AFEB. Unit slip has occurred over the area AFEB. A step has been created on the surface of the crystal figure (2.6). The figure shows a screw dislocation in the simple cubic crystal. Atomic planes above and below are shown in figure (2.7).1 The figure clearly shows why this type of dislocation is called a screw dislocation. The crystal in the region of dislocations is not made up of parallel atomic planes, rather it is a single atomic plane in the form of a helicoid. In the case of a screw dislocation there is always a step on the uppermost surface. The step is shown in figure (2.6). There are two types of screw dislocation, right and left handed.

2.7 Crystal Growth and Screw Dislocation

It has been mentioned earlier that when all the steps have been eliminated by the advancement, forming complete layers, it is necessary to have a nucleus or step created on the surface in order for growth to

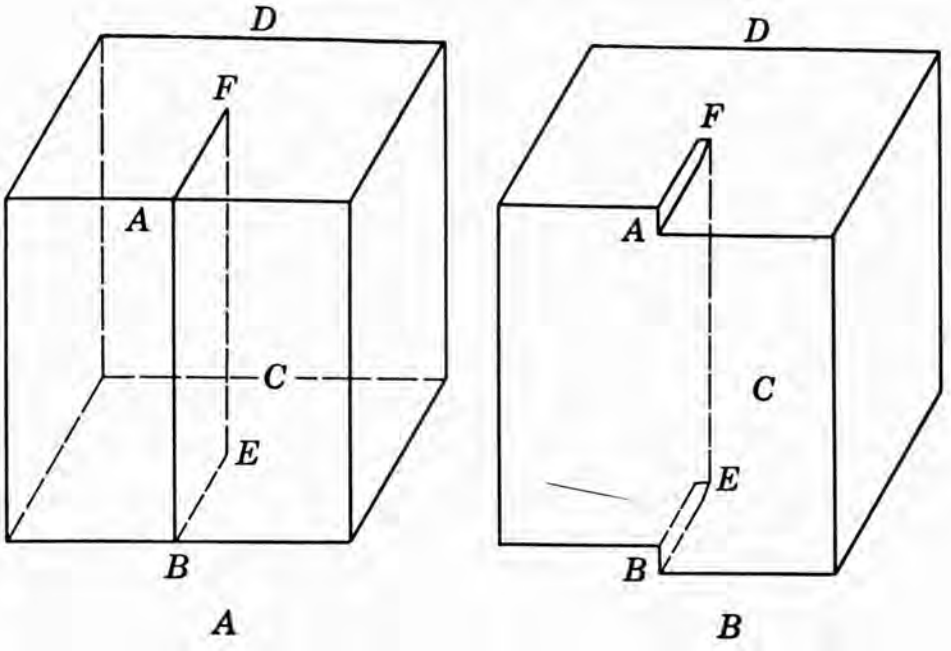

Figure 2.5.

The formation of a screw dislocation

(From Verma & Krishna)

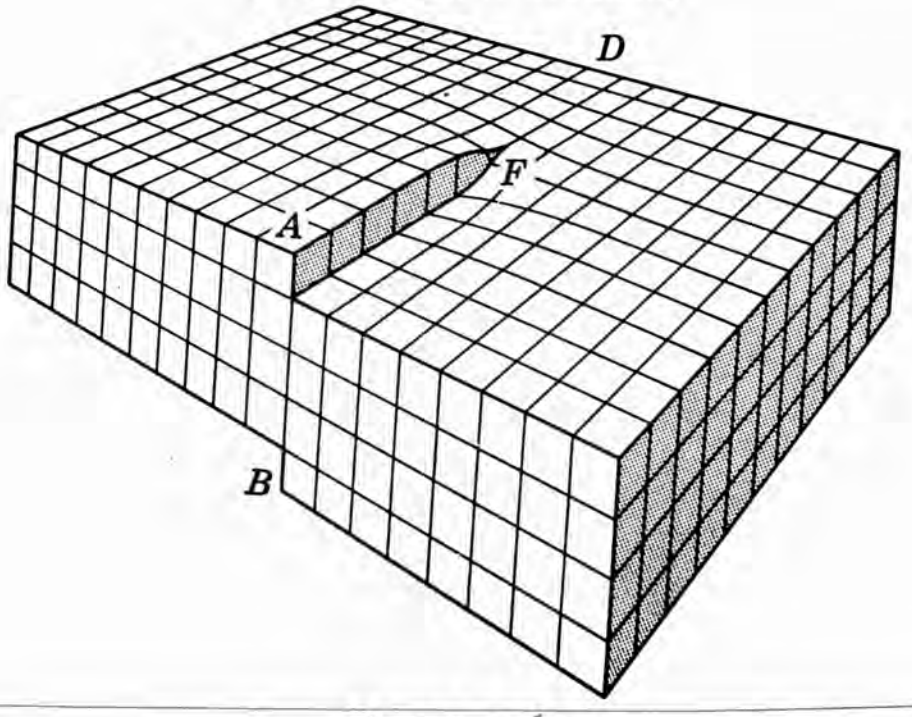

Figure 2.6.

The end of a screw dislocation

(From Verma & Krishna)

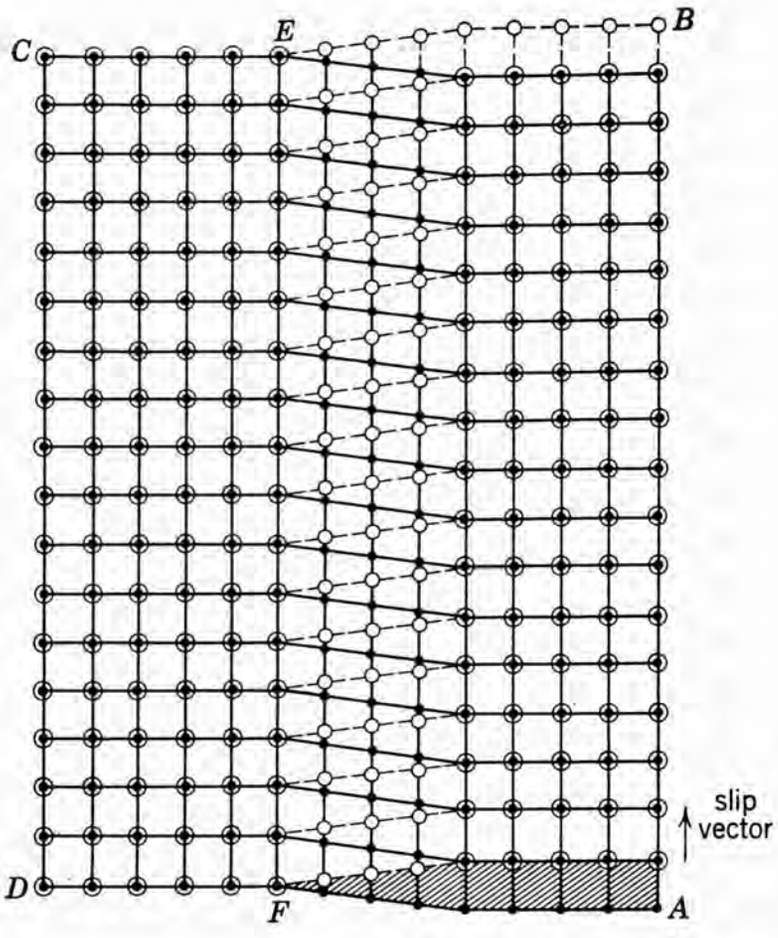

Figure 2.7.

Structure of a screw dislocation

(From Verma & Krishna)

proceed. Frank (1949) suggested that the presence of the step associated with the defect in the particular dislocation having a component of displacement vector normal to the crystal face, may catalyze the growth. These dislocations provide the continuous steps which play a key role in the crystal growth at low super-saturations. Atoms are adsorbed on the surface, and diffuse to steps which then advance. However, the steps can never grow so as to produce a completed atomic layer, since the upper surface is a spiral ramp. Frank (1949) has shown that when the crystal is growing under supersaturated environment, the steps due to the dislocation winds itself in a spiral, in such a way that a single screw dislocation sends out successive turns of steps. If the spiral is due to a right and left handed pair of dislocations, they will send out closed loops, provided their distance apart is greater than the diameter of the critical nucleus. In both cases dislocations will form pyramids. This gives an interpretation of the pyramids of vicinal faces long recognized as a normal feature of slow crystal growth (Mier, 1903 and 1904).

Direct evidence for the occurrence of this process was provided by Griffin (1950). Verma (1951) has obtained phase contrast photo-micrograph of spirals originating from various single and multiple dislocations on silicon carbide crystals grown from vapour. The step heights as measured by Verma are integral multiples of 15Å, the cell constant. Amelinckx (1951) also observed similar spirals. Forty (1952) has photographed growth spirals in cadmium and magnesium crystals grown from vapour. Recently growth spirals have been observed on various crystals. Though no such growth spirals have so far been observed on the natural diamond surfaces. Tolanksy and Sunagawa (1959, 1960 a, b and c) observed spirals on cubic faces of synthetic diamonds. Patel and Goswami (1964) and Patel and Ramachandrah (1968) have reported spirals on {111} faces of synthetic diamonds.

Seager (1953) having observed that a number of growth layers on the crystal surface have a common origin, suggested that it is very likely that growth layers might have originated at dislocations.

In the case of diamond, dislocations have been observed by various workers. Frank and Lang (1959) have

tried to correlate the dislocation pattern in diamonds with trigon formation. According to Lang's (1964) X-ray topographical studies on diamonds, all pyramidal trigons are situated where the dislocations outcrop on the surface. No obvious relationship was found between the Burgers vector and the shape of the trigon.

Evans and Phaal (1962) during their transmission electron-microscopical studies after thinning the crystal observed many dislocations in diamond.

2.8 Origin of Dislocations

The question arises: what is the origin of dislocations which are necessary for the growth of the crystal?

According to Frank (1949), imperfections are sometimes trapped in during the rapid growth of crystals at high supersaturation. The nucleation of layers in the correct and incorrect orientation also gives rise to dislocations. Due to the adsorbed impurities, a curvature develops and this causes the layers to grow in abnormal orientation, thereby producing dislocation. Sometimes aggregations of molecular vacancies give rise to dislocations. Dislocations can also be caused by

mechanical stresses.

Forty (1954) explained the formation of dislocations by the occlusion of impurities. He suggested that buckling of thin crystals arises due to non-uniform distribution of stresses, after which the stress is relieved by a slip of the structure. The buckling is produced due to the non-uniform distribution of impurities or by stress which sometimes arises due to the pressure of the neighbouring crystals.

Thus these various considerations indicate that dislocations, necessary for crystal growth, are formed inevitably in the conditions needed for nucleation.

CHAPTER 3

SYNTHESIS OF DIAMOND

3.1 Introduction

The modern development of high pressure research has made the synthesis of diamonds possible. Diamonds have now been made by many groups in a number of countries, all using temperature in the range of approximately 1,500 to 2,400°C and pressure from 45,000 to 100,000 atmospheres (Berman 1965).

The equilibrium line between diamond and graphite on the phase diagram was first calculated on thermodynamical grounds, taking the physical properties and the heat of formation of diamond and graphite into consideration. The experimental physical properties data were not available beyond 1,200°C and therefore the equilibrium line was at first simply extrapolated (Berman & Simon 1955) (figure 3.1). Until the recent synthesis of diamonds in the laboratory there had been no way to study this equilibrium curve by direct experiments.

However, the phase-diagram can only show whether the reaction has thermodynamical permission to run. The rate at which the reaction runs, depends upon

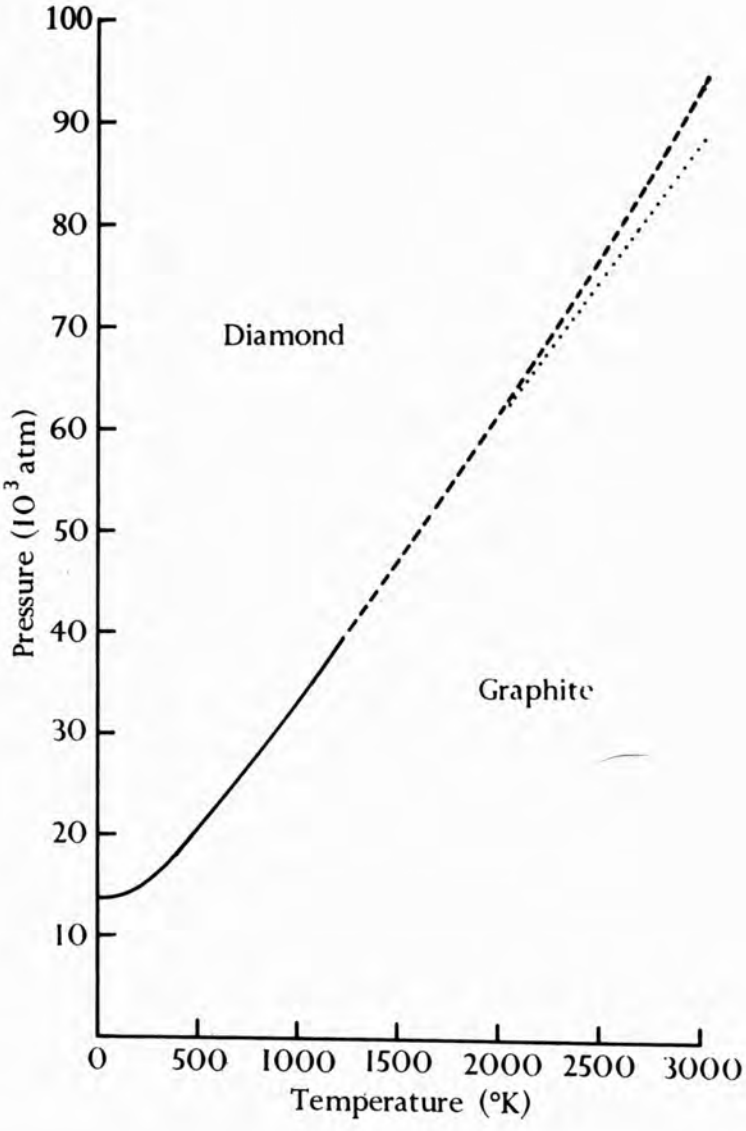

Figure 3.1.

The Graphite-Diamond Equilibrium Curve

(After Berman & Simon, 1955)

the nucleation centres of the new phase, the activation energy of transformation, where an intermediate state is involved, and the rate of incidence of energy pulses capable of exciting the change (Bundy et al. 1961).

Hall (1956) has studied in detail the question of direct transformation from graphite to diamond on the basis of the reaction rate and thermodynamic stability. He found that, high temperature will be necessary before much crystallization of diamond occurs. Even at 12kbar pressure and 2700°C temperature, no synthesis was possible (Bovenkerk et al. 1959). Because of high heat of vapourization of diamond at very high pressure, excess of thermodynamical potential is required to initiate the nucleation of the new phase.

3.2 Diamond Synthesis using Metal Catalysts

Experiments have shown that the diamond synthesis occurred readily in the presence of molten metals of group VIII (or alloys) and best results were obtained when graphite and metal were in relatively large pieces adjacent to each other (Bundy et al. 1961).

Diamonds were found to be formed at the interface area and the reaction progressed as the wave front of molten metal penetrated through the graphite. The reaction stops where the local temperature dropped below the melting point of metal-carbon eutectic. Bovenkerk et al. (1959) have shown that diamond synthesis has occurred at pressure and temperature appropriate for the thermodynamical stability of diamond. They verified the curve for the temperature range 1500°C - 2700°C and studied various systems for the synthesis of diamond revealing that the system involving carbon, dissolved in molten metals, was the most fruitful. After detailed studies about diamond synthesis they arrived at the following conclusions.

1 - Temperature and the pressure of the system should be those for which diamond is thermodynamically stable.

2 - Temperature must be high enough to ensure that the catalyst metal, saturated with carbon is molten.

3 - Diamonds can form whether there are diamond seed crystals present or not.

4 - If the synthesis pressure and temperature are moved further in into the diamond stable region, away

from the diamond-graphite equilibrium curve, the rate of nucleation and growth of diamonds increases but the average crystal size decreases.

5 - Bovenkerk (1961 a,b) and Bovenkerk (1959) suggested that the growth rate of synthetic diamonds is high, 0·1 to 0·3 mm per minute. This rate is influenced by the temperature gradient, because of the dependence of the solubility of carbon on temperature. Growth rate is higher if the gradient is steeper.

6 - However, high growth rate results in the clustering of crystals, as it is very difficult to prevent nucleation. The edges of the crystals tend to grow faster with growth advancing towards the centre of the crystal faces. This leads to hopper or skeletal structure.

7 - The transformation from carbon to diamond occurs across a very thin film, about ·1 mm thick, which separates carbon from the diamond. Thus the transformation is direct but the catalyst is essential.

8 - As the growth rate of synthetic diamonds is high, they easily include or grow around foreign particles present in the mixture. Particularly due to the rapid

growth, some of the catalyst metal is often trapped inside the growing crystals.

9 - Higher temperatures appear to favour growth of octahedral faces exclusively. At the lower temperatures cubo-octahedra and cubes predominate. Litvin and Butuzov (1969) have also studied the crystal habit in relation to the temperature of production. According to them, different solubilities are responsible for the production of different forms. This is the solubility of various faces and of graphite in the metal solvents. According to them octahedra are formed only in the Mn - C system.

10 - Most of the synthetic diamonds so far available have been made by dissolving carbon in molten nickel, but various other catalyst materials can be used, e.g. manganese, iron, cobalt, ruthenium, rhodium, palladium, osmium, iridium, chromium or nickel or platinum (Bovenkerk et al. 1959). Some catalysts are more effective than others (Bovenkerk et al. 1959).

11 - Carbon is used in the form of commercial graphite, carbon-black or sugar charcoal, but graphite is to be

preferred.

The colours of the synthetic diamonds vary through from black, grey, greenish-yellow, yellow, amber, blue to colourless. The colourless crystals are formed at the higher temperature. In many cases the colour does not depend on the particular catalyst used but depends upon the operating temperature, relative to the melting.point of the catalyst-carbon mixture. The colour might have been caused by imperfections in the crystal lattice.

Thus in this method, metals are used for dissolving graphite and allowing recrystallization at pressure and temperatures where diamond is stable. Usually temperatures and pressures of the order of 1400 - 1600°C and 56 - 60 kbar are used now (Wentorf 1966). Most of the world's synthetic diamond production (several tons per year) is based upon this method. However there are other methods too.

3.3 Shock Synthesis of Diamond

The quickest way is to expose graphite to the intense pressures and temperatures generated by a compressive shock wave, usually produced by high explosives

(De Carli and Jamieson 1961, Cowal et al. 1968). By this method diamond forms in a few micro-seconds and the main problem is to recover it afterwards. The crystal size is usually small, of the order of a few microns, because of the intense mechanical disruption of the specimen and the short times available for crystal growth. Both hexagonal and cubic modifications of diamond are produced. This method is used in manufacturing shock synthesized diamonds from Du Pont Inc.

3.4 Direct Convertion of Graphite into Diamond

Another method consists of heating graphite to about 3000°K while it is held at pressures near 130 kbar (Bundy 1963). In this method because of the high temperatures and pressures involved, rapid cooling takes place and the crystal size is small, e.g. 0·01 mm to ·1 mm.

3.5 Synthesis of Gem Diamonds

Recently Strong and Wentorf (1972) have reported

a method for synthesizing diamonds upto 6 mm in diameter. This method consists in dissolving very small diamonds or diamond powder in a molten catalyst metal e.g. Fe, Ni, Co etc., at pressures and temperatures of the order of 50 - 60 kbar and 1400 - 1500°C respectively, in a hot region and depositing upon a seed crystal in slightly cooler regions. Several days are required to produce high quality single crystals. The cost is excessively high.

CHAPTER 4

ETCHING OR DISSOLUTION OF CRYSTALS

4.1 Introduction

Etching is a reliable tool for the direct investigation of defects in crystals. The method consists in immersing crystals in a suitable medium which could be a liquid, a solution or a gaseous chemical reagent. When the crystals are subjected to the corrosive action of the solvents, characteristic markings are produced and such markings are known as "etch figures".

Honess (1927) has defined "etch figures" as "definitely shaped solution cavities produced by the momentary or prolonged action of some natural or artificial solvents upon the faces of the crystals, the shape and distribution of the cavities being directly attributable to the solvent and to the molecular configuration of the face upon which they occur". Pits were found to vary in shape from conical to pyramidal, the latter form usually displaying the

symmetry of the crystal plane in which the pits occurred. Being essentially a phenomenon reverse to crystal growth, the concepts that play a role in crystal growth do so in dissolution as well.

Etching is the most convenient method for revealing dislocations in many crystals. Shockley and Read (1949) were the first to suggest that etch pits corresponding to individual dislocations might be seen microscopically. Successful, deliberate attempts to etch the surface terminal points of dislocations were made by Horn (1952), Gevers et al. (1952) and Gevers (1953). They produced etch pits within growth spirals in silicon carbide. Soon after Vogel et al. (1953) showed that in germanium the spacing of etch pits in grain boundaries corresponded to predictions based on the theoretical model of Burgers (1940) and Bragg (1940). This strongly supported the idea that etch pits can be formed at dislocation terminals. By etching matched cleavages of crystals, Patel and Tolansky (1957 a,b) and Gilman et al. (1958), among others, have shown how etch patterns form mirror images establishing that linear defects can be cut into pairs by a cleavage crack.

4.2 Etch Pit Formation

Growth and dissolution are thought to occur by the advance and retreat of monomolecular steps across the surface of crystals (Burton et al. 1951). Individual molecules may be deposited or removed at kinks.

When a perfect crystal is exposed to a solvent, dissolution is supposed to begin by the nucleation of unit pits of one molecule depth at other places in addition to dislocation terminals, e.g. cleavage steps, inclusions etc. These unit pits grow as steps and retreat across the crystal surface. As said above dislocation sites serve as preferential points for the nucleation of unit pits and repeated nucleation at a dislocation leads to the formation of an etch pit. Cabrera (1957) emphasized the role of the dislocation energy in the nucleation of pits, pointed out that effectiveness of a dislocation as a nucleation site depends on, among other factors, the character of dislocation and the impurity content. The dislocation energy that contributes to the nucleation of pits is made up of the core energy plus a small fraction of the total elastic strain energy. The existence of several

types of pits suggests that the etch is sensitive to more than one type of dislocation. Also nucleation rates may depend upon the character of dislocations. The pit size is bigger in the case of edge dislocations because of their higher energy (Gilman et al. 1958).

The different crystallographic planes are susceptible to different etchants to a different extent, producing pits of different shapes, having different crystallographic orientations. Orem (1957) having subjected a sphere of aluminium to alkali and acid etchants, found that it tended to become a cube in alkalis while an octahedron in acid etchants. Gilman and Johnston (1957) obtained pits of different orientation in alkali and acid media indicating that different etchants are effective to different planes to a differing extent. Patel and Ramanathan (1962) obtained pits of different orientations with different etchants.

The formation of visible dislocation etch pits depends on the nucleation rate for unit pits at the sites of the dislocations and the rates of motion across the surface. The two quantities depend on the linear solution rates normal to the surface at a dislocation and

parallel to the surface. In the figure 4.1 if Vn and Vs represent these rates and if $Vn \ll Vs$, very shallow pits would be formed. These pits however will be difficult to see under ordinary conditions. To obtain relatively visible pits Vn/Vs should be appreciable. The ratio Vn/Vs can be increased by:

(a) increasing Vn, as in the case of most etchants for metals which utilize a segregated impurity for this purpose (Wyon and Lacombe 1955, Gilman 1956, Suits and Low 1957).

(b) decreasing Vs by the addition of an inhibitor.

(c) varying the temperature to take advantage of the difference in the temperature-dependence of Vn and Vs (Gilman et al. 1958).

If a dislocation is moved during the etching process, the dissolution rate normal to the surface Vn, at the original position of the dislocation becomes negligible. Since the velocity of the steps, Vs remains the same, the pit will assume a flat-bottomed shape as shown in figure 4.1.

4.3 Effect of Surface Orientation

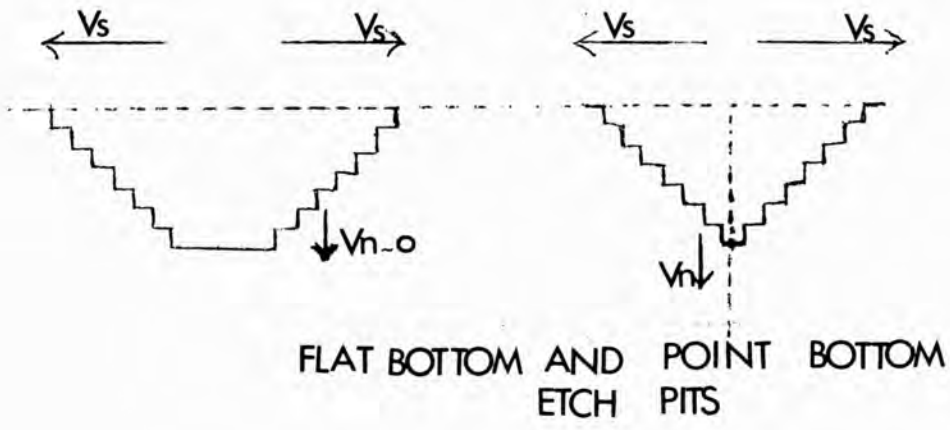

Figure 4.1.

Flat-bottom and Point-bottom Etch Pits

The orientation of a surface has a pronounced effect on its etching behaviour. As a rule, the close-packed planes are more easily etched than others (Amelinckx 1964). The pits have been observed only within 15° of {111} in germanium (Holmes 1959), 7° from {111} in copper (Bertocci et al. 1963), 4° from {100} in iron (Sestak and Kadeckova 1966), 2·5° from {111} in silver (Levinstein and Robinson 1962) and 2·3° from {111} planes in copper (Livingston 1960). Outside these ranges, the general surface dissolution is comparative to etch rate at the defect sites and therefore no pit would be formed.

4.4 Information from the Etch Pits

Etch pits essentially reveal the emergence points of dislocations, on the surface of a crystal and therefore provides a direct measure of dislocation densities. The evidence that all the dislocations in LiF crystals are revealed by the etch pit method, has been provided by X-ray studies (Gilman and Johnston 1957). More detailed studies about the etch pits marking the terminal points of dislocations, have been made by Newkirk (1959) and various other workers. Since the etch

pits have certain depth, they also give some indication concerning the general directions of the dislocation lines (Amelinckx 1956). If the line intersects the surface perpendicularly, a symmetrical pit would arise; if the line is oblique the pit becomes slightly assymetrical and from the assymetry the inclination of the line can be deduced.

For the etch pits on {111} faces of natural diamond crystals, Patel (1961) showed that the dislocation must be straight and along {111} planes within the crystals. Removal of surface layers alternated with etching permits the exploration of dislocation configuration in space. This technique was employed by Gilman and Johnston (1957) for mapping dislocation loops.

If the dislocation line is perpendicular to the surface and has a helical shape, the etch pit acquires the form of a conical spiral (Amelinckx et al. 1957).

Information can be obtained about edge and screw dislocations, because they etch slightly differently. The pits produced at edge dislocations are deeper and symmetrical while the pits at the screw dislocations are

slightly assymmetrical.

Etching is inhibited or accelerated by some segregated impurities at dislocations, therefore aged and fresh dislocations etch much differently (Gilman et al. 1957).

Damiano and Herman (1959) were able to produce spiral etch patterns on basal planes of zinc. Thus the method of etch gave the evidence of screw dislocations in the crystals.

Etching can be used to determine the orientation of the crystals (Loh 1969).

Etching studies therefore provide an efficient and powerful tool for surface as well as bulk studies of crystals and the evergrowing literature is direct proof of its reliability.

CHAPTER 5

SURFACE TOPOGRAPHICAL STUDIES ON NATURAL AND SYNTHETIC DIAMONDS BY PREVIOUS WORKERS

Natural diamonds are frequently found as octahedral or dodecahedral forms. The cubic form is comparatively rare except in the Congo. Octahedral faces are often smooth while the cubic faces are well known for being rough. Dodecahedral diamonds usually have curved faces and are often striated.

Markings on diamond surfaces have long interested geologists and physicists. Most diamonds show a variety of surface detail which varies considerably from diamond to diamond. These markings must be the record of the geological history of the diamonds. According to Tolansky (1955) "The surface topography which can be seen on any diamond is a frozen-in picture of the last stages of growth". Surface studies should therefore give some clues regarding the growth of diamonds in particular and possibly crystals in general.

5.1 Studies on Octahedral Faces

The octahedral faces are characterized by the presence of triangular cavities: the so-called "trigons" (Sutton 1928), having their corners pointing towards the edges of the octahedral faces. Figure (5.1) shows trigons on an octahedral face.

There has been a long-standing controversy as to the formation of these cavities. Trigons have been studied and discussed by various workers. There are two schools of thought about the origin of trigons. Crookes (1907), Fersmann and Goldschmidt (1911), Van der Veen (1913), Sutton (1928), Williams (1932), Tolansky and Wilcock (1947), Wilcock (1951), Halperin (1954), Tolansky (1955, 1960, 1962, 1965) and Varma (1967 a,d) conceived trigons to have originated in growth.

Van der Veen (1913) supposed that trigons are formed by three growth layers approaching from the three sides at 60°. The advancing sheets leave a triangular pit, when their ends touch. The rectilinearity of the sides of the trigons and the curvature of the growth sheets outside were explained by postulating that the limits of the newer layers remained curved while those

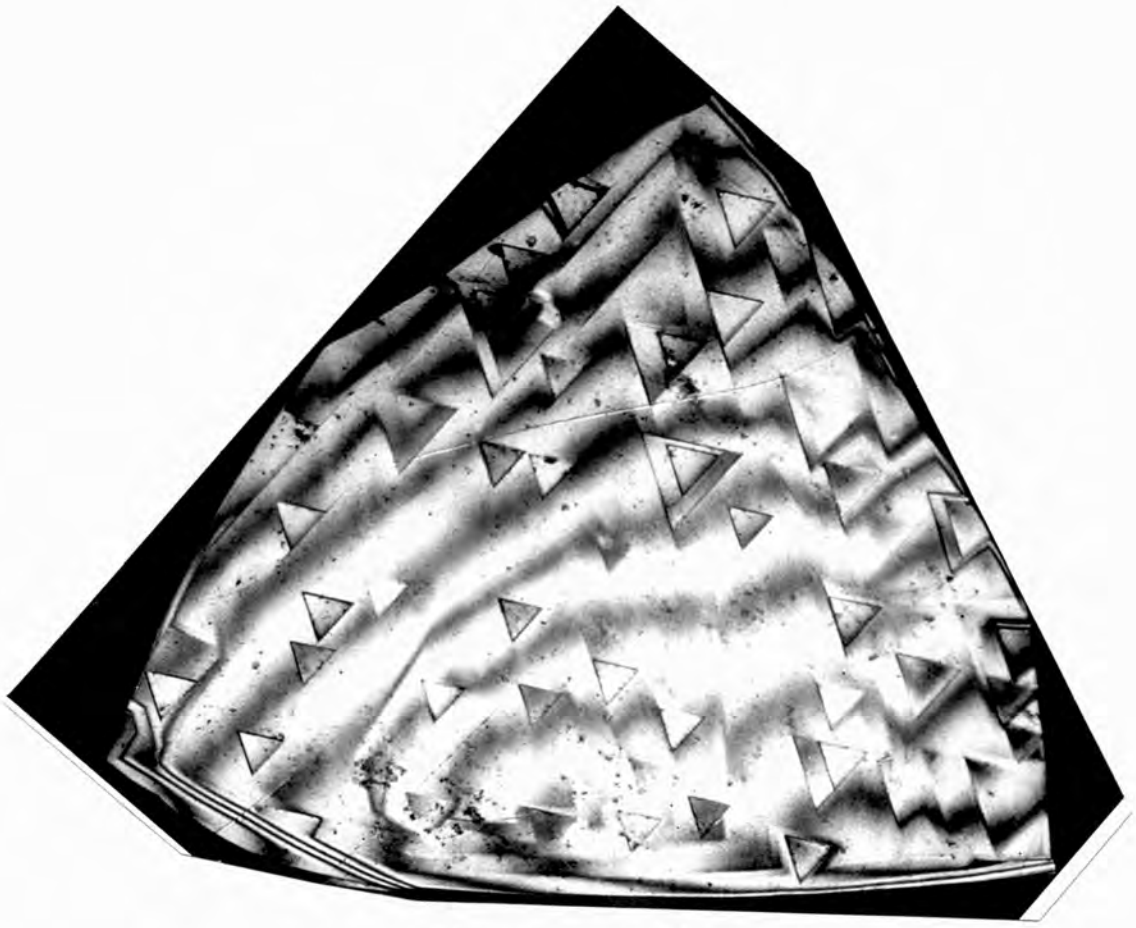

Figure 5.1. (X 200)

of the older ones became straight. Figure (5.2) shows the mechanism conceived by Van der Veen.

Tolansky (1953 a,b; 1955; 1960; 1965) made an extensive study of trigons by applying the sensitive technique of multiple-beam interferometry. The technique gives a resolution of the order of a few angstroms in the vertical direction. He observed that trigons are "ubiquitous" in that they are almost always present on the octahedral faces. He gave the simple and straightforward explanation that trigon formation is essentially a growth process arising from the building up of octahedral diamond with a succession of plane growth sheets. When these layers, which are inclined at an angle of 60°, get arrested, an equiangular triangular cavity would form, having its base at the same level as the outer region with an intervening plateau (Tolansky and Wilcock 1946, 1947). Occasionally these growth layers advancing at 60° to each other also leave hexagonal cavities (Tolansky and Wilcock 1946). (Such features were frequently observed during the present studies with an electron microscope).

Wilcock (1951) gave an alternate explanation

Figure 5.2.

Van der Veens Mechanism of "Trigon" formation.

(After Van der Veen, 1913).

for the formation of trigons. He suggested that trigons are formed when the advancing layer stops due to some obstruction, forming a stationary front. According to him the layer advances on either side of the stationary front, then grow inwards from either side, halt as the ends touch and so form the trigon. A similar argument was put forward by Halperin (1954) who proposed that trigon formation would take place when the advancing layer is disturbed by some surface defect like imperfect steps or an accumulation of interstitial faults in the lattice. This layer bends round the corners, leaving the triangular cavity.

Tolansky (1965) made a microscopic examination of the "kerf", the scratch that professional cleavers make while cleaving diamonds. He observed in a number of cases a curious phenomenon that the kerf invariably skirted round well defined trigons. Tolansky interpreted this as indicating that the physical nature of trigon boundary is different from that of the surrounding region such that it could hold up the splintering shock and deflect it away. This was indirect evidence, supporting the growth theory of trigons that Tolansky

has established by other observations.

Varma (1967 a,d) studied trigons in relation to the surrounding features and observed certain characteristics which he stated were inalienable. The maintenance of these characteristics, he observed was possible only if the trigons did not change their present sizes. As etch pits can and do change in size by continued etching, he suggested that this was additional evidence in support of the growth origin of trigons.

Wilks (1961) suggested that low-angled point-bottomed pyramidal trigons are formed by etch while steep-sided flat-bottomed trigons arise due to some different mechanism.

Wilks' ideas were supported by Seal (1962 a).

According to the other school of thought, trigons are attributed to an etch (Frank et al. 1958; Frank and Puttick 1958; Patel and Ramanathan 1962; Lang 1964; Patel and Patel 1968 a, b, 1969, Patel and Patel 1971).

Frank et al. (1958) have emphasized that the precise contact of one of the corners of a trigon with the side of another, a characteristic often observed, is a very significant diagnostic feature leading to an

explanation of trigon formation. They suggested that the trigons seen in contact have approached this contact either by enlargement from non-contact or shrinkage from overlapping. They further suggested that trigons never overlap because as soon as the contact is reached, "a new process operates to restore the contact". Frank and Puttick claim to have produced pits of trigon orientation, by etching diamonds in fused kimberlite at 1450°C. This claim has however to be looked upon carefully.

Tolansky (1965) emphasized how trigons are sometimes extremely shallow and can therefore be missed. When etching takes place it will develop their boundaries. Hence the pre-existing trigons could be missed and after being etched might be mis-interpreted to be etch pits.

Lang (1964) made X-ray topographic studies on a number of high quality diamonds, and observed that whereas dislocations outcropped at point-bottomed trigons, no dislocations outcropped at flat-bottomed trigons. He also found that several pyramidal trigons showing a complex structure at their bottom were found to correspond to close pairs or triplets of dislocations. Since the

sites of dislocations would be attacked preferentially, Lang came to the conclusion that his observations provided strong support for etch pit hypothesis for the origin of trigons.

Also supporting the etch hypothesis are Patel and Ramanathan (1962); Patel et al. (1964); Patel and Agarwal (1965); Patel, Agarwal and Desai (1966) and Patel and Patel (1968 a.b, 1969).

However, it is certain that etch pits of both orientation i.e. positive, having sides parallel to the octahedral edges and negative i.e. having corners pointing towards the face edges can be produced on octahedral faces, by varying etchant, and other physical conditions like temperature and pressure. The point still remains that if trigons are etch pits then why their topography is different from artificially produced etch pits. Also if all the pits on octahedra from all sources are always in negative orientation, this would mean that all the diamonds irrespective of their origin are subjected to the right etchant at the right temperature and pressure. Further the origin of flat-bottomed trigons still remains unexplained (Wilks 1961).

In addition to trigons other features are occasionally observed on octahedral faces. Crystallographic slip is not very common in natural diamonds. Tolansky and Omar (1953b) were the first to report crystallographic slip. They studied it interferometrically and suggested that the slip plane made an angle of $70 \cdot 5^{\circ}$ with the surface. Also Tolansky et al. (1958) has reported the evidence of crystallographic slip on $\{111\}$ faces. The slip was observed as a straight line running across the crystal face in $\langle 110 \rangle$ directions. The slip line passed through the centre of trigons. Recently slip on $\{111\}$ faces was also reported by Patel and Agarwal (1967a).

Varma (1970) has produced evidence to show that these linear discontinuities are the result of plastic deformation producing twinning. It was suggested that the twinning could have occurred even as the diamonds were growing in nature.

Tolansky and Emara (1958) reported six-sided growth features containing alternate angles of approximately 90° and 150°. They suggested that edges of these features were parallel to $\langle 431 \rangle$ directions, and they may possibly arise due to the intersection of $\{221\}$ planes

with (111) face. This they suggested, indicated favoured growth along {221} planes.

Patel (1964) reported polygons on a twin boundary. He observed that on the twinned region of natural octahedral faces of diamond, various parallelogram-like or six-sided features are seen. He suggested that an etch mechanism is responsible for the formation of such features on the twin boundary.

Halperin (1958) reported an uncommon growth feature on diamond (111) face, which he suggested indicated plane sheet mechanism of growth for diamond.

Patel and Agarwal (1966 a) reported unusual microstructures on South African diamonds. The crystals revealed a multitude of crystallographic and non-crystallographic hillocks, which they attributed to dissolution in nature.

Thus these unusual features also shed some light on the mechanism of diamond growth in nature.

(During the present studies various unusual features were observed which are described in Chapter 12).

5.2 Studies on Dodecahedral Diamonds

The dodecahdra usually have rounded faces.

Like the 'trigons' on the octahedral faces the curvature of the dodecahedral faces has been the subject of extensive study and controversy.

Fersmann and Goldschmidt (1911) attributed the curvature to partial dissolution in nature. They conceived diamond to be immersed in a mother liqour allowing free movement of crystallization and dissolution currents and suggested that there is a delicate balance between growth and solution. A current meeting the crystal deposits, or rather grows diamond, while the current leaving removes the material. These ideas were further elaborated by Shafranovsky (1940 and 1941) and Kukharenko (1946).

Raman and Ramasheshan (1946) suggested that the curvature is direct consequence of the solidification of diamond from a drop of liquid carbon. This idea was further developed by Ramasheshan (1946) who attempted to show that the curvature of the faces would correspond to the curvature of such a drop.

Taylor (1947) indicating the intrinsic difficulty in the proposition, pointed out how this would require the ad-hoc assumption that a high degree of directed valency bonding would exist before solidification.

Frank and Puttick (1958) suggested that the curvature is due to natural dissolution, while Williams (1932) and Varma (1967 b) explained that dodecahedral form is the result of piling up of layers of diminishing sizes on octahedral faces. Varma (1967 b) suggested that striations "the channel-like features running parallel to the longer diagonal of the rhomb" are the spaces between the successive layers in $\{111\}$ planes.

Detailed surface studies were undertaken by Tolansky and Pandya (1954), Emara and Tolansky (1957) and Pandya and Tolansky (1961).

Tolansky and Pandya (1954) and Emara and Tolansky (1957) found that striations are often less than 50 Angstroms deep. They also observed a network pattern consisting of very shallow ruts, either curved or straight, with the straight ruts crystallographically oriented. The crystallographic and irregular network pattern was attributed to the etching of crystals in nature, because the etch experiments gave similar pattern, while the pre-existing one deepened on further etching. The non-crystallographic network pattern was suggested to be due to invisible dislocations on the surface of the

natural dodecahedra, the outlines of which are the regions to be etched preferentially.

The crystallographic network pattern was studied by Emara and Tolansky (1957) and Pandeya (1959). They found that this was made up of either ridges or grooves in ⟨110⟩ directions. The angles were 110° and 70°. On further etching, the channels became deeper and wider. The crystallographic pattern was explained by preferential etching of the projections of {111} planes on the dodecahedral faces. As diamond grows by layer deposition on {111} planes (Pandya and Tolansky 1954), some of these layers may be more susceptible to an etch and thus forming the network pattern, having V-shaped grooves. The included angles are approximately 70·5° and 109·5°. They also reported the formation of this crystallographic pattern by artificial etching. Thus the crystallographic pattern was suggested to be due to the traces of {111} planes which are perpendicular to {110} planes on (110) faces, while the striations were suggested to be the traces of {111} planes making an angle of 35·5° with the dodecahedral planes.

During the present work such features have been observed for the first time on the faces of synthetic

diamonds (Chapter 8).

In addition to these network patterns, another surface structure at times observed on the dodecahedral faces is a disk pattern. Sutton (1928) observed such a pattern. It was also reported by Tolansky and Pandya (1958), Kvohov (1959) and Kucharenko (1960). Pandya and Tolansky (1961) have made a detailed interferometric study of such features and suggested that these are due to the protective effect of bubbles on the crystals which were being subjected to a mild etch in nature.

5.3 Surface Studies on the Faces of Cubic Natural Diamonds

The cubic diamonds are rarer in nature compared to the octahedral and dodecahedral forms. Studies on the cubic diamond faces were reported by Fersmann and Goldschmidt (1911), Sutton (1928), Williams (1932), Tolansky and Sunagawa (1959, 1960 c), Tolansky (1961 a) and Harrison (1964). All that was reported by these workers was that the faces are full of square shaped cavities having their sides in ⟨110⟩ directions i.e. the cavities have so-called negative orientation with respect of the crystal face. Tolansky and Sunagawa

(1960 c) have suggested the name "quadrons" to match with the name "trigons".

Similar to the case of trigons, Fersmann and Goldschmidt (1911) and Patel and Agarwal (1967) have attributed these cavities to dissolution in nature, while Williams (1932) and Tolansky and Sunagawa (1960 c) and Harrison (1964) have attributed these to growth.

Because the faces are extremely rough detailed studies are intrinsically difficult and were not therefore undertaken by earlier workers.

During the present work the cubic crystals are studied electron microscopically (Chapter 11).

5.4 Surface Topographical Studies on Synthetic Diamonds, Reported by Previous Workers

The surface structures on synthetics are ordinarily quite different from those on the naturals (Tolansky and Sunagawa 1959, 1960 a,b,c; Tolansky 1961 a; Seal 1961, 1962 a).

The surface markings may provide some clues to the growth mechanism responsible for diamonds in nature and may lead to the devising of more efficient and easier ways of synthesizing diamonds. Moreover the surface markings on synthetic diamonds are important with regards

to the use of such diamonds as abrasive grits, since the surface conditions play an important role for the bonding between diamonds and resin. The life of a tool depends on the surface structure present on the diamonds. The diamond grinding wheels are made by bonding diamonds with a suitable material such as organic resin or glass or sintered metal. The efficiency of the wheel is determined by the strength of bonding between the metal and diamonds.

In comparison to the vast literature present on the surface topographical studies of natural diamonds, less work has so far been reported on the synthetic diamonds. The work is tedious and time-consuming owing to the extremely small size of present-day available synthetic diamonds.

However a brief review of the surface studies on synthetic diamonds from various sources will be described here.

Tolansky and Sunagawa (1959; 1960 a,b and c; 1961) were the first to study the surfaces of synthetic diamonds in detail. They applied various optical techniques to study the various surface markings on the faces of synthetic diamonds and observed that surfaces

of the synthetic diamonds are different from those of the natural diamonds in four ways:

1 - The cubic faces of the synthetic diamonds at times show growth spirals (Tolansky and Sunagawa 1959, 1960 a,b and c; Tolansky 1961 b, 1962 a,b).

2 - The cubic face on the synthetic crystals are often very smooth, in contrast to the cubic faces of the natural cubic diamonds (Tolansky and Sunagawa 1960 a,b and c; Tolansky 1961 a).

3 - In the case of synthetic diamonds dendritic - patterns are present on cubic as well as octahedral faces (Tolansky and Sunagawa 1959, 1960 a,b and c; Tolansky 1961 a, 1962 a).

4 - Slip lines are very frequently seen on the octahedral faces of synthetic diamonds, while in the case of natural diamonds crystallographic slip is not observed so frequently (Tolansky and Sunagawa 1960 a,b; Tolansky 1961 a, 1962 b).

Slip on the faces of synthetic diamonds was also reported by Patel and Ramachandran (1967).

Surface studies on the synthetic diamonds were mostly performed with the help of two-beam interferometry because the crystals were too small to be studied by

multiple-beam methods (Tolansky and Sunagawa 1960 a,b).

According to Tolansky and Sunagawa (1960 a), the two-beam fringes obtained from synthetic diamonds have much better contrast compared to the contrast in the case of natural faces, owing to the lower reflectivity of the synthetic diamond surfaces.

Spirals on the cubic faces of synthetic diamonds were later reported by Patel, Goswami and Ramanathan (1963), while Patel and Goswami (1964) and Patel and Ramachandran (1968) reported the occurence of spiral growth patterns on the octahedral faces of synthetic diamonds.

Bochko and Deryagin (1969) observed right and left-hand spiral growth on the diamond faces, which they attributed to the presence of positive and negative dislocations.

Tolansky and Sunagawa (1960 a,b) and Tolansky (1961 a, 1962 b) have described the frequently observed hopper growth on the faces of synthetic diamonds. Lemmlein et al. (1964) also reported the hopper formation on the faces of synthetic diamonds.

The so-called dendritic pattern on the surface

of synthetic diamonds was commonly observed by various workers (Tolansky and Sunagawa 1960 b, c; Tolansky 1962 a, b; Bovenkerk 1961 a, b). They observed these to be elevations. Bovenkerk (1961 a) explained this veined surface structure by postulating that during the last stage of growth of diamond, the catalyst could be in a semi-solid state with dendrites freezing in the metal and thereby being imprinted on the diamond surface. Such features however, are observed by Tolansky (1971) on the faces of natural crystals during his extensive surface topographical studies on Premier Mine micro-crystals.

This surface veining was also reported by Seal (1961, 1962 a).

Occurence of trigons on G.E.C. synthetic diamonds was reported by Tolansky (1962 a, b). He suggested that trigons are a relative rarity in synthetic diamonds. As suggested by Tolansky (1955) for natural diamonds, Bovenkerk (1961 a) also reported that in case of synthetic diamonds the intersection of growth layers leads to trigon formation.

Apart from trigons, crystallographically oriented

growth hillocks were also reported on the octahedral as well as cubic faces of synthetics.

Patel and Ramanathan (1963), during their optical studies on G.E.C. synthetics reported triangular growth hillocks on the {111} faces. Such hillocks were also observed by Seal (1961 and 1962 a, b). The growth hillocks on the {100} faces were studied by Patel and Ramachandran (1967 b).

The present studies were for the first time carried-out on the de Beers synthetic diamonds. In addition to the optical studies, detailed electron-microscopical surface studies were performed for the first time and therefore in addition to the features described above, various other new features were seen because of the high lateral resolution.

Crystallographic growth hillocks, trigons, spirals and various other features were seen for the first time electron-optically.

(The details of the surface features observed are given in Chapter 8).

CHAPTER 6

FORMER EXPERIMENTS ON DIAMOND ETCHING

The history of diamond etching goes back as early as 1892, when Luzy heated diamonds in blue ground. He heated diamonds in the blast furnace at 1770°C for 20 - 30 minutes and observed that the surfaces of the diamonds which were previously very smooth became covered with irregular oval and hemispherical cavities, due to the presence of oxygen in the fuse. The etch pattern obtained by Luzy did not reveal any crystallographic symmetry.

Another series of experiments on diamond etching was performed by Fersmann and Goldschmidt (1911). They tried to explain the presence of naturally occurring triangular cavities (the so-called trigons) on the octahedral faces of natural diamonds, on the basis of an etch mechanism. They etched diamonds with natural growth and cleavage faces in KNO_3 and soda fluxes at 900°C for a few hours. They did not study the pattern in detail.

Sutton (1928) etched diamond octahedra with KNO_3 at 900°C and obtained roughly circular and equilateral triangular cavities on them. On etching dodecahedral faces he obtained boat-shaped features which he described as resembling chisel marks parallel to the shorter diagonal of the face. He also etched polished cubic faces and obtained concentric squares oriented in conformity to the face.

Williams (1932) studied the etch phenomenon in greater detail and provided some photographical records of the diamond surfaces. He obtained triangular cavities by heating diamonds at 900°C in fused KNO_3 for 2 hours, and observed that these cavities ranged from flat-bottomed to pyramidal. On prolonged etching he noted that the cavities overlap. On the whole, the cavities reflected the crystal symmetry. Williams stated that on heating the crystals no rounding of the corners or edges was observable.

Wilcock (1951) was the first to realise that the etching used in previous studies on diamonds was so heavy as to obscure much of the required detail, and he started etching the crystals at low temperatures from

200°C to 600°C in KNO_3. As the etch rate of diamonds is much too small at these temperatures, even the very sensitive multiple beam interferometry was not able to resolve much detail.

Tolansky and Omar (1953a) etched diamonds at temperatures ranging from 525°C to 625°C. They observed that in case of octahedral faces etching commenced at 525°C in the regions of ring cracks, micro-cracks and along the surface damages. They studied the surface with the help of multiple-beam interferometry and observed what looked like an etch spiral on (111) face of diamond.

Omar, Pandya and Tolansky (1954) performed more controlled experiments on the etching of diamonds with fused KNO_3 at temperatures starting from 500°C. During the course of their studies they observed that the surface flaws are etched preferentially. They divided the etch mechanism in the range 500°C to 700°C roughly in three stages. In the first stage there is preferential attack on ring cracks, cracks and other surface defects and large numbers of micro-pits are produced on the surface. They found that inside the trigons, the density

of pits is lower, possibly because there is lower density of dislocations in the regions. This would indicate that the trigons were growth features, since dislocations encourage growth. In the next stage at 575°C the etch pits increase in size, merge into one another and consequently decrease in number. The corners become rounded and various flat-bottomed pits result.

In the third and the final stage the whole of the original surface is eaten away and a block formation results. The blocks have planes which are mainly {212} and further etch develops {313}. Ultimately they tend to become {334}.

They have also described the mechanism of etching of trigons. How trigon-sides are etched preferentially leading to hexagons is shown.

Pandya and Tolansky (1954) extended the etch studies to polished cubic and dodecahedral faces. On the dodecahedral faces they obtained boat-shaped pits, while on cubic faces, square cavities in conformity with the face. In addition to pits on dodecahedral faces they also obtained a crystallographically oriented rectilinear pattern. This pattern was hexagonal and

revealed for the first time a laminar structure inside the body of the crystal. The rectilinear pattern was also observed on the cubic faces.

The results indicated that the laminae grew under differing growth conditions.

Emara and Tolansky (1957) after their extensive etch studies on dodecahedral faces reported that etch is most severe on the {110} faces.

Further studies were done by Tolansky and Patel (1957) and Patel and Tolansky (1957). According to them etch even starts at 475°C and rectilinear etch pits are produced. Above 500°C they observed that pits start rounding off. While etching matched cleavages Patel and Tolansky (1957) observed one to one correspondence of the etch pattern. They observed that the arrangement of pits exhibits etch laminae, indicating different temperature and pressure during formation.

Omar and Kenawi (1957) performed their etching experiments with gases. They etched diamonds on hot molybdenum filament at 1000°C in oxygen at $2 \cdot 5 \times 10^{-3}$ torr pressure. They claimed that pits so obtained were similar in all respects, except their orientation to the

natural features, trigons.

Further experiments on gas etching of diamonds were done by Frank and Puttick (1958). In an attempt to produce trigons they etched diamonds in monovalent radicals. Because the negative steps (steps bounding trigons) on the {111} faces are triply bonded, they thought that these radicals will be able to stabilize the steps and hence trigons which have negative orientation, will be formed. According to Frank et al. (1958), the doubly bonded steps are stabilized because of the favourable orientation of the free bonds to form carbon-oxygen complexes e.g. a c-o-c-o zig zag chain, such as is present in polyoxymethylene polymers of aldehyele.

This led them to attempt the etching of natural {111} faces with monovalent radicals such as hydrogen, halogen etc. But these attempts to etch diamonds in monovalent radicals were unsuccessful. Etching with wet H2 resulted in non-crystallographic pits. Etching with water vapour and chlorine at about 800^{o}C gave positive pits. Thus their experiments according to them were inconclusive. However, they claim to have produced negative pits of trigon orientation by heating diamonds

in fused kimberlite at about 1450°C.

The work of gas etching was further extended by Evans and Sauter (1961). They etched natural octahedral and dodecahedral faces and polished cubic faces at reduced pressure in air in the temperature range 800°C to 1400°C. They observed that as the temperature was increased, change in orientation of the pit took place. The pits on {100} and {110} faces changed their orientation at about 1400°C, while in the {111} faces the change occurred at 1000°C. In an attempt to find out which of the constituents of air are responsible for the etch pit formation, they subjected octahedra to various mixtures of gases found in nature. They concluded that oxygen and water vapour are the responsible reagents for pit formation. They also performed experiments with carbon dioxide and found that at about 900°C, CO_2 attacks diamonds heavily. They explained the change of orientation by mentioning the different stabilities at different temperatures of carbon-oxygen complexes, formed at the various steps.

Patel (1961) during his etch studies on diamond octahedra and cleavages classified the pits into three groups, flat-bottomed, terraced and point-bottomed.

According to him in the case of point-bottomed pits the dislocations which may be linear are not completely etched away, while in the case of flat-bottomed pits they are completely removed by the etch. The eccentricity observed in the case of flat-bottomed and point-bottomed pits was attributed to the inclination of these linear dislocations, which he calculated to be 70^{o} to the crystal surface.

Patel (1962) further described linear defects and point defects on the surface of the crystals. While etching $\{111\}$ surfaces, he obtained rod like and trapezium shape pits in addition to the normal triangular pits. In the advanced stage of etch these all are converted into triangular cavities. Patel and Ramanathan (1962) etched natural and cleavage octahedral faces and polished cubic faces in strong oxidising agents e.g. $KClO_3$, $KMNO_4$, $K_2Cr_0O_7$, $NaClO_4$, and the alkali halicles like KCl and KBr.

With these reagents they obtained pits of both orientations at different temperatures. According to them the higher kinetic energy of oxygen atoms from these reagents is responsible for the negative etch pit formation.

Seal (1962 c, d) studied the polished sections of diamonds from different origins. The etching was done in fused KNO_3. He found that many natural diamonds are very inhomogeneous in their internal structure. In the case of the section of dodecahedral crystals, Seal found that all the diamonds showed evidence of being dissolved at some stage in their geological history.

Seal (1962 c) suggested that there are indications of differences between the diamonds of different origins.

Harrison and Tolanksy (1964) applied the method of etch to reveal the growth history of diamond crystals. They studied diamond slabs by sawing and polishing diamond octahedra and subsequently subjecting them to a mild etch. Stratigraphic etch pattern was obtained on these sawn and polished {100} faces. The pattern revealed a lamella structure inside the crystals. It was suggested that laminae had different conditions of growth and hence different defect concentration which in turn leads to the difference in ultraviolet absorption properties. They found that the ultraviolet transparent type II laminae had nearly 1500 pits per square mm, while

the type I layers nearly 5 x 10^5 pits per square mm.

Seal (1965) extended this method of etch to sections of natural octahedra as well as synthetic diamonds. According to him nearly 67% of the natural diamonds show the stratigraphic patterns, indicating the layered growth on {111} planes. He concluded that growth is followed by dissolution and regrowth. Sometimes complex patterns are obtained due to segregation of impurities. He also confirmed the findings of Harrison and Tolansky (1964) that etch is more severe on type I layers than on type II layers. On the polished and etched cubic sections of synthetic diamonds stratigraphic patterns were found parallel to ⟨100⟩ and ⟨110⟩ directions, indicating that growth had taken place on other than {111} planes.

Evans and Phaal (1961) reported their experiments on the rate of oxidation of diamond single crystals. All low index faces were studied. It was found that in the pressure range 5 x 10^{-2} torr to 0·5 torr, the rate was linearly dependent on oxygen pressure. At about 650°C in the case of octahedral and dodecahedral faces, surface blackening due to carbon deposition was observed; in this range of pressure on the cubic faces surface

blackening appeared at 850°C. When the pressure was increased to atmospheric pressure, surface blackening appeared at higher temperatures; 700°C in the case of {110} and {111} faces. It was found that cubic faces etch at the slowest rate below 1000°C, while above 1000°C the reaction rate for all the faces was identical becoming maximum at 1050°C, and decreasing drastically above this. According to them blackening observed was not due to graphite formation, because at 0·4 torr pressure graphitisation does not take place below 1350°C. At about 1000°C the carbon layer becomes quite thick and thus the rate of etching is identical for all the faces because it is governed by the diffusion of oxygen atoms through the carbon layer.

Rudenko et al. (1965) reported the comparative etch studies with alkali-metal-hydroxides, carbonates, oxygen and carbon dioxide and water vapour.

According to them atmospheric oxygen is a very strong oxidising agent. At about 850°C it is 30 times stronger than CO_2 and 150 times stronger than water vapour. They suggested further that these salts just act as catalysts and do not take part in the reaction because the etch rate solely depends on the volume of incoming

air. They found that CO_2 is produced as a result of oxidation. At about 800°C they observed that in the case of water vapour and CO_2 etching, very rectilinear pits are produced.

Phaal (1965 a, b) extended the work reported by Evans and Phaal (1961). In this case the range of oxygen pressure investigated was from 10^{-2} torr to atmospheric pressure. He again found the surface blackening on all the low index faces at low pressure. As pressure was increased this surface blackening started appearing at higher temperature. Above 1·5 torr pressure, even at 700°C all the surfaces were clear of surface blackening.

He suggested that etch rate is given by the relation $R = KP^n$, where K is the rate constant depending on the temperature and particular face of crystal, R is the measured etch rate, P the pressure and n the order of reaction. At low pressure n = 1, while at high pressure n is equal to zero.

According to him above 1000°C the carbon layer thickness and thus the rate is governed by diffusion of O_2 through the carbon layer and hence it is identical for

all the faces. This is indicated by the change in the slope of the etch rate versus temperature curve, which shows that after reaching 1050°C etch rate starts decreasing suddenly. Thus the etch is not a simple conversion of diamond to CO and CO_2 but involves an intermediate process of carbon formation. The rate of etching depends on the oxidation of this carbon layer and also on its thickness. He emphasized the presence of surface carbon and the various carbon complexes in the temperature range 500 - 900°C. According to him the by-products of the reaction CO and CO_2 also affect the etch rate, and hence the etching is a very complex phenomenon. He suggested further that the stability of the carbon-oxygen complexes at positive and negative steps would be different. Knowing their stabilities the final shapes of the pits can be predicted. The complexes at the positive steps, where the atoms are doubly bonded, are more stable at lower temperature than the complexes on the triply bonded steps. Therefore the pits on the {111} faces are predicted as having a positive orientation. According to him this would follow from the observed experimental fact that {100} faces, which have doubly bonded atoms have the

slowest etch rate. Above 1000°C he observed the etch rate to be identical for all the low index faces and therefore he argued that the change in the orientation observed by Evans and Sauter (1961) was the result of the action of the by-products, carbon dioxide and not the temperature.

In addition to the experiments with the said gases, Phaal also etched diamond surfaces with various other gases: H_2, Cl_2, Br_2, HCl etc. upto 1400°C and found that none of these gases, except H_2 in presence of metal catalyst such as Fe, attacked diamonds. In the case of cubic faces, he observed pits forming arrays in $\langle 100 \rangle$ directions. He noted further a reversal in etch pit orientation at about 1350°C with CO_2.

Patel and Agarwal (1966 b) observed that in the case of natural diamond crystals etch rate is fastest on $\{111\}$ faces, intermediate on $\{110\}$ faces slowest on $\{100\}$ faces. In the case of synthetic diamonds Patel and Ramachandran (1968 b) found similar results.

Patel and Patel (1968 b, 1968) etched diamonds by heating in a carbon arc and subsequently treating with $NaNO_2$ solution. Having observed pits of both orientations

on natural {111} faces, they concluded that the 'trigons' - the naturally occurring triangular cavities - are the result of natural dissolution. They applied the same technique to etch natural cubic faces (1968 b) and suggested that "quadrons" - the naturally occurring square cavities - reduce in size and no new pits nucleate. However they were unable to produce quadron-like features by their method of etching.

Patel and Patel (1971) applied the same method to synthetic diamonds and claim to have produced trigon patterns on the octahedral faces of the crystals while Patel and Ramanathan (1964), etched octahedral cleavages of natural diamonds in $NaClO_4$ at 850°C. They obtained triangular pits of both orientation, and some hexagonal pits. They suggested that the difference in the dislocation energies is responsible for producing the pits of both orientations simultaneously. According to them, because the energy of the oxidising atoms is constant at a particular temperature, the difference in the energy of the carbon atoms at the sites of dislocations and away from them, would produce etch pits having boundaries in different orientation.

Patel and Goswami (1963) etched G.E.C. synthetics with $KClO_3$ and KNO_3. They suggested that in the case of cleavages of synthetic diamonds, the change of orientation takes place at higher temperature and therefore the synthetic diamonds are more resistant to etch as compared with the natural diamonds. Their findings conflict with the findings of the present investigation. During the present work it has been observed that the synthetic diamonds etch faster than natural diamonds. Patel and Goswami however observed that the etch pits on the synthetic diamonds have more rectilinear boundaries compared to the boundaries of the pits on natural faces. Similar results were observed during the present studies.

Sappox and Boehm (1968) studied the formation and properties of surface oxides in the case of etching diamond powder. According to their infrared studies they found that the amount of chemisorbed oxygen increases from 25° to 420°C while carbon dioxide is evolved as a result.

Karklina and Maslakovets (1969) studied comparative etch rates with sodium and potassium nitrates, hydroxides and oxides. They observed that etch rate

varies exponentially with temperature in the range 560°C to 700°C. Having observed the same activation energy as that of etching of diamond with air, they concluded that any of the above salts do not have any effect on diamond below 880°C, and that the mechanism of etching is the same as in air. Their results are in agreement with the views of Rudenko and Kulakova (1965).

So far the etching experiments were done by fused alkalies or strong oxidising agents and gases, but Murphy and Ritter (1970) tried to etch diamond surfaces with laser and electron beams.* They subjected freshly cleaved diamonds to a 100 KeV electron-beam. Etch pits having positive orientation were observed. Some of the pits were seen to have spiral shape. Electron microscopic studies revealed various complexes and intermediate products formed during the process. It was found that oxygen is chemisorbed even at room temperature. The amount of absorbed oxygen increases until the temperature is 400 - 500°C and carbon-oxygen complexes are formed. The energy of absorption of oxygen was found to be equal

* Though it seems impossible to estimate real temperature of interaction in case of (1) electron impact (2) laser impact

to that of formation of carbon dioxide. They observed these complexes to be converted into gaseous oxides at about 500°C and found that carbon dioxide so produced starts reacting with the surface at about 650°C.

CHAPTER 7

EXPERIMENTAL TECHNIQUES

In this chapter different optical and electron optical techniques employed during the present investigation are discussed. The techniques used are two-beam interferometry, multiple-beam interferometry, light profile microscopy, phase-contrast microscopy and electron microscopy.

7.1 Interferometry

The contour map of a surface using two-beam fringes was first studied by Fizeau (1862). Siegbahn (1932) for the first time used this technique to study the surface topography of crystals. Two-beam interferometry is a very powerful and easy technique, so far as the microscopical studies of the surfaces are concerned. The two-beam fringes produced between the crystal and glass slide represent the contour map of the surfaces. Each fringe shows the change in height or depth of $\lambda/2$, whilst changes of 1/15th or 1/10th order can be detected. Thus the features of height or depth of approximating a few hundred angstroms can be distinguished. The two-

beam interference pattern enhances the contrast to a great extent. In order to be useful, there should be several fringes in the field of view, which implies a higher wedge angle at higher magnification. The intensity distribution in the two-beam fringes follows a $\cos^2$ law, such that the light and dark parts are equal in width. Thus it scans much more area compared to the multiple-beam fringes. Kayser (1944) was the first to apply interference method to diamond surfaces.

7.2 Multiple-Beam Interferometry

Multiple-beam interferometry instead of two-beams has led to very important advances. Multiple-beam means to employ succession of coherent beams all in specially related phase and intensity. This is achieved by increasing the reflectivity of the surface. Boulouch (1893) realizing the significance of this pointed out that a profound change in appearance of the interference fringes takes place when the coefficient of reflectivity is increased.

Airy's Formula

The theory of multiple-beam fringes was given

by Airy (1831). Figure 7.1 shows two parallel surfaces A and B separated by a distance 't'. If R and T are the coefficients of reflection and transmission respectively for the two surfaces, then Airy's summation in the transmitted system is given by the formula:

$$I_T = \frac{T^2}{(1-R)^2} \quad \frac{1}{1 + \frac{4R}{(1-R)^2}} \quad \mathrm{Sin}^2 \quad \delta/2 \quad - \quad (1)$$

Where $\delta = \frac{2\pi}{\lambda} \cdot 2\mu t \cos \phi$, ϕ being the angle at which the light is incident on the system. μ is the refractive index of the medium enclosed between the parallel plates separated by 't'. In the case of air μ is equal to 1.

The equation indicates that the intensity distribution is not a Cos^2 function. In the absence of absorption

$$I_{max} = \frac{T^2}{(1-R)^2} = 1 \quad - \quad (2)$$

The intensity minima $I_{min} = \frac{(1-R)^2}{(1+R)^2}$

The fringe shape is independent of T and determined by reflectivity R only.

In (1897) Fabry and Perot developed their multiple-beam interferometer consisting of two silvered plane parallel plates. They also attempted this technique to wedge consisting of silvered planes, but they did not

realize the necessary conditions to produce sharp fringes. Tolansky (1946) was the first to analyze the conditions necessary for the wedge fringes which are described briefly below.

Figure (7.2) illustrates the intensity distribution in multiple-beam fringes.

7.3 Effect of Absorption

It was long recognized that any absorption in the silver film will reduce the intensity of the transmitted system, but it was not until 1946 when Tolansky showed that absorption has a much more pronounced effect. Whenever there is absorption the total intensity distribution is affected through the transmitted fringe shape remains the same. The equation (1) gives the intensity distribution in case of the transmitted system for the interferometer consisting of two silvered parallel plates. The equation can be written as

$$I_T = \left(\frac{T^2}{1-R}\right)^2 \cdot \frac{1}{1+F} \sin^2 \delta/2 \quad \text{where } F = \frac{4R}{(1-R)^2}$$

F is called the coefficient of fineness, since it determines the fringe shape. If A is the fraction of

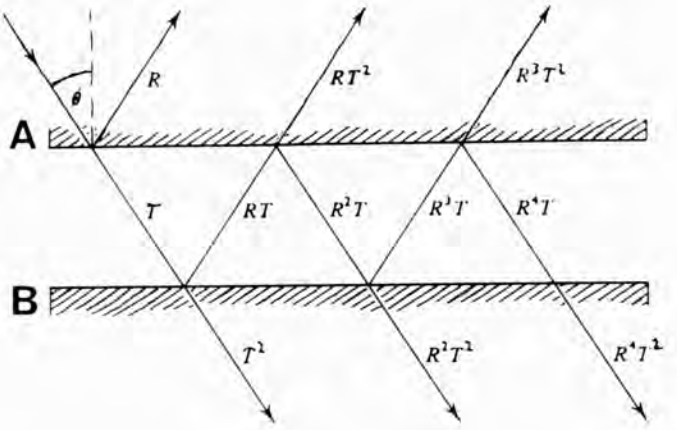

Figure 7.1.

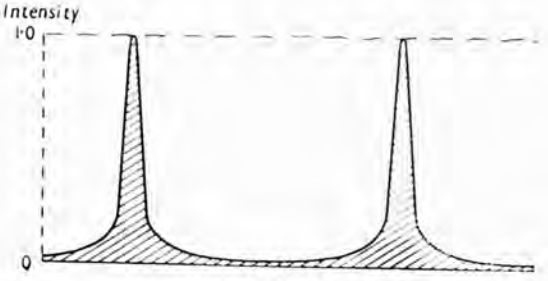

Figure 7.2.

light absorbed at each silver film, then $T^1 + R + A = 1$

and $\left(\frac{T^1}{1-R}\right)^2$ will become $\left(\frac{1}{1 + \frac{A}{T^1}}\right)^2 = k$ (say)

This means that the whole pattern is reduced in intensity by the factor k. Figure 7.3 shows the effect of absorption on the fringe system. In the reflected system since $T^1 < T$, the minima does not go down to zero and hence the visibility is poor (Tolansky 1954).

The important difference between the parallel system and wedge system is that, in the former the phase difference, between the successive reflected beams is constant, whereas in the latter it alters progressively with the order of reflection. Considering the two plates inclined at an angle θ, (figure 7.4) it is clear that the phase difference between the successive beams is not constant.

7.4 Phase Condition

Tolansky (1946) has given a simple method for finding the path difference between the first and the n^{th} beam in the case of a wedge. The retardation lag behind the arithmetical value for the n^{th} beam is given by

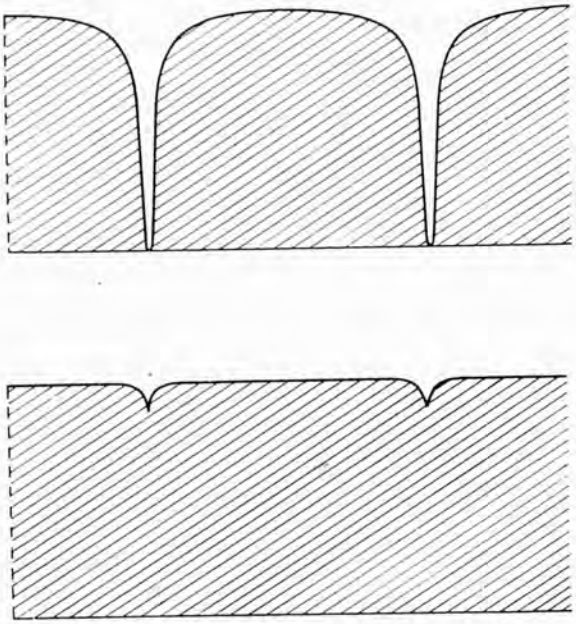

Figure 7.3.

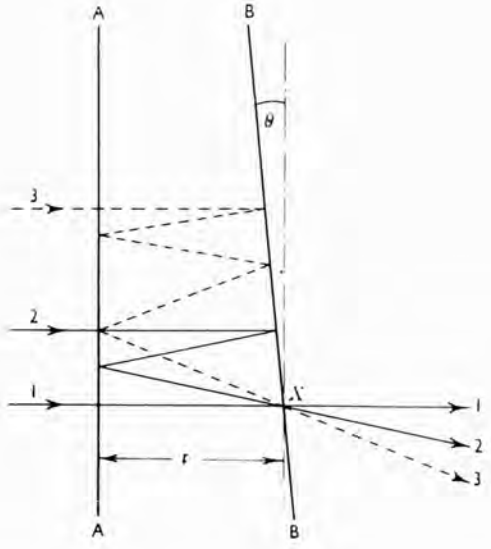

Figure 7.4.

$$2\frac{\eta}{\delta}(2n^2 + 1)\theta^2 t$$

as shown in the figure 7.5, Where 't' is the thickness of the air gap. From this equation this is clear that higher orders get out of step with the first beam and no longer assist the Airy summation. Indeed when the retardation is $\lambda/2$, such a beam tends to destroy the condition of sharpness. If 'n' is high enough, then the expression reduces to the form

$$4/3\ n^3\theta^2 t.$$

In the case of n = 60, $\lambda = 5{\cdot}46 \times 10^{-5}$ cm and in the case of 10 fringes/cm the value of 't' should be of the order of $1{\cdot}2 \times 10^{-3}$ cm. Hence in the case of wedge fringes, the separation between the two surfaces must be as small as possible.

7.5 Linear Displacement of the Beam

The magnitude of the phase lag effect is dependent upon the linear displacement of the successive beams. The linear displacement is not only dependent on θ, the wedge angle, but also upon the angle of incidence if it is other than normal. It is essential

to view interference from beams which have scanned as small an area as possible if confusion due to beams from different topographical features meeting at arbitrary point is not to occur (Tolansky 1948).

The linear separation between the first and n^{th} beam is approximately

$$dn = 2n^2 t\theta$$

If X is the number of fringes/cm, then $\theta = \frac{X\lambda}{2}$.
If X = 10 fringes per cm. and t = 1/1000 mm; as is desirable for the phase condition, then 60^{th} beam comes from a region only 1/400 mm. away from the first beam. Thus all the relevant beams come from a region which is within the resolving limit of a low-power microscope. It is therefore clear that the value of t required is substantially the same as that necessitated by the phase condition.

7.6 Errors in Collimation

Fabry (1922) was first to realize the fringe broadening due to lack of parallelism in the incident beam.

For normal incidence, $n = \frac{2t}{\lambda}$.

For the incidence at an angle ϕ, this diminishes to

$$n - \delta n = \frac{2t \cos \phi}{\lambda}$$

Calculating δn in terms of ϕ,

$$\phi = \left(\frac{\lambda \delta n}{t}\right)^{\frac{1}{2}}$$

The fringes usually have a half width of about $1/40^{th}$ order, and if the fringes are not to be increased in width by more than a fifth of this, $\delta n = 1/200$, giving for $\lambda = 5 \times 10^{-5}$ cm.

$$\phi = \frac{5 \times 10^{-4}}{\sqrt{t}} \text{ radians} = \frac{3 \times 10^{-2}}{\sqrt{t}} \text{ degree.}$$

This shows that the accuracy of parallelism is directly dependent on the separation 't', the stop diameter is also critical.

Summarising the discussion, the following conditions are necessary for sharp multiple-beam fringes (Tolansky 1948).

(1) The surface should be coated with highly reflecting film of minimum absorption.

(2) The thickness of the film should be very uniform.

(3) Monochromatic light should be used.

(4) The interfering surfaces should be very close, few wave-lengths approximately.

(5) The incidence should be normal.

(6) A parallel beam should be used, divergence should not exceed from 1^{o} to 3^{o}.

Multiple-beam technique is a very sensitive and delicate technique; the height changes of the order of few angstroms can be detected and measured accurately. Figure 7.6 shows polishing marks on a cube section of a natural diamond crystal. The fringe deviation definitely enables the estimation of the height changes of the order of few angstroms.

7.7 Light Profile Microscopy

This technique was introduced by Tolansky (1952) for the estimation of height and depth of various surface features during the microtopographical survey of the surfaces, particularly when the structure is coarse from the interferometric point of view. The method is an improvement over Schmaltz's light cut method.

Figure 7.7 indicates the experimental set up. A is a monochromatic source which sends light through the

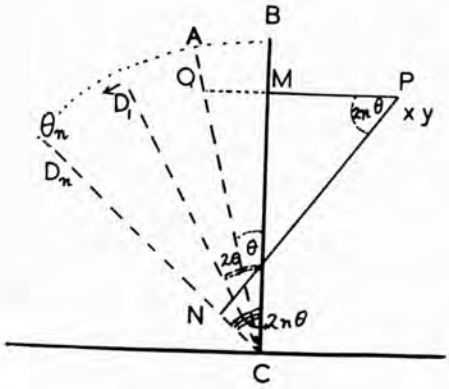

Figure 7.5.

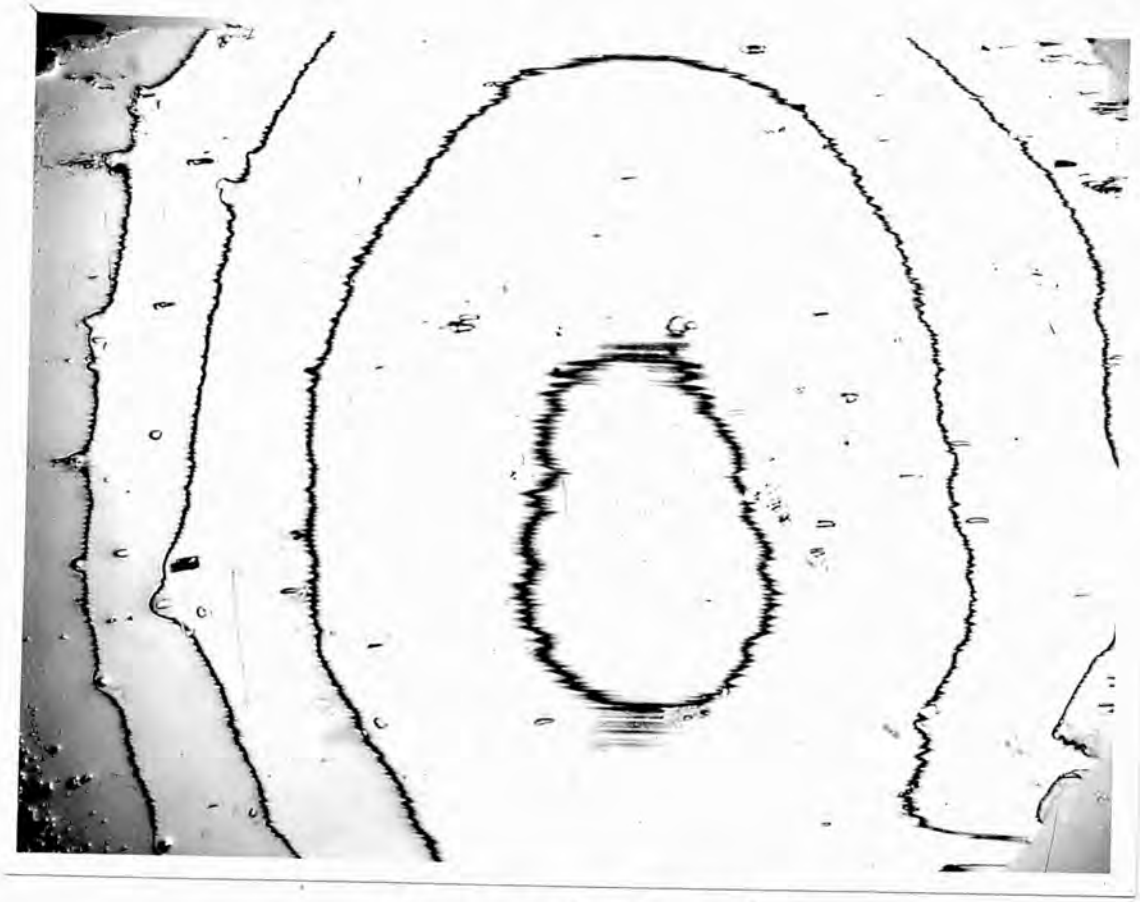

Figure 7.6. (X 100)

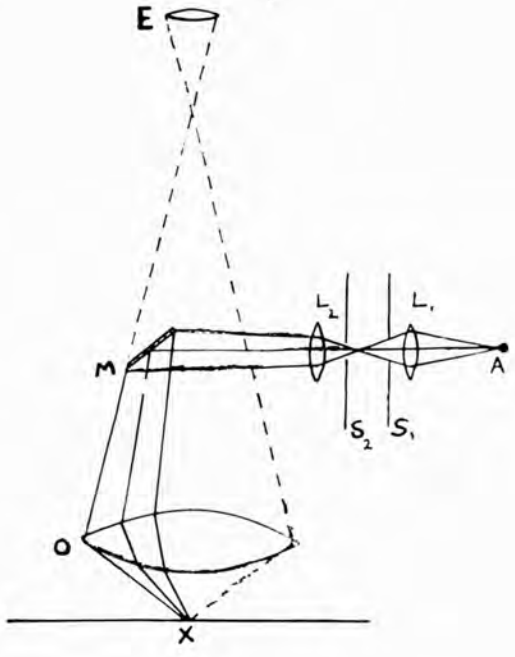

Figure 7.7.

condenser lens L& field iris S_2. The profile which can be a fine wire, a hair, a scratch or an etch line on glass, is placed nearby S_2. M is a metal tongue reflector which sends an off-centred pencil as shown in the diagram. The surface to be studied is placed at X, and the microscope is adjusted to get a very well focussed image of the surface at E. The profile is then inserted near S_2 and is moved forward and backward so that it is well focussed and a sharp image is formed on the surface.

Tolansky has shown that the profile magnification

$$M_1 = 2M \cdot \frac{\tan i}{n}$$

Where M is the linear magnification of the microscope, n is the refractive index of the medium in which the surface is immersed and i is the angle of incidence of the off-centred pencil.

In the above expression

$$\frac{M_1}{M} = \frac{2\tan i}{n} = R \text{ (Lens Constant)}$$

and this is constant for a particular objective. The values of R used with the microscope in this laboratory have been obtained by Tolansky and it is 0·56 in case of 8 mm objective used for the value of $i = 15{\cdot}5^{\circ}$.

The technique is simple and it is useful for the coarser surfaces. The resolution of the order of 0·25 micron can be secured.

The height or depth of the feature is given by

$$h = \frac{\text{Shift on the plate}}{\text{Lens constant RX Magnification M}}$$

7.8 Phase-Contrast Microscopy

The phase-contrast microscope, which is due to Zernicke (1934) is essentially an interference microscope, in which interference is so contrived that no fringes are produced, but the areas on the specimen of different level appear in the image as areas of different brightness so long as they are not too large.

Theory - Figure (7.8) shows that if the object X is an amplitude grating the vectors (full-line) of object, Fraunhofer diffraction spectra and image will be as shown in figure 7.8(a). If the grating is now moved by half a pitch the vectors of spectra changes by π, since superposition of the two cases, i.e. removal of the grating, causes the disappearance of spectra. The dotted lines represent these changed vectors.

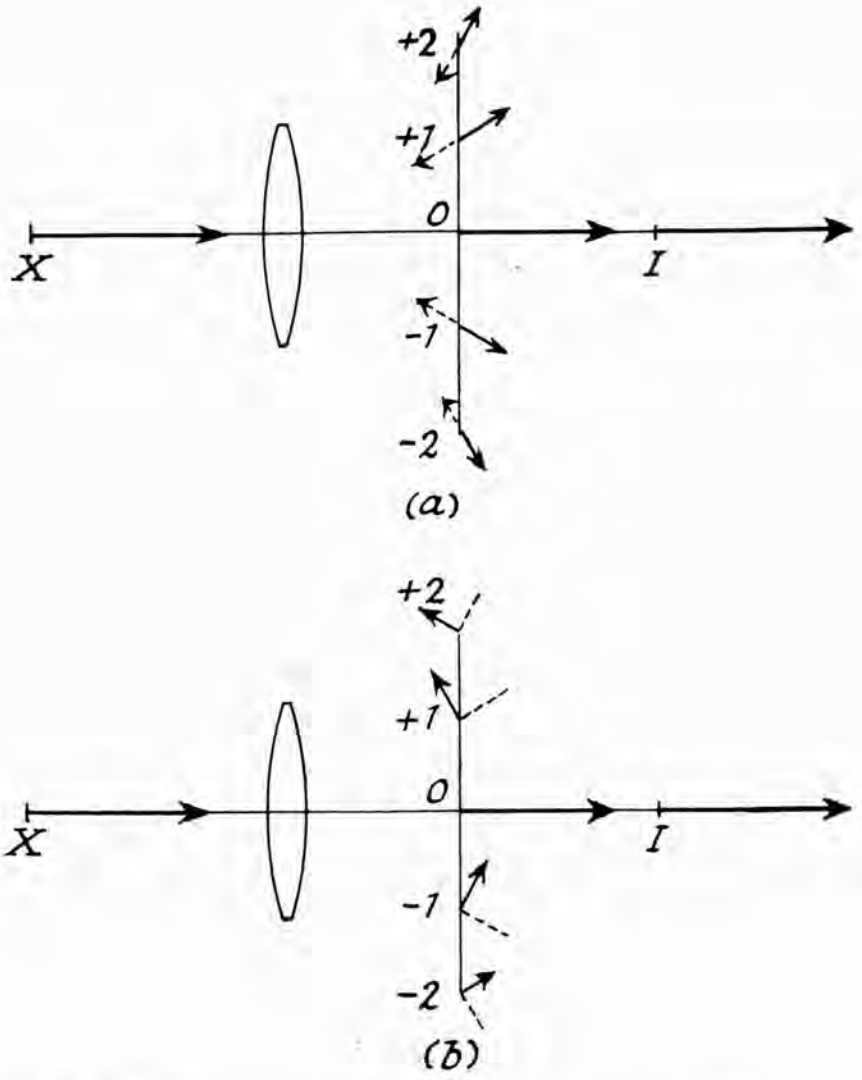

Fig. 7, 8. Distribution of light between different diffraction orders (zero, first and second) in back focal plane of objective: (*a*) amplitude object; (*b*) phase object.

If the object is not amplitude grating, but composed of strips of slightly different refractive index, it produces small phase differences without changes in amplitude. If this object is considered as a summation of two gratings displaced relatively one half pitch, then there is not complete cancellation of vectors for the higher order Fraunhofer spectra as these are not exactly anti-phase. Instead there are small resultants about $\pi/2$ to the phase of those for an amplitude grating as shown in the figure 7.8 (b). Evidently the components of the symmetrically opposite parts of the higher order Fraunhofer diffraction images in the direction of zero order diffraction image cancel, and cannot contribute to image formation. It will be noted that the components at right angles to the zero order diffraction image do have a resultant. Therefore it is possible to obtain an image if the zero order diffraction image is: (1) suppressed by a suitable stop or (2) suitably weakened and either advanced or retarded in phase by $\pi/2$. The effect of the latter is that the intensity of the zero order diffraction image is reduced to about the same level as that of the diffraction images of higher order, and its phase is shifted to be approximately in phase or

π out of phase with that of the latter. Result is that the reinforcement or cancellation occurs. As the intensity of the diffraction images of higher order than zero depend upon the phase differences produced by the specimen, the image intensity at any point is a function of the phase difference at the corresponding point on the specimen surface and therefore of the height of this point on the surface relative to adjacent parts of the surface. When the zero order diffraction image is advanced in phase the so-called 'positive' phase contrast is produced, in which surface elevations appear brighter and depressions darker; if zero order diffraction image is retarded in phase, 'negative' phase contrast is produced, giving the reverse effect.

Practical arrangement -

The normal modifications required to convert a normal microscope to phase-contrast are shown in figure (7.9). They involve the addition of (i) a stop A and (ii) a phase plate B or (C). The stop is so positioned that its image, after reflection at the specimen, falls on the phase plate, which carries a phase advancing or retarding step of shape and size identical with that of zero order image of the stop A;

stop is also made to absorb a proportion (e.g. 80 per cent) of the intensity of the zero order image. Annular stops and plates are usually used with a mean radius of $\frac{1}{2}$ or 2/3 of the full aperture and a width 1/15 of the full aperture. A series of interchangeable phase plates of different degrees of absorption and phase shift can be mounted in a single glass strip that can be moved to located positions.

7.9 Electron Microscopy

Although the vertical resolution of multiple-beam interferometry is very high and height changes of the order of 10 angstroms can be measured (Tolansky 1960), the lateral resolution is necessarily limited by the optical microscopy. Thus for the detailed surface topographical studies, electron-microscopy is a useful supplement.

For the study of the crystal surfaces by electron-microscopy, surface replicas must be prepared. The replicas are thin films of electron transparent material, corresponding exactly to the topography of the surface. The first replication was done by Mahl (1940 a,b). He used collodion to reproduce the surface structure. For

the best results the replica should have the following characteristics.

(a) It should faithfully reproduce the surface details.

(b) It should retain the details when stripped.

(c) It should itself contain no structure down to the resolution of the microscope.

(d) It should give adequate contrast for the various surface details.

A number of different materials are used in the manufacture of replicas but each requires its own particular specimen preparation technique. The choice of the material depends upon, whether it is to be used to prepare a preliminary impression of the specimen, from which the final replica is to be made (the two stage), or whether the material is to form the final replica (the single stage). Different materials used, fulfil different conditions and requirements (Kay 1965).

Plastic replicas using collodion, form-var, methacrylates, polystyrene or cellulose compounds, adequately fulfil the conditions (a) and (b) but do not stand up well to the other conditions.

Metal replicas using evaporated metals like silver, aluminium etc. are satisfactory for the conditions

(a), (b) and (d) but fail to fulfil (c). The two stage plastic-carbon replicas give good results but lack rigidity and contrast. Oxide replicas using silicon monoxide also lack contrast.

In addition to the above conditions the final replicas must be sufficiently strong to be self-supporting and must be resistant to the electron bombardment. Plastic replicas sometimes charge up during bombardment. This problem is overcome by coating the plastic replica with carbon, which makes it conducting.

Ultimately the choice of the final replica depends upon the size, shape, solubility of the specimen and also on the surface structure of the specimen and finally on the resolution desired.

Carbon replicas were found to be the most suitable for the present work. Carbon replicas are usually 200Å to 500Å thick films of spectroscopically pure carbon evaporated under high vacua, 10^{-5} torr so as to conform, strictly to the surface structure. Carbon is evaporated by passing alternating (30 V 60 A) current through the points of two carbon rods, lightly pressed together. The best working distance is about 3 to 10 cms and the thickness can be estimated by comparing the

colouration produced on the white porcelain with a neighbouring area of porcelain protected by a drop of oil.

7.10 Shadow Casting

As mentioned above the carbon replicas lack contrast. In order to overcome this carbon can be evaporated at an angle, but because of the transparency of carbon film, the contrast is not all that good. Moreover, an excessively thick film will produce geometric distortion by piling up of material on the side facing the source. According to Bradley (1954), sharp shadows can never be obtained in this method of self-shadowing. It therefore is necessary that material of high electron scattering power, e.g. palladium, gold-palladium, platinum, uranium and few oxides of tungsten, be used for the shadow-casting. The shadowing layer must have least possible self-structure, and one of the best combination from this point of view is platinum/carbon. Platinum/carbon has the further advantage that the final replica can be made from the shadowing material itself (Bradley 1959). Platinum/carbon shadow-casting using composite platinum/carbon electrodes is capable of

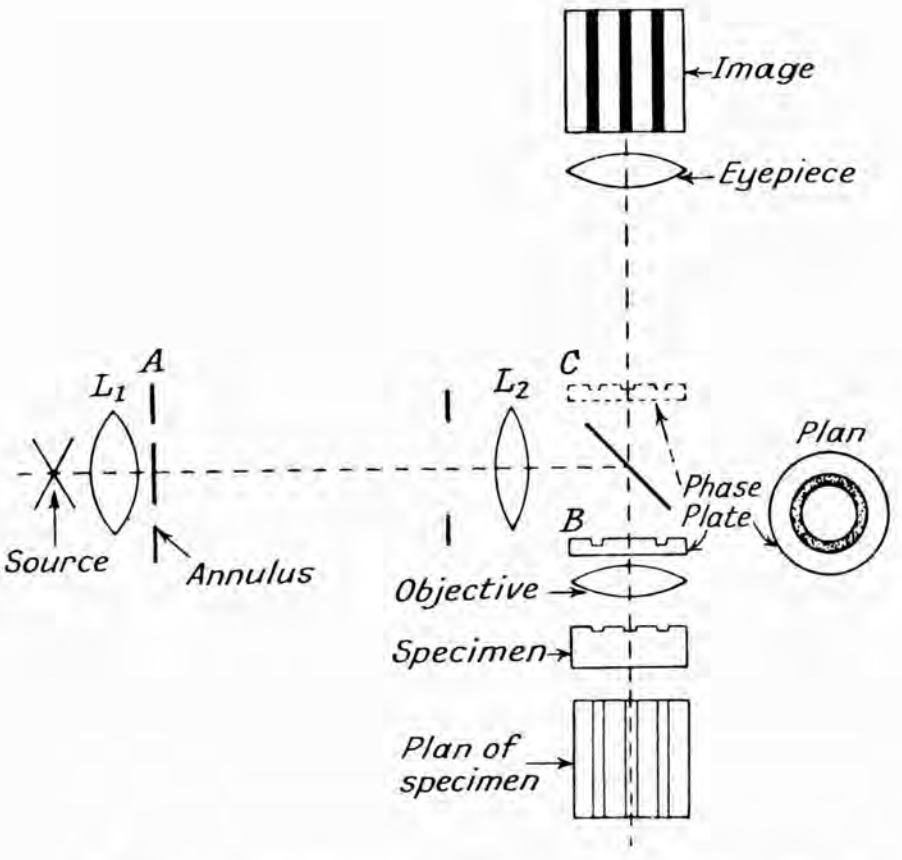

Fig. 7, 9. Arrangement of phase-contrast microscope.

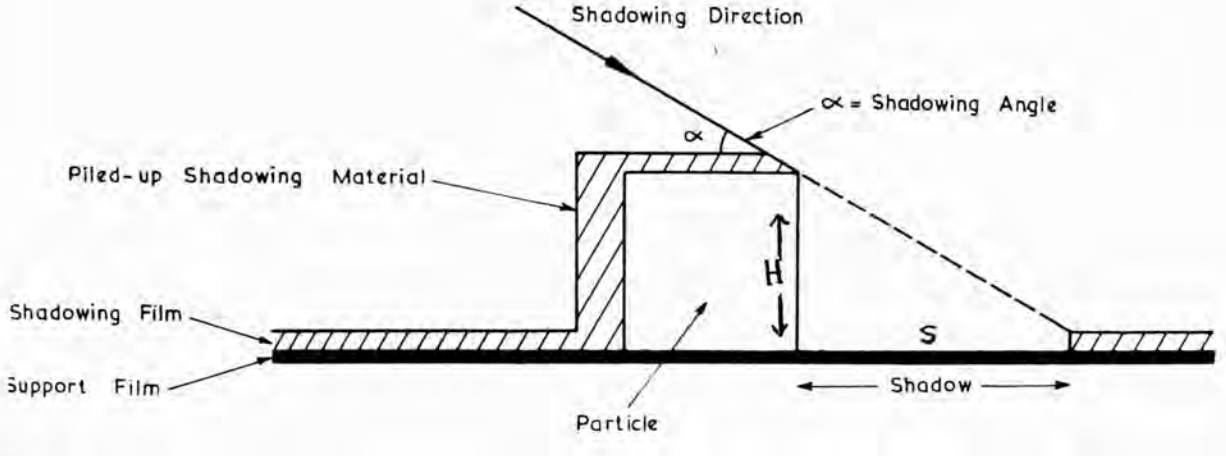

Figure 7.10.

Diagrammatic representation of a shadowed particle.

producing resolution of the order of 10Å.

In addition the illuminating system of the electron-microscope produces an electron beam, the intensity of which differs, so that the platinum/carbon rods of varying composition can be required, according to the type of instrument used. In that case platinum-on-carbon catalyst pellets can be used, (Kranitz and Seal 1962) and hence the platinum/carbon composition can be varied. However in the present investigation the platinum/carbon rods supplied by Polaron Instrument Company were used and they were found to be satisfactory. By using the method of shadow casting with platinum/carbon electrodes, not only the contrast is enhanced but the step height of the order of 50Å were satisfactorily measured. As shown in the figure 7.10 if S is the width of the shadow, M is the magnification of the microscope, the step height H is given by

$$H = \frac{S}{M} \tan \alpha$$

where α is the angle of shadowing. Recently many techniques have been developed for the replication of various types of specimen (Kay 1965) depending on the extent, shape and the nature of the surface.

Diamond surfaces, because of their insolubility

and chemical inertness under ordinary conditions require special techniques. Various techniques can be applied depending further on the size and shape of the crystallites. Whenever possible it is more satisfactory to use a single stage procedure, it usually requires the destruction of the specimen, usually by solution. Since diamond is insoluble, under normal conditions, the single stage replication is very difficult. This is one of the reasons that very little replication work has been done on diamond surfaces so far.

Eckert (1968) studied the mechanism of wear of natural and synthetic diamonds in grinding wheels and drilling crowns and saws. The replication was done using water soluble carboxymethyl cellulose (Cellofas B-50) solution. He prepared a film of this water soluble plastic by dissolving it in water and spreading on a glass slide. This film when dried was moistened very slightly just before the crystal was pressed on it. The crystal was then removed when the plastic had hardened. This technique limits the size of the crystal to be studied, moreover the removal of the crystal from the dry plastic mechanically might affect the surface impressions produced.

Bartoshinskii and Makorov (1967) were able to get replicas of Russian synthetic diamonds by mounting them in polystyrene.

Patel and Patel (1967c) prepared carbon replicas of diamond surfaces by evaporating an intermediate layer of NaCl.

Diamond studies using electron microscopy are meagre compared to what has been done by conventional microscopy.

In order to study the surfaces of the Du-Pont diamonds which are nearly 30 microns in size, a replica technique was developed during the present work. These diamonds are particularly well suited for use as lapping or polishing compounds. The particles are exceedingly small in size and need very careful replication. To make a single stage replication of these particles is very difficult, but after various trials a single stage technique was developed (Miller and Punglia 1970). The single stage technique is preferred to the multi-stage process because any additional operation in the replica increases the likelihood of artefacts and loss of resolution. For studying such particles two stage replication is usually used (Tuerb 1968), by partly

embedding the crystals in formvar for example, and then finally it is replicated by cellulose acetate.

Actually during the present studies it was possible to make single stage replicas for these particles, using direct platinum/carbon evaporation.

7.11 A Single Stage Replica Technique for Electron Microscopy of the Micro-Diamond Surfaces

A piece of acetyl cellulose film, 0·034 mm thick (Biodon R.F.A.; Polaron Instrument Ltd.), is moistened with methyl acetate and placed on a glass microscope slide. The micro-diamonds are sprinkled on the film as shown in the diagram (figure 7.11 S_b) and then it is covered by another glass slide which is held in position by clips and kept at 80°C for 30 minutes. This partly embeds the crystals and prevents the film from curling during subsequent evaporation. The upper slide is then removed and the film and diamonds are subjected to platinum/carbon evaporation in vacuum in the usual manner. The plastic/crystallites/Pt-c composite is shown in figure 7.11 (S_c). It is then stripped from its glass slide and placed, Platinum/carbon downwards, on to another glass slide which has just been dipped into paraffin

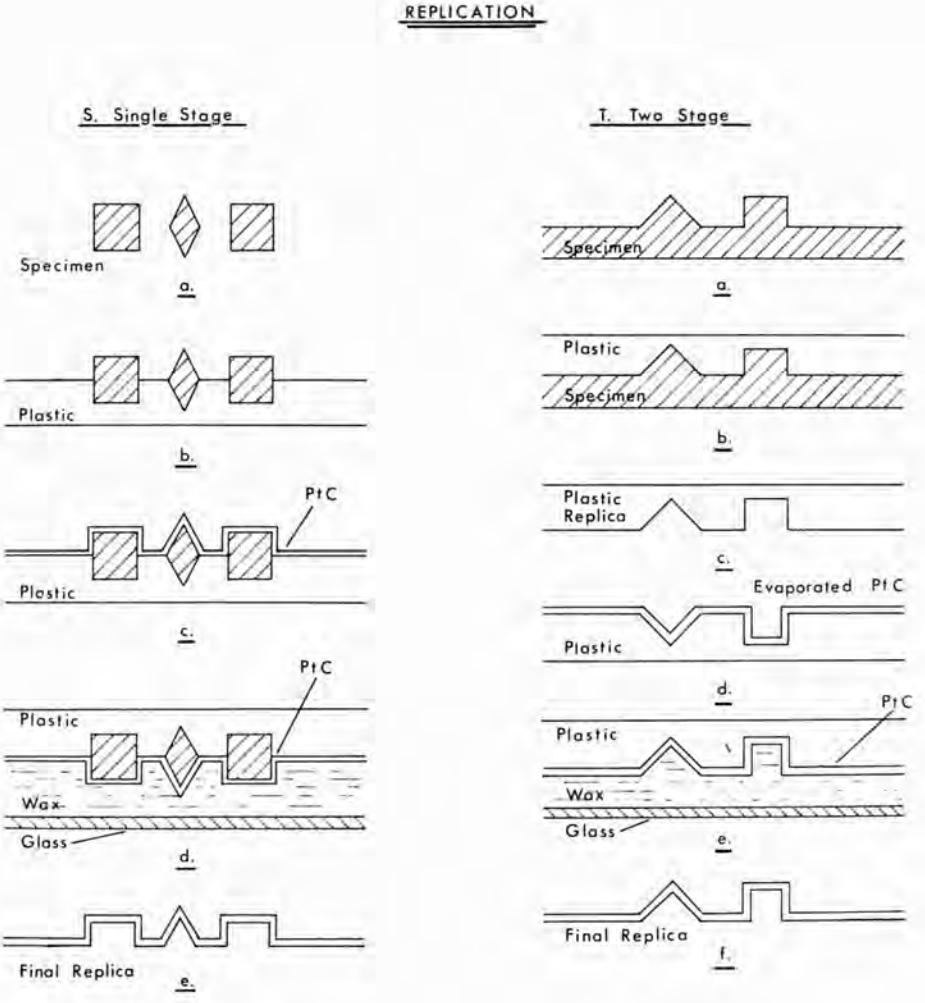
REPLICATION
S. Single Stage
Specimen
a.
Plastic
b.
Pt C
Plastic
c.
Pt C
Plastic
Wax
Glass
d.
Final Replica
e.
T. Two Stage
Specimen
a.
Plastic
Specimen
b.
Plastic
Replica
c.
Evaporated Pt C
Plastic
d.
Pt C
Plastic
Wax
Glass
e.
Final Replica
f.

Figure 7.11.

wax (M.P. 65°C). It is shown in the figure 7.11 (S_d). The whole is now placed in methyl acetate at room temperature to dissolve the plastic. The slide is then transferred to another dish of methyl acetate which is gradually brought to 50°C, at which temperature wax rapidly dissolves and releases the platinum/carbon replica together with crystals. At this stage the replica curls and flexes, releasing the crystals which collect at the bottom of the dish. After repeated washings in fresh methyl acetate, the replica is transferred to an acetone bath and then to distilled water, where it floats on the surface and is stretched flat by surface tension. This also removes the crystallites sticking to the replica. The replicas may then be picked up and mounted for examination.

The technique is non-destructive and can be equally used for other minerals provided they are insoluble in methyl acetate. Moreover there is no intermediate soluble layer evaporated on the crystals which can increase the possibility of artefact and loss of resolution.

The technique progressively becomes less successful for the particle size greater than 100microns,

owing to the breakage of the replica at the crystal edges during the flexing process. Figures 7.12, 7.13, 7.14, 7.15, 7.16 and 7.17 show the various electron micrographs of such micro-crystals using this technique. These crystallites are about 20 to 40 microns in size. High resolution ($\lesssim 100\text{Å}$) of surface details is easily obtained. Figures 7.12 and 7.13 show the surfaces of the shock synthesized Du-Pont diamonds. Figures 7.14 and 7.17 show the particles of diamond grinding power. It is suprising to see the characteristic features on the particles which are extremely small and constitute a very fine powder. Figure 7.14 clearly shows the growth layers; while figure 7.15 shows perhaps a cleavage face. Figure 7.16 reveals various steps and these may be cleavage steps or the multiple slip line caused by mechanical stress or other reasons. Steps are clearly resolved and step heights $<100\text{Å}$ can be easily seen. Figure 7.17 also shows an interesting crystallographic pattern on the particle of size 20 - 40 microns. The figure probably indicates a portion of a crushed cubic face. The technique can therefore be used for studying crystallographic cleavage and abrasion properties of such crystals.

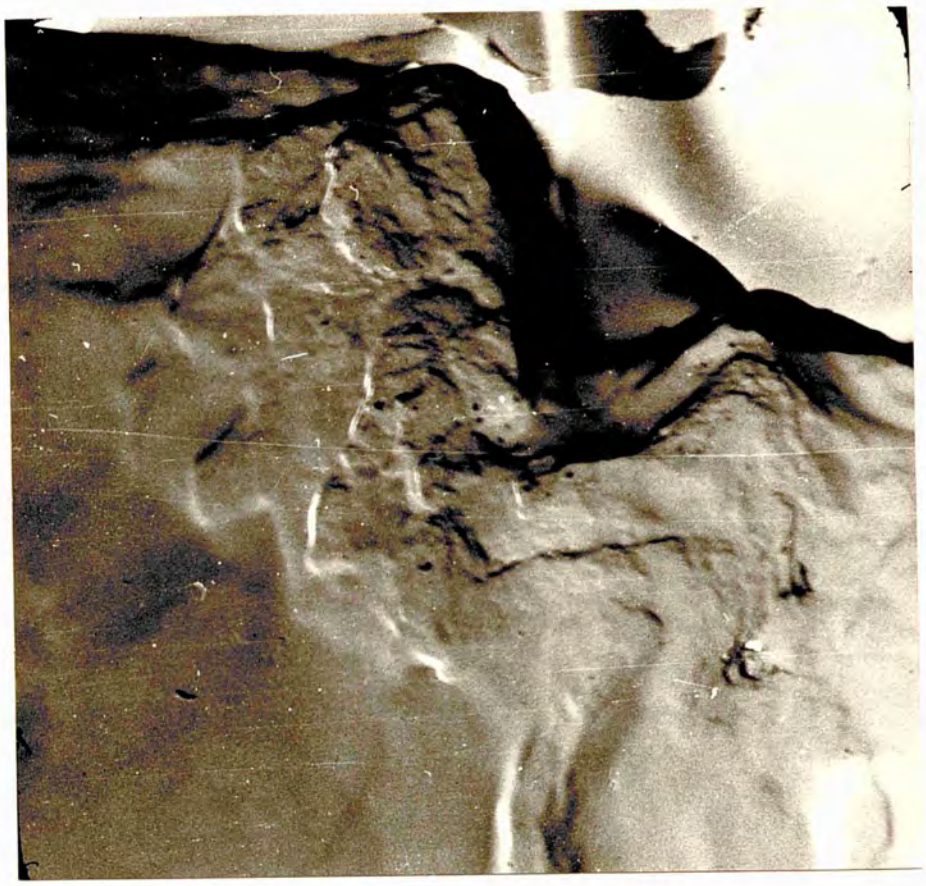

Figure 7.12. (X 10,000)

Figure 7.13. (X 10,000)

Figure 7.14. (X 10,000)

Figure 7.15. (X 10,000)

Figure 7.16. (X 10,000)

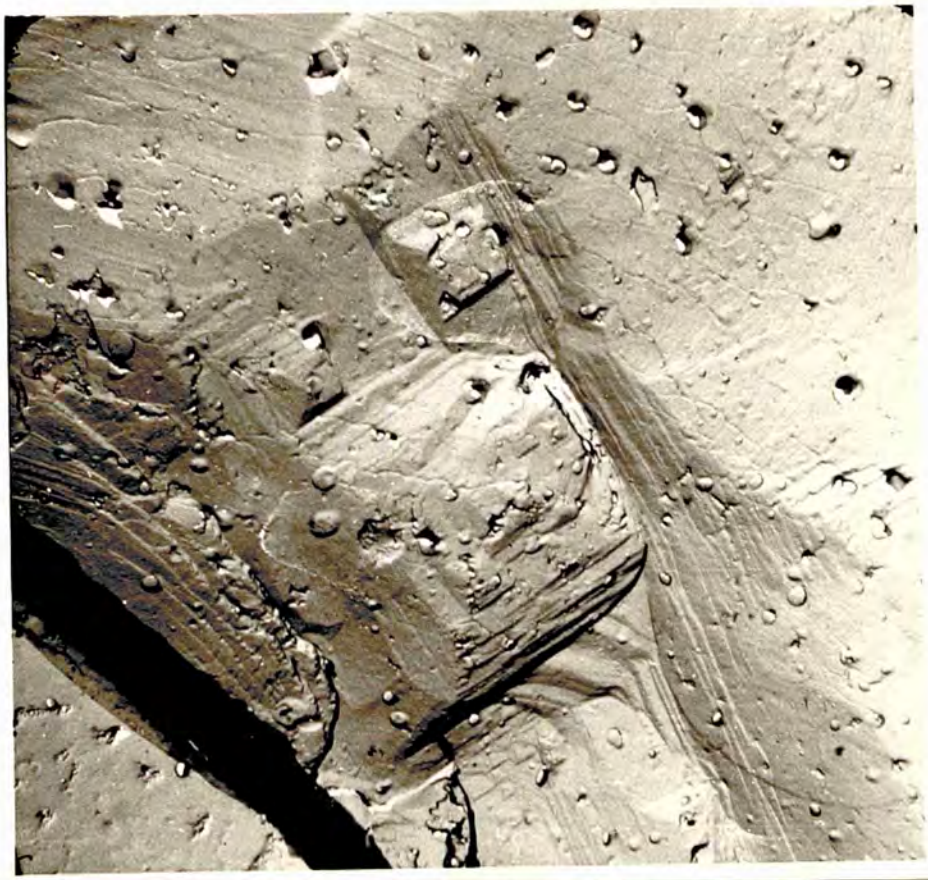

Figure 7.17. (X 10,000)

Figures 7.12 and 7.13 on the other hand show very rough looking surfaces of shock synthesized Du-Pont micro-crystals. Attempts were made to study the crystallographic properties of these crystals by the method of etching. Because the crystal is very tiny it was impossible to etch them in any liquid or solid reagents without losing them. The crystals were therefore etched by oxygen in a cylindrical oven. The crystals (in the form of fine powder) were placed in a quartz boat in a long quartz tube, which was just fitting in the cylindrical oven, and oxygen was passed through the tube. The oven was calibrated beforehand for the temperature distribution by a simple thermocouple. However it was difficult to control the etch parameter for the crystals of such a size and it was found difficult to etch the crystals satisfactorily to the desired extent for the replication work.

7.12 Replica Technique for De Beers Synthetic Diamonds of (1/5 to $\frac{1}{3}$ mm size) and Premier Mine Micro-diamonds

In order to study the surface topography of De Beers synthetic diamonds of 1/5 to $\frac{1}{3}$ mm size and also Premier Mine natural diamonds of 30 - 40 mesh size another

replica technique was developed.

The diamonds to be replicated were very small in size, the faces of the order of 10^{-4} sq. cm were to be replicated. In order to study the surfaces optically and electron-optically after making replicas, it was necessary to mount the crystals in a suitable medium. This should be insoluble in methyl acetate (which is used in replication process), but should be soluble in some other solvent, so that the crystal can be removed from the mount and can be re-examined on the other face. It was also necessary that the mounting material should soften when heated so that the crystal can be mounted with its face perfectly flat for the interferometric work. After investigation of many common materials, orange shellac (B.D.H.) was found to be the only suitable material. After mounting the crystals they are first cleaned with water and then by preliminary replication. The acetyl cellulose plastic film as described above is moistened in methyl acetate and placed and lightly pressed on the crystal surfaces, as shown in figure 7.11 (T,b). After the plastic dries off, it was stripped and placed on clean glass slide. As many as five to six replicas were taken at a time to ensure that fairly representative sample

is obtained. All of these replicas were pressed between two glass slides, which are held in position by clips and then the composite was held at 80° for 30 minutes. The subsequent operations are similar to those described above and shown in figure 7.11 (T; c, d, e and f), the only difference being that in this case there are no crystallites sticking to the final platinum/carbon replicas. This is a two stage replication used during the present work. Usually platinum/carbon is evaporated at an angle to give contrast to the various features on the replicas. During the present work platinum/carbon was evaporated approximately at an angle of 25°.

The replicas obtained were picked upon grids type 100 supplied by Polaron Instrument Company. The grids are specially suitable for studying various rare features.

Replicas were studied with the AEI, EM6 electron microscope (figure 7.18). The figure 7.19 shows the (ray diagram) functioning of an electron microscope under normal condition and under the condition for diffraction patterns.

Photographs were taken on ILFORD N50 fine grain

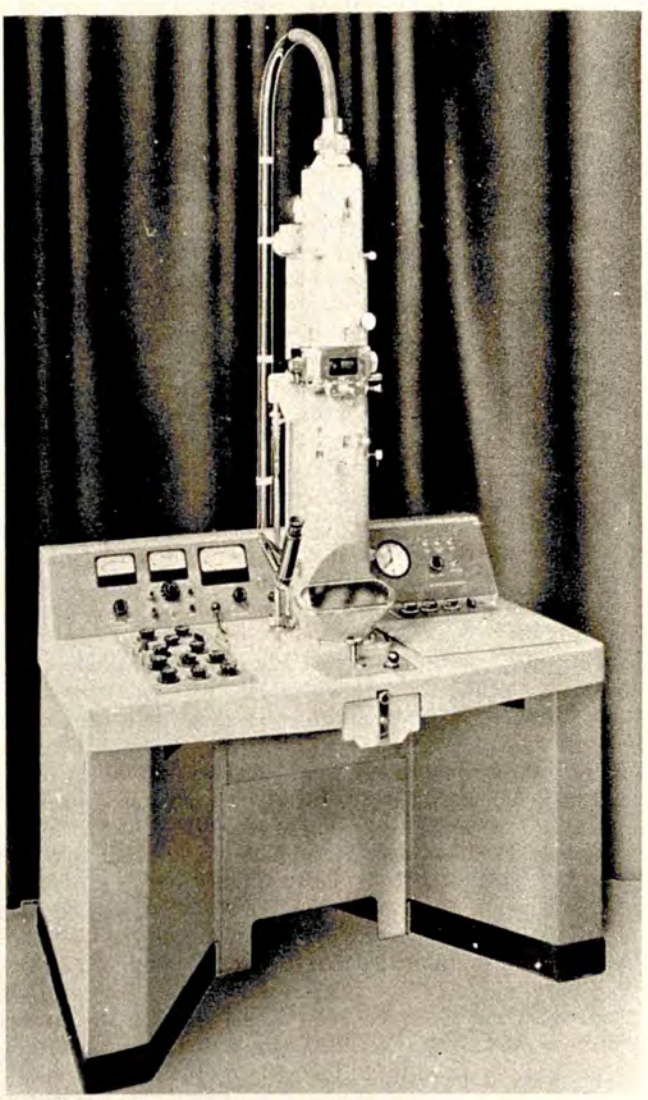

Figure 7.18.

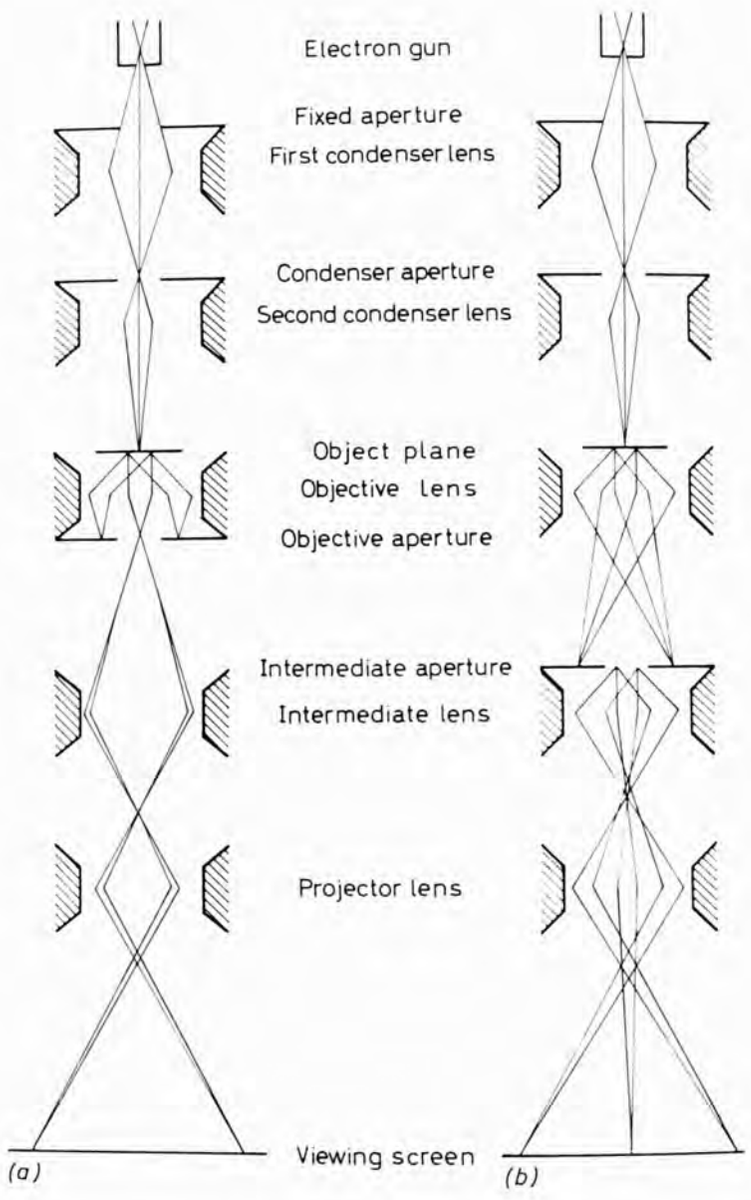

Figure 7.19.

Electron optics of transmission electron microscope:

(a) image formation.

(b) selected area electron diffraction.

plates, allowing plate magnification upto 10 - 15 times. For various beam intensities an exposure time 3 to 10 seconds was given.

7.13 Vacuum System

The platinum/carbon evaporation for preparing replicas was carried out in an Edward 12EA/204 coating unit. It consists of oil vapour diffusion pump, water cooled, backed by oil rotary pump, having P_2O_5 trap. The upper limit of evacuation goes to a pressure, approximately 5×10^{-6} torr. The evacuation is done to start with the rotary pump (usually from 0·05 torr pressure to $2{\cdot}5 \times 10^{-5}$ torr pressure). A Pirani gauge was used to measure the backing pressure over the range 0·5 to 0·001 torr. A Penning gauge was used to measure pressures from 5×10^{-3} to 2×10^{-6} torr.

It is unlikely that synthetic and natural diamonds used during the present work were rigorously cleaned, therefore they were pre-cleaned by boiling in concentrated nitric acid and then washing with soap solution ultrasonically and finally refluxing in acetone.

For etching, KNO_3 provided by B.D.H. was used and it was carried out in a Gallenkamp oven. The temperature accuracy was of the order of $\pm$ 10°C.

Some of the synthetic diamonds were etched in a rotating crucible in a cylindrical oven (figure 9.34). The crucible had a long stem and was rotated by attaching this stem, to a 50 rpm motor.

The interferometric work was carried out with a Vicker's microscope.

CHAPTER 8

OPTICAL AND ELECTRON-OPTICAL STUDIES OF THE SURFACE FEATURES OF de BEERS SYNTHETIC DIAMONDS

8.1 Optical Studies

de Beers synthetic diamonds are of size 1/5 to $\frac{1}{3}$ mm. In shape they are cubo-octahedral: in some crystals cube faces are the more prominent, while in others the octahedral faces are more developed. Figure 8.1 shows some de Beers synthetic diamonds. There is a considerable number of diamond crystals (nearly 2000÷3000) in a carat. Nearly 75% of the 50 carat sample are well shaped crystals but this was specially selected for us. The colour of the crystals usually varies from black to dark green, yellowish-green, yellow and even to colourless. Handling of such crystals is tedious for microscopy and also for electron-microscopy. The crystals are cleaned first by boiling in concentrated nitric acid, then washing in soap solution ultrasonically and then refluxing in organic solvents such as alcohol or acetone, to remove surface contamination and grease etc.

For electron microscopy various well shaped crystals were selected. These crystals showed very little

surface structure under the optical microscope, except the river pattern or so-called dendritic overgrowths (Tolansky 1961 a, 1962 a) of possibly metal carbides. Figure 8.2 shows such a pattern on a cubic face. The crystals were studied in phase-contrast microscope but they showed no structure at all. The very sensitive multiple-beam interferometry could not be applied because of the tiny size of the crystals. Each of the 14 faces of the crystals are of the order of 10^{-4} sq. cm. in area. It may be noted that Tolansky finds such dendritic patterns on natural diamond. They may be solution effects.

However, out of few hundreds of diamonds studied in the present work, only a few showed some interesting features in two-beam interferometry. As mentioned above, handling of these small crystals was difficult, since they were easily lost, and also the relocation of a specific face was difficult. In order to minimise the chances of losing the specimen during interferometric observation, a hole was made in a plastic dish, on which was then placed the crystal over its supporting glass slide. This glass slide is locally smooth upto $\lambda/20$, and was suitable for the production of interferograms.

Figure 8.1. (X 75)

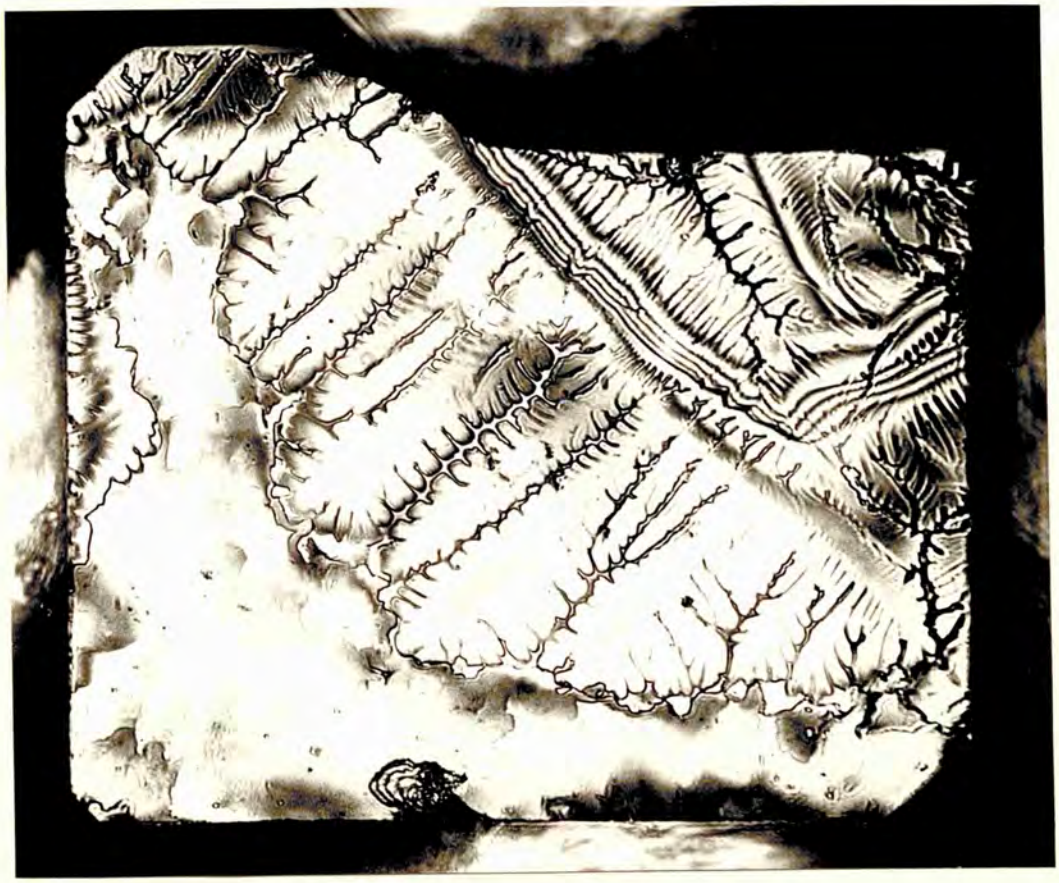

Figure 8.2. (X 315)

Interference between the glass slide and the crystal surface produced Fizeau fringes which are a contour map of the crystal surfaces. Because of the comparable reflectivity of these crystals with that of glass, fringe contrast is very good. In the case of natural diamonds reflectivity of the crystals is much higher than that of glass, and therefore a good fringe contrast is difficult to achieve (Tolansky and Sunagawa 1960 a). The visibility of the fringes varies from crystal to crystal and face to face, moreover it varies on the different parts of the same face.

Cubic faces on synthetic diamonds are unusually smooth in comparison to the faces on natural cubes (Tolansky and Sunagawa 1960 a, b, and c; Tolansky 1961 a). Figure 8.2 shows one of the cubic faces of the de Beers synthetic diamonds. The two-beam interferogram reveals the smoothness of the face. Apart from the dendritic pattern no other structure is present. Dendrites are elevations and in the present case their height above the surrounding surface varies from 1500Å to 3000Å. Dendrites are often present on the faces of synthetic diamonds. Figure 8.3 is another example showing dendritic pattern on the octahedral faces of a synthetic

diamond. Tolansky (1961 a, 1962 b) also found these to be elevations. Bovenkerk (1961 a, b) suggested these to be the imprints of metal carbides (however similar dendrites are on natural diamonds).

Hopper formation is also frequently seen on the octahedral as well as cubic faces of de Beers synthetics. About one in five of the nearly 2000 faces examined showed this character. Figure 8.4 shows a hoppered cubic face. Figure 8.5 shows the hopper formation on an octahedral face. Hopper formation on the faces of synthetic diamonds was first reported by Tolansky and Sunagawa (1960 a, b) and Tolansky (1961 a, 1962 b). According to Lemmlein et al. (1964) the heat of crystallization from the vertices and edges can be discharged more easily than from the central part of the crystal face. Hence the supercooling and consequently the probability of nuclei approaching around the vertices and edges, is greater than in the centre of the faces. The steps arising at the periphery will move towards the centre of the face, and at vertices and edges new ones will arise to replace them. New layers may develop long before the preceeding ones have actually covered the whole face. This results in the hopper formation, at the face centre. The time for a

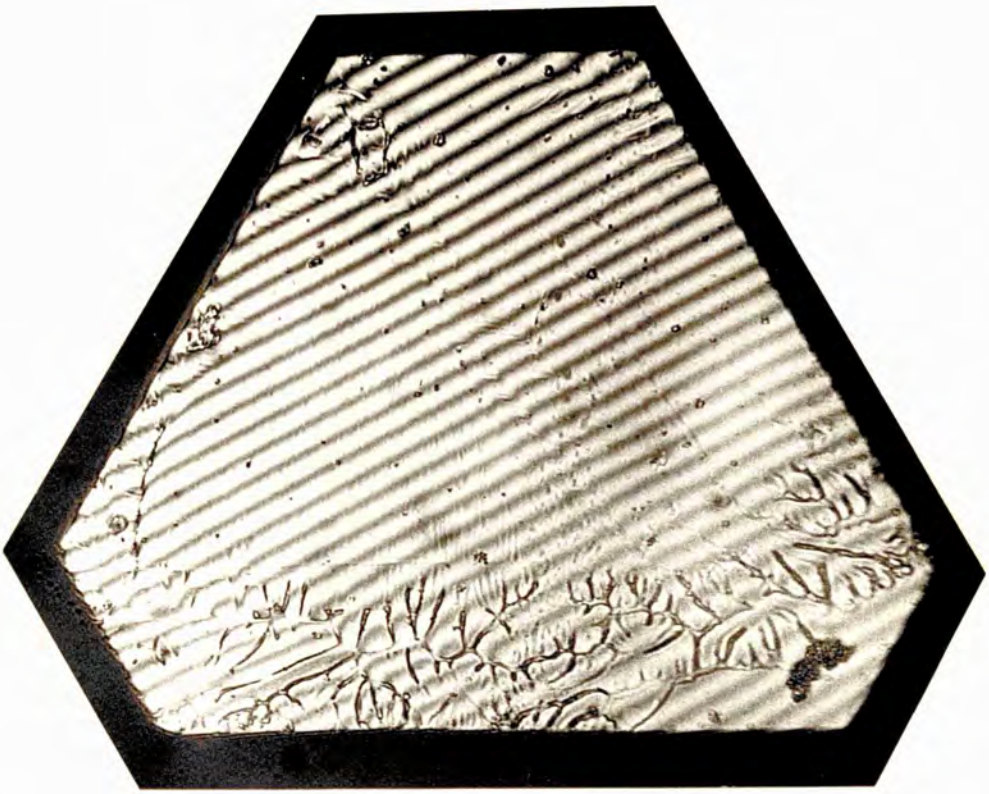

Figure 8.3. (X 315)

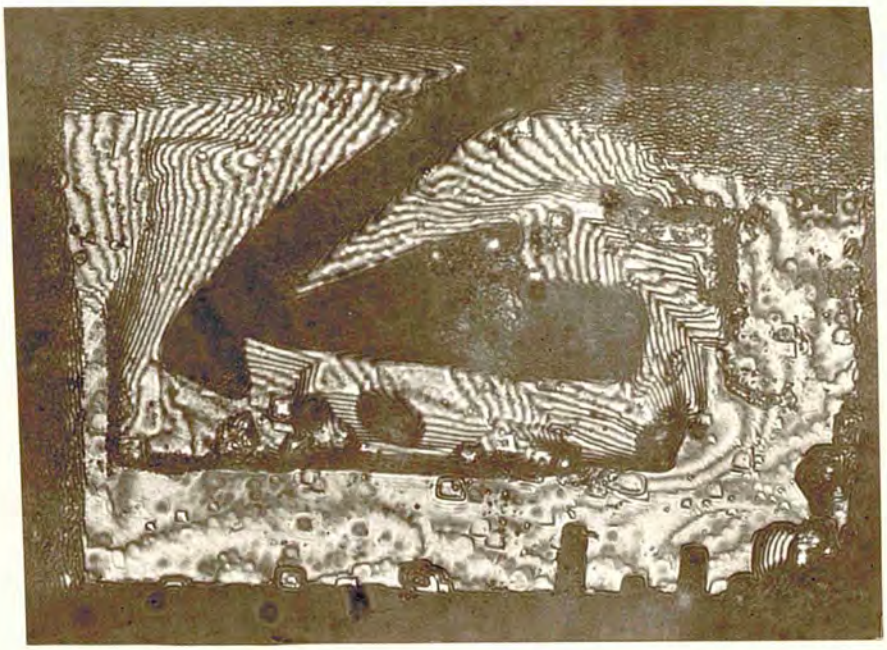

Figure 8.4. (X 315)

layer to propagate across the face is proportional to its extent, so that skeletal structure should only arise on those crystals whose size exceeds a certain value depending on the conditions of growth.

Figure 8.6 shows a cubic face which is bounded by ⟨110⟩ directions. On the surface there is a growth hillock the top of which is nearly 15000Å high above the surrounding surface. Dendrites are conspicuously seen on the face. Such a hillock was also observed by Tolansky (1962 a) during the course of studies on G.E.C. synthetics.

Figure 8.7 shows another cubic face. There are some crystallographic hillocks on the face. The orientation of these hillocks is positive i.e. sides are roughly parallel to ⟨100⟩ directions. These hillocks are elevations and this is confirmed by white light fringes.

During their studies on G.E.C. diamonds, Patel and Ramachandran (1967) also came across such hillocks. According to them hillocks are formed by preferential growth at screw dislocations. They suggested that somehow during the growth dislocations move away and this leads to the formation of flat top-surfaces of the hillocks.

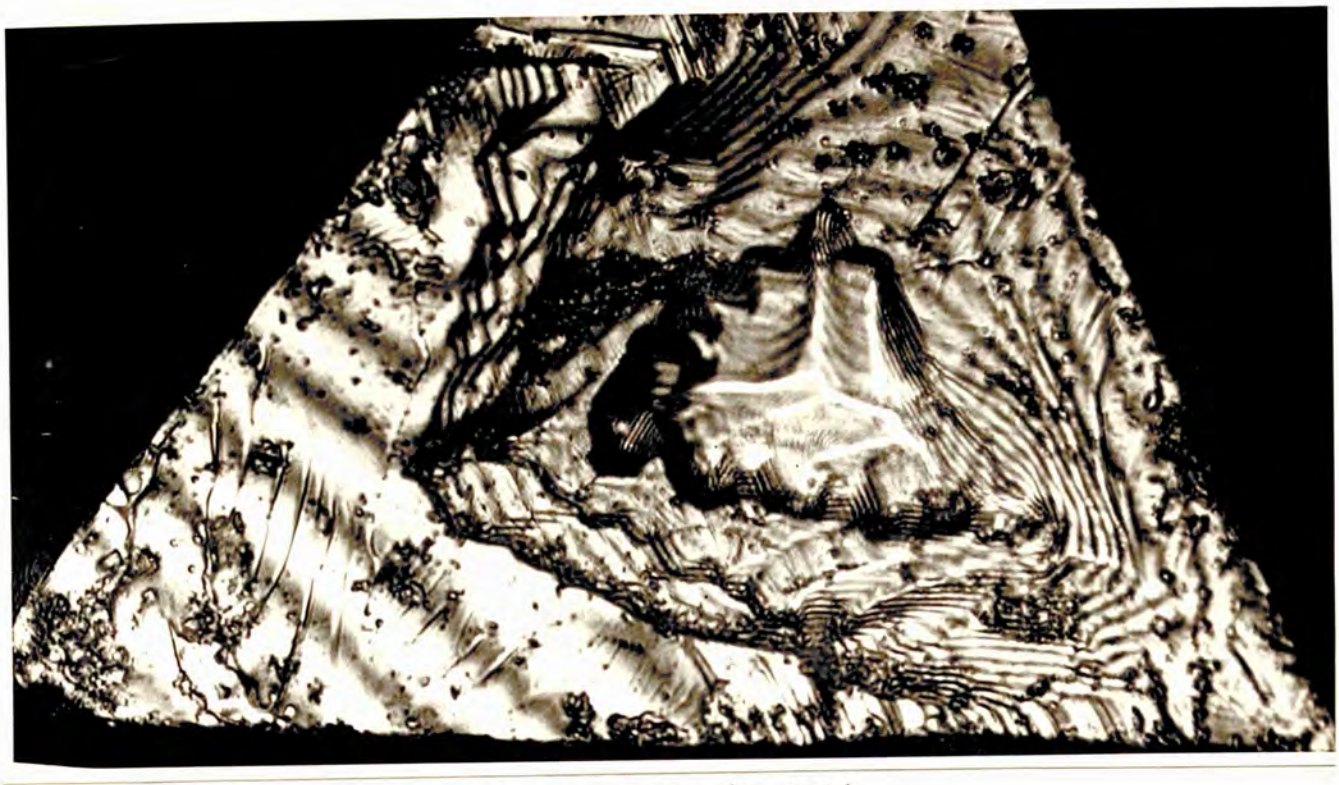

Figure 8.5. (X 630)

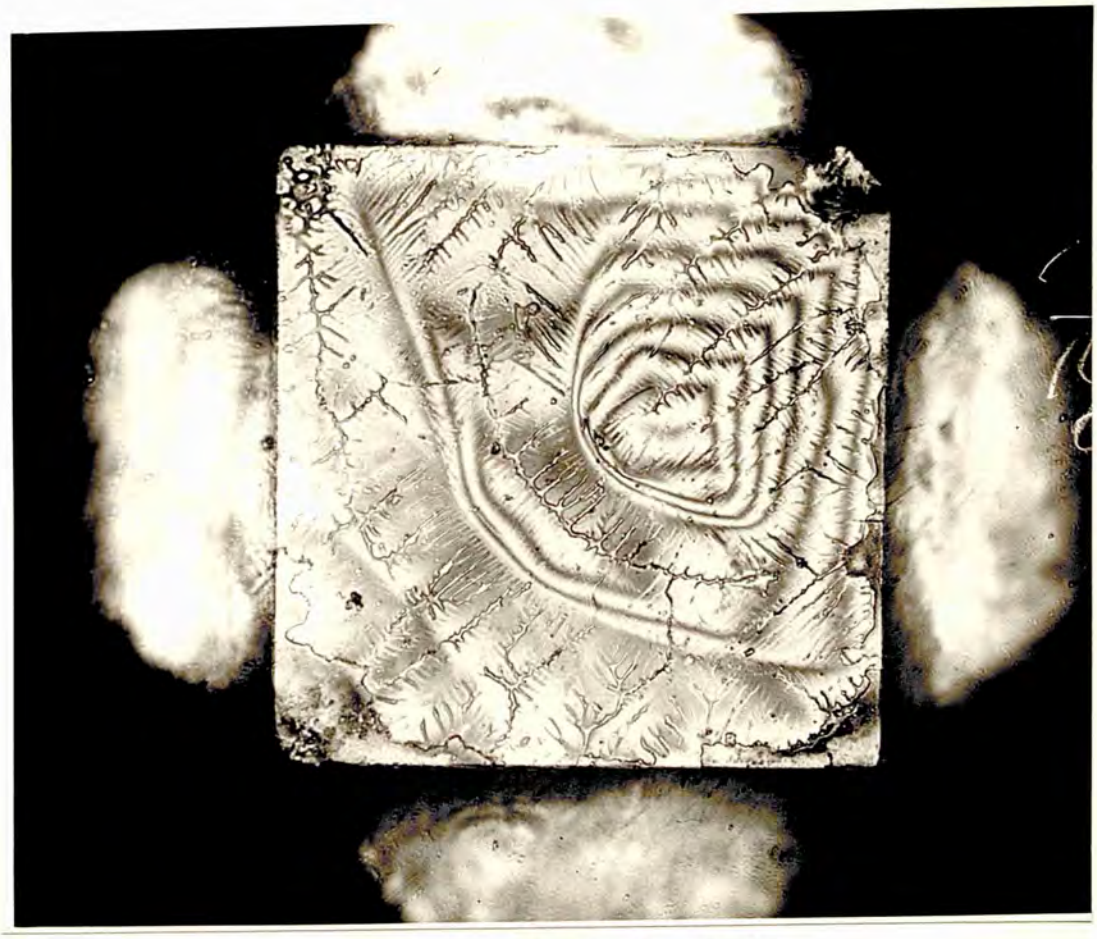

Figure 8.6. (X 320)

Figure 8.7. (X 530)

Figure 8.8. (X 320)

As reported by earlier workers during their studies on G.E.C. synthetics, trigons are a rarity and this is true also of de Beers diamonds. Figure 8.8 is an octahedral face showing numerous trigon-like features. The features are depressions. Orientation of these depressions is negative which was confirmed by seeing the crystal as a whole at low magnification. Trigons are formed by the intersections of growth layers proceeding at 60^{o} to each other.

Figure 8.9 shows one of the octahedral faces having some topographical features, which show up in two-beam interferometry. The face shows a spiral-like feature in bottom right hand corner of the photograph, which is nearly 25000Å high above the surrounding region. There are triangular features on various terraces on the crystal face. These were found to be hillocks by the method of light-profile microscopy (Tolansky 1952). Since there are features on the terraces and some of the hillocks have zig zag sides it is conjectured that these features arise from a mild etch during the process of manufacturing. Similar hillocks were reported by Patel and Ramanathan (1963) and Seal (1961, 1962 a, b). Spirals on the faces of

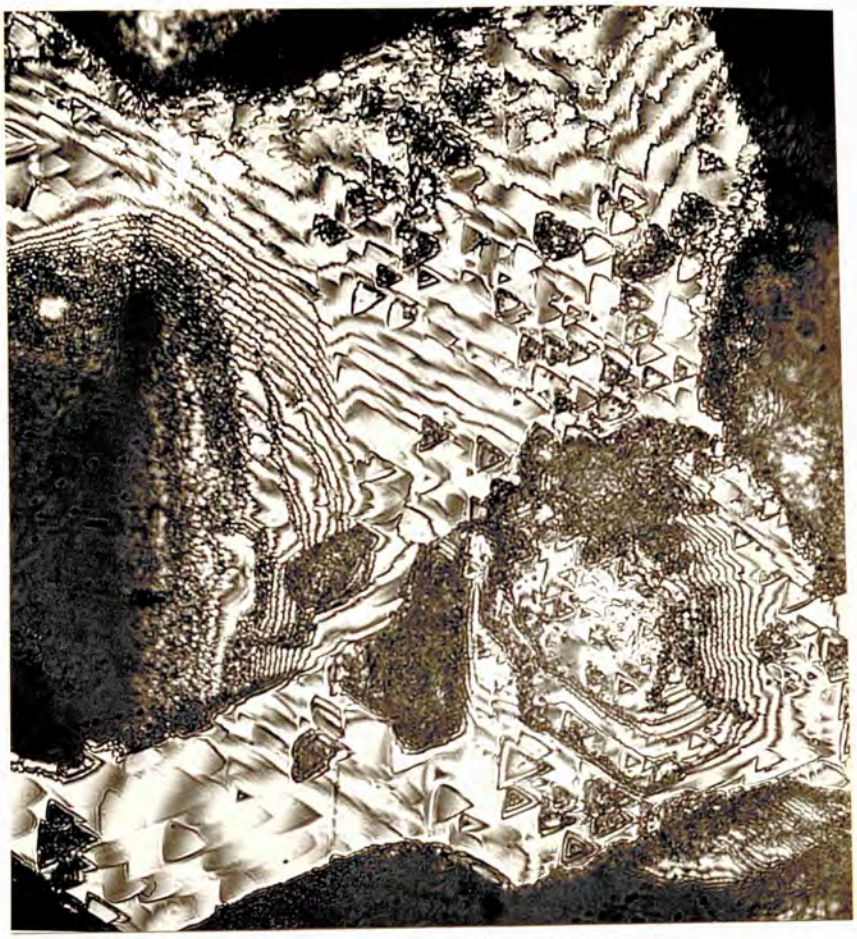

Figure 8.9. (X 320)

Figure 8.10. (X 320)

synthetic diamonds is an occasionally occurring feature. On the cubic faces of synthetic diamonds they were reported by Tolansky and Sunagawa (1959, 1960 a, b, c) and Tolansky (1961 b, 1962 a, b). They were also reported by Patel and Goswami (1964) and Patel and Ramachandran (1968) on the octahedral faces of G.E.C. synthetics.

In the case of de Beers diamonds, spirals are not very frequently seen either on $\{100\}$ or $\{111\}$ faces.

Figure 8.10 shows the octahedral face of another synthetic diamond in two-beam interference. These features have positive orientation with respect to the crystal face and are depressions as shown by white light fringes and light profile method and hence can be attributed to an etch during manufacture.

Figure 8.11 shows a network of positively oriented triangular cavities. A remarkably similar pattern was observed by Tolansky (1962 a) on G.E.C. synthetics. Because the pits have positive orientation and curvilinear sides these are also likely to be due to mild dissolution during manufacture.

Slip is another commonly observed feature on synthetic diamonds. Figures 8.12 and 8.13 show slip

lines on octahedral faces. The lines are in ⟨110⟩ directions. In the case of the figure 8.12 the slip goes right across the crystal face, while figure 8.13 shows that its step height gradually reduces and ultimately disappears. As reported by Tolansky and Sunagawa (1960 a, b) high density of inclusion in the synthetic diamonds may well be responsible for the frequent occurrence of such a feature in the synthetic diamonds.

Out of nearly 2000 faces examined optically only the few described above showed features which were detectable by light microscopy. The rest of the faces were very smooth, having dendritic pattern and hoppers only. They were studied electron-microscopically.

8.2 Electron Microscopic Studies

For electron microscopic studies, well shaped crystals having plane faces selected by two-beam interference and phase-contrast microscopy, were chosen from a considerable number of crystals. Nothing was detectable on the surface of these crystals, apart from the so-called dendritic patterns.

The crystals prior to replication were cleaned by the usual procedure. Faces having an area of the

Figure 8.11. (X 320)

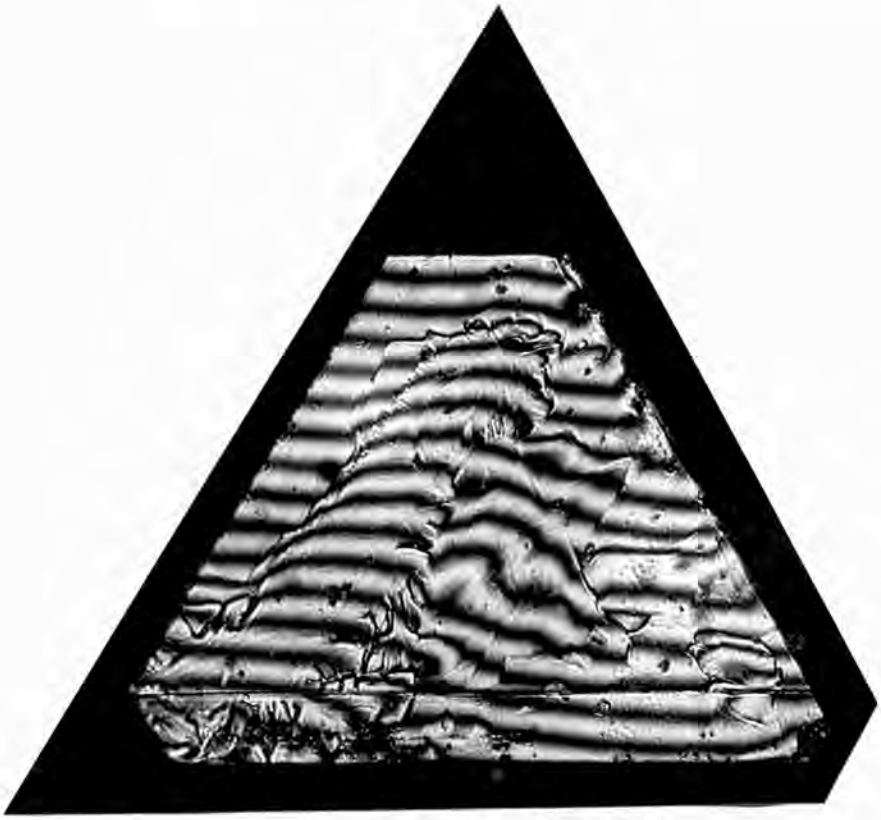

Figure 8.12. (X 320)

order of 10^{-4} square centimeter were involved. Ultimately after various trials and errors a replica technique was developed and the crystals were mounted and replicated as described in section 7.12.

Compared to the extensive topographical studies on natural crystals very little work has been done on the synthetic diamonds because of the very small size of the present day available synthetic diamonds. However, recently some interferometric and other optical studies on G.E.C. synthetic diamonds have been reported (Chapter 5).

Detailed electron microscopic studies are here reported on de Beers synthetic diamonds.

Electron microscopy proves very useful. It reveals a wealth of information regarding the surface structure of these micro-crystals. The surface details obtained can be divided into four groups.

1 - Structure on the octahedral surfaces.

2 - Structure on the cubic faces.

3 - Structure on the rarely occurring dodecahedral surfaces.

4 - Miscellaneous features.

(1) Structure on Octahedral faces

The so-called dendritic overgrowth on the faces of synthetic diamonds is frequently observed. Tolansky

(1961 a, 1962 a) has observed these to be elevations. Bovenkerk (1961 a, b) also observed this veined surface structure. He suggested that when the metal during synthesis is in a semi-solid form, dendrites freeze in the metal and they get replicated on the growing diamonds, which are in their last stage of growth. He also observed dendrites to be elevations. However dendritic pattern was also observed on the faces of cubo-octahedral crystals (Tolansky 1971).

Figure 8.14 shows the pattern on the faces of synthetic diamonds at high magnification. It is obvious that the structure looks like veins and is an elevation on the surface. Since it is suggested that the pattern on the natural faces arise due to dissolution a similar mechanism may be responsible for the formation of dendritic-like pattern on the faces of the synthetic diamonds. Moreover various features on the synthetics show that they have undergone dissolution.

Figure 8.15 shows a crystallographic hillock. The sides of the hillocks are fairly rectilinear and crystallographically oriented. The layered growth is easily seen. Hillock is nearly 1000Å high above the surrounding surface level.

Figure 8.13. (X 400)

Figure 8.14. (X 23,000)

Figure 8.16 shows another example of the crystallographic growth hillock. The hillock is only 100Å above the surrounding area and it is crystallographically oriented and the bounding lines are strictly rectilinear. Hillocks indicate that growth is only taking place over that restricted region, because of the restricted amount of carbon reaching there.

Figure 8.17 shows growth layers intersecting at 60°. The layers are nearly 400Å thick. There is a trigon-like feature in the corner of the photograph. Figure 8.18 also shows growth which presents zig zag appearance, the rectilinear segments of which are in crystallographic directions. If another growth layer can be imagined to meet these two-sided features at 60°, trigons would form. Figure 8.19 shows such features formed by the growth layers proceeding at 60° to each other. Whenever growth layers at 60° intersect they give rise to v-shaped features with numerous re-entrant angles as shown in figures. Trigons are formed when the growth layers at 60° are arrested from three directions (Tolansky 1955, 1960).

Figures 8.20, 8.21 and 8.22 provide further examples showing the layers spreading at 60°. The

Figure 8.15. (X 19,000)

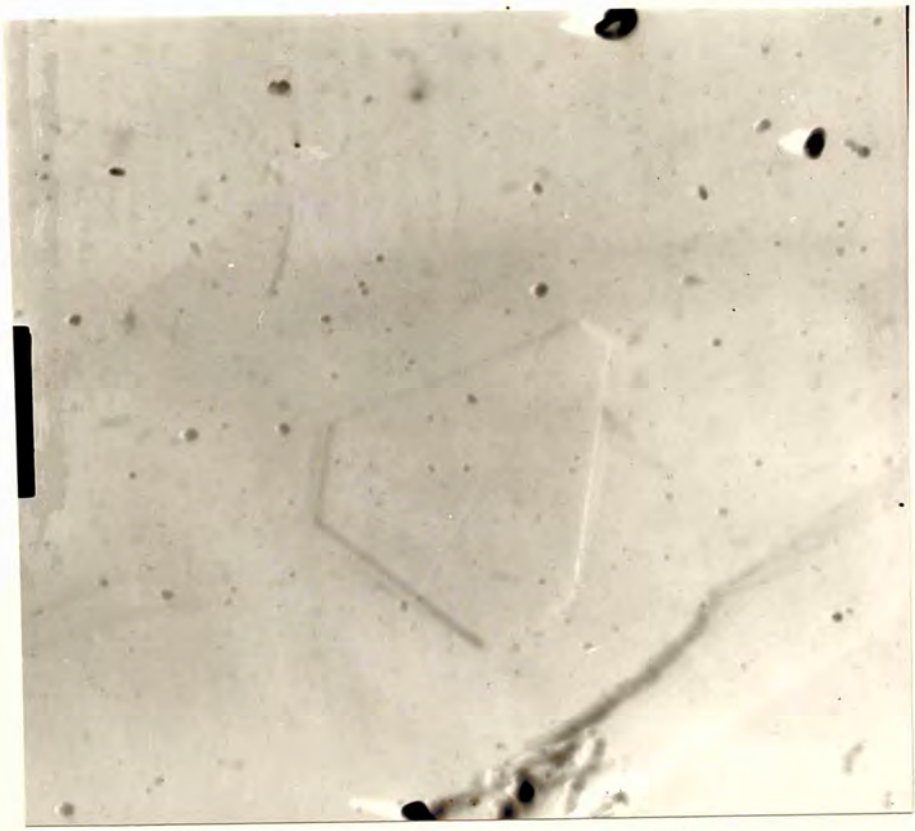

Figure 8.16. (X 23,000)

Figure 8.17. (X 15,500)

Figure 8.18. (X 20,000)

Figure 8.19. (X 11,500)

Figure 8.20. (X 17,000)

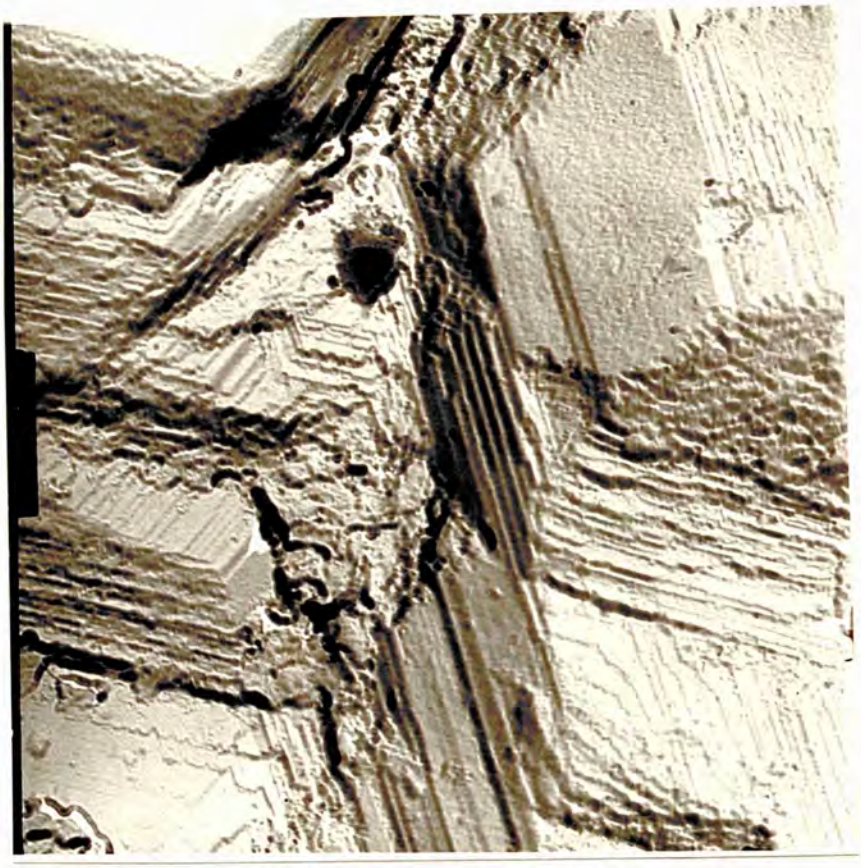

Figure 8.21. (X 10,500)

Figure 8.22. (X 10,000)

piling up of these layers produces various three-dimensional features. In addition to trigons, various parallelogram-like features are also observed on the faces of de Beers synthetics. Figure 8.23 is one example of this type. The mechanism of formation of such features seems similar to that of trigons.

Figure 8.24 shows some peculiar features. They are depressions and all of them are nearly of the same depth, some 850Å approximately. Their lateral size is approximately 0·5 micron. It is suggested that these are growth features, because they are flat-bottomed and have similar depths. Etching would be unlikely to cause such characteristics. These are more likely to be due to the obstruction of growth layers, either by point obstructions or due to deficiency in the amount of carbon reaching these regions during the growth process.

Another observation of interest is the growth spirals, examined here for the first time electron microscopically. Figure 8.25 shows a growth spiral. The angle between the adjacent arms is 120°. The picture shows that the spiral is a hexagonal elevation. The step height is approximately 240Å.

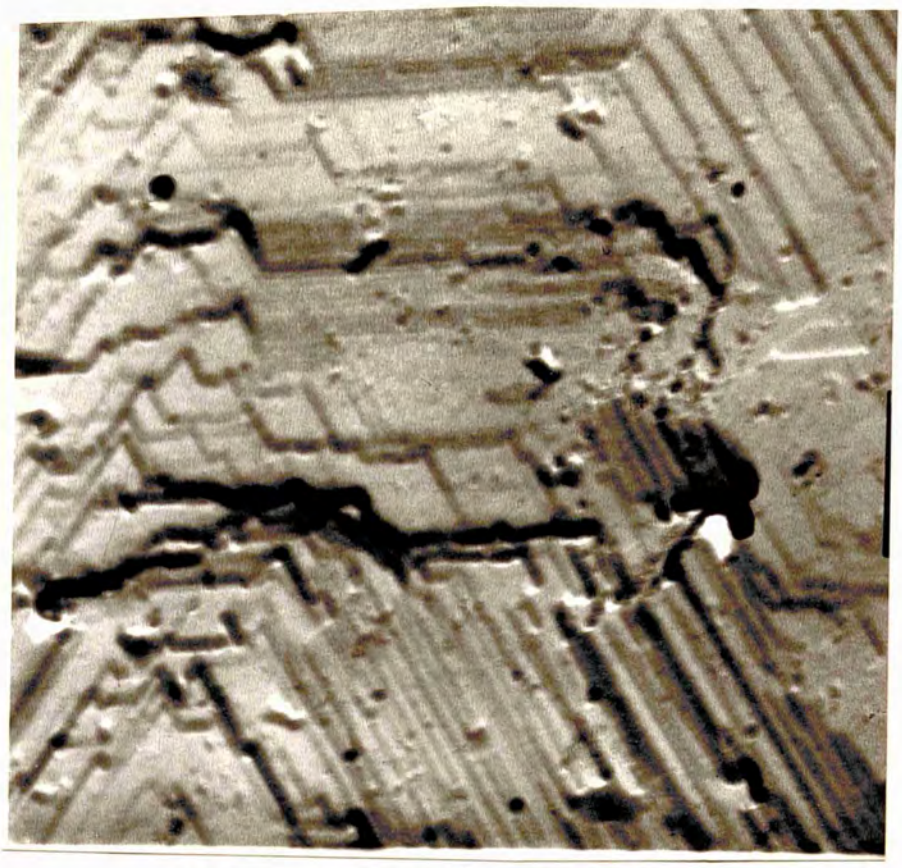

Figure 8.23. (X 21,000)

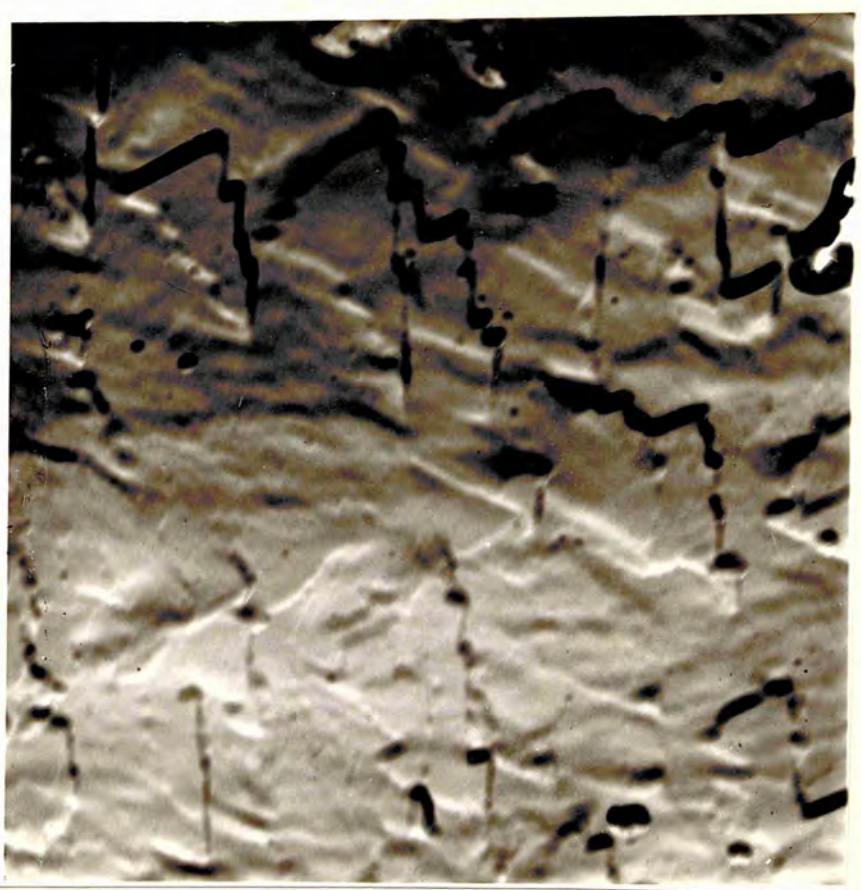

Figure 8.24. (X 22,000)

Growth spirals on synthetic diamonds have been reported by various workers but not yet studied electron microscopically. Detailed electron microscopic studies indicate that the areas between the successive steps are very smooth and there is no sub micro-structure present.

Figures 8.26 and 8.27 show an unusual structure on the de Beers synthetics. Nucleation occurs continuously on the steps and because of the succeeding thick layers not proceeding fast enough to cover the whole surface of the crystal, due to the rapid growth rate, local regions of layered growth are formed.

Apart from growth there are various features attributable to an etch. They vary in size, shape and character from face to face; those observed on the octahedral face display the three-fold symmetry.

Figure 8.28 shows triangular features. They are clearly depressions, all of which have a depth of nearly 170Å and are similar in size (nearly 0·25 micron). These features also occur in crystallographically aligned arrays as seen in figure 8.29. Patel and Tolansky (1957) observed similar stratigraphic pattern on mildly etched octahedral cleavages of natural diamonds.

Figures 8.30 and 8.31 show more examples of

Figure 8.25. (X 20,000)

Figure 8.26. (X 15,000)

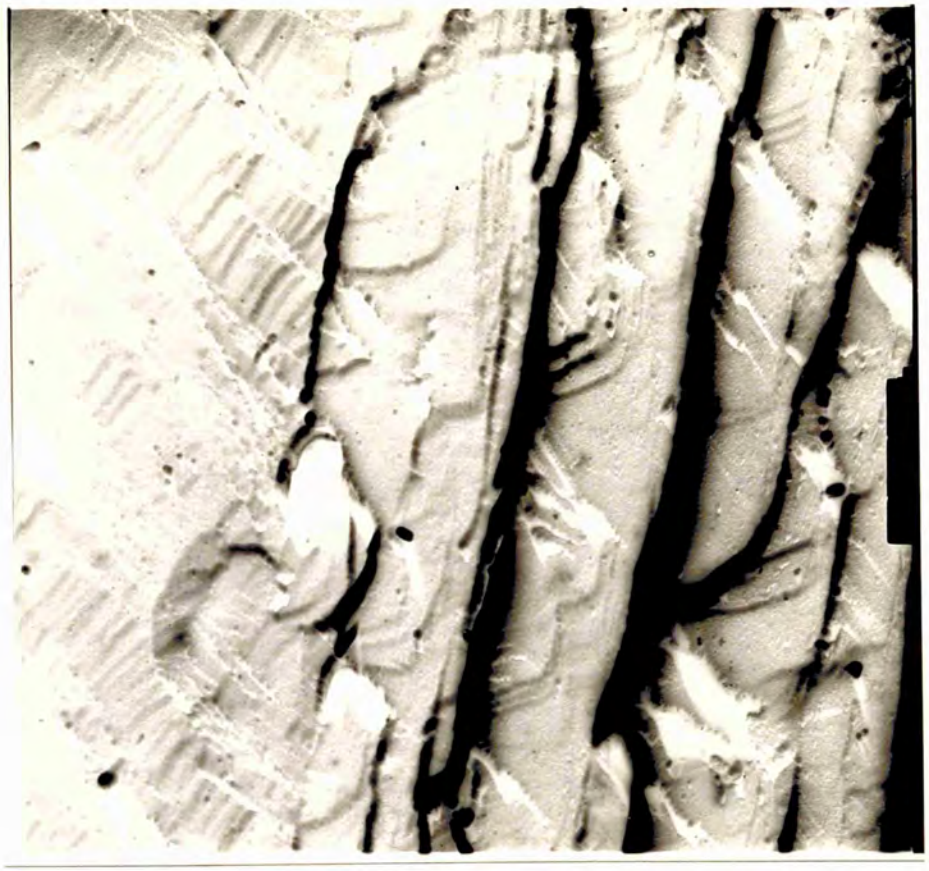

Figure 8.27. (X 14,500)

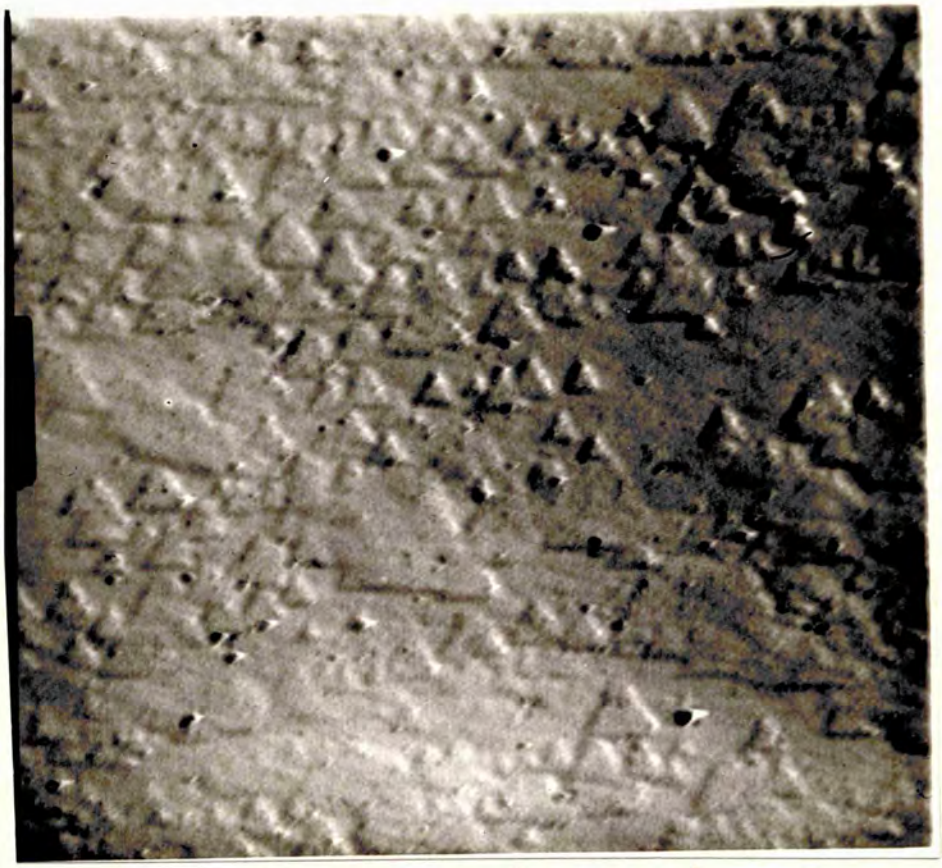

Figure 8.28. (X 23,000)

Figure 8.29. (X 23,000)

Figure 8.30. (X 5,100)

such a feature on the octahedral faces of synthetic diamonds, which are presumed to be due to etch for the following reasons:

1 - Photographs indicate separately that the pits are similar in size and shape.

2 - They overlap and occasionally have rounded edges.

Since trigons do not show these characteristics the cavities observed here on the octahedral faces are likely to be due to dissolution during manufacture.

Figure 8.32 shows pyramidal hillocks on the $\{111\}$ faces. The area surrounding the hillocks, which is not plane and exhibits solution channels, indicates the surface has undergone dissolution. Thus these features which are elevations, are likely to be the result of dissolution. Such features were also reported on Russian synthetic diamonds by Bartoshiniskii and Makorov (1967). They ascribed these features to 'surface relief' and termed them 'thorn-like' features.

(2) Features on the Cubic Faces of the Synthetic Diamond

Cubic faces of the synthetic diamonds also exhibit similar features, the only difference being that they represent the four-fold symmetry of the face.

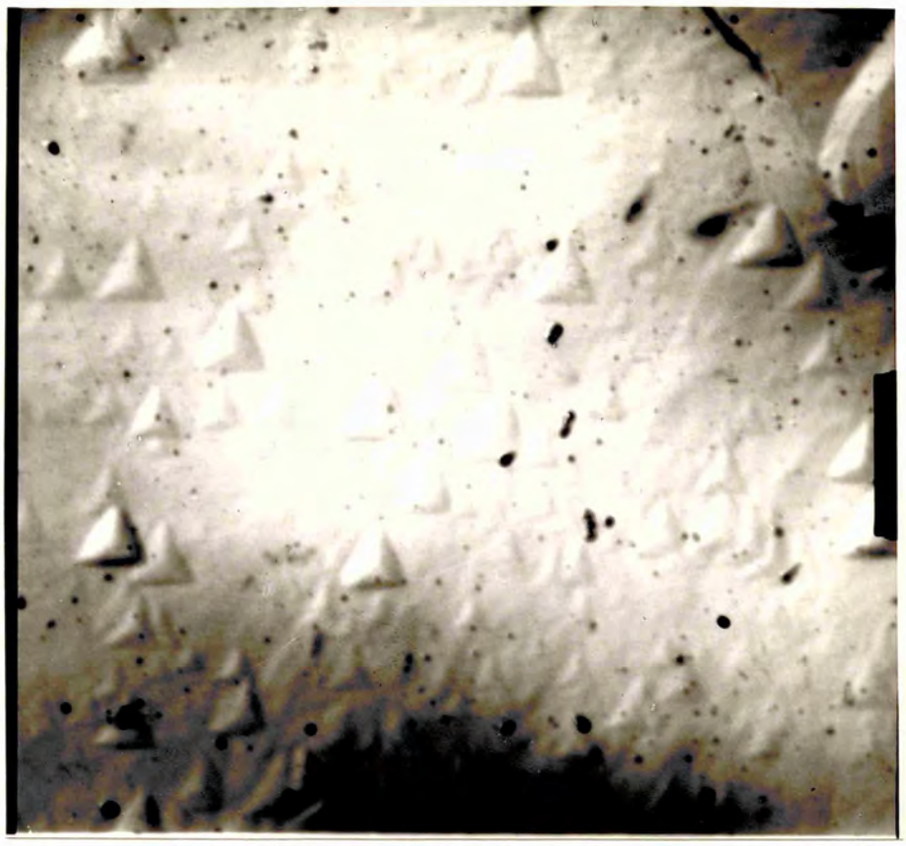

Figure 8.31. (X 18,500)

Figure 8.32. (X 6,000)

Figure 8.33. (X 16,000)

Figure 8.34. (X 19,000)

Figure 8.33 shows growth layers at 90° to each other, intersecting to form a stepped structure with numerous re-entrant angles. This we suggest is similar in origin to the V-shaped structure on the {111} faces. The step height is generally of the order of 300Å.

Figures 8.34 and 8.35 both show thick growth layers proceeding at 90° to each other. Pictures clearly indicate that growth on the cubic faces also take place by layer deposition and these layers are inclined to each other at 90°, conforming to the symmetry of the face. Figure 8.36 is another example of such a type. The step height ranges from 100Å to 200Å.

In addition to these various types of growth patterns, many etch patterns were also observed. Figure 8.37 shows one of such patterns. The surface looks like having undergone an etch. Layers at 90° are showing.

Figure 8.38 shows some elevated hillocks, observed on the de Beers synthetic diamonds. The sides of the hillocks are curved and appear to be mildly etched.

Figure 8.39 shows an etched cubic face. There are various tiny cavities. In addition to these there

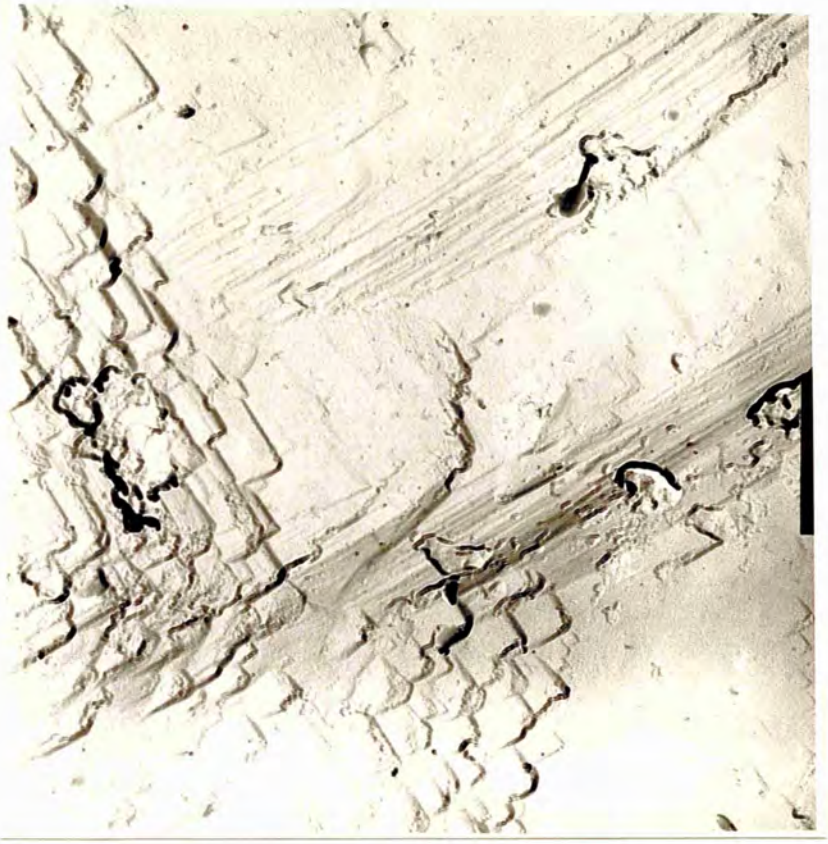

Figure 8.35. (X 17,000)

Figure 8.36. (X 13,000)

Figure 8.37. (X 19,000)

Figure 8.38. (X 19,000)

is a rectilinear pattern. Such pattern is observed here on the synthetic diamonds for the first time. Harrison and Tolansky (1964) have reported a 90° rectilinear pattern on the sectioned, polished and subsequently etched faces of a natural diamond.

Figure 8.40 shows an interesting block-pattern. The pattern shows the layered growth. The layers seem to have undergone a mild etch. Figure 8.41 also exhibits an etched cubic face. The face is heavily etched and the multitude of tiny pits appear like constituting a block-pattern on the cubic face. Since the pits are overlapping and the surface is very rough these can reasonably be attributed to an etch during the manufacture.

Various other growth and etch patterns were observed but only the representatives of the class have been described here.

(3) Structure on the Rarely Occurring Dodecahedral Faces

Tolansky and Pandya (1954), Emara and Tolansky (1957) and Pandeya and Tolansky (1961) have reported various types of etch patterns on the dodecahedral faces of natural diamonds:

1 - Irregular network pattern.

2 - Elevated disk pattern.

Figure 8.39. (X 22,500)

Figure 8.40. (X 26,500)

3 - Boat-shaped features.

4 - The rectilinear and crystallographically oriented network patterns.

A similar crystallographic network pattern has been seen on the synthetic diamonds for the first time. This rectilinear pattern is made up of grooves. There are two parallel sets which meet at an angle of 108^{o}.

Figures 8.42 and 8.43 show such a pattern. The grooves look V-shaped in nature, they are strictly rectilinear and uniform. They seem to be oriented crystallographically. The depth of the grooves is approximately 550Å while their width is 2500Å.

Emara and Tolansky (1957) have produced such a pattern on the natural dodecahedral diamonds by etching the faces artificially, at 550^{o}, in potassium nitrate. According to their optical studies, these are the regions of intersection of less perfect octahedral planes on the dodecahedral faces. These planes are more susceptible to an etch and this gives rise to crystallographic grooves.

Pandeya (1959) also observed a similar pattern. He found that striations bisect the obtuse angle (108^{o}). Figure 8.43 shows striations in addition to the V-shaped

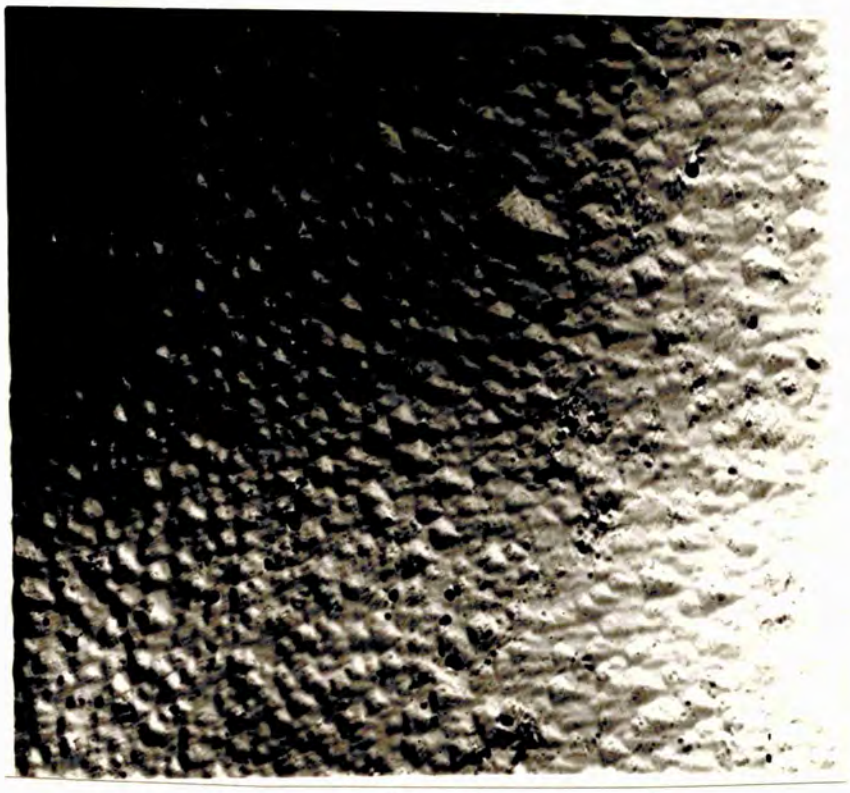

Figure 8.41. (X 11,000)

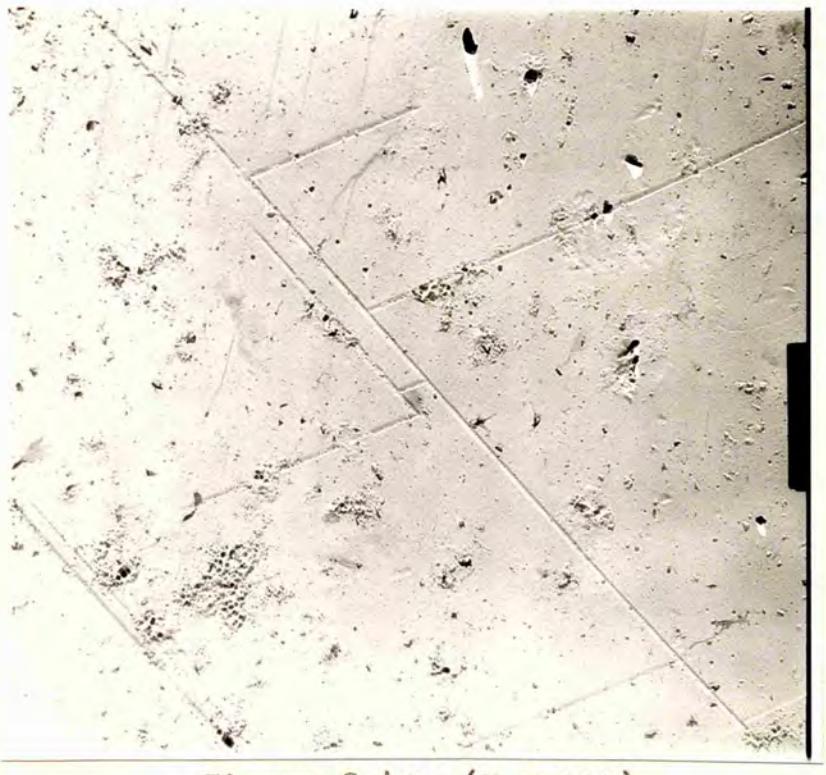

Figure 8.42. (X 2,000)

grooves. These striations present, also bisect the obtuse angle approximately. Pandeya suggested that the V-shaped grooves are the intersections of {111} planes which are at 90° to {110} faces, while the striations are the intersections of those octahedral planes which are inclined at 36·5° to the dodecahedral faces.

This type of pattern has been observed for the first time on the synthetic diamonds, and may be reasonably supposed to be similar in origin to that observed on the natural diamonds.

Another type of commonly observed features on the dodecahedral faces of natural diamonds is boat-shaped features. Figure 8.44 for the first time shows such features on the faces of synthetic diamonds.

(4) Miscellaneous Features

Figures 8.45 and 8.46 show the layered growth. The features indicate that the growth layers are obstructed by surface irregularities, which could be metal impurities etc. The layers are at 60° to each other. They indicate that surfaces are lightly etched, perhaps when the growth had ceased, leaving big holes in place of metallic inclusions. Figure 8.46 shows how a growth layer advances around an impurity. The basal-extension

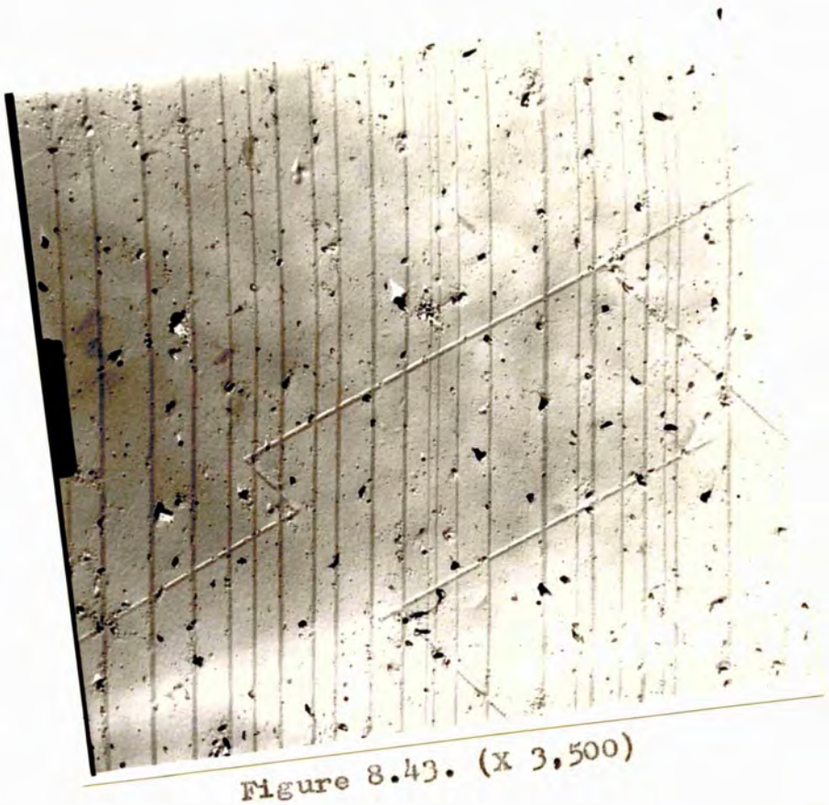

Figure 8.43. (X 3,500)

Figure 8.44. (X 22,500)

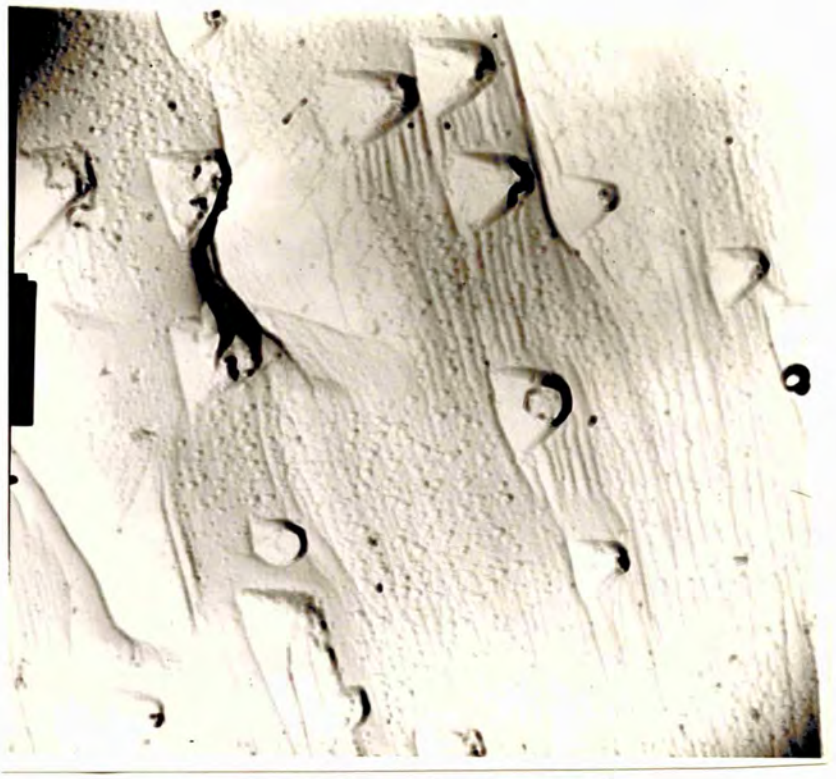

Figure 8.45. (X 11,000)

Figure 8.46. (X 11,500)

type features showing here are formed by the ends of the growth layers.

Figure 8.47 shows a rather beautiful and unusual pattern. The surface appears to have multiple cracks along the cleavage directions on the octahedral face. The depths of the cracks look different at different points, indicating a variable local shear.

Figure 8.48 indicates a structure similar to that observed by Seal (1961). It is an unusual structure and exhibits 'flow type' features and stepped formation. This type of feature has also been reported by Zapffe and Worden (1949), on ammonium hydrogen phosphate. According to Fisher and Gilman (1955) these features are associated with the presence of twist boundary between the adjacent subgrains of the crystal, each line is initiated by screw dislocations emerging in the surface.

Thus electron microscopical observations show features and patterns on the surfaces of synthetic diamonds in detail and provide very high lateral magnification compared to the conventional optical techniques. It therefore not only allows the studies of the features which escape observations during the optical studies but also allows the detailed study of previously observed features.

Figure 8.47. (X 11,000)

Figure 8.48. (X 11,500)

CHAPTER 9

THE ETCH STUDIES ON DE BEERS SYNTHETIC DIAMONDS: THE CHANGE OF ORIENTATION OF THE ETCH PITS

9.1 Introduction

After studying the crystals optically and electron optically, etching experiments were made on the de Beers synthetic diamonds. Crystals were etched with fused KNO_3 from a temperature of 500°C to 800°C at intervals of 25°C or 50°C, in a muffle furnace. The temperature accuracy was ± 10°C. The crystals subjected to an etch were selected from the sample having minimum disturbing surface structure. Figure 9.1 shows one of the representative surfaces with two beam interferometry. These crystals were etched together with the natural diamonds from the Premier Mine. These natural crystals were 30 - 40 mesh octahedra or macles and were also selected from minimum possible surface structure. Thus these crystals were comparative in size to the de Beers synthetic diamonds and also had the advantage of being small. As suggested by Honess (1927),

"small crystals give better results".

9.2 Etching at Temperature 500°C to 600°C

At every temperature fresh crystals were etched and hence the etch was the characteristic of that particular temperature and had no connection with the previous experiments.

The crystals were etched at 500°C for 8 hours. The surfaces did not show any remarkable change in the topography when examined with a Vickers microscope. They were therefore etched further for 10 hours. After 18 hours of etching, some etch effect became noticeable. Dendrites became less prominent and there were a few micro-pits on the surfaces. The pits were very small and thus it was difficult to assess their orientation.

Pits on the {100} faces of synthetic diamonds formed arrays in ⟨100⟩ directions.

The temperature was then increased to 530°C. New crystals were etched for $8\frac{1}{2}$ hours. Pits are very small and just big enough to be resolved microscopically.

On the natural {111} faces percussion marks seem to be developed. However the pits are very small,

their orientation is positive which is indicated by the figure 9.2. Pits on the {111} faces of synthetic diamonds are nearly $1\frac{1}{2}$ times bigger in area compared with the pits on the natural surfaces (figure 9.3). The orientation of these pits on the octahedral faces of synthetic diamonds is positive - this was confirmed further by viewing the crystal at low magnification.

On the cubic faces of synthetic diamonds as shown in the figure 9.4, there are a few resolvable pits. These pits form the chains or arrays in ⟨110⟩ directions. There are a few arrays in ⟨100⟩ directions too.

Thus at 530°C the {111} faces of the synthetic diamonds appear to be the fastest etching faces. The temperature was increased to 560°C and new crystals were etched for $4\frac{1}{2}$ hours at this temperature to study the effect of temperature on etching. At this temperature the size of the pits increases drastically, though the number of pits remains nearly the same.

Figure 9.5 shows the etch pattern on natural {111} faces. Pits are now nearly 4 times in area

Figure 9.1. (X 300)

Figure 9.2. (X 200)

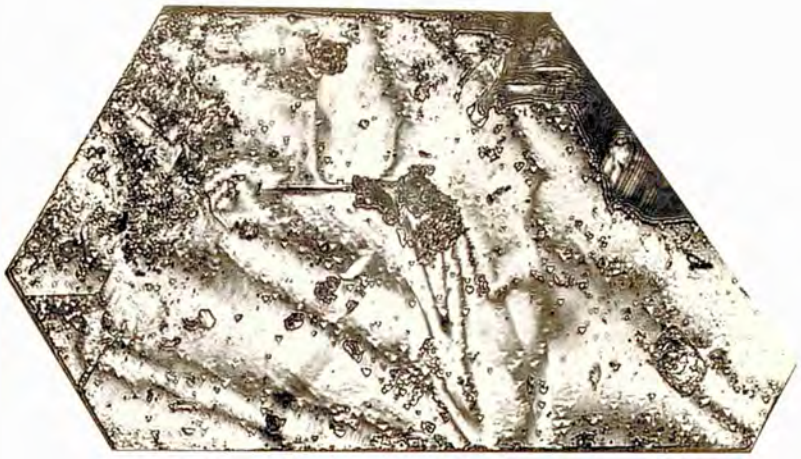

Figure 9.3. (X 250)

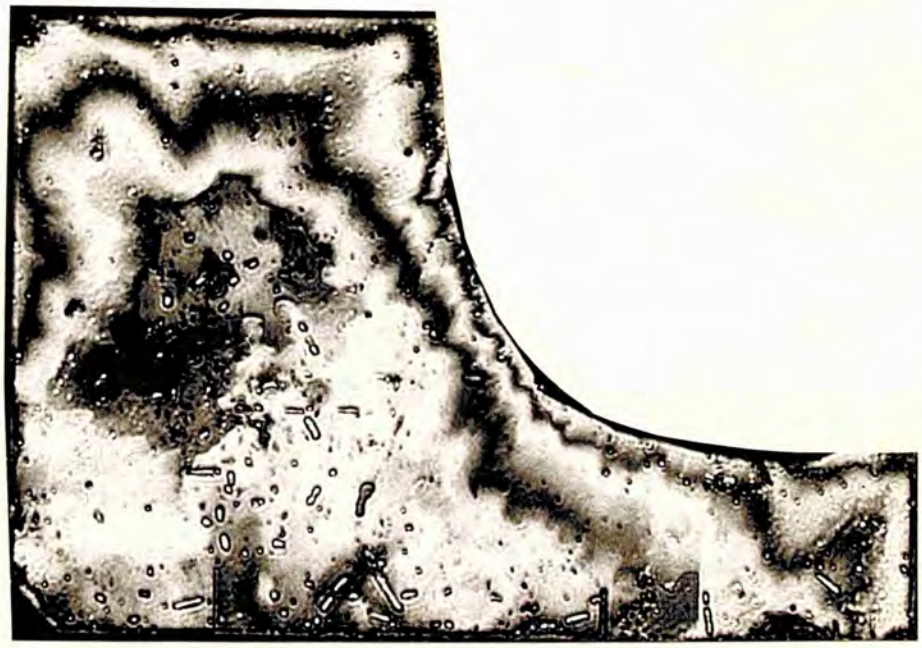

Figure 9.4. (X 425)

compared to the pits at 530°C. A few of the pits are well developed while there are numerous small pits on the surface. Pits as shown in figure 9.5 start rounding off their corners. The rounding of the corners and their rectilinearity was first studied in detail by Tolansky and Patel (1957). Figure 9.6 reveals the etch pattern produced on the {111} face of a synthetic diamond. The etch pattern is well developed. There are numerous bigger pits. The density of the bigger pits is nearly 4 times that of the pit density on the natural octahedral face. Remarkable enough these pits are more rectilinear than the pits on the natural {111} faces at the same temperature. The same effect was observed by Patel and Goswami (1963) during their etch studies on G.E.C. synthetics. A comparison of the figures 9.6 and 9.7 shows that the dendrites on the face after being etched are very faintly visible.

Pits on the cubic faces are shown in the figure 9.8. Pits on {100} faces are small in comparison with the pits on the octahedral faces. On the whole the pit density increases on the cubic faces, but the size of the pits do not change very much by altering the temperature

Figure 9.5. (X 250)

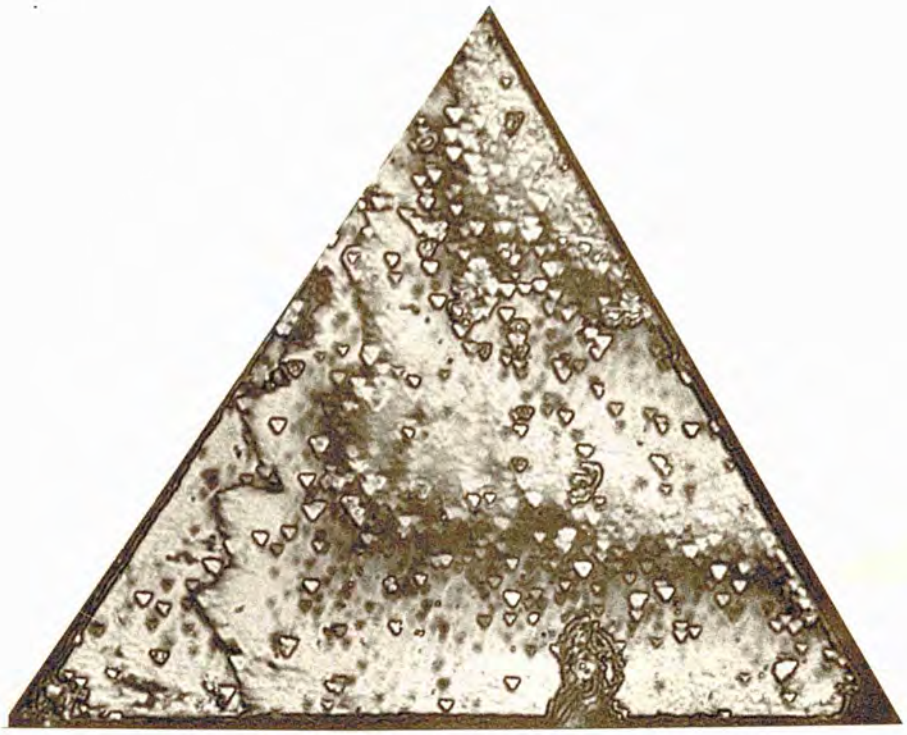

Figure 9.6. (X 400)

Figure 9.7. (X 400)

from 530°C to 560°C. Pits forming arrays can be seen on the photograph.

Thus at 560°C the etch rate is fastest on the {111} faces of synthetic diamonds, intermediate on the {111} faces of natural diamonds and it is slowest on the cubic faces of synthetic diamonds.

This agrees with the results obtained by Patel and Ramachandran (1968).

The pits are in negative orientation on the {100} faces. Temperature was further increased to 600°C and the time was reduced to $3\frac{1}{2}$ hours. At this temperature the etch rate increased abruptly.

On the {111} faces of natural diamonds (figures 9.9 and 9.10) the size of the pits increased approximately 2 to 3 times and number of bigger pits increased and hence the pit density as a whole decreased. Pits are rounded (as shown in figures). Some of the pits seem to form an array in ⟨110⟩ directions.

On the synthetic {111} faces the etch rate is faster still. The pits start overlapping. At this temperature, the size and number of the bigger pits are more than that on the natural surface. Figure 9.11 shows a two-beam interferogram of a (111) face of

Figure 9.8. (X 400)

Figure 9.9. (X 400)

Figure 9.10. (X 200)

Figure 9.11. (X 330)

synthetic diamond etched at 600°C for $3\frac{1}{2}$ hours. The pits have side length of nearly 10 microns.

The $\{100\}$ faces show a surprising effect. There are numerous bigger and smaller pits. The number of the bigger pits is least in the case of cubic faces (figure 9.12). It is obvious from the photograph that pits which are deeper and bigger in area start changing their orientation through 45°. This would mean that pits on the cubic faces are in negative orientation, only the pits which are bigger and deeper change their orientation through 45° and hence they are in positive orientation.

Figure 9.13 shows an interesting pattern on the cubic face of a synthetic diamond etched at 600°C for $3\frac{1}{2}$ hours.

The pattern shows arrays of pits forming a rectangular network. The arrays are in $\langle 110 \rangle$ direction. It is likely that they are projection of $\{111\}$ planes on this face, the planes having higher impurity concentration. Because of this high impurity concentration these projections are preferentially attacked when etched.

Thus the observation at 600°C suggested that

Figure 9.12. (X 240)

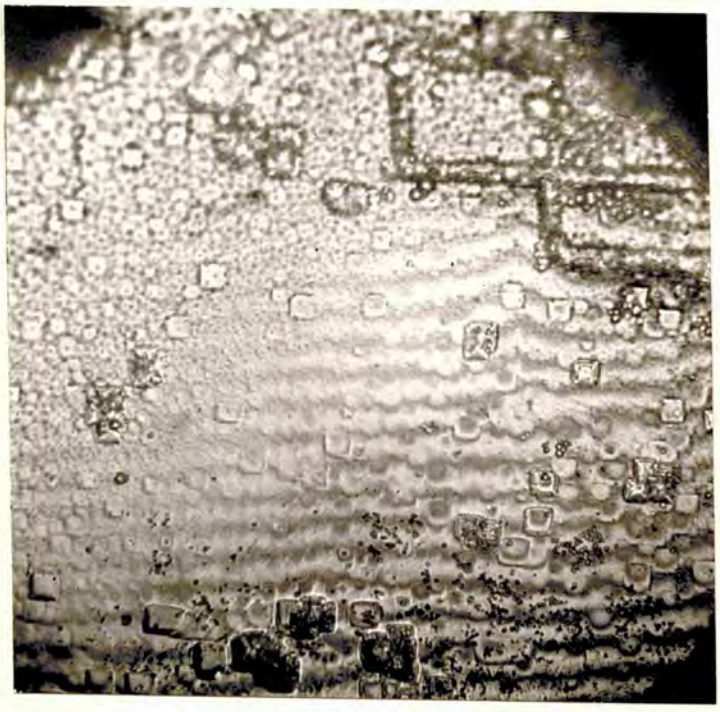

Figure 9.13. (X 300)

Etch rate is highest on the octahedral faces of synthetic diamonds and lesser on the natural octahedral and cubic faces of synthetic diamonds.

9.3 Etching at 650°C and 700°C (Formation of Block-Patterns and Change of Orientation)

Temperature was increased further to 650°C and the etching time was reduced to $1\frac{3}{4}$ hours.

On the octahedral faces of synthetic diamonds at this temperature an interesting block-pattern results. Also at this temperature the etch rate is very high which is evident from the figure (9.14). Pits are very deep: one of the pits is nearly 29 fringes deep i.e. nearly 84000Å. Unlike pits on the natural {111} faces which have curved sides and very rounded corners, these pits have sides which are fairly straight and corners very sharp. If the faces are photographed in reflection, they would give the block-pattern, similar to that observed by Omar, Pandya and Tolansky (1954) on natural {111} faces.

Figure 9.15 shows an etch-pattern at a slip-line, on an octahedral face of a synthetic diamond. The step height can be measured at various points, knowing the

Figure 9.14. (X 450)

Figure 9.15. (X 440)

fringe shift. At 'A' the step height is approximately 6000Å. The step is inclined rather than vertical. Slip on the octahedral faces of natural diamonds was observed for the first time by Tolansky and Omar (1953). It was also studied by Tolansky, Halperin and Emara (1958). According to Tolansky and Omar the slip takes place on $\{111\}$ planes and hence makes an angle of $70^{\circ}\cdot5$ with the face.

The $\{111\}$ faces of natural diamonds showed the usual block-pattern at $650^{\circ}C$. Figure 9.16 shows such a pattern. The pits are very deep and the whole original surface is eaten away. The figure shows the pattern in two-beam interference.

The $\{100\}$ faces of the synthetic diamonds gave striking results (figures 9.17, 9.18,9.19 and 9.20). The surfaces become covered with micro-pits and bigger cavities. As the pits grow bigger and deeper they appear to change orientation. First they become octagonal and as they become deeper still the sides parallel to the $\langle 110 \rangle$ directions diminish in length and the sides in $\langle 100 \rangle$ directions become more pronounced, hence the result is that the pits change their orientation

Figure 9.16. (X 400)

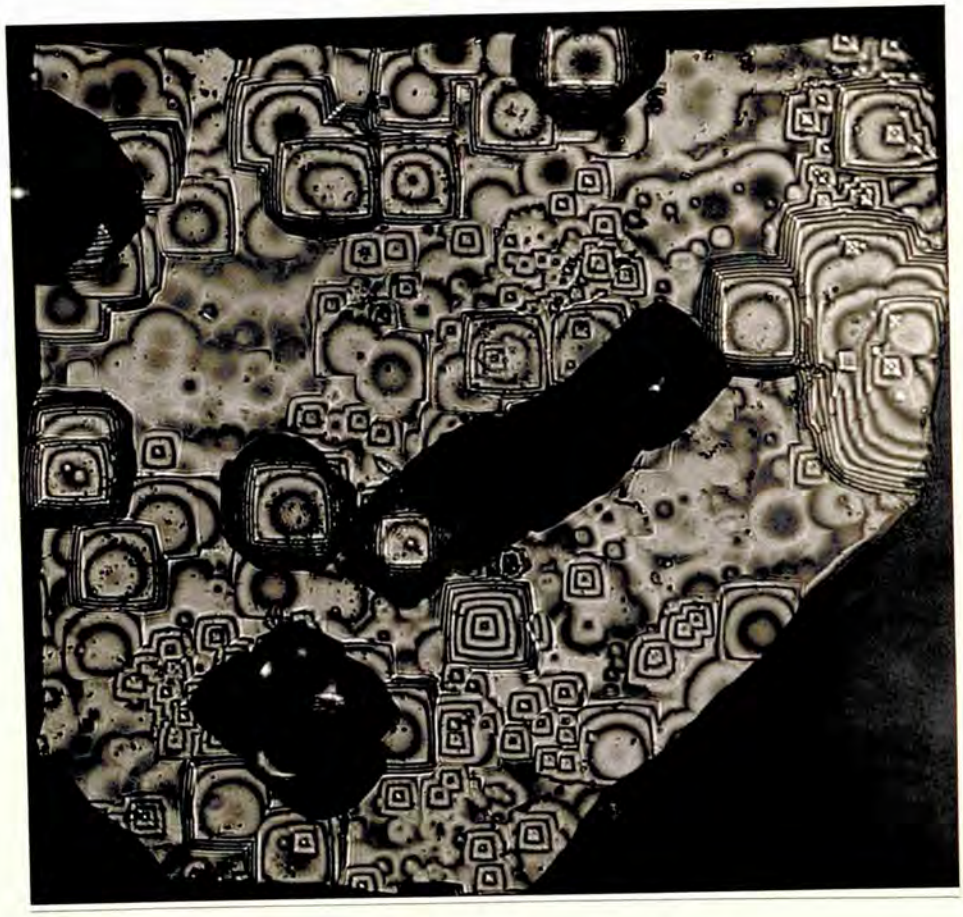

Figure 9.17. (X 345)

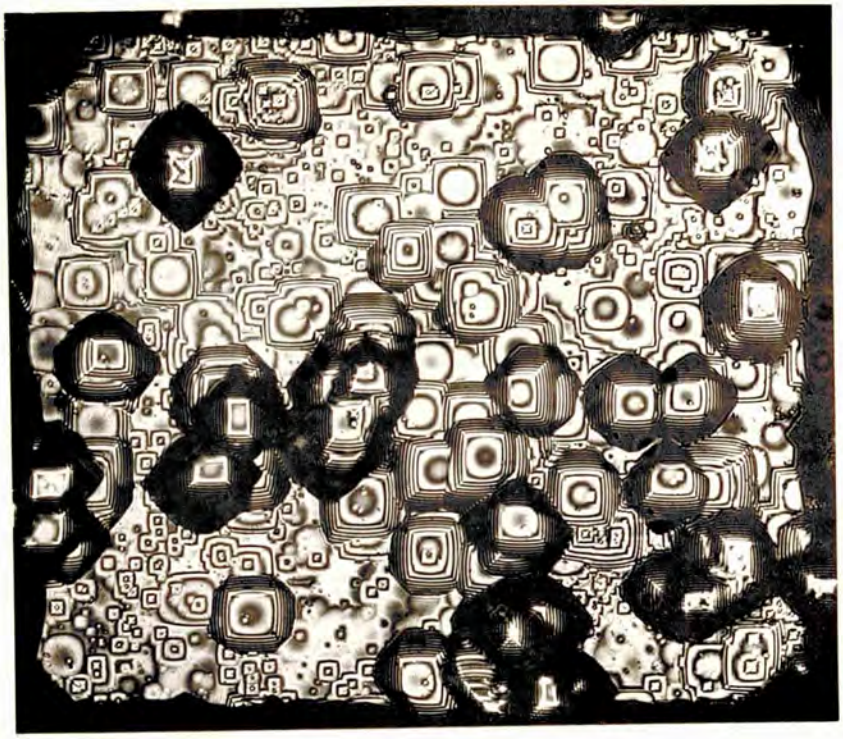

Figure 9.18. (X 250)

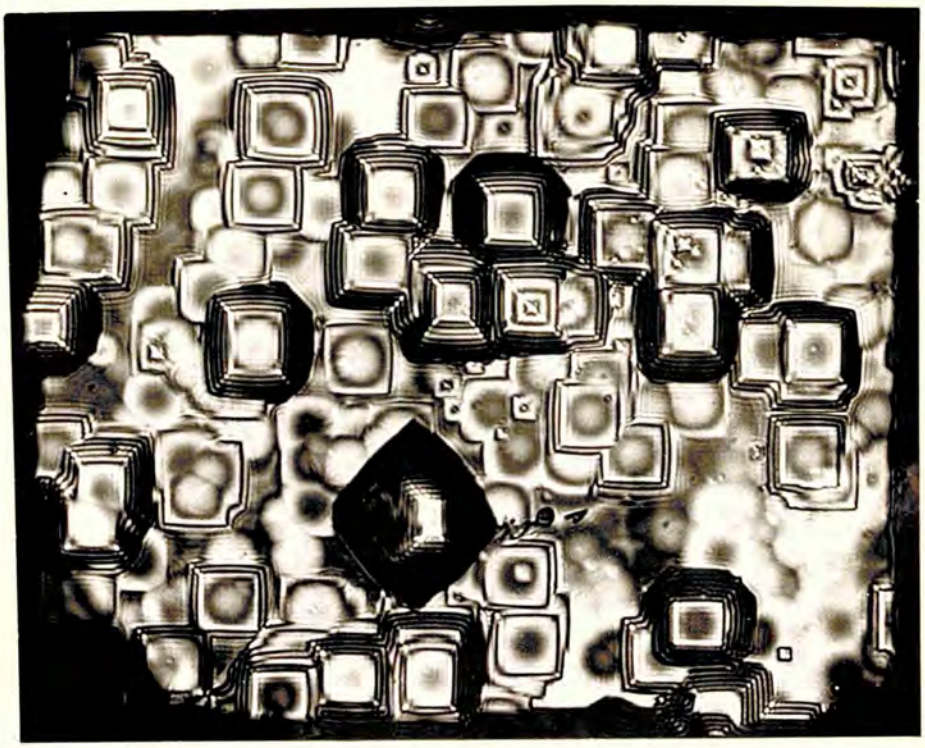

Figure 9.19. (X 400)

through 45^{o} as their depths and extent increase. The figure 9.21 is the schematic diagram illustrating the observed phenomenon. The pits at the various stages of an etch are shown. It is evident from the diagram that as the pits become bigger and deeper, their sides parallel to ⟨110⟩ directions gradually reduce in length and the new sides parallel to ⟨100⟩ directions develop at the cost of the sides in ⟨110⟩ directions. As the depth increases the pits change their orientation completely through 45^{o}. Figures 9.17, 9.18, 9.19 and 9.20 are good examples showing the change of orientation phenomenon. In figure 9.18 there are numerous pits which are big so far as the area is concerned, compared to the micro-pits on the face, but since they are not deep their orientation does not change.

Figure 9.22 shows another interesting feature on the cubic face etched at this temperature - 'a spiral'. This spiral is an elevation. There are various pits arranged along the arms of the spiral. The spirals are an occasional feature on synthetic diamonds (Tolansky and Sunagawa 1959, 1960 a.b.c; Tolansky 1961 b; 1962 a,b).

Figure 9.20. (X 350)

SCHEMATIC DIAGRAM SHOWING THE CHANGE OF ORIENTATION OF THE ETCH PITS

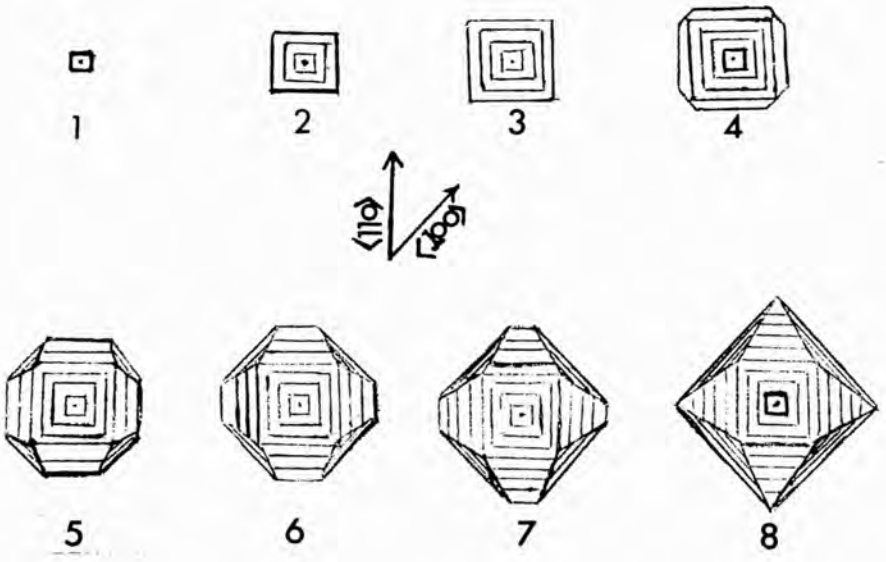

Figure 9.21.

They occasionally observed spirals on the synthetic diamonds from G.E.C. In the present investigation on de Beers synthetics, spirals are not seen very frequently.

To observe and study the effect of the increase in temperature on the change of orientation of the etch pits, the temperature of etching was increased to 700°C, while the etching time was reduced to 45 minutes only.

At this temperature the octahedral faces of synthetic diamonds give striking block-formation. Figure 9.23 shows the pattern obtained at 700°C after etching for 45 minutes. The cavities are very deep on this face. One of the pits is nearly 20 fringes deep (in the top-left corner of the photograph) showing the fierce etching at this point. The pits which are very deep tend to become a little circular. The surface can be photographed in reflection and they give similar block-pattern as obtained by Omar, Pandya and Tolansky (1954) on the octahedral faces of natural diamonds.

Figure 9.24 shows another face. The slope of the pits seems to differ from one pit to the other. One of the pits in the bottom left hand corner is nearly

Figure 9.22. (X 300)

Figure 9.23. (X 400)

Figure 9.24. (X 550)

Figure 9.25. (X 500)

20 fringes deep i.e. 55000Å deep. Sides and corners of these pits on the octahedral faces of the synthetic diamonds are less curved and rounded compared to the pits on the natural octahedral faces.

Figure 9.25 shows one more example. In this figure some of the pits are pyramidal while others are flat-bottomed. The pits range in depth from 6000Å to 24000Å. Pits have sides which are not very curved while the corners are very sharp. The flat bottoms of the pits are amazingly smooth as shown by the two-beam fringes. Figure 9.26 shows the light-profile picture of the face shown in figure 9.25. The shift of the profile indicates that the flat-surfaced feature is a depression.

Figure 9.27 shows the pattern obtained on a natural octahedral face. The original surface has been washed away by etching, and the block-formation results.

Figure 9.28 shows another block-pattern in reflection. The cavities here look like forming the rectangular blocks piled up on one another. This optical illusion was studied in detail for the first time by Omar, Pandya and Tolansky (1954).

The {100} faces of the synthetic diamonds give

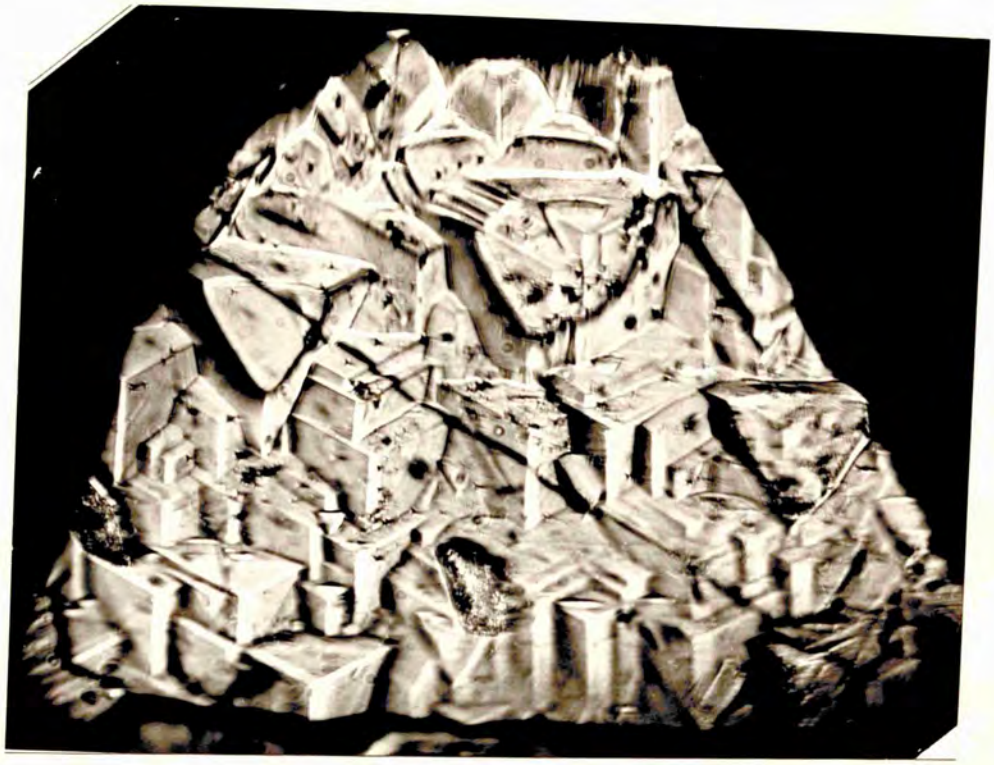

Figure 9.26. (X 500)

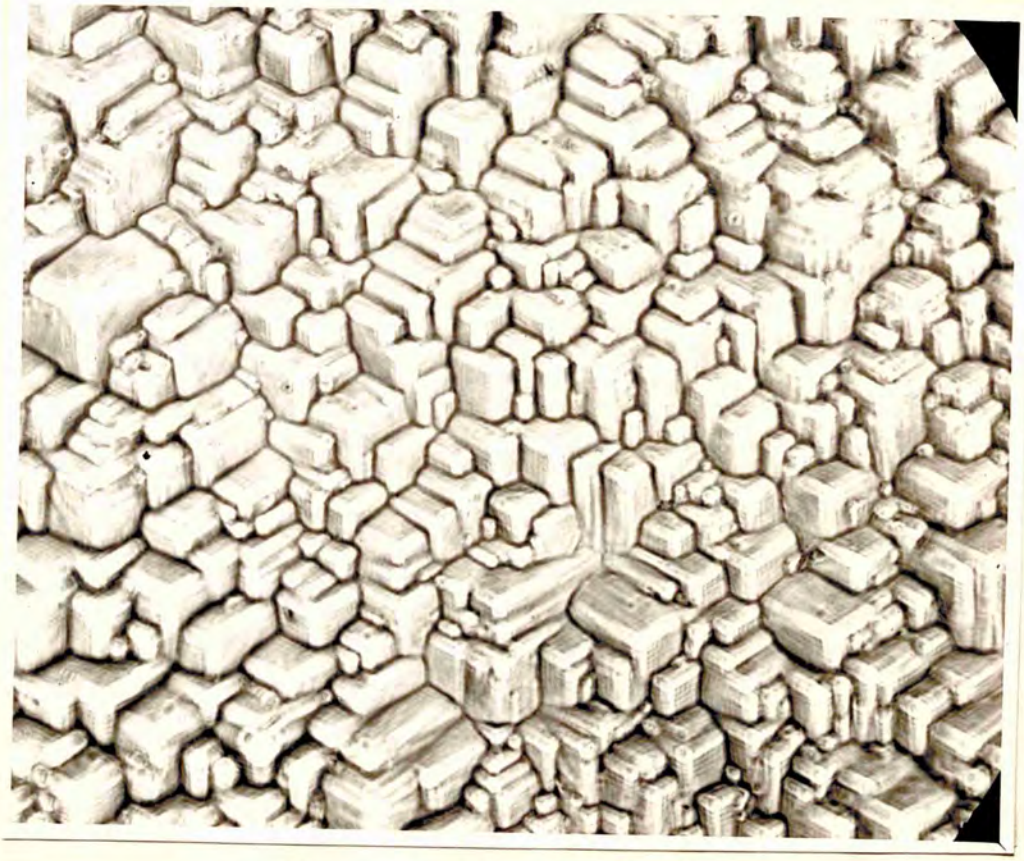

Figure 9.27. (X 150)

similar results. Figures 9.29, 9.30 and 9.31 show the {100} faces of the synthetic diamonds etched at 700°C for 45 minutes. There are very deep cavities on the faces. They exhibit the change of orientation phenomenon. From the figures it is evident that as the depth of the pits increases they tend to become octagonal and if they become deeper still their orientation changes completely through 45°. The minute examination of the pits indicates that they always nucleate in one orientation, but as the pits develop, their relative etch rates in ⟨100⟩ and ⟨110⟩ directions change and hence the pits start changing their orientation. The larger pits in which the orientation has changed, usually become flat-bottomed. The bottom is actually bowl-shaped which is shown by the circular fringes at the centre of the pits.

When the pits change their orientation, the new facets develop in ⟨100⟩ directions. These new facets have steeper slope with the cubic face, which is shown by the dark corners of the pits in two-beam interferograms. These new facets appear on specific planes. The developments of these facets is schematically shown in the

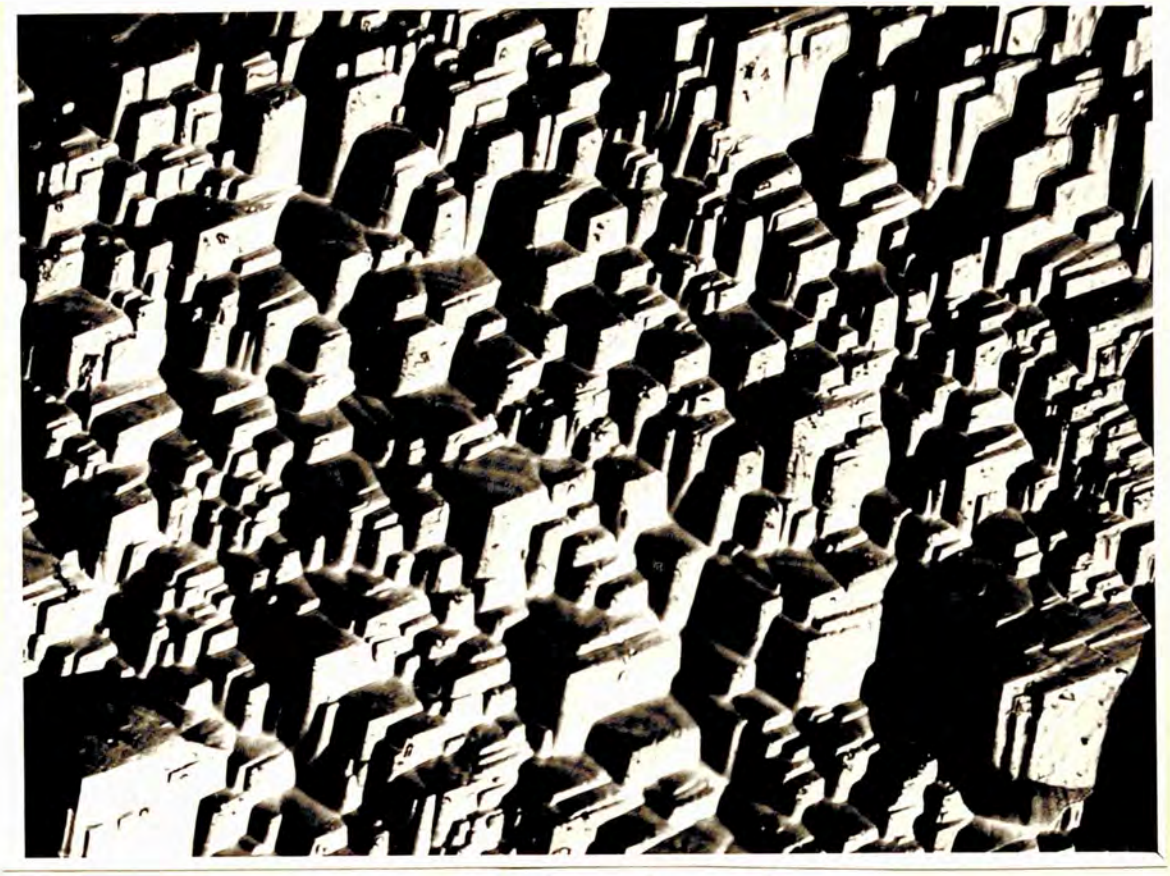

Figure 9.28. (X 150)

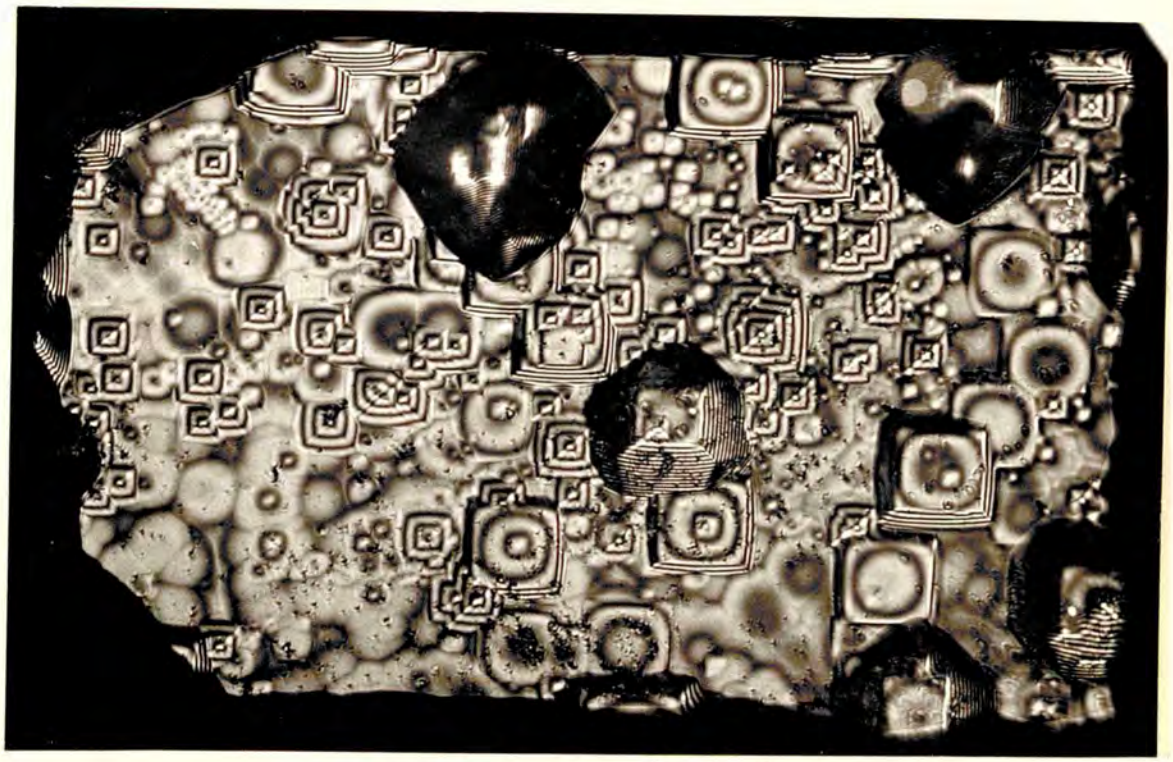

Figure 9.29. (X 400)

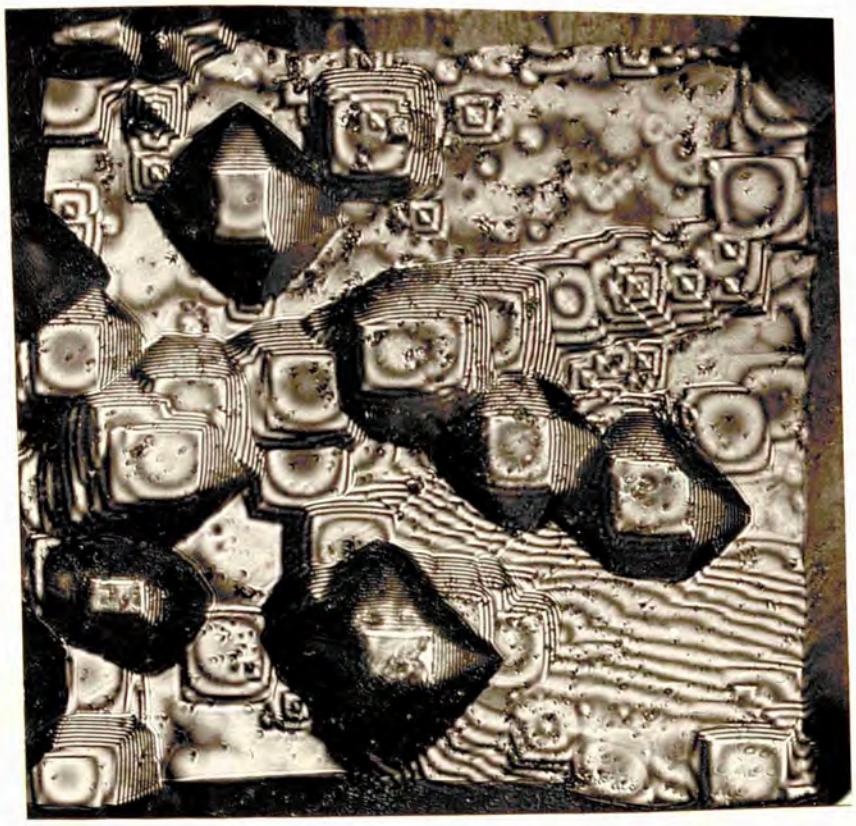

Figure 9.30. (x 400)

Figure 9.31. (x 325)

diagram (figure 9.21). Whether these planes are some fixed planes or these are at random, was checked and it was found that they represent some fixed planes which are of the form $\{102\}$ in the $\langle 100 \rangle$ directions, while $\{114\}$ in the $\langle 110 \rangle$ directions.

The change of orientation takes place only in the case of cubic faces and even here only the bigger and deeper pits change their orientation. This presents a very intricate problem. The fact that only a few pits on the faces change their orientation while the rest maintain theirs would indicate that this is not a characteristic of temperature for otherwise all pits on the face at that temperature would have changed their orientation. One might also think it possible that all pits perhaps develop in the same orientation and as the time of etching increases, some pits tend to change in orientation. But it was found that time of etching had absolutely no effect on the number of pits changing their orientation. This was checked by etching a crystal at $660^{\circ}C$ for $1\frac{1}{2}$ hours and again at the same temperature for a further $1\frac{1}{2}$ hours, when no alteration in the number of pits changing orientation was observed.

9.4 Etching of Polished {100} Section of Natural Octahedral Diamond

Whether the change of orientation is the property of the synthetic diamonds only, or it is the property of cubic planes in general is a question deserving investigation. A cubic face obtained by sectioning and subsequently polishing an octahedron, was therefore etched exactly in the manner described above. It was found that etching proceeded in the same way as with the synthetic diamonds. Figures 9.32 and 9.33 show the etch patterns obtained: most pits are in negative orientation but the bigger and deeper pits (very deep in this case) are in positive orientation (figure 9.32). In addition to the etch pits a stratigraphic pattern similar to that obtained by Harrison and Tolansky (1964) is also seen conspicuously on the face. Figure 9.33 also shows that the orientation of the bigger and deeper pits is opposite to that of the smaller pits. Though the polishing marks and rough surface finish of the cubic face produced anomalous etching making the pattern complicated, it is evident that change of orientation also takes place on the natural faces at about the same

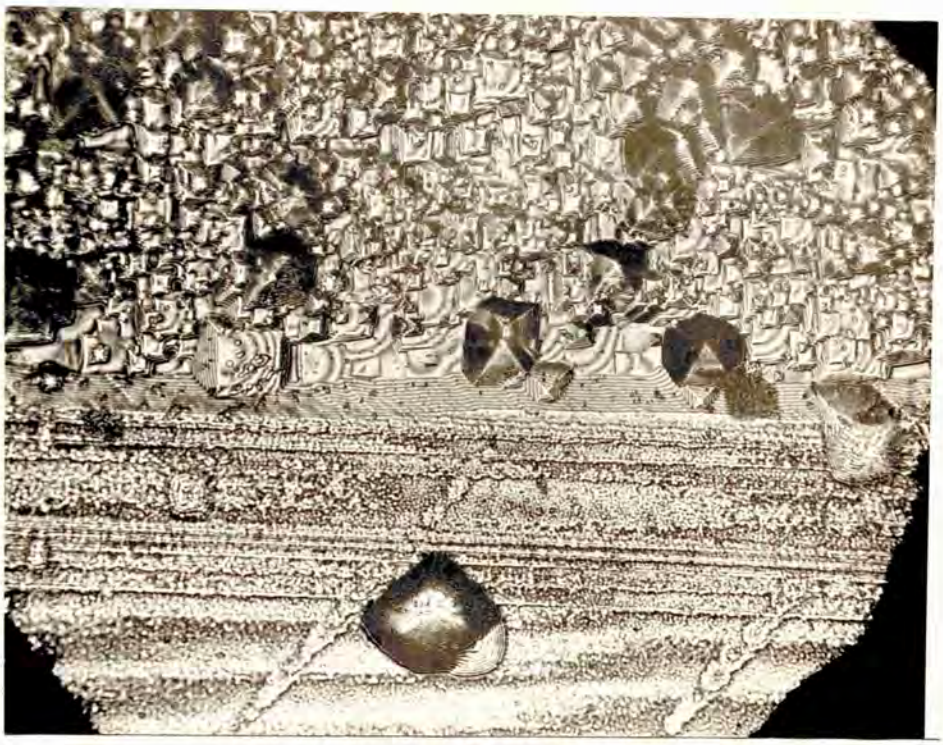

Figure 9.32. (X 150)

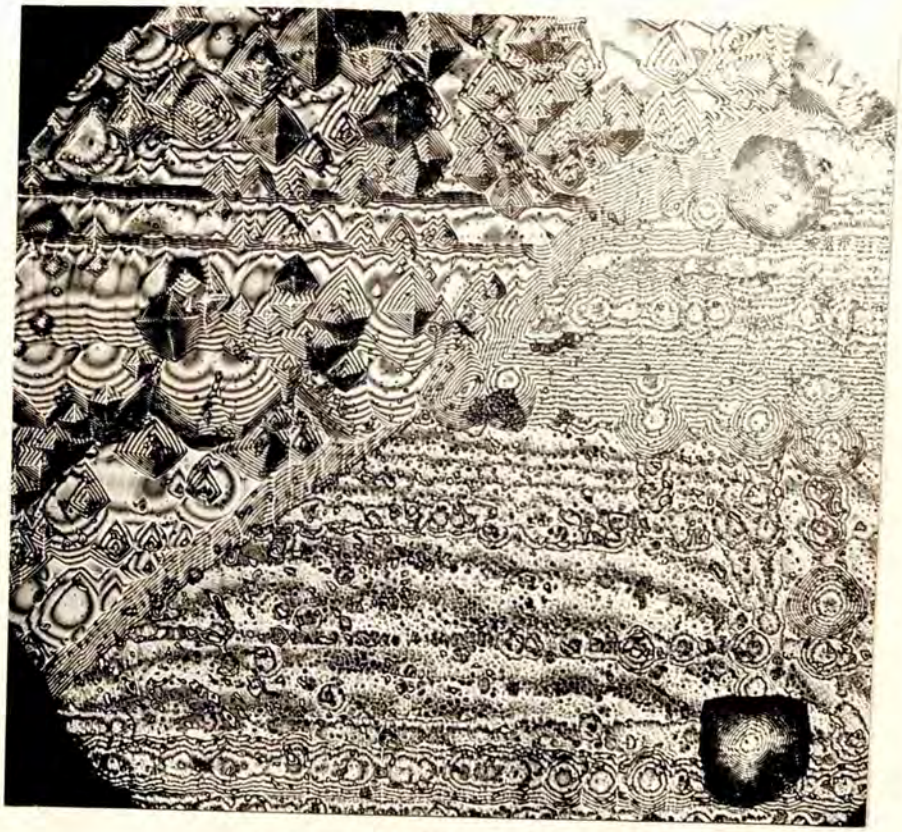

Figure 9.33. (X 150)

temperature. It was confirmed further by etching unusually plane cubic faces of natural cubo-octahedron diamonds (Chapter 10).

9.5 Etching of the Synthetic Diamonds in a Rotating Crucible

Tiwary (1964) observed that as temperature was increased the etch pits on the cubic faces of synthetic diamonds became octagonal. He interpreted this in terms of an explanation given by Honess (1927). According to Honess the pits conform to the shape of the face. Since the cubo-octahedral synthetic diamonds occasionally have octagonal faces, the formation of octagonal pits was considered to be the consequence of the shape of the crystal face. However it is evident from the photographs that faces which are four sided, five sided, six sided and eight sided, all invariably show pits which are square, octagonal and ultimately four sided again but changed in orientation through 45°.

Patel and Ramanathan (1964) obtained etch pits of both orientation by heating the octahedral cleavages of natural diamonds at $850^{\circ}C$ in sodium chlorate. They attributed this to the difference in the energy of the

carbon atoms as one moves away from the site of dislocations, where the pits nucleate preferentially. However if this would have been the case here, all the pits bigger in area irrespective of their depth would have changed their orientation. But figure 9.18 clearly shows that change of orientation is not dependent only upon the extent of the pits.

The observations indicate that the deeper and bigger pits only change their orientation. This would mean that only at the points where the etch rate is fast the orientation change occurs. Since the etch system used was static, it is conjectured that the by-products of the reaction at the points of higher etch rate may not get enough time to escape and could therefore be responsible for the observed change of orientation.

If the etch system is anyhow agitated then this change could be avoided to some extent. To check this, a cylindrical quartz crucible was constructed, having a long co-axial stem attached to a 50 rpm motor (figure 9.34). The crucible, containing a mixture of synthetic diamonds and potassium nitrate, was placed in

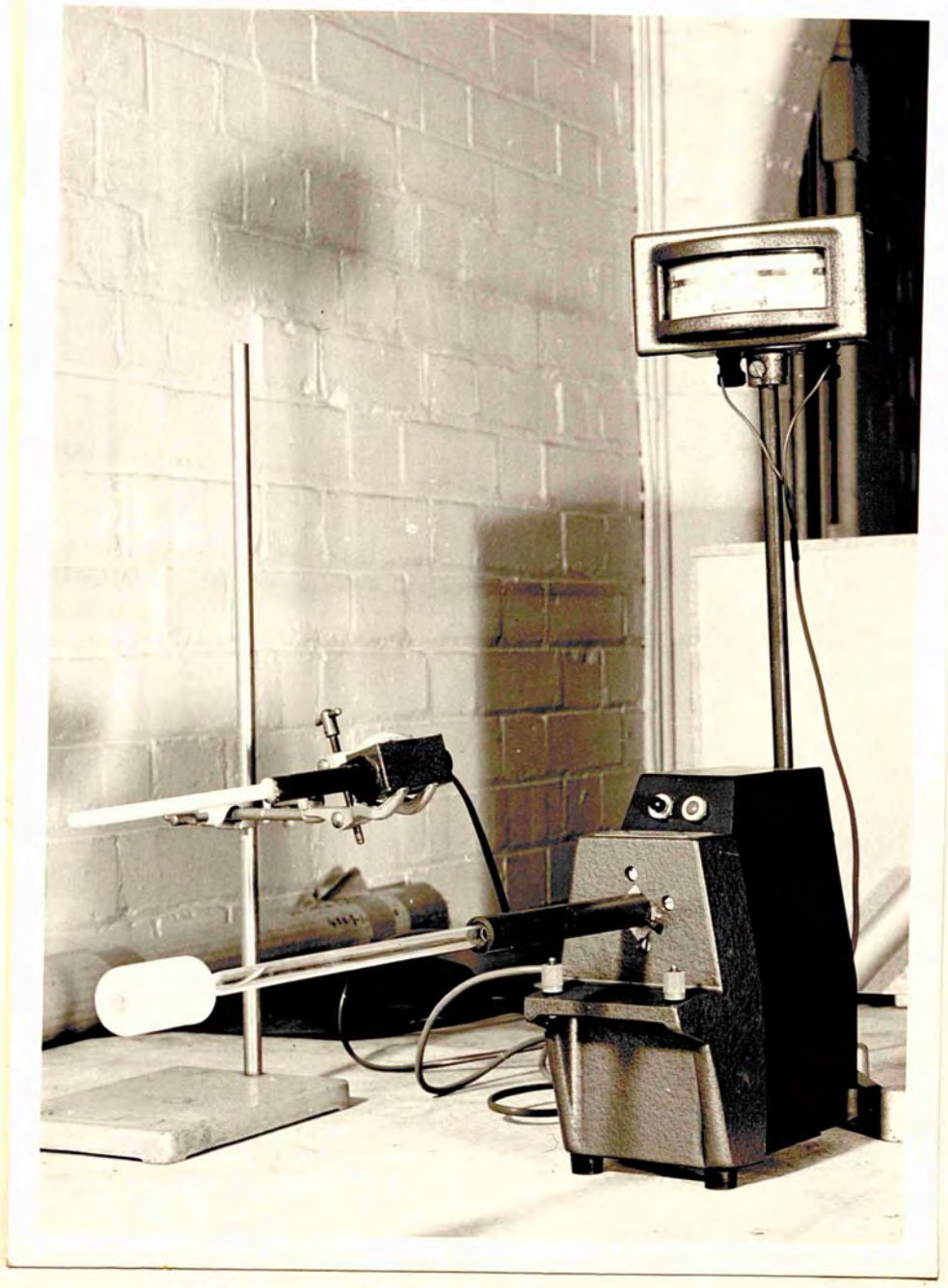

Figure 9.34. (Rotating Crucible)

the cylindrical oven at 680°C (much above the temperature at which the orientation changes start) for 1½ hours.

Figures 9.35 and 9.36 show the characteristic etch patterns obtained in such a system. Although the temperature is much higher than that at which the orientation change previously took place, even then the deeper pits show no change of orientation. Usually at 650°C and at 700°C pits which are 3 fringes deep start changing their orientation but figures 9.35 and 9.36 clearly indicate that the pits much deeper than 3 fringes remain in the same orientation. In figure 9.35 there are various pits having depth of about 9 fringes and another very dark pit having depth of about 15 fringes. They all seem to maintain their orientation.

9.6 Further Discussion about the change of Orientation of the Etch Pits

Having decided that the change of orientation of the pits is a consequence of fast etching where the by-products of the reaction start reacting with the surface, the question arises as to what these by-products may be.

Figure 9.35. (X 400)

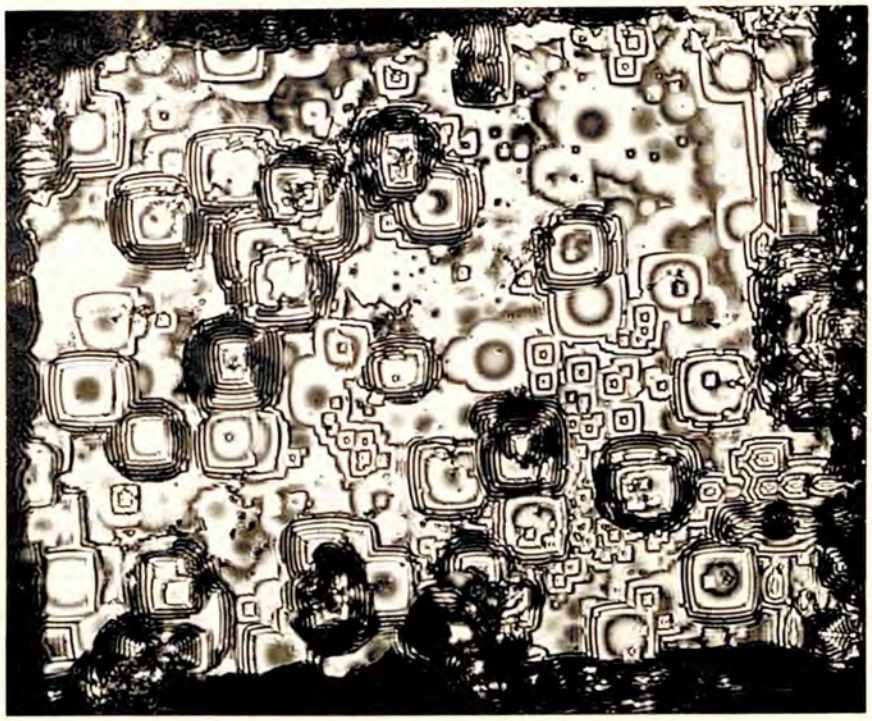

Figure 9.36. (X 400)

Rudenko and Kulakova et al. (1965) during their experiments with alkali-metal hydroxides and carbonates suggested that these salts just act as catalysts, and diamond is etched by the atmospheric oxygen. They established further that carbon dioxide is the product of the reaction. At about 800°C they obtained positive pits with carbon dioxide.

Karklina and Mastakovets (1969) during their etch experiments with KOH, KNO_3, NaOH, Na NO_3 and Na_2 O_2 separately as well as mixture, concluded that the mechanism of etching in the above alkalies and salts is similar to that in air, because the activation energy within the temperature range 560°C to 700°C was the same (45 ± 2KCal/Mol) as obtained by etching diamond in air. This indicates that carbon dioxide is the by-product of the reaction of diamond etching with potassium nitrate.

Sappox and Boehm (1968) performed infrared spectroscopy on the surface of etching diamond powder and observed that oxygen is chemisorbed even at room temperature and carbon dioxide is produced at about 500°C.

Similar observations were made by Murphy and Ritter (1970) during their etch studies with electron beams. They observed that carbon dioxide is produced at

about 500°C and at about 650°C the carbon dioxide starts attacking diamond.

Thus it is likely that carbon dioxide is produced as a result of heating the crystals in potassium nitrate and this carbon dioxide so produced may be the agent which causes etching at about 600°C - 650°C leading to the change in the orientation of the etch pits. Additional proof was provided by etching the crystals in the rotating cylinder so that the by-products of the reaction were encouraged to escape partly and thus the change of orientation was partially prevented.

An explanation has therefore been suggested as to why the pits which always nucleate in one orientation, start changing their orientation at about 600°C to 650°C. Since the by-product of the reaction carbon dioxide, which is the likely reagent responsible for the change in the orientation is evolved at the above temperature in large amounts at the sites of fast etching, the orientation change takes place only at these points.

Similar orientation change was observed in case of the natural cubic faces (Chapter 10) which proves that the change of orientation of the etch pits is the inherent property of the cubic faces.

CHAPTER 10

STUDIES ON CUBO-OCTAHEDRAL FORM OF NATURAL DIAMONDS

10.1 Introduction

The work described so far, has been upon synthetic diamonds from de Beers and Co. South Africa, studied optically and electron-optically and by the method of etch. While carrying out etch studies these crystals were etched simultaneously with Premier Mine diamonds of comparable size in order to study the two types comparatively under identical conditions. The synthetic diamonds were cubo-octahedral in form and therefore had cubic as well as octahedral faces, while in the case of the natural micro-crystals from Premier Mine, which were either octahedral or macle, only {111} faces were present. Thus the comparative studies were incomplete, until the cubic faces of the natural diamonds were studied by the method of etch.

The naturally occurring {100} faces on cubic diamonds are extremely rough and therefore are unsuitable for precision etch studies. This is the reason for the

extensive literature describing surface topographical and etch studies on the octahedral faces in contrast with the infrequently reported studies on natural {100} faces. However Pandya and Tolansky (1954), Seal (1962 c,d), Patel and Ramanathan (1962) and Harrison and Tolansky (1964) have studied polished {100} faces of the natural diamonds. These workers tried to study surface etch phenomenon by sectioning, polishing and subsequently etching the sections. But according to Honess (1927) "The surface characteristics of the face and crystal in general have an important bearing upon the features revealed by etching. Scratches may produce anomalous features, therefore great care is needed in selecting the crystals. As a rule small crystals having natural surfaces give better results".

In view of this, etch studies on cut and polished faces are liable to artefacts introduced by the preparation process. Thus far, the only etch studies reported for {100} diamond faces have been on such surfaces. The present work describes for the first time studies on good <u>natural</u> {100} faces of the cubo-octahedral diamonds.

While studying Premier Mine micro-diamonds in detail, cubo-octahedral natural diamonds were discovered. Nearly 1% of the perfect water-white crystals of nearly 30 - 40 mesh size are cubo-octahedral in habit. These are perfectly water-white octahedra having few or all corners truncated. Both in shape and size they are comparable to the synthetic diamonds. This similarity of shape and size of the natural and synthetic diamonds should allow meaningful comparative studies to be made.

These natural cubo-octahedral crystals were also studied optically and electron-optically and finally by the method of an etch.

10.2 Studies by Two-Beam Interferometry

The cubic faces of these diamonds are smooth and specular, unlike the faces of the natural cubes. Figures 10.1 and 10.2 show the typical examples. Faces are very flat and smooth. Sometimes because of the extremely small size of these faces (which is of the order of 10^{-4} sq. cm.), it is very difficult to re-locate a particular face. Moreover their minute size and difficulty of manipulation renders multiple-beam inter-

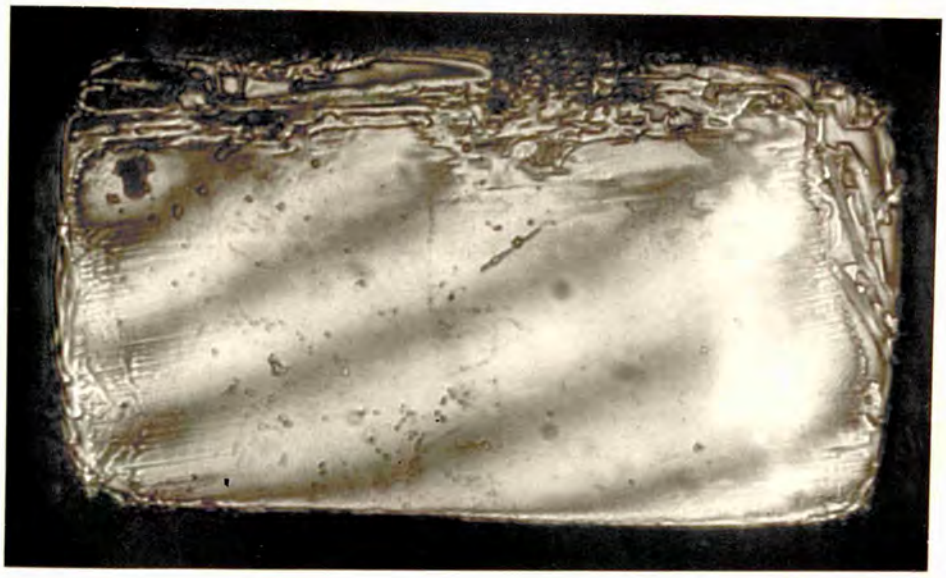

Figure 10.1. (X 300)

Figure 10.2. (X 350)

ferometry impossible, they were therefore studied by two-beam interferometry which proved adequate.

As two-beam interferometry reveals, some of the cubic faces are very smooth and flat, while others show very remarkable surface pittings. This pattern is crystallographically oriented, and relates to the symmetry of the face. The pits have their sides parallel to ⟨110⟩ directions. Figures 10.3, 10.4 and 10.5 show faces of this type. The fringes show the pits to be on very smooth areas. The pits are not very deep and are flat-bottomed. Their sizes are fairly similar. The pits have sharp corners forming an angle of 90^{o}. The sides of the pits are usually rectilinear. In addition to these pits there are some rectangular channel-like features. These channels are parallel to the face edges and hence are crystallographically oriented in ⟨110⟩ directions. There are some pits (figure 10.5) showing truncation of corners. Truncation of the corners of the natural square cavity on {100} faces has been seen for the first time.

Whether these surface markings are due to a natural etch or are due to growth, presents a very

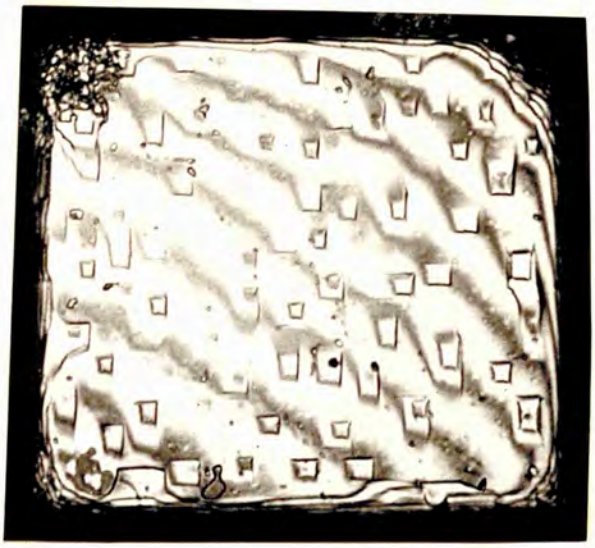

Figure 10.3. (X 450)

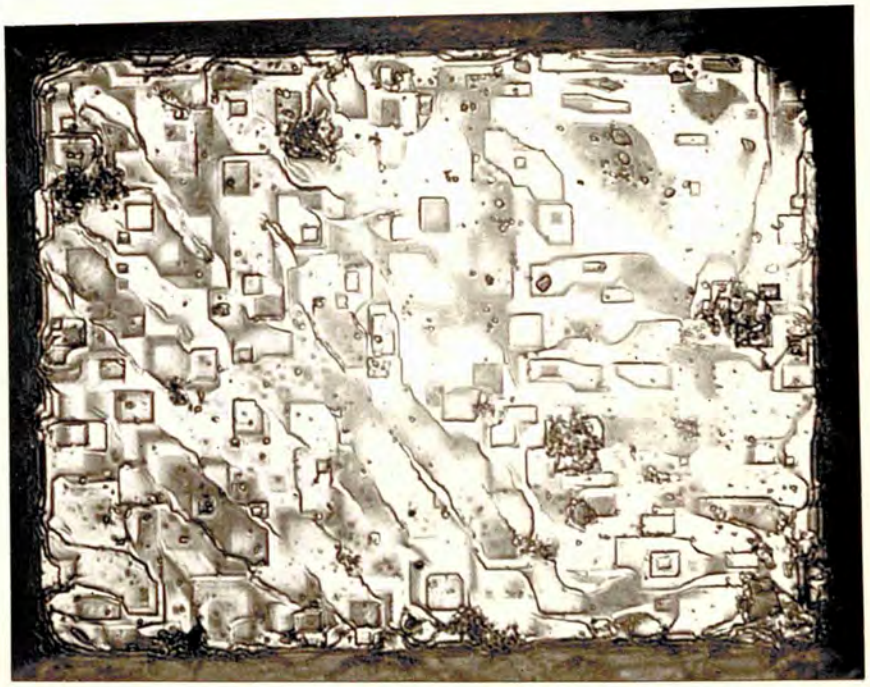

Figure 10.4. (X 380)

Figure 10.5. (X 550)

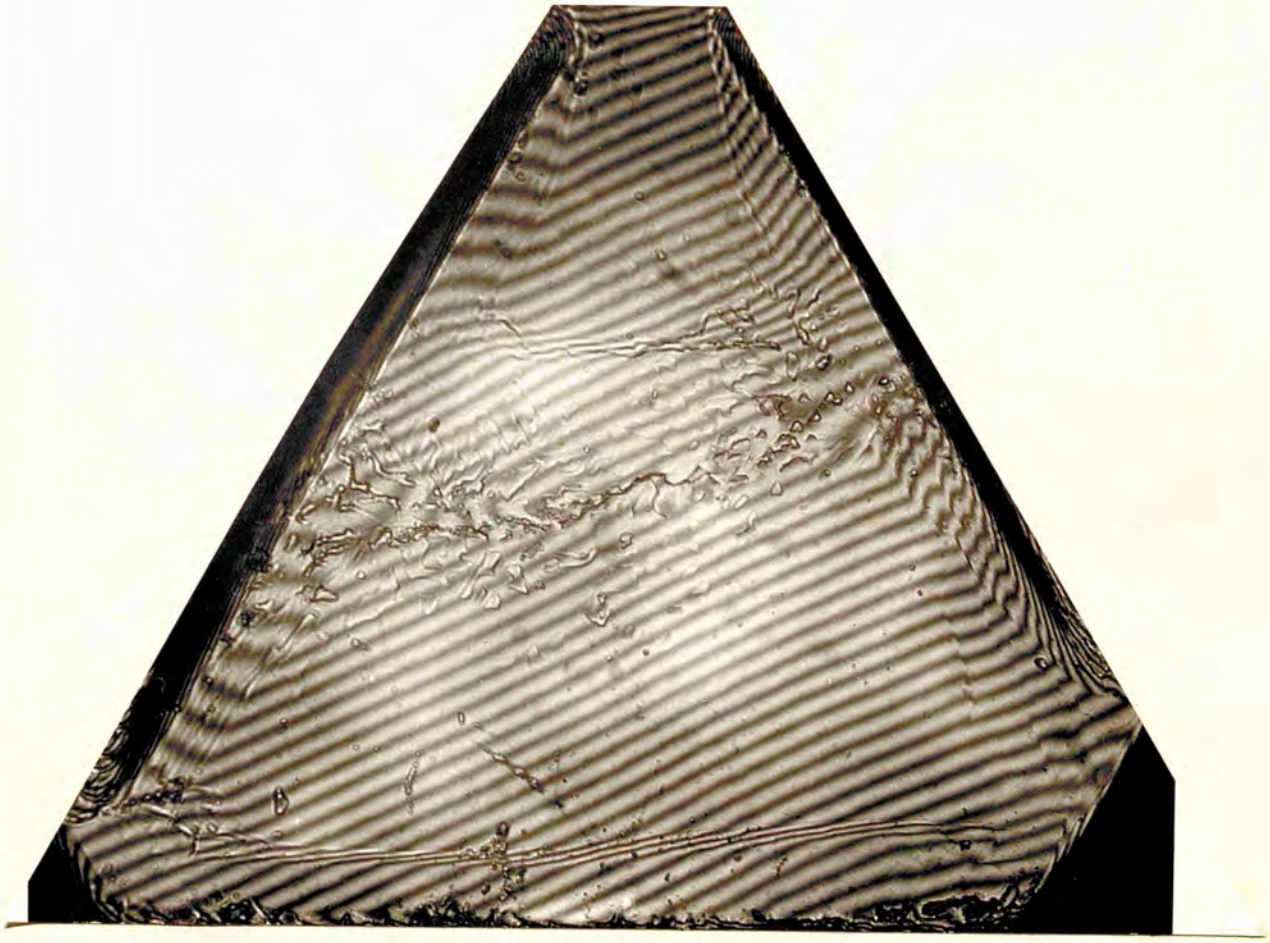

Figure 10.6. (X 300)

interesting problem. In order to decide this, each crystal was studied in detail. As indicated above, the majority of the faces are plane or show very shallow surface pittings which are crystallographically oriented. Some of the faces show the crystallographic channels. In addition to these, there are channels on some faces which show zig zag sides (figures 10.7 and 10.8) and some of these channels are along ⟨100⟩ directions (figure 10.8). The channels look like dendritic pattern which is always present on the faces of synthetic diamonds.

Like the long-standing controversy about the trigons on octahedral faces and so-called quadrons on cubic faces and the rounded form of the dodecahedral crystals, whether these forms are due to an etch or are the result of growth under different conditions of temperature and pressure presents a similar dilemma.

The two-beam interference pictures indicate that the topography of the cubic faces of cubo-octahedra is different in various aspects from the topography of the cubic faces of natural cubes, though in both cases the cavities are square and have sides parallel to ⟨110⟩ directions. The differences are as follows:-

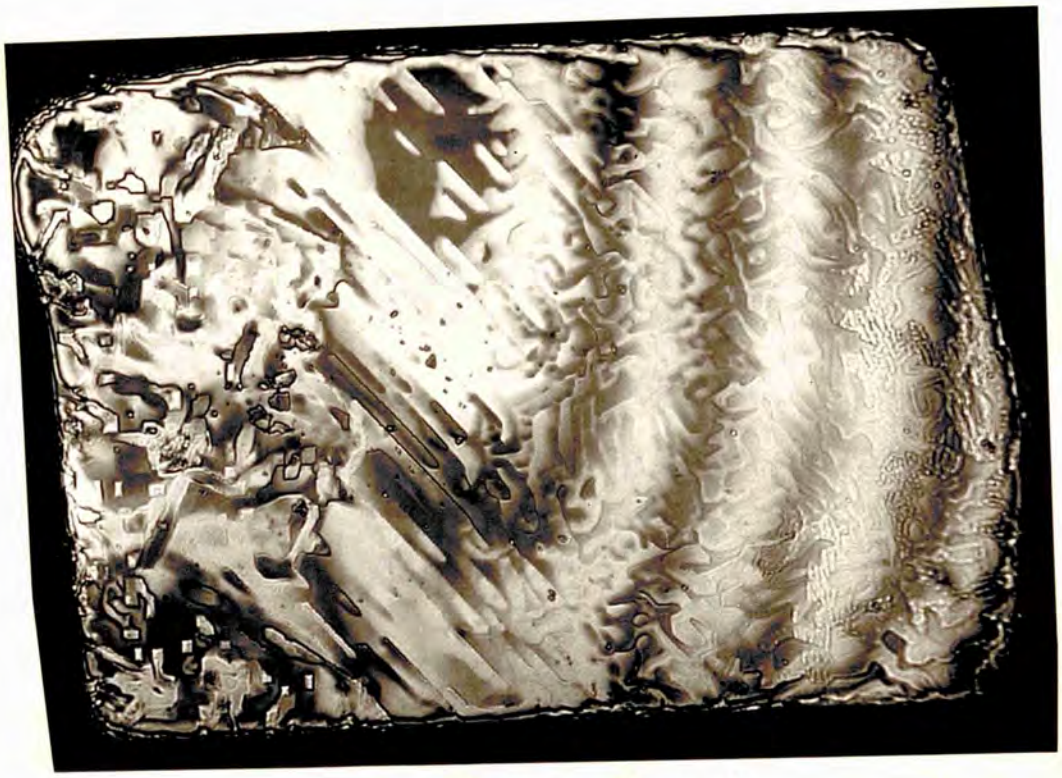

Figure 10.7. (X 350)

Figure 10.8. (X 300)

1 - The "quadrons" are usually point-bottomed, while the cavities on the cubo-octahedra are flat-bottomed (figures 10.3, 10.4 and 10.5).

2 - "Quadrons" show terraces and layers and they are deeper in comparison to cubo-octahedral pits which are shallow and usually show no terraces.

3 - In the case of natural cubic faces there are no crystallographic or zig zag channels present. Moreover the "quadrons" have never been seen, having truncated corners, while in the case of the pits on the cubic faces of cubo-octahedra, there are some crystallographically oriented and zig zag channels and some of the pits have truncated corners (figures 10.3, 10.4 and 10.5).

4 - "Quadrons" are usually good squares (Chapter 11) while the pits on cubo-octahedra are sometimes rectangular as well as square (figures 10.4 and 10.5).

5 - In contrast to the natural cubic faces which are very rough these cubic faces on cubo-octahedra are very smooth and specular, as shown by the figures 10.1 and 10.2.

All these points evidently show that the topography of the cubic faces of natural cubo-octahedra is different from that of the natural cubic faces and it

also seems clear that surfaces have undergone a mild etch in nature. This is further confirmed by the presence of etch-like cavities on very smooth {111} faces of the crystals (figure 10.6). The cavities are positively oriented.

10.3 Studies by the Method of Etching

In order to study further, whether the faces were etched in nature or not, the crystals were etched in potassium nitrate at various temperatures, starting from 550°C. All the cubic faces of these crystals were photographed at all these stages of an etch. Figures 10.1, 10.2, 10.7, 10.8 and 10.9 show the representative cubic faces before etching, while figures 10.6 and 10.10 show octahedral faces, which are also unusually smooth and plane as revealed by the interference fringes.

Crystals were etched at 560°C for 3 hours. The pits formed were very small, therefore the crystals were etched again for $2\frac{1}{2}$ hours. After etching for $5\frac{1}{2}$ hours altogether though the pit density increased, the pits were still too small to be clearly resolved by two-beam interferometry. Figures 10.11 and 10.12 show one of the cubic and octahedral faces respectively, etched

Figure 10.9. (X 300)

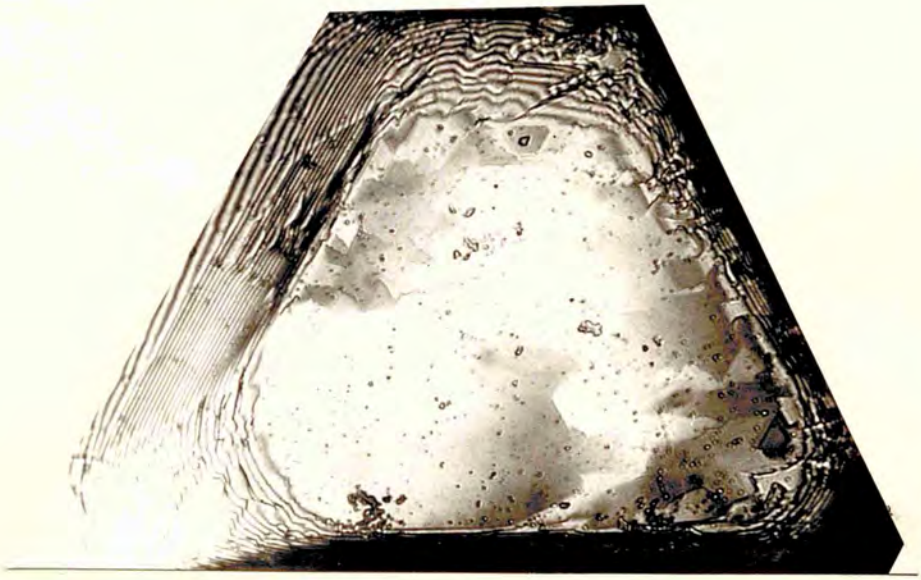

Figure 10.10. (X 300)

at 560°C for $5\frac{1}{2}$ hours. In the case of the cubic face (figure 10.11) the pits are negative i.e. have sides parallel to ⟨110⟩ directions. In the case of octahedral faces the pits are positive. This was confirmed by viewing the crystal at low magnification in a stereo-microscope. The pit density is higher on octahedral faces, which agrees with the observations on the synthetic diamonds during the present work and also with the observations on natural and synthetic diamonds by other workers (Evans and Phaal 1961; Patel and Agarwal 1966 b).

The crystals were etched further for $2\frac{1}{4}$ hours but now at 600°C. At this temperature the pits became bigger in size. Figure 10.13 shows the octahedral face after being etched at 600°C for $2\frac{1}{4}$ hours. The face shows that because of the increase in the temperature of etching, the overall pit-density has not increased but the number of bigger pits has increased suddenly. There are rows of etch pits seen on this figure in ⟨110⟩ directions. These rows become more prominent as the temperature is increased. This pattern may be the result of either a local slip or a crack formed by impact. Figure 10.14 shows one of the cubic faces. Pits are

Figure 10.11. (X 300)

Figure 10.12. (X 200)

Figure 10.13. (X 225)

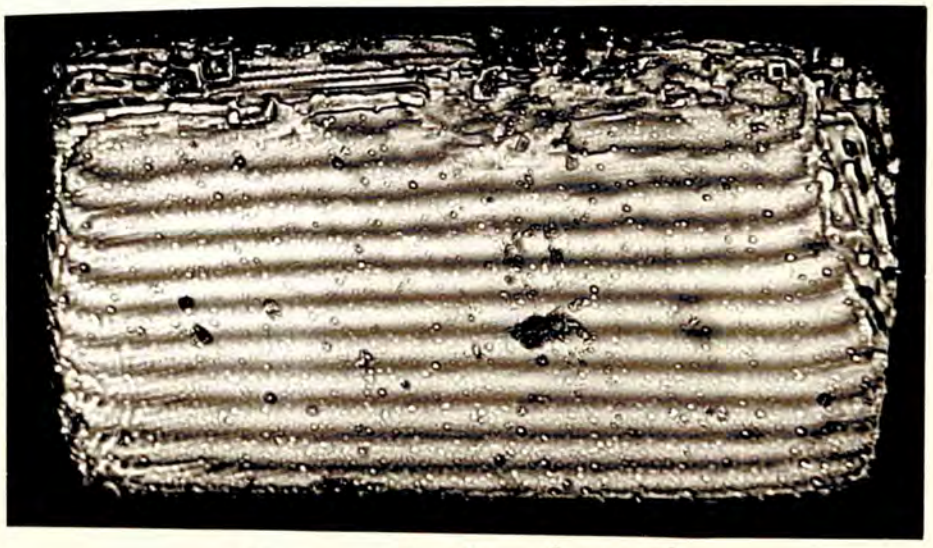

Figure 10.14. (X 300)

generally still very small. Their orientation is such that their sides are parallel to face edges.

Figure 10.15 shows the micrograph of the face shown in figure 10.8, after etching. The comparison shows that even after etching for $2\frac{1}{4}$ hours at 600°C, the initially existing channels are still visible, but have become wider. The previously occurring pits on the unetched faces definitely become bigger and many new pits nucleate having the same negative orientation as that of the pre-existing pits. The pits are numerous and tend to overlap.

Figure 10.16 illustrates another cubic face, shown in figure 10.9 prior to etching. The comparison of the two micrographs shows that naturally occurring channel-like features are still visible. The majority of the pits have negative orientation, while there are a few pits near the corners of the photograph having positive orientation i.e. having their sides parallel to $\langle 100 \rangle$ directions. These pits are too small for any change of orientation to be clearly observed, therefore the crystals were etched further for $1\frac{1}{2}$ hours at 650°C, and when perceptible changes did not occur, they were etched further

Figure 10.15. (X 300)

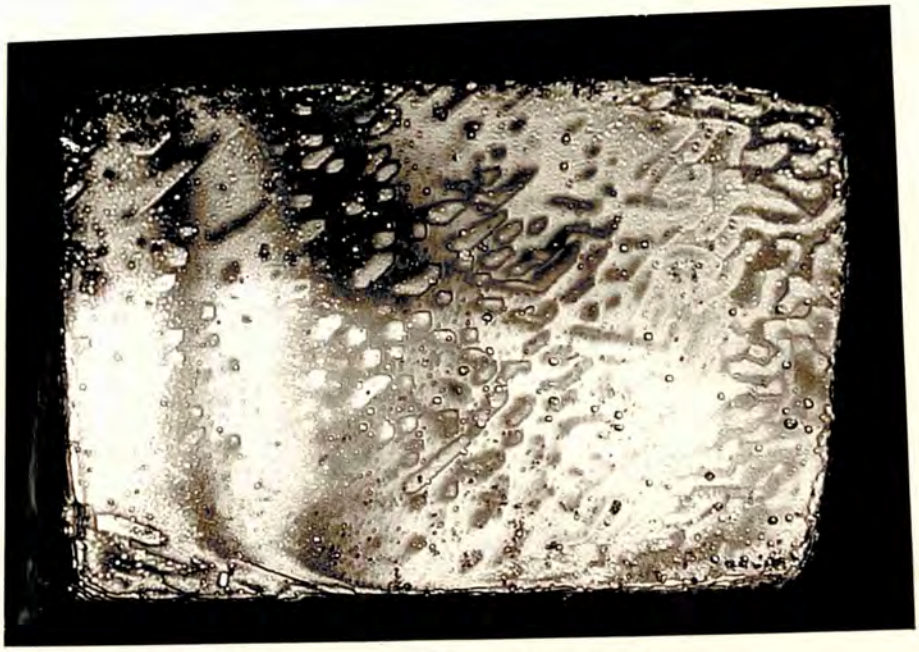

Figure 10.16. (X 300)

at the same temperature for another 1 hour.

Figure 10.17 illustrates the face shown in figure 10.1 after being etched at various stages. It is notable that even in the case of these natural crystals, as with synthetic crystals, the pits which are deeper and bigger change their orientation through 45°.

Figure 10.18 illustrates the cubic face, shown in figure 10.2 before etching. The figure 10.18 shows the face after being etched at $650^{\circ}C$ for $2\frac{1}{2}$ hours. It is quite evident from this micrograph that larger and deeper pits are at 45° to the remaining pits. Thus it is clear that only larger and deeper pits change to positive orientation i.e. having sides parallel to $\langle 100 \rangle$ directions, while the smaller pits have orientation in negative direction.

Figures 10.19, 10.20 and 10.21 exhibit the faces shown in figures 10.7, 10.8 and 10.9 respectively, after being etched through various stages. The faces invariably show the same result as that shown by the cubic faces of synthetic diamonds. Here also the pits nucleate in the negative orientation and at about $600^{\circ}C$ or $650^{\circ}C$, when the etch rate is appreciable at certain

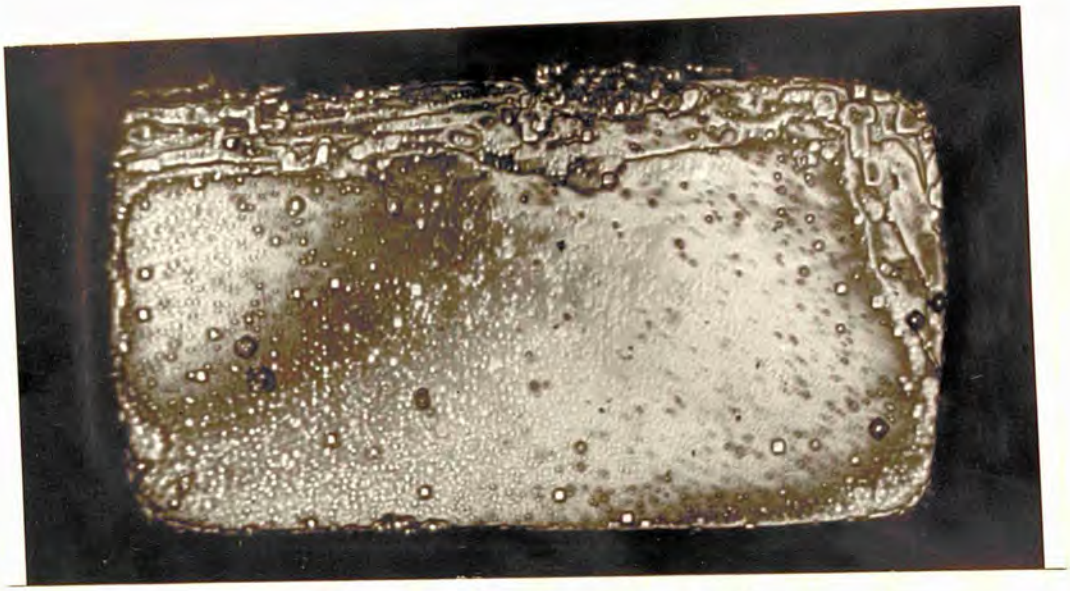

Figure 10.17. (X 300)

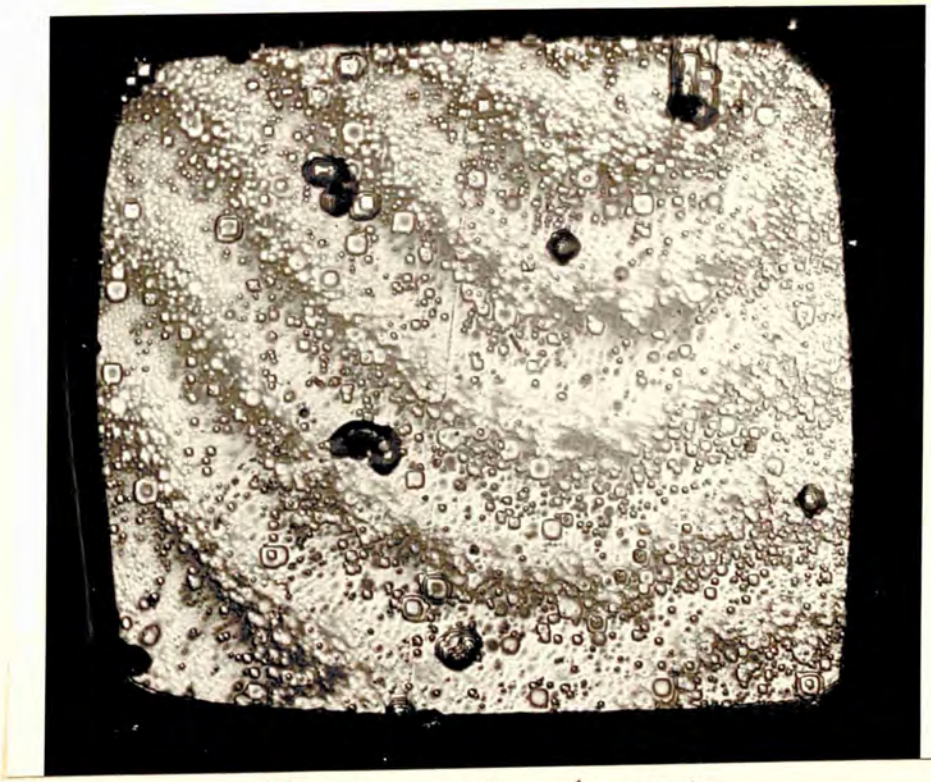

Figure 10.18. (X 350)

points, then the pits start changing their orientation.

The only difference between the synthetic diamonds and these natural crystals is that, there are very few points on the natural surfaces where the etch-rate is high, while in synthetic diamonds, because of the high density of inclusions, the etch-rate at many points is high and thus the orientation change takes place at all these points.

The octahedral faces show the usual block-pattern (figure 10.22).

These etch experiments indicate that at low temperature the pits produced by etching have the same orientation and are exactly similar to the naturally occurring pits on the {100} faces of the cubo-octahedra. It therefore seems likely that crystals have undergone a mild etch in nature. Secondly, these experiments on these natural cubo-octahedral crystals indicate that change of orientation always occurs at the same temperature in synthetic as well as natural crystals.

10.4 Electron Microscopic Studies

The faces of these crystals as mentioned above are very rare and unusually smooth; therefore they were

Figure 10.19. (X 350)

Figure 10.20. (X 300)

Figure 10.21. (X 280)

Figure 10.22. (X 350)

studied in detail with the help of an electron microscope. The crystals were mounted for one particular face of interest. After studying the faces by two-beam interferometry the usual two-stage replication was carried out. The replicas so obtained were examined in the A.E.I. EM_6 electron microscope. The crystals were remounted for studying the other faces of interest.

Figures 10.23 and 10.24 show two of the most smooth-looking crystal faces. These faces were replicated and it was found that electron micrographs revealed further details about these faces.

Figure 10.25 shows the rectangular pits and stripes most likely to be formed by the arrays of the etch pits. As expected, these pits represent the four fold symmetry of the face. Electron microscopy confirms that the pits look very smooth and have very flat bases. Some of the pits overlap to form an array. The estimated depth of the pits from shadow cast, varies from 200Å to 700Å. Figure 10.26 shows the etch-like features on such faces. The pits are crystallographically oriented but their sides are not very straight. There are various micro-pits on the bottoms of these features.

Figure 10.23. (X 200)

Figure 10.24. (X 300)

Figure 10.25. (X 11,000)

Figure 10.26. (X 10,000)

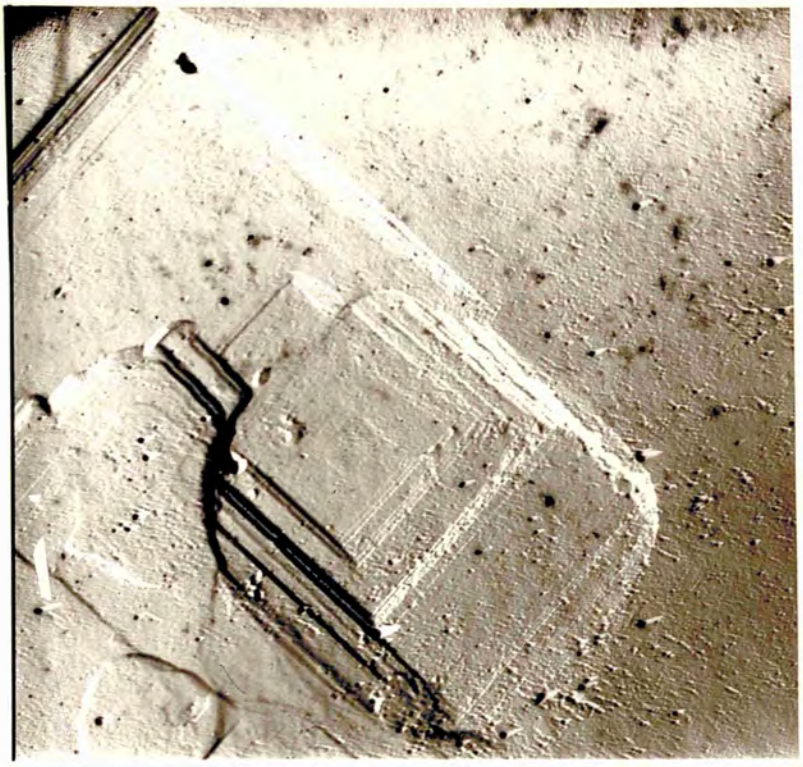

Figure 10.27. (X 9,000)

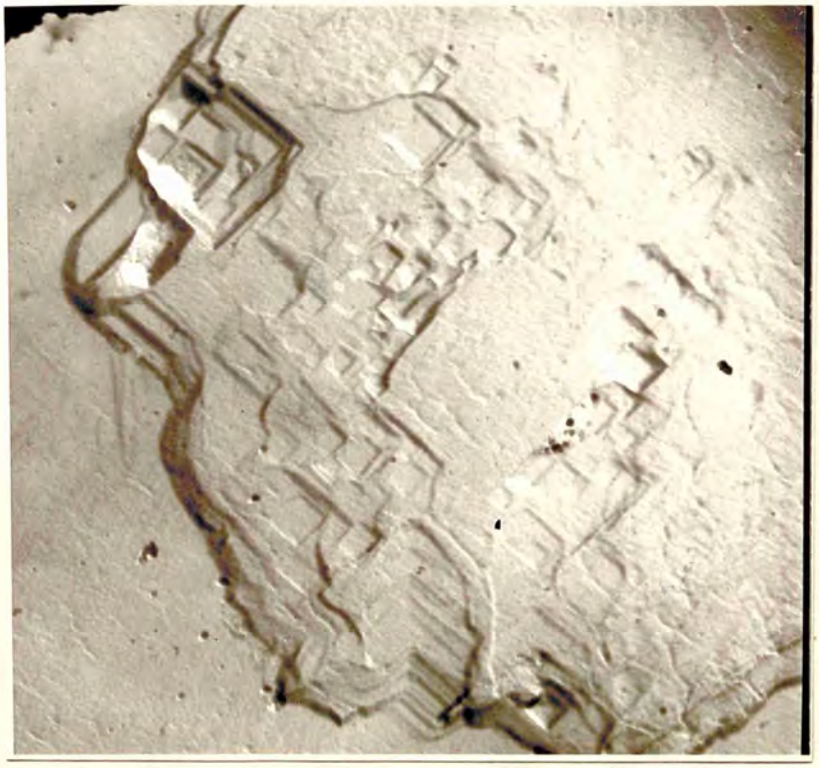

Figure 10.28. (X 10,000)

Figure 10.27 shows some larger pits. There are various layers revealed on the sides of these pits. Layers upto an estimated 50Å can be easily resolved. Figure 10.28 shows features which are apparantly due to etch. There looks like a solution hillock on the face, upon which there are various micro-pits. This picture definitely shows an etch effect. Similarly figure 10.29 shows square cavities on the face, which are most probably due to dissolution.

Figure 10.30 shows etch-like network pattern. The pits are nearly all of the same size and their depth is also nearly the same ranging from 500Å to 1000Å. All the pits have sharp corners with angle of 90° and are flat-bottomed, suggesting a dissolution effect.

Figures 10.31 and 10.32 show terraced pits and solution channels. The pits have perfectly rectangular corners.

Thus the minute surface details observed by an electron microscope suggest that the surface has been etched in nature.

10.5 Discussion

Having decided that the crystals have undergone

Figure 10.29. (X 17,000)

Figure 10.30. (X 10,000)

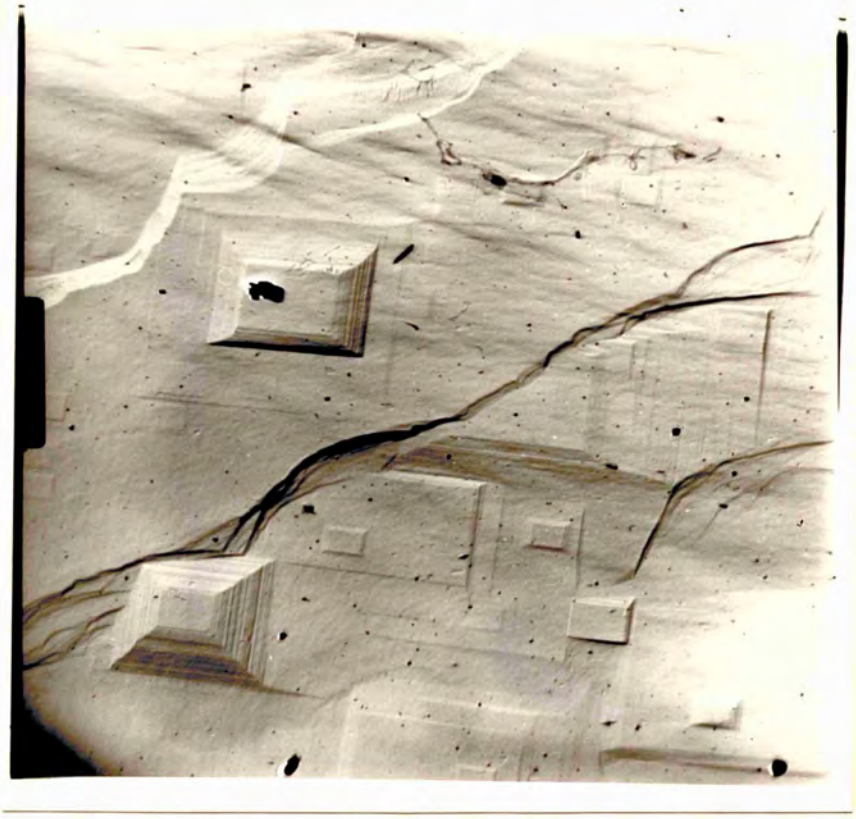

Figure 10.31. (X 8,000)

Figure 10.32. (X 8,500)

a mild etch in nature another question arises: whether the cubo-octahedra are due to growth, or dissolution in nature. The following points suggest that these are very likely to be the outcome of natural dissolution.

1 - The crystals have very smooth, flat and small cubic faces (figures 10.1 and 10.2). Some of the faces show appearance of characteristic cube face etch pattern (figures 10.3, 10.4 and 10.5). These pits are very shallow and are different from the point-bottomed "quadrons" on the faces of natural cubes. In addition to pits there are solution channels on the faces which show the effect of being etched in nature (figures 10.7 and 10.8).

2 - Octahedral faces too are unusually smooth (figures 10.6 and 10.10) and some of them also show the effect of being etched in nature (figure 10.6).

3 - Etching experiments also produce exactly similar pits in the same orientation as that of the naturally occurring pits.

4 - Sometimes the crystals exhibit the cube-truncated planes at all the corners forming a perfect cubo-octahedron whilst in other cases, the truncation appears at few of the corners.

The foregoing evidence suggests that the cubic faces are etched mildly in nature and that the faces themselves may be the result of an etch.

It can be argued that, as with the synthetic diamonds, different forms are produced under the different conditions of temperature and pressure (Litvin & Butuzov 1969) and therefore these cubo-octahedra may be the result of growth under different conditions. But as the crystals are sometimes partly cubo-octahedral this argument does not support the growth hypothesis, and hence it is more likely that the cubo-octahedra are the result of an etch in nature.

CHAPTER 11

ELECTRON MICROSCOPIC STUDIES ON NATURAL CUBIC DIAMONDS

Cubic diamonds are less abundant in nature than other types. They are found only in the Congo. Moreover the faces of these diamonds are extremely rough and unsuitable for precision optical studies. This extreme roughness is responsible for the fact that very little interest has so far been taken in studying the surface topography of the natural cubic faces in the past.

The faces of these crystals are faceted and these facets, reflect light specularly which makes the optical studies very difficult. Various topographical details do not show up at all (Tolansky and Sunagawa 1960 c). As a consequence, little has been discovered about these surfaces other than that they are very rough and full of square shaped cavities.

Fersmann and Goldschmidt (1913) claimed that these cavities are the result of natural dissolution, while Williams (1928); Tolansky and Sunagawa (1959, 1960 c)& Tolansky (1961 a) attributed them to growth.

As the direct optical studies are not very easy

and do not show details, Harrison (1964) replicated the surfaces with perspex acrylic sheet. The replication was done by applying heat and pressure. The replicas so obtained were studied by ordinary microscopy and interferometry. He compared the surface features on natural cubic diamonds to the surface features on Bi crystals grown from the melt (studied earlier by Hurle 1962) and observed the features to be similarly terraced. He also found that the features are similar to those on sodium chloride crystals grown from solution, and hence that the cavities on natural cubic diamonds could be attributed to growth. Harrison's work was done at medium magnifications (X 50∽300).

Another type of low magnification study on natural cubes was made by Varma (1967 c). According to him the cubic form of natural diamond crystal is a consequence of layered-growth mechanism and the layers are in the {111} planes. He studied the crystal in such a way that the trigonal axis of the cube coincided with the axis of the microscope, and suggested that the facets are the boundaries of the octahedral plane.

During the present work, the high magnification

and lateral resolution of electron microscopy was used to examine the cube faces in greater detail than before. This work extends that due to Patel and Agarwal (1967), who carried out electron microscopical studies on cubo-octahedral diamond. The octahedral faces of the latter show trigons, which Patel and Agarwal believed to be caused by natural etching. They attributed the co-existing rectangular features, "quadrons", on the cubic faces to the same mechanism. However, they were unable to produce such features by any artificial etch methods.

The crystals studied during the present work were almost perfect cubes from alluvial deposits of the Congo. There is a large variation in colour and size and surface roughness, and generally speaking these diamonds are markedly faceted. Various diamonds were studied first optically and then electron optically.

Figures 11.1, 11.2 and 11.3 show optical micrographs. The micrographs conspicuously show that the surfaces are very rough and that there are various square pits, whose corners point towards the face edges. The bending of the layers in the vicinity of "quadrons" can be seen in some of the figures. Most of the pits

Figure 11.1.
(X 200)

Figure 11.2.
(X 200)

are approximately quadrilateral and on the terraces of the bigger pits, there are to be seen smaller pits (figures 11.1 and 11.2). Being very rough and uneven the whole of the surface is not simultaneously in focus.

From various diamonds studied optically, a few perfect cubes, having sharp corners were chosen. One of them was a yellowish crystal of about 2 mm edge, another was a water white crystal of nearly 1·5 mm edge. A few yellowish crystals of nearly 1·25 to - 1·5 mm in extent were available.

The crystals were first cleaned by boiling in concentrated nitric acid, then washing with soap solution and subsequently refluxing in alcohol. After the simple studies with an optical microscope, the surfaces were studied electron-microscopically. The electron microscopic studies give a wealth of information about the surface structure of these very rough-looking surfaces.

The following points are worth mentioning:-

1 - Nearly all the pits are pyramidal and terraced. The growth layers, are quite clearly resolved, by the replica down to 50$\mathring{A}$. Flat-bottomed pits are extremely rare.

2 - There are various small pits on the terraces of

the bigger pits. Like trigons, quadrons are also of various sizes in the same region.

3 - The regions outside the quadrons are very smooth and show no sign of surface dissolution.

4 - Quadrons strictly conform to the symmetry of the face. The layers intersect each other at right angles, and are strictly rectilinear and crystallographically oriented.

5 - The apex of an inverted pyramidal cavity is not necessarily always at the centre of the pit.

6 - The boundaries of the quadrons are not necessarily square or rectangular. One or two corners of the quadrons can be elongated, to give a kite-like appearance, these elongations of the corners (tails) of the different quadrons in the same region, point in the same direction.

7 - Like the basal extension in the case of trigons, quadrons may have one or two of their sides extended.

8 - The surface layers usually bend in the vicinity of quadrons. This indicates the mechanism of quadron formation i.e. how the layers bend when they meet an obstruction in their way leading to quadron formation.

9 - Like trigons, quadrons may form a linear array.

Figure 11.4 shows various characteristics of

Figure 11.3.
(X 200)

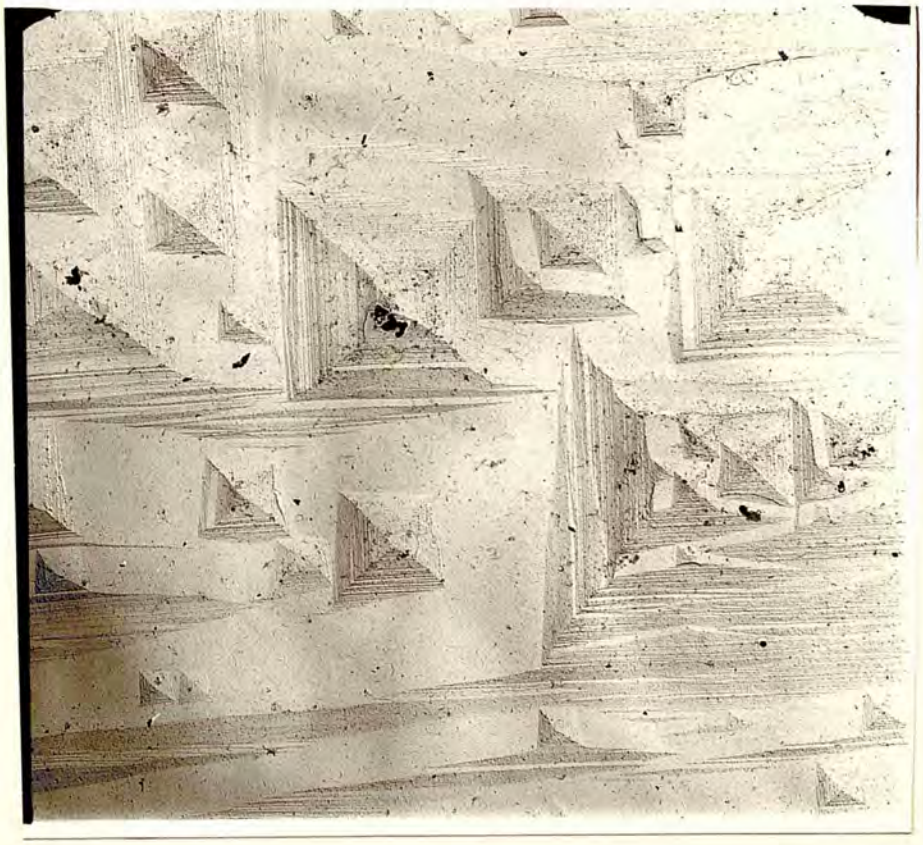

Figure 11.4.
(X 6,000)

quadrons. All the pits are four-sided and invariably have a pyramidal structure. They are of differing sizes and some are clearly assymmetric. The layers which are approximately 50Å thick, are clearly shown.

Figure 11.5 shows that even at high magnification (X 22000), perfectly rectilinear layers intersecting at 90° are conspicuous. They strictly conform to the symmetry of the face as the layers on the octahedral faces, forming trigons.

Figure 11.6 shows that the quadrons are terraced whilst their sides may extend like the frequent basal-extension shown by trigons. The layers are however, straight and crystallographic, but the outlines of the cavities are not necessarily square. One of the corners of the pits may be elongated and this gives the pit an appearance like a kite.

Figures 11.4 and 11.7 show some of the extensions of these corners of the quadrons, and the clear layered growth.

Figure 11.8 shows that in a particular region, these tails of various quadrons point in one direction.

Figures 11.9 and 11.10 clearly indicate that unlike the etch pits the quadrons are sitting on perfectly

Figure 11.5.
(X 22,000)

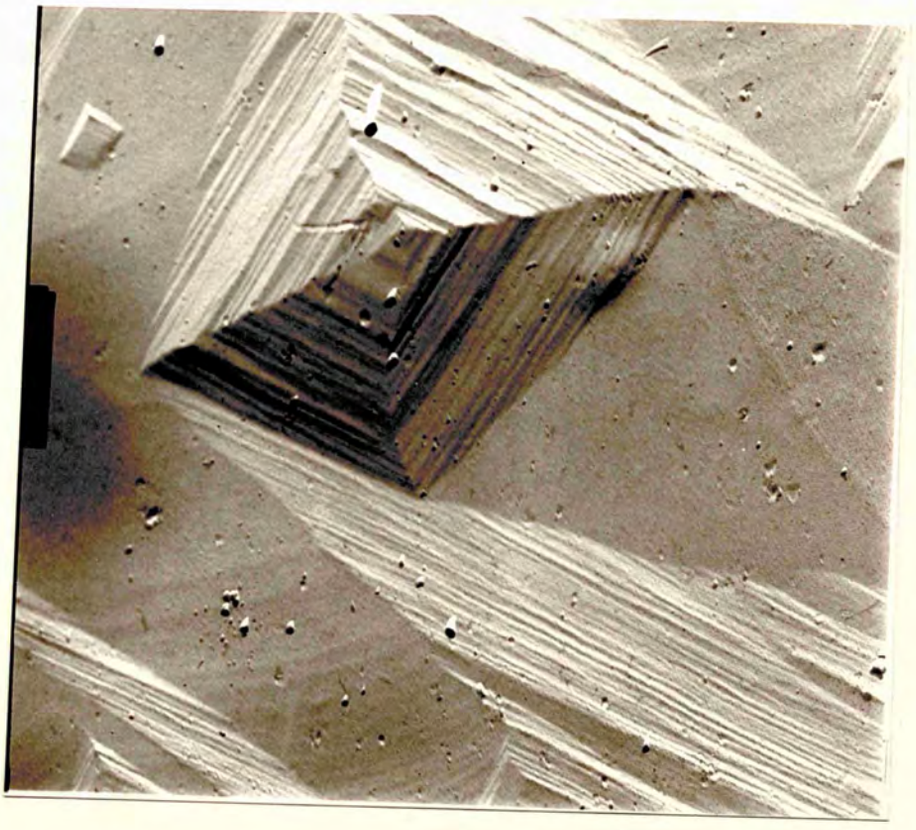

Figure 11.6.
(X 22,000)

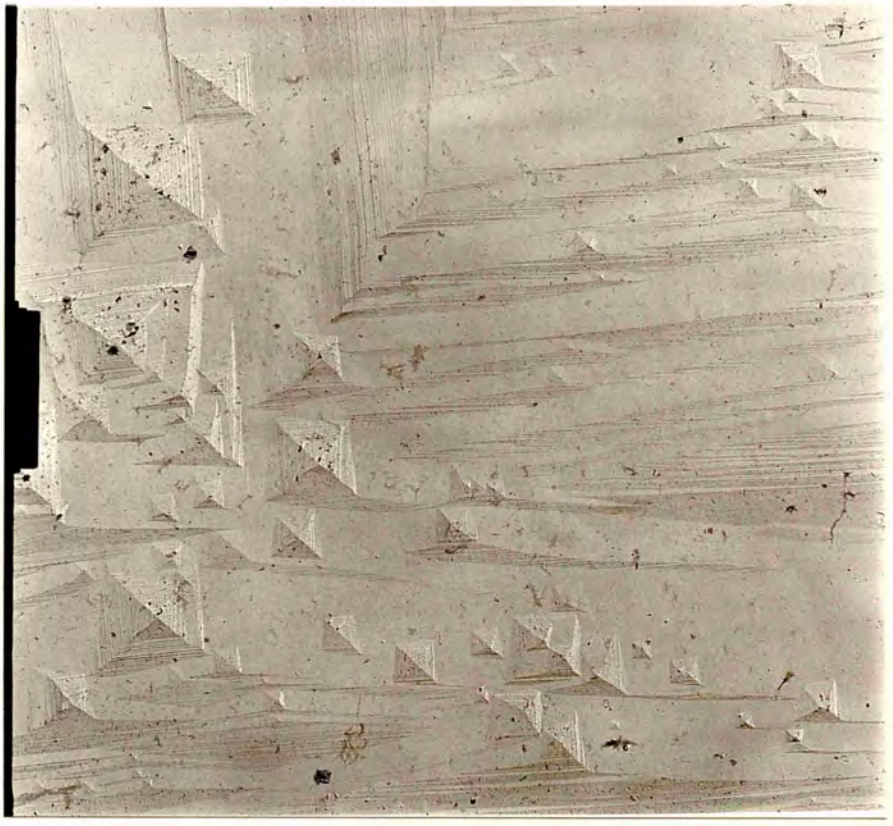

Figure 11.7.
(X 6,000)

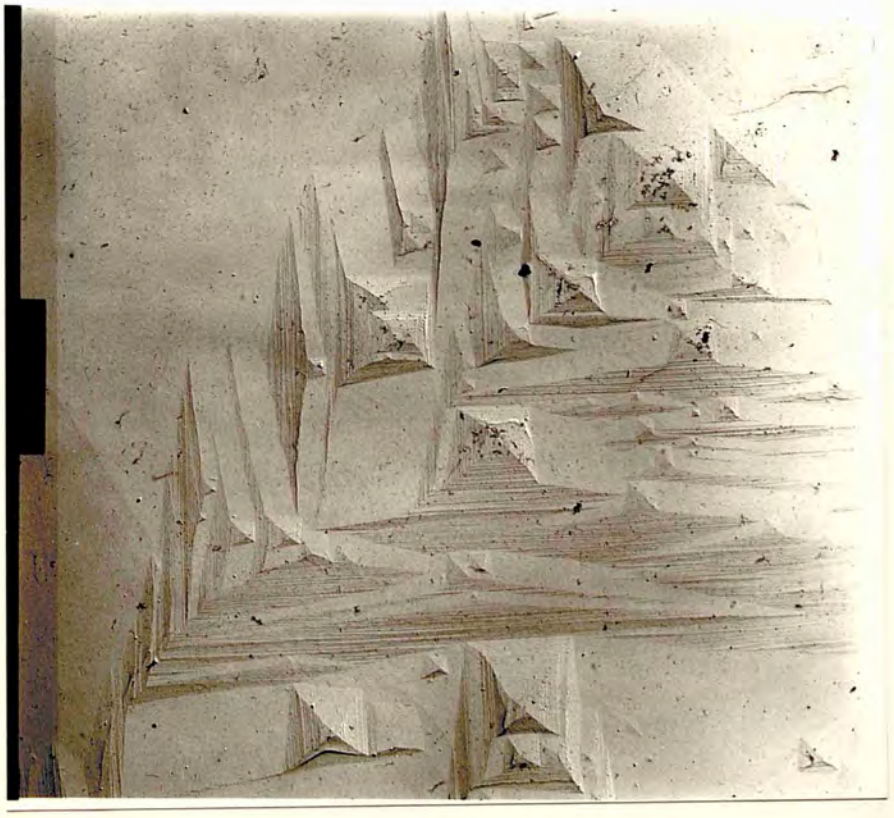

Figure 11.8.
(X 4,500)

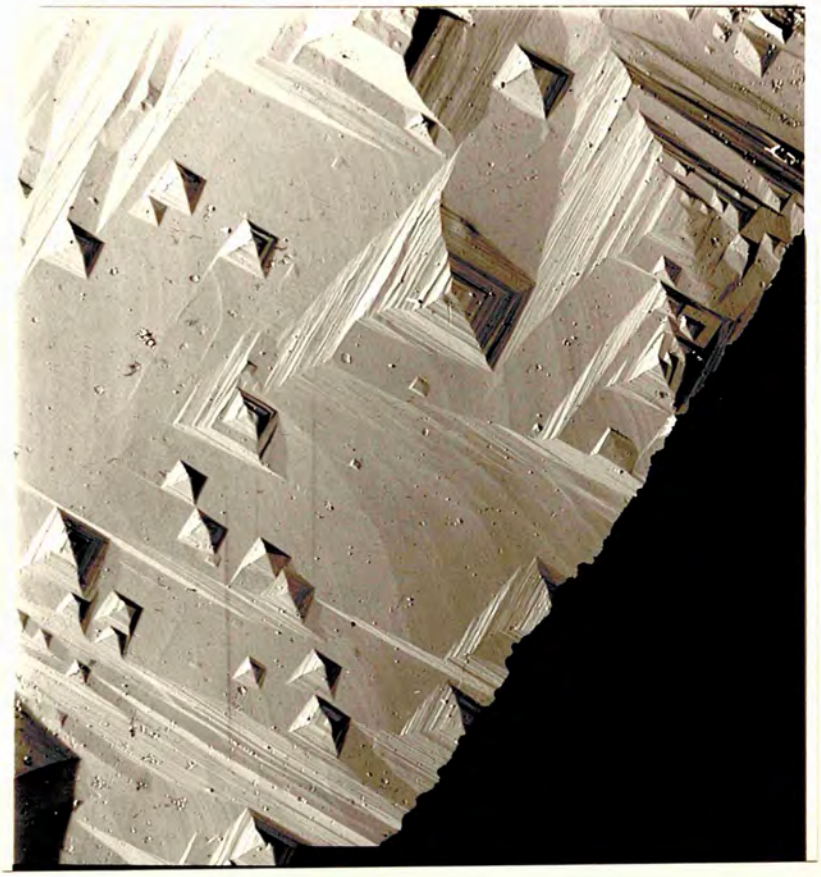

Figure 11.9.
(X 4,500)

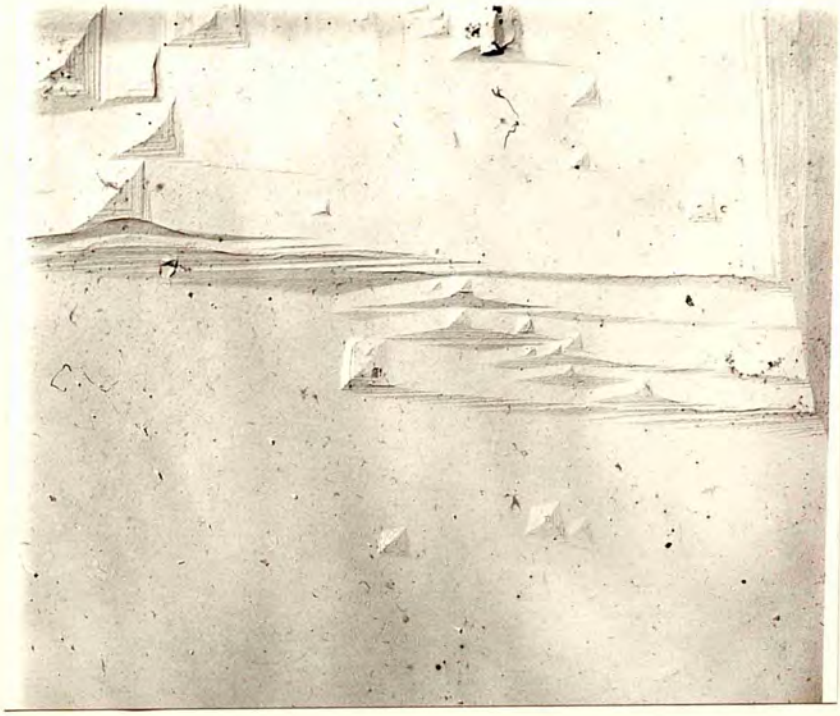

Figure 11.10.
(X 6,000)

plane areas. The basal-extension like layers are also shown.

Figure 11.11 shows the only flat-bottomed quadrons we have observed. On the top of the picture, it clearly shows how layers bend when they meet obstructions and thus the quadrons are formed.

Figure 11.12 shows quadrons forming a linear array. In this picture the growth layers can be easily seen. Quadrons are situated on the plane areas between the terraces. Figure 11.13 shows layers bending to form quadrons (In middle of the picture). The same effect is shown in the bottom right hand corner of the figure 11.14 at higher magnification. The photographs clearly reveal the perfect geometry of the layers forming quadrons.

Discussion

All the above evidence indicates that the cubic crystals grow by layer deposition. The theories of crystal growth also suggest that crystals grow by layer deposition on all the faces (Bunn 1964), though the velocity of growth in the direction of their face normals may differ from face to face depending on the super-saturation and also on the indices of the face (Seager 1953). When these advancing layers meet obstructions

Figure 11.11.
(X 4,500)

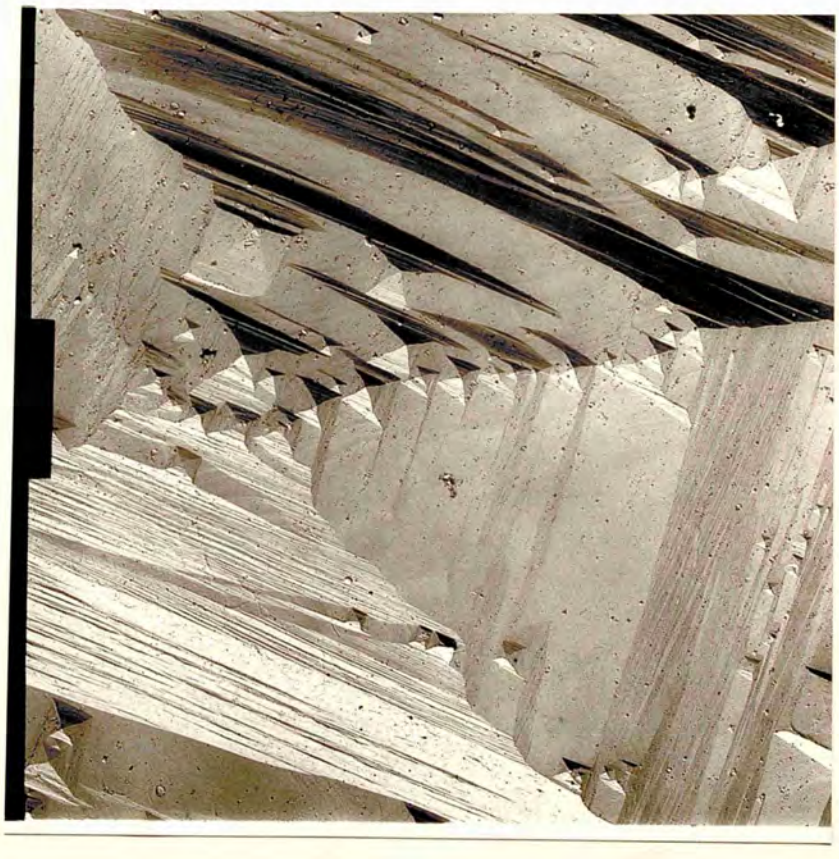

Figure 11.12.
(X 4,500)

Figure 11.13.
(X 4,500)

Figure 11.14.
(X 10,000)

the quadrons are formed by the incompletion of the layers in the region of obstruction. Unlike the etch pits, almost all the quadrons are pyramidal and are of various sizes in the same region. The area surrounding quadrons is smooth and quadrons never overlap. They are made up of layers and terraces which are perfectly rectilinear and crystallographically oriented. The layers intersecting sharply at 90^{o} can be clearly seen from the photographs. This proves Tolansky and Sunagawa's (1960 c) conjecture that "Cubes grow by plane sheet mechanism as revealed by layers and terracing. Just as the trigons on {111} faces, so with quadrons here, the incompletion of growth layers leaves terraced pits because of the sheet character of the growth".

Moreover figures 11.11, 11.13 and 11.14 clearly show how the layers are obstructed and bent from their normal course to form quadrons. This indicates that mechanism of quadron formation is the same as suggested by (Tolansky and Wilcock 1946) and Halperin (1954) for trigons on the {111} faces of diamond.

If these quadrons were produced by etching, one will have to assume that all the cubic diamonds irrespective of their origin are always subjected to the

same etchant at the same temperature (Because temperature changes the orientation of the etch pits on the cubic faces Chapter 9). Moreover they must also always etch in such a way that all the pits so formed are pyramidal. Thus it seems improbable that quadrons are formed by natural dissolution. Harrison (1964) during his etch studies on the polished cubic faces, polished a cubic face very slightly so that the natural pattern just disappeared. He then etched the crystal in order to study the correlation between the pre-existing pattern and the pattern obtained after polishing and subsequently etching. No correlation was obtained, as would be expected by an etch-hypothesis. According to etch hypothesis the pyramidal pits are formed where the dislocations are not completely etched away. Because almost all the pits on the cubic faces are pyramidal, it can therefore be assumed that dislocations are still inside the body of the crystal and hence further etch should give the pits corresponding to previous distribution on the face. Because no such correlation was observed, quadrons could not be explained on the basis of etch theory.

All the surface details observed here at higher

magnification undoubtedly also indicate that quadrons are not etch pits, but are the result of incompletion of the growth layers.

Hence quadrons are the close analogue of the trigons on {111} faces of diamond. As shown by the photographs, they have every character present in trigons (allowing for the difference in symmetry) and therefore quadrons can be logically attributed to the same growth mechanism, of spreading layers (Tolansky and Wilcock 1947; Tolansky and Sunagawa 1960 c).

CHAPTER 12

UNUSUAL MICRO-STRUCTURES ON THE PREMIER MINE DIAMONDS

12.1 Introduction

Micro-structures present on the Premier Mine diamonds, South Africa, are studied in detail. These diamonds are of 20 - 40 mesh size and hence the 200 carats sample contained some 200,000 separate objects. Nearly a thousand well-shaped crystals were extracted and studied. The extensive optical and electron-optical studies on these micro-crystals reveal interesting and complex structures.

The diamonds are octahedra, macles and dodecahedra in form. These diamonds have been also studied by Tolansky and Rawle-Cope (1968), for their ultra-violet absorption. Apart from two-beam interferometric method various other techniques were employed in the present work. They are:-

1 - Phase-contrast microscopy.

2 - Oblique illumination.

3 - White light fringes (two-beam interference).

4 - Electron microscopy.

Multiple-beam interferometry could not be applied to these crystals satisfactorily, because of their small size. Electron microscopy proved very satisfactory because of its high lateral resolution. The Premier Mine crystals during the present work, for the first time have been studied electron microscopically and therefore various unusual features along with the expected trigons and growth hillocks, were observed.

First, nearly a thousand well-shaped crystals were studied optically under the ordinary microscope. Crystals showing peculiar features were sorted out and were studied in detail using the above techniques. This detailed study of the micro-structures of the Premier Mine diamonds presents various interesting features, including polygons and hook-like features. Some crystals are also cube-octahedral in shape.

12.2 The Polygons on Diamonds

Out of numerous crystals examined, a few show polygonal surface features in addition to trigons, i.e. four, five and six-sided features all crystallographically oriented (the rest of such crystals show the usual trigons on the faces). Such features were

studied in detail electron microscopically and are reported on here for the first time.

Crystal No. 4 was a clear transparent water-white crystal nearly 0·5 mm across, and one which showed considerable birefringence. This crystal had polygons on its various faces, together with many trigons. The size, density and shape of the polygons differ from face to face, but most of the faces of the crystal show polygons.

Figure 12.1 shows one of the faces using phase contrast. Figure 12.2 shows the same face with oblique illumination. It is obvious that in addition to trigons there are various polygons or truncated triangular features on the face. The polygonal features are terraced like trigons (figure 12.2), and there are smaller trigons on the terraces. All these features are depression, as proved by white light fringes and electron microscopic methods. The growth layers seen on the pictures are fairly rectilinear and crystallographically oriented. A minute study of the crystal as a whole and face shows that there is no sign of its having been etched. All the pits are crystallographically arranged, having straight edges and sharp corners. There are no pits

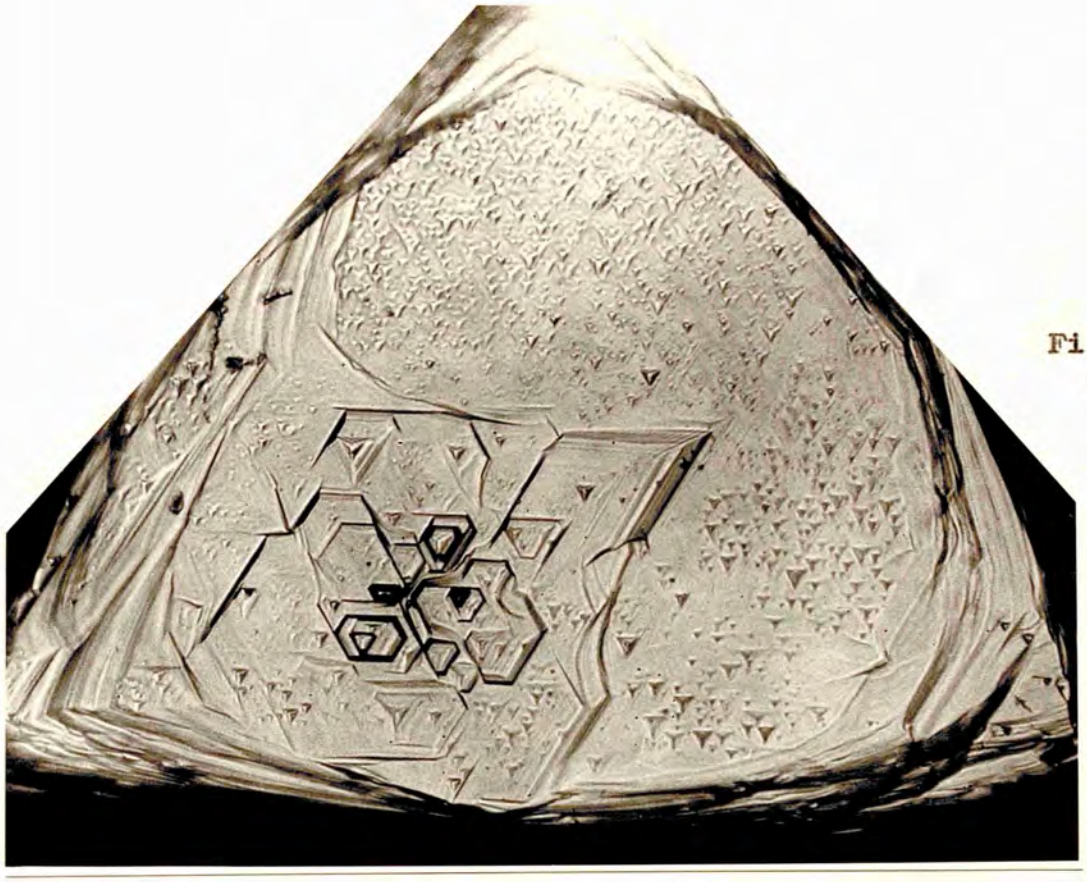

Figure 12.1.
(X 150)

Figure 12.2.
(X 300)

with orientation opposite to that of the trigons. The features often associated with trigons, such as salients are also visible in some region of the figure 12.2. Other faces of the crystal show similar features in association with trigons, but there are fewer polygons on them and some show trigons only.

Diamond No. 3 is another crystal with similar features on some of the faces. The crystal is ($1 \times 0{\cdot}3 \times 0{\cdot}3$ mm^3) in size. This crystal also looks white and transparent though shows birefringence.

Figure 12.3 is the phase-contrast picture of one of the faces of the crystal. Again polygons conspicuously accompany the trigons. The polygons are terraced and there are a few trigons on the terraces. The general appearance of the crystal indicates that it has not undergone any surface dissolution. There is not a single pit with orientation opposite to that of a trigon. These polygons also have rectilinear sides, and sharp corners and there are trigons both, inside and outside these features. Electron microscopic studies show that the regions inside the various polygons are

Figure 12.3. (X 300)

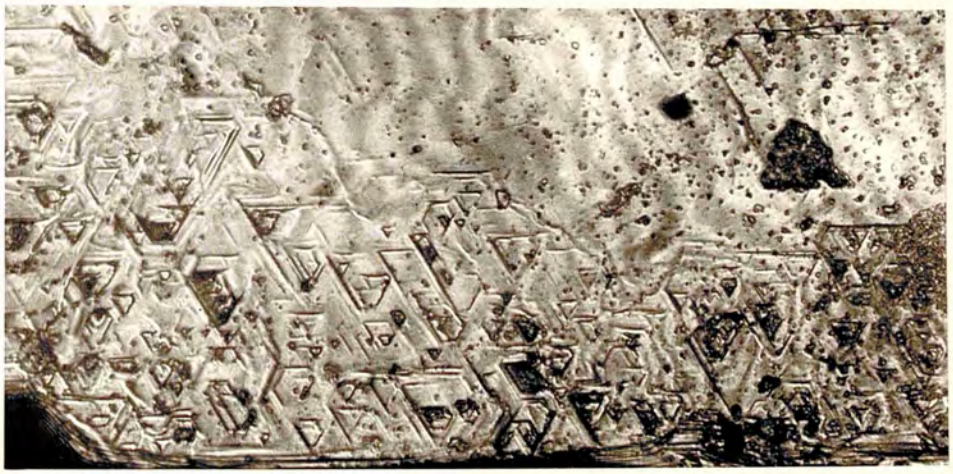

Figure 12.4. (X 300)

smooth and flat. These features however, are too big for electron microscopic studies and thus only a few electron micrographs were taken. The crystals were mostly studied by phase-contrast, oblique illumination, white light fringes and ultimately etching.

Crystal No. 2 is a clear white macle $(0{\cdot}4 \times 0{\cdot}3 \times 0{\cdot}4)$ mm^3 in size. This crystal shows peculiar features. Three of the faces of the crystal show spiral-like features along with the usual trigons. Figures 12.4 and 12.5 show such features, though they are too small to be resolved properly. The pictures show two-beam fringe patterns. The crystal faces have various thick layers forming a growth plateau (figure 12.5). This reduces the quality of the two-beam interferograms, because the crystal surface is not resting close to the supporting glass slide. However, it is clear from the pictures that there are quite a few trigon-like features and crystallographic triangular spiral-like features.

Such a feature was also reported by Patel and Ramachandran (1966) on the octahedral faces of the diamond from South Africa. They studied the faces optically at very low magnification. Because it roughly looked like

a spiral, Patel and Ramachandran interpreted that there are spirals on the natural octahedral faces and because it was a depression they attributed this and the co-existing trigons on the face as a result of natural dissolution.

However, the features observed here are numerous. Two of the faces of the crystal show multitude of such features while on the third face these are few and far between. After optical studies the crystal was mounted and replicated and the replicas so obtained were studied electron microscopically in the usual manner. These studies proved very useful as would be seen below.-

Figure 12.6 shows the portion of the face shown in figure 12.5 at higher magnification. The true character of the surface and of the features becomes clear at higher magnification and what may look like spirals, at lower magnification, are in fact shown to be not spirals but simply polygons or truncated trigons. The various crystallographically oriented rectilinear layers show up clearly. Unlike etch pits, the polygons (Features having more than 3 sides) are of various shapes and sizes in the same region of the crystal face (Figures 12.6 and 12.7). They are all flat-bottomed

Figure 12.5.
(X 375)

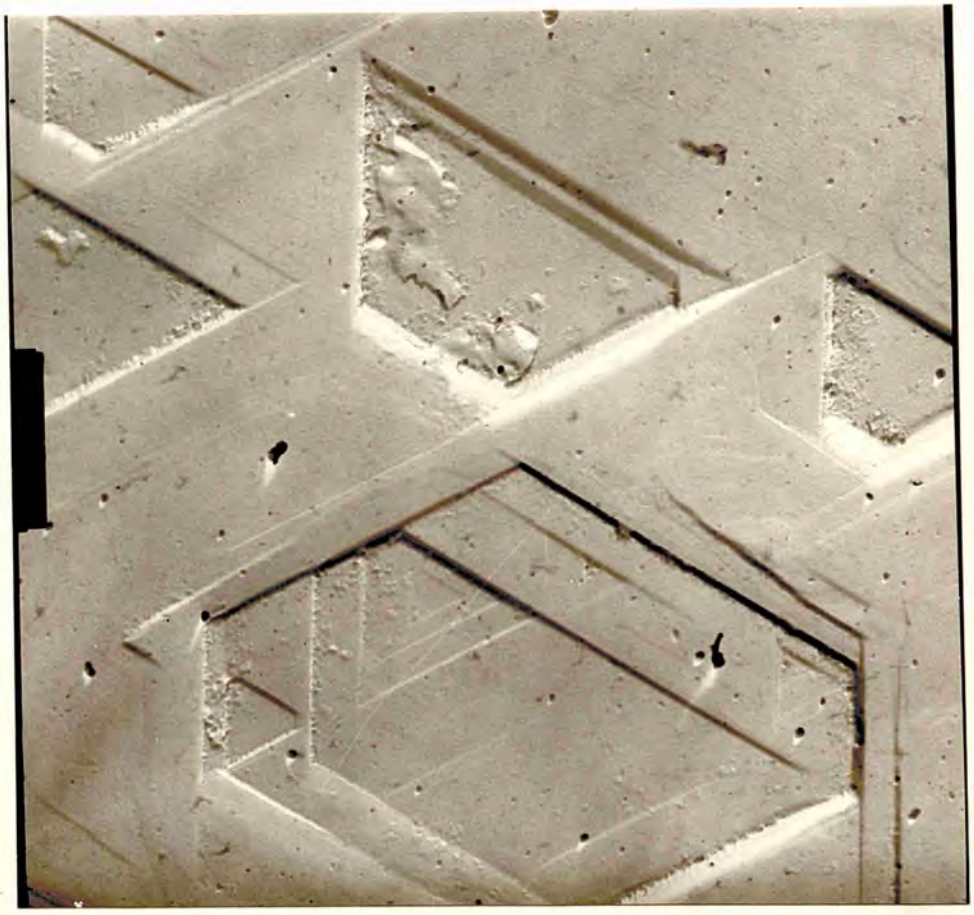

Figure 12.6.
(X 10,000)

and have very smooth bases and are situated on a very smooth region which does not appear to have undergone natural dissolution. On the terraces of bigger polygons, there exists smaller trigon features (figure 12.6). The maximum depth of the feature is 2 microns. The thick layers are nearly 0·08 microns in thickness.

Figure 12.8 is another good example of polygons of various shapes and sizes. In the corner of the picture is a big polygonal feature which could well be mistaken for a spiral at low magnification. On this feature the triangular and parallelogram-like features are situated. The region inside the features and outside is fairly flat and the layers crystallographic and corners are very sharp.

Figure 12.9 also shows the very flat, strictly rectilinear and crystallographic features, all of different shape and size. The trigon-like features in the corners, indicate how the growth layers start truncating the trigon corners. Such a high degree of rectilinearity of the sides and smoothness of the bases cannot be explained on the dissolution hypothesis. The basal-extension-like layers which often appear in association with trigons (Tolansky and Wilcock 1947), can also

Figure 12.7.
(X 10,000)

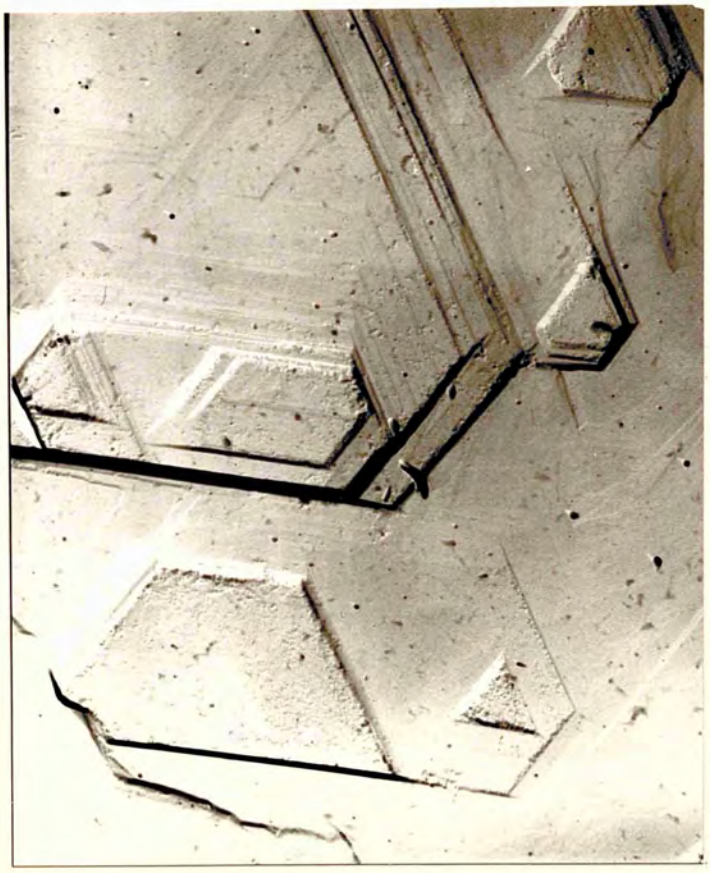

Figure 12.8.
(X 11,000)

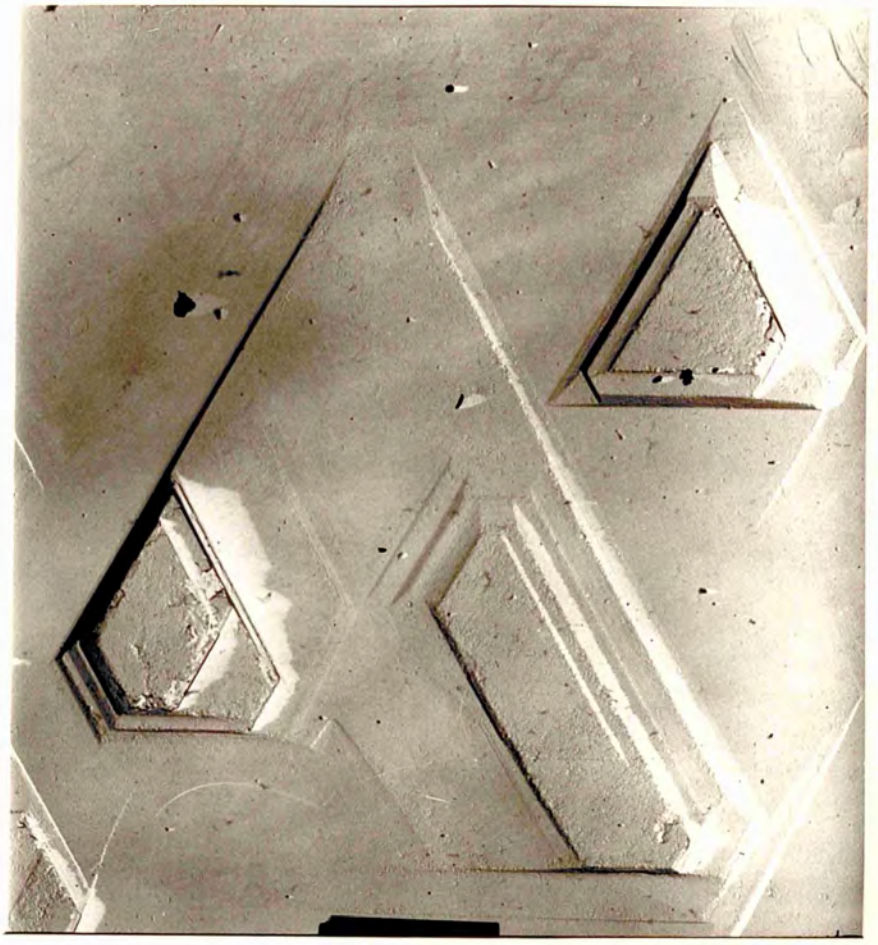

Figure 12.9.
(X 10,000)

Figure 12.10.
(X 12,000)

be seen in the picture. Figure 12.10 also shows similar features which indicate the process of crystallographic layers advancing and forming trigons and polygons as suggested by Tolansky and Wilcock (1946, 1947).

Figures 12.11, 12.12 and 12.13 all show six-sided features of various shapes. As the pictures reveal, they do not seem to be spirals but just polygons and hexagons. The layered growth and the extension of the sides can be easily seen. The features are terraced and the terraces are not symmetrical (Figure 12.13).

Figure 12.14 is a little defocussed but shows an interesting pattern which might look like a spiral at low magnification. There are features of different character on the face in the same region. The feature shows layered growth in three directions at 60^{o}. There are triangular features on the terraces. These features too have sharp corners and there is no sign of rounding or any surface dissolution.

Figure 12.15 shows the usual trigon features and indicates how growth starts at one of the corners making it a four-sided feature. A feature with a triangular outline is shown clearly in the bottom left-

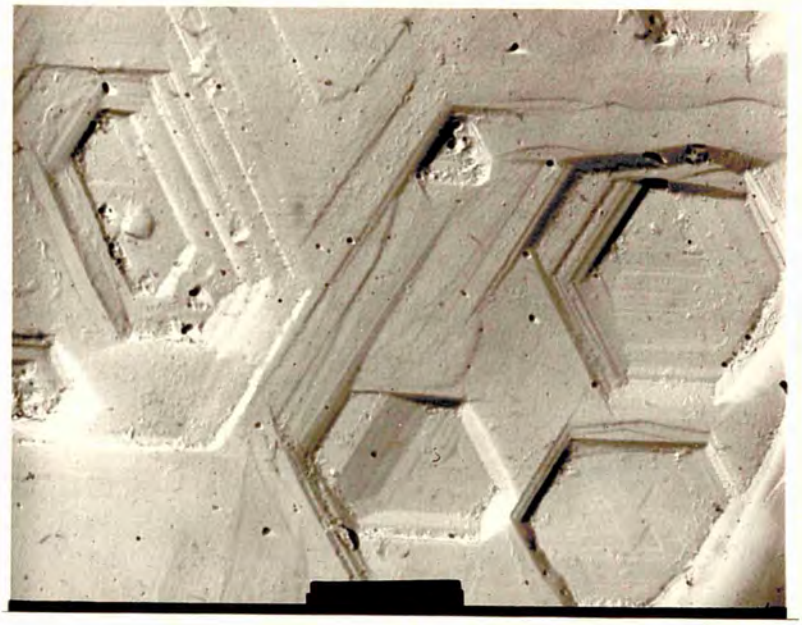

Figure 12.11.
(X 9,000)

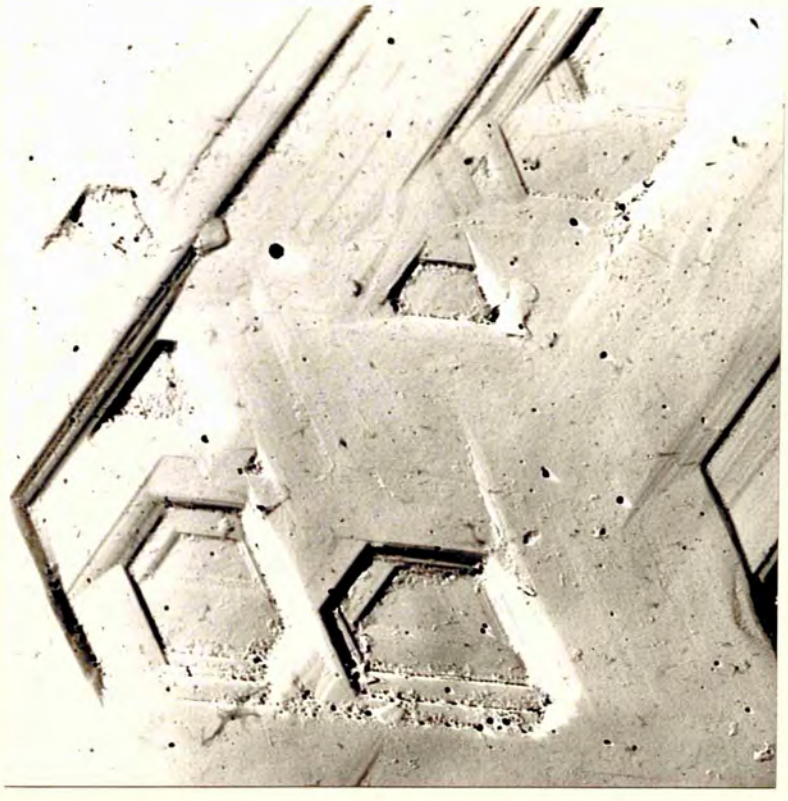

Figure 12.12.
(X 9,000)

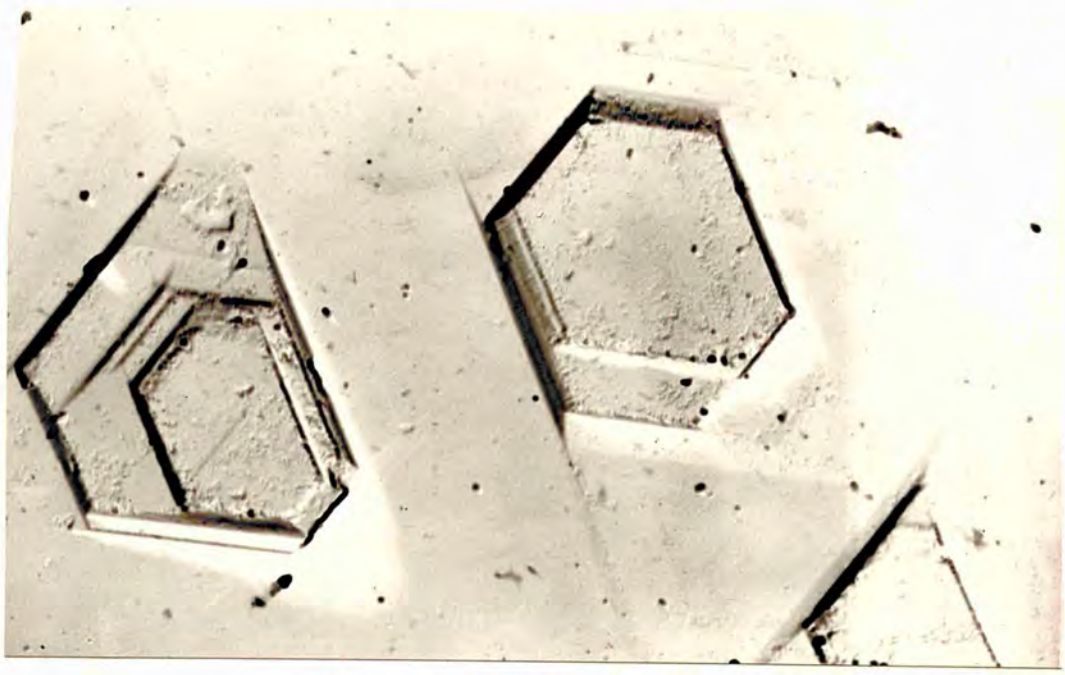

Figure 12.13. (X 10,000)

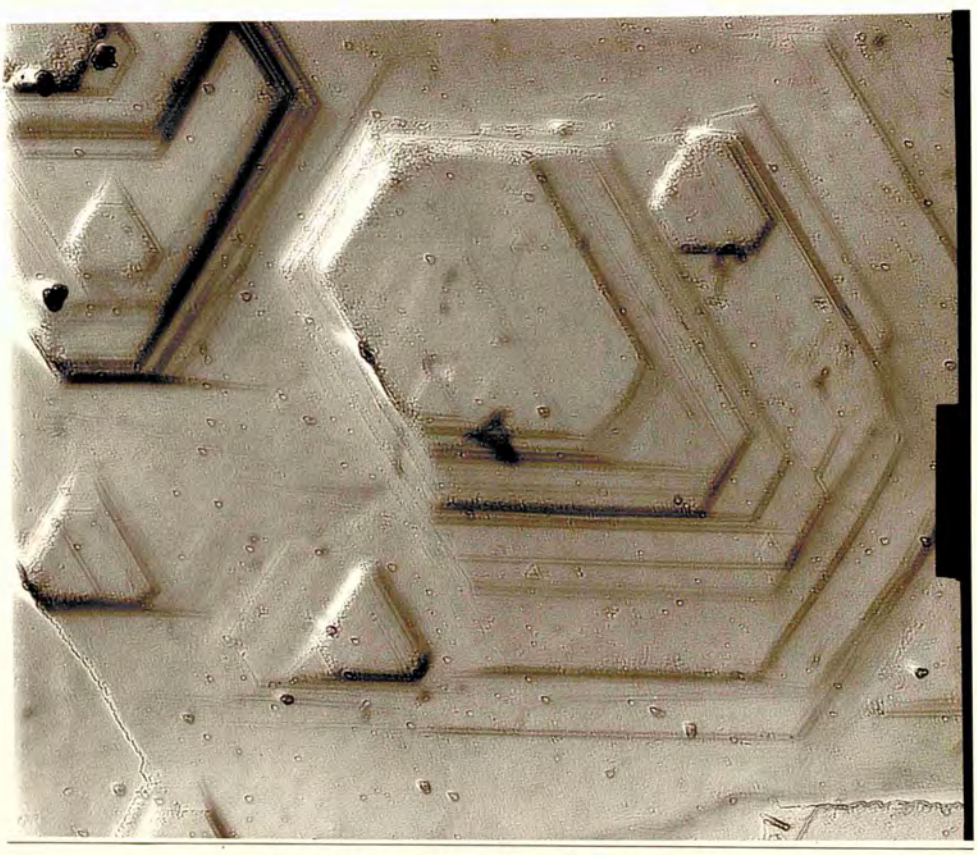

Figure 12.14. (X 9,000)

hand corner of the photograph but due to growth occurring in one or two of the corners, the trigons become truncated to form a four-sided feature. The same effect appears in figure 12.9 indicating how trigons can look like four-sided, five-sided and six-sided figures. Figure 12.16 shows such a mechanism of formation of hexagons clearly. How the layers start moving towards the trigon corners can be easily seen. The layers are crystallographic and the bottom of the feature is smooth indicating no sign of surface dissolution.

By the method of shadow casting and double stage replication all the features described above, are proved to be depressions.

12.3 Discussion

The above features, inspite of their different shapes, sizes and depths, are crystallographically oriented, having sides parallel to $\langle 110 \rangle$. They all invariably show layered growth. They all are flat-bottomed and situated on smooth areas and where there is no sign of surface dissolution either inside or outside the pits. Corners of the features are sharp and the boundaries strictly rectilinear and crystallographic.

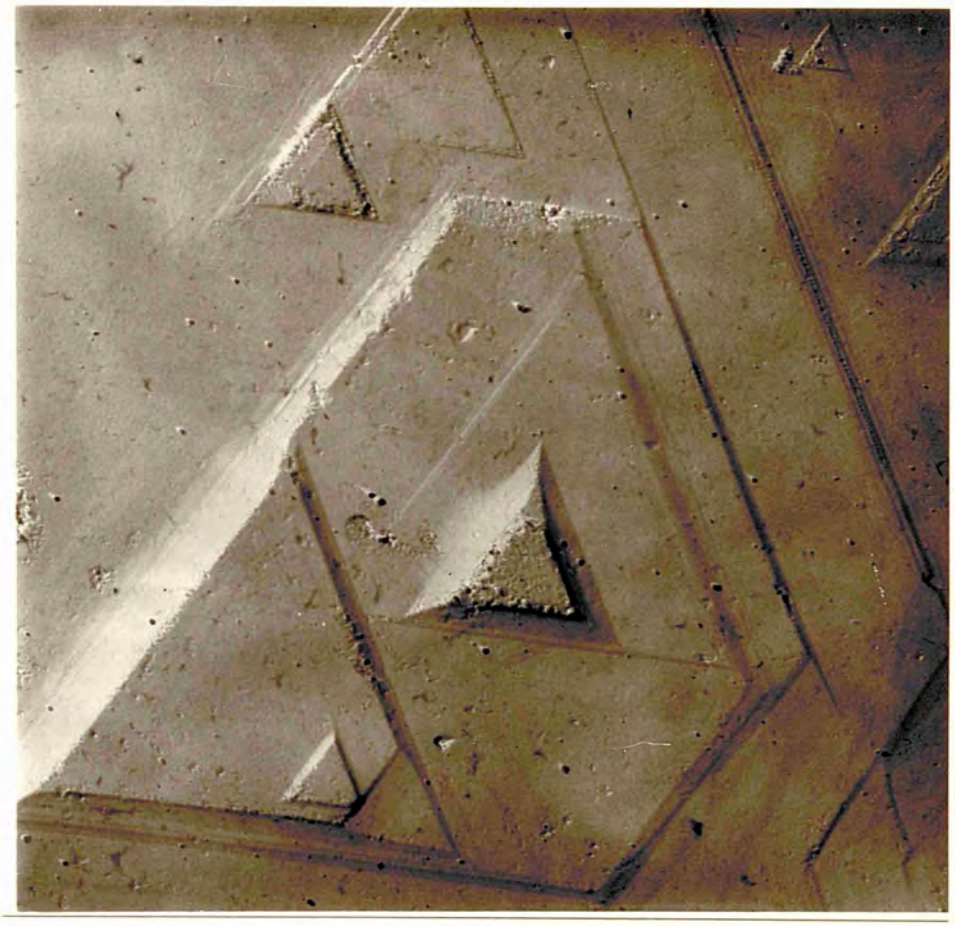

Figure 12.15.
(X 6,000)

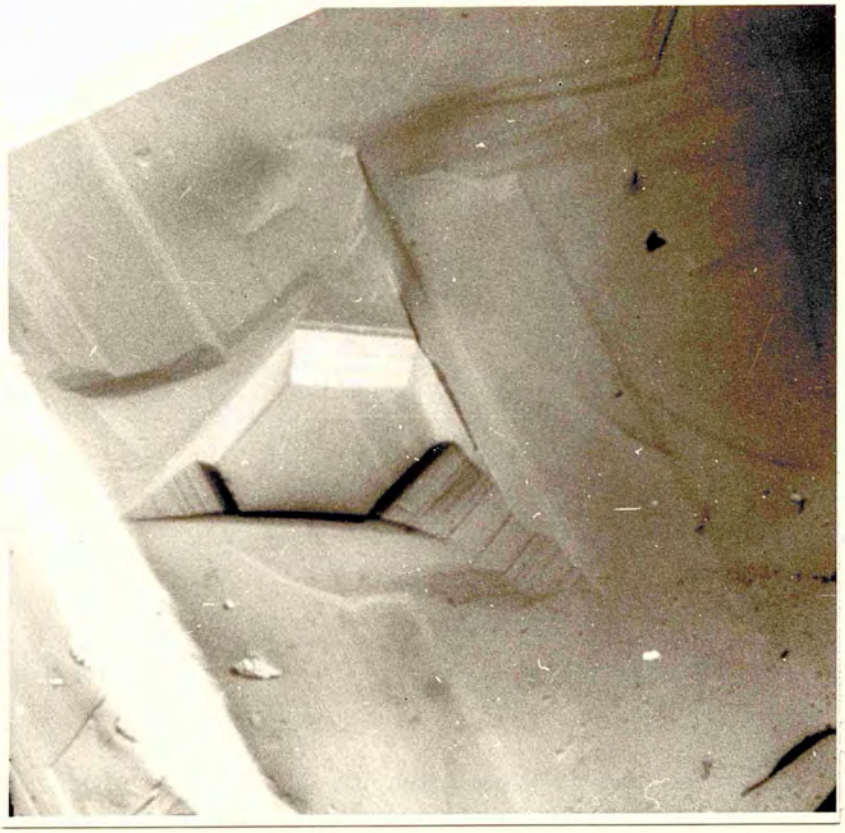

Figure 12.16.
(X12,000)

All this evidence indicates that the features are a result of plane sheet growth at 60^{o} as suggested by Tolansky and Wilcock (1946, 1947) for the case of trigons on octahedral faces.

However, it can be argued that these features may be the result of surface dissolution, yet all these features without any exception have very flat bases showing no trace of surface dissolution, which is difficult to conceive on the basis of an etch for the two reasons:

1 - The pits due to etching will be flat-bottomed as well as pyramidal (Patel 1961).

2 - Secondly the etching would produce micro-pitting inside and outside the main features.

This is absent in case of the present features and hence an etch theory cannot explain the formation of the polygons. Moreover the existing immense literature on the subject of dissolution suggests that features on a particular face conform to the symmetry of the face (Honess 1927) i.e. they are similar in shape on a particular face, and on a particular region they are nearly the same in size. Here the features are of different shapes and size on the same face, moreover in

the same portion of the crystal face (figures 12.6, 12.7 and 12.9).

Etching produces rounding of the corners and sometimes edges, which are completely absent in the case of the features studied here. They have perfectly rectilinear, crystallographically oriented sides and sharp corners.

Finally it can be argued that some of the hexagons may be the result of an etching of pre-existing trigons which are almost ubiquitous on the octahedral faces (Tolansky 1953 a).

Actually it has been shown (Omar, Pandya and Tolansky 1954; Patel and Patel 1968) that trigons convert into hexagons on etching. In this case there are trigons and polygons co-existing. But in order to convert trigons to hexagons, conditions of etching should be such that positive pits having orientation opposite to that of trigons are produced as a result of which the trigon corners become truncated and hexagons are produced. But no such features having orientation opposite to trigons are present on the faces here and hence it is very unlikely that the features are the result of surface

dissolution.

Thus all the evidence indicates that these polygons are most likely to be due to growth. If on the other hand one were to postulate an etch mechanism to explain the formation of such features, formidable difficulties would arise to explain all the characteristics of these features having different shape and sizes on the same region of same crystal face.

Patel (1964) has observed hexagonal and parallelogram-like features on the twin-boundaries of a macle. He attributed these to etching of dislocations present on the twin boundary of the crystal. In the present work such features are present all over the crystal faces and it is unlikely that there would be local twins all over the surface of the crystal.

Tolansky and Wilcock (1946 and 1947) proposed that trigons are growth features and are formed when growth layers, advancing at 60° to each other, are arrested. They also described that such a mechanism sometimes might lead to the formation of truncated trigons, or hexagons. Thus they suggested that trigons or truncated trigons or hexagons arise entirely due to the failure of completion of the growth layers. A similar

mechanism can be proposed to account for the polygonal features observed here.

In order to study the features by the method of etching, some of the crystals on which the polygons were big enough for optical studies were etched at 600°C for 1½ hours. The etch proved too fierce.

Figures 12.17 and 12.18 show the faces of the crystal No. 3, after being etched. As usual various positive pits develop on the surface. Some of the pre-existing small trigons look like hexagons because of being etched. The pre-existing polygons just widen up because of being etched. Within the regions of polygons it is clear from the figure 12.17 that the density of the micro-pits is lower, which suggests the polygons to be growth features, similar in origin to trigons (Omar, Pandya and Tolansky 1954).

Secondly, the polygons as seen in the figure (12.17) do become shallower than before, indicating that surface dissolution is higher than the dissolution within the polygons. This also indicates that the polygons are due to growth.

Thirdly, figure 12.18 shows a strange rounded feature, which was a polygon prior to etching. An

Figure 12.17. (X 300)

Figure 12.18. (X 300)

exactly similar etch pit formation was observed by Givargizov and Sheftal (1966) on etching bi-trigonal growth pits on germanium. The bi-trigonal growth pits were the consequence of the growth of germanium crystal from vapour. According to Givargizov and Sheftal pits develop under conditions where lateral spreading of layers along the ⟨211⟩ directions is retarded by impurities. They further suggested that layered growth and formation of such pits is the characteristic of the crystals with diamond or germanium structure. The different shapes of the pits were attributed to the different distributions of impurities in various direction in which the growth layers advance, which impedes the growth in various directions to a different extent, producing rectilinear and crystallographically oriented features in ⟨110⟩ directions.

Thus a growth mechanism satisfactorily explains the formation of these unusual features, which co-exist with trigons on the crystal faces.

The features evidently indicate the existence of layered growth in ⟨110⟩ on the octahedral faces and also suggests that trigons are growth features, which co-exist on the faces with polygons.

12.4 Hook Features

Occurring alongside with trigons and polygons, these features were however a rarity, having been observed only on 4 crystals, out of nearly one thousand studied optically. As with trigons, the study of these features might throw some light on the growth mechanism of diamonds.

The first crystal studied was a transparent birefringent octahedral crystal, about 0·7 mm across. The crystal showed no apparant sign of dissolution rounding. Some of the faces of the crystal were quite smooth, showing very few trigons and no sign of etch pitting. Only two faces of the crystal showed the 'hook' like features. After studying the crystal face by phase - contrast microscopy, two-beam interferometry and oblique illumination, the usual two-stage platinum/carbon replicas were made and studied in the electron microscope.

Figures 12.19, 12.20, 12.21 and 12.23 show clearly that in addition to the polygons, there are various hook-like features. The polygons can be regarded as trigons with one, or more truncated corners. In most cases, these hook-like features start from one of the corners of a trigon (figures 12.19, 12.20, 12.21 and 12.24).

Figure 12.19.
(X 3,000)

Figure 12.20.
(X 2,500)

Figure 12.21. (X 300)

Figure 12.22. (X 20,000)

The channels forming the 'hook' features may change direction one, two or more times. The features usually have one corner, thus resembling a hook in the plane view. The depths of the features varies from 500Å to 4000Å and appear to be constant for a particular channel. The features show the following general characteristics.

1 - Hooks are crystallographically oriented features. The straight sections lie along ⟨112⟩ dierctions, i.e. they are perpendicular to the sides of the trigons (figures 12.19, 12.20 and 12.24).

2 - The photographs suggest that hooks and their associated features, i.e. polygons, are often at the same level. The regions inside and outside the hook are smooth, figures (12.19, 12.24 and 12.25).

3 - The sides of these features are not quite rectilinear, but they show a rippled appearance (figure 12.27). The boundaries of the ends of the hooks are in ⟨110⟩ directions, i.e. parallel to the sides of the trigons. These boundaries are strictly rectilinear and clearly show layered growth steps figure (12.27).

4 - The ends of the hooks are bounded by the crystallographic layers, making internal angles of 150°, 120°,

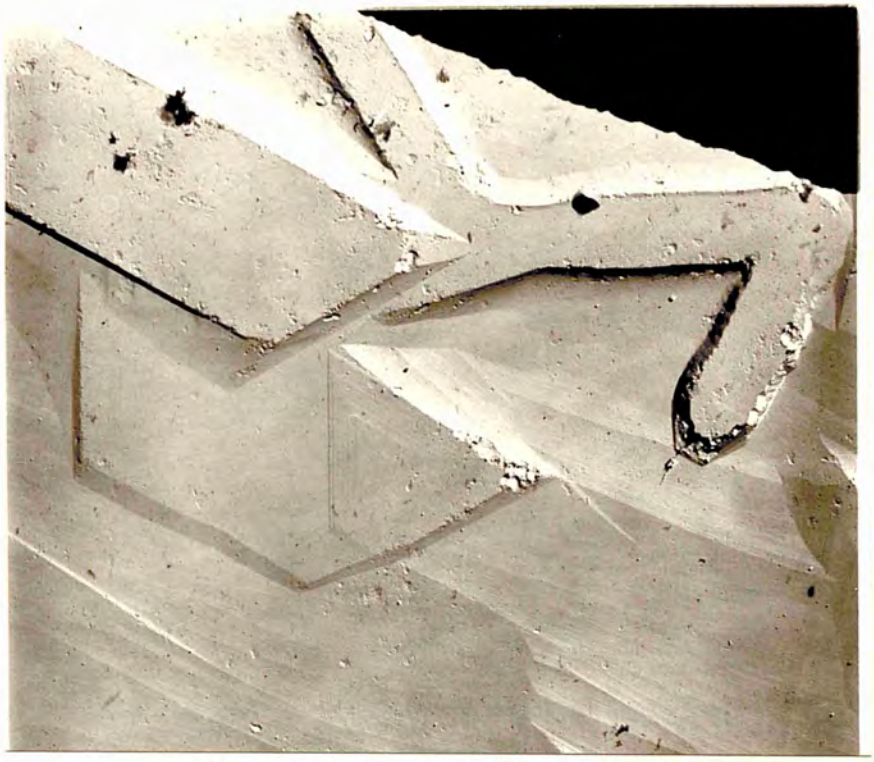

Figure 12.23. (X 2,500)

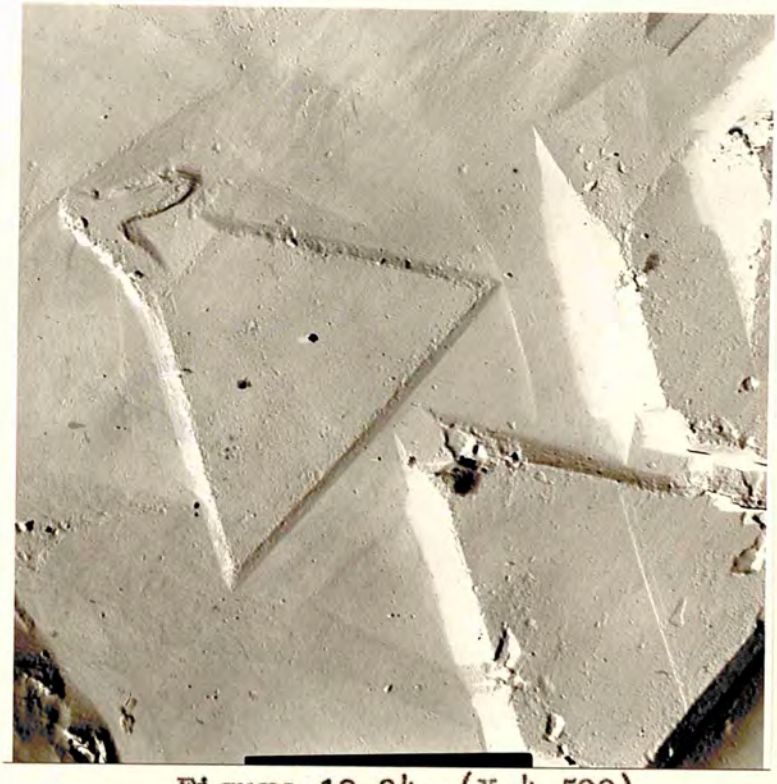

Figure 12.24. (X 4,500)

Figure 12.25. (X 6,000)

Figure 12.26. (X 300)

120° and 150°. This is true in all the cases observed (figure 12.20 and 12.27).

5 - Some of the hook features show branching (figure 12.19).

6 - In a few cases the width of the channels forming the hook features decreases gradually figures (12.22 and 12.30).

7 - Trigons co-exist closely with the hooks on the face. Figures 12.30 and 12.31 clearly show a trigon adjacent to the hook feature.

8 - Angle btween the branches of the hook is approximately 60° (figures 12.22, 12.27 and 12.28).

Other crystals studied optically and electron optically show similar features (figure 12.26).

12.5 Discussion

Trigons and polygons co-exist with the hook-features on the octahedral faces of the diamonds. The areas inside and outside the features are smooth. The smoothness of the regions outside and inside the features suggests that these features are due to growth rather than dissolution, because if the features were caused by natural dissolution one would expect pits or surface

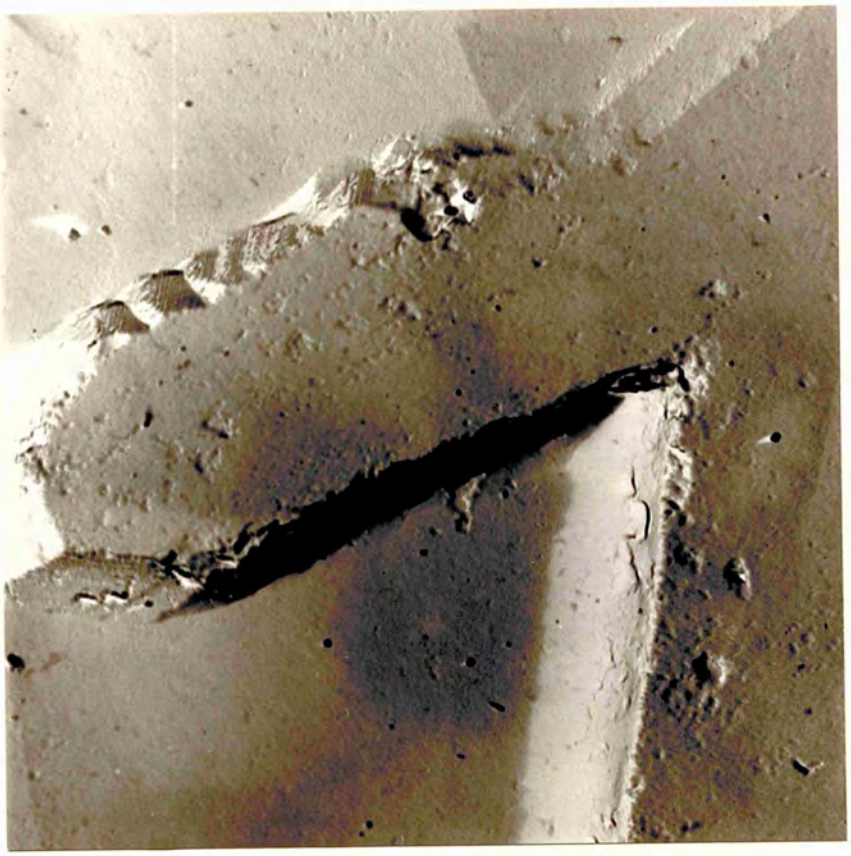

Figure 12.27.
(X 14,000)

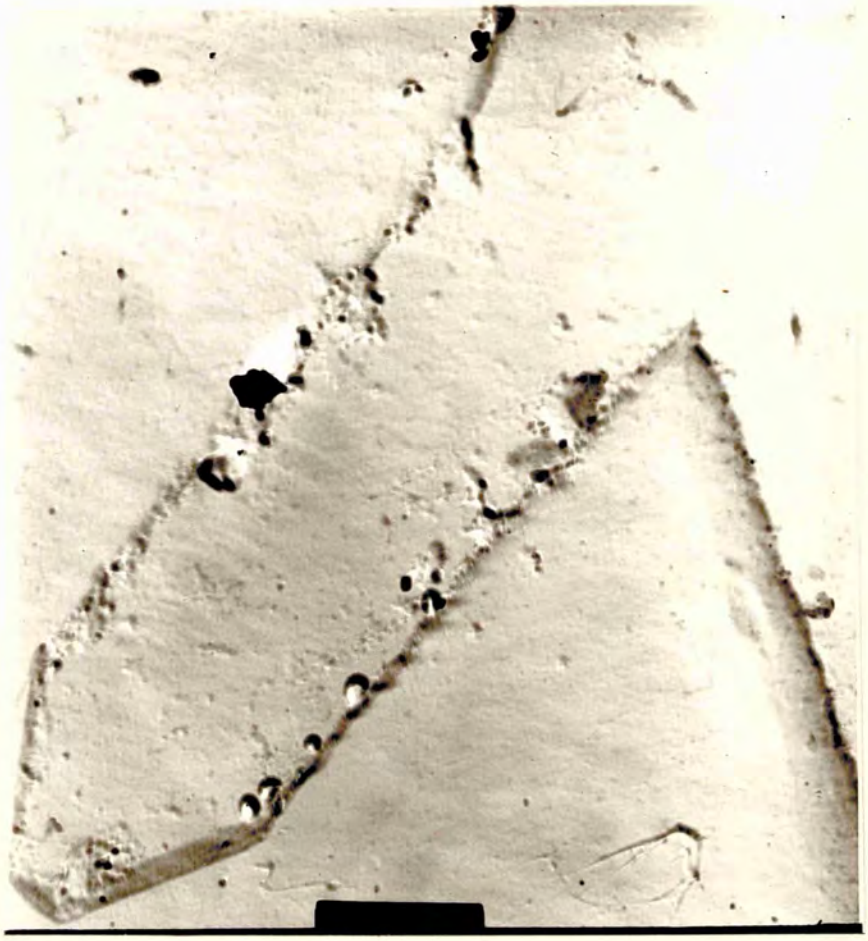

Figure 12.28.
(X 12,000)

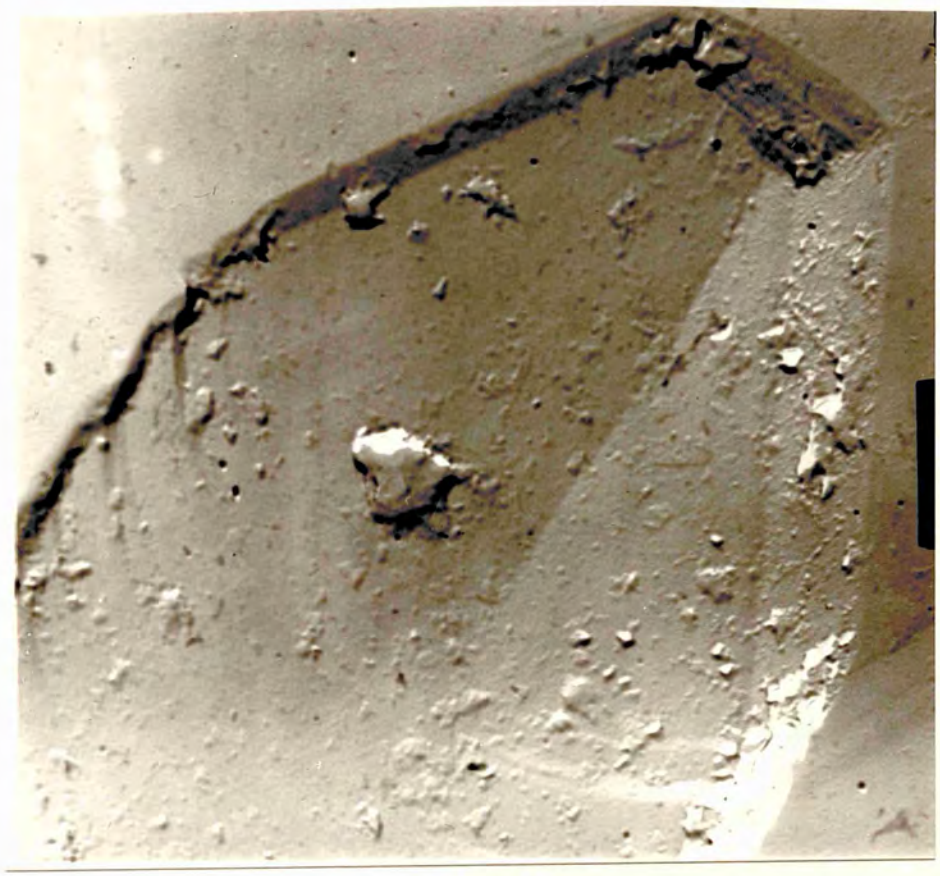

Figure 12.29.
(X 24,000)

Figure 12.30.
(X 2,500)

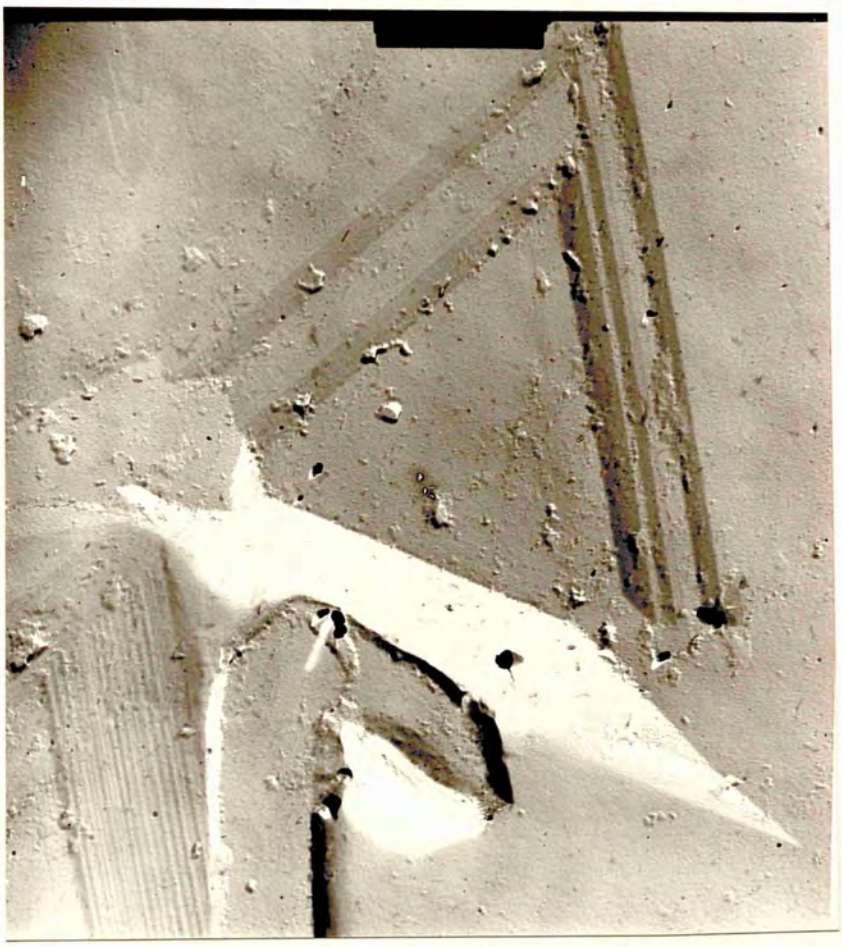

Figure 12.31. (X 6,000)

roughness to be present. Figures 12.19, 12.20, 12.23 and 12.24 all clearly indicate that the features are quite smooth and therefore it is unlikely that they are due to dissolution.

Not only are the channel beds of the hook features smooth but the associated features are also smooth-surfaced and in the most cases hooks and the trigons adjacent to them are at the same level. Figures 12,19 and 12.24 show this characteristic which is difficult to be explained on the basis of an etch hypothesis.

It is reasonably well established, that diamonds grow by layer deposition (Tolansky and Wilcock 1946, 1947; Tolansky 1966; Pandya and Tolansky 1954; Harrison and Tolansky 1964; Tolansky and Rawle-Cope 1968). On the $\{111\}$ faces growth layers proceeding in $\langle 112 \rangle$ directions become arrested and trigons form (Tolansky and Wilcock 1946, 1947). Also even if a single growth layer meets an obstruction, trigon formation may occur (Halperin 1954). It is quite likely that at very high pressure and temperature (conditions under which diamonds grow), the impurities or obstructions might be in the form of gaseous or liquid

bubble or a drop which might give rise to such a feature. However more detailed studies of such features might give clear ideas about the mechanism of formation of these features. But it seems evident that these features are a consequence of plane sheet mechanism of growth on the {111} faces of diamonds.

CHAPTER 13

DISCUSSION AND CONCLUSIONS

Compared with the vast literature available on the surface topographical studies of diamond crystals using conventional methods, relatively few reports exist of surface studies on diamonds using the electron microscope. Therefore, during the present investigation, the surfaces were studied whenever possible using both electron microscopy and interferometry, because electron microscopy, with its high lateral resolution can usefully complement interferometry. Crystals were studied by the method of replication.

13.1 Replica Technique used in the Sudy of Du Pont Synthetic Diamonds

A single stage replica technique has been developed for micro-crystals of the size of a few microns. The surfaces of the Du Pont diamonds were studied by this method and appeared to be extremely rough. Since it was difficult to control the etch parameters for crystals of such a size, it was found difficult to etch the crystals satisfactorily to the desired extent for

the replication work and the experiments were inconclusive.

13.2 Electron Microscopic Studies of de Beers Synthetic Diamonds

de Beers diamonds are very small, weighing nearly 1/3000th to 1/2000th of a carat. These crystals have been studied in detail, optically and then electron optically and finally by the method of etching. The studies reveal various interesting surface details. All the features reveal the layered growth on various low-index faces. Evidence suggest that growth layers pile-up on {111} as well as {100} planes.

In addition to growth patterns various etch patterns have been seen, similar to those observed by Tolansky (1961 a) on the octahedral faces of G.E.C. synthetic diamonds. The etch patterns observed indicate that the crystals are etched slightly during or after the growth process.

The layered growth on the octahedral faces produced patterns, other than trigons, suggesting a plane sheet mechanism of growth at 60° to each other.

The surface structure on the cubic faces also indicates layered growth at 90° to each other. Hopper formation is observed on octahedral as well as cubic

faces, indicating growth on both types of faces.

However, since the manufacturing conditions (and as a consequence the surface structure) varies from batch to batch, the conclusions drawn here may only be applicable to those synthetic diamonds which are examined during the present work.

13.3 Etching of de Beers Synthetic Diamonds

A comparative etch study was done on the natural micro-crystals from the Premier Mine (South Africa) and synthetic diamonds from de Beers. Since the crystals were comparable in size, it was thought that the comparative studies might give some useful information. It was observed that due to the high density of inclusions in the synthetic crystals the etch rate is much higher than that of the natural crystals.

The cubic faces of the synthetic diamonds give etch pits in a negative orientation, but it is surprising to see that at about 600° to 650°C those pits which are bigger and deeper start changing their orientation through 45°. Changes in the orientation of etch pits have also been observed by various workers in many other crystals. Gilman and Johnston (1957) observed a change in the etch

pit orientation on LiF crystals with alkali and acid media.

Amelinckx et al. (1960) observed a change in the orientation of pits on silicon carbide crystals and attributed this to the film of SiO_2 on the surfaces of the silicon carbide crystals.

Hughes et al. (1962) and Thomas et al. (1963) have observed changes in the etch pit orientation during their etch studies on graphite crystals with oxygen. As the temperature was increased, etch pits were found to change orientation. They ascribed this to an anisotropy of etching which is temperature dependent. The change in the etch pits orientation was also observed by Patel and Bahl (1965), who observed that changing the pressure of the etching system caused the etch pits to rotate through 30°. Similarly Haribabu et al. (1969) observed changes in the etch pit orientation on sodium chloride crystals, produced by varying the quantity of mercuric chloride in the etchant ethyl alcohol.

Joshi and Ittyachen (1967) reported a change in the etch pit orientation in the case of apophyllite ($KF\ Ca_4\ (Si_2\ 05)_4\ 8H_2O$) crystals.

All the above investigators attributed these changes to the changes in the etch parameters.

At higher temperatures (above 1000°C) the change in the orientation of the etch pit in the case of diamond was reported by Frank and Puttick (1958) and Evans and Sauter (1961).

Phaal (1965 a, b) having observed the change in the etch-pit orientation by etching in oxygen at various pressures and temperatures, suggested that the variation in the etch rates of the low-index faces at higher temperatures is responsible for the etch-pit re-orientation on the faces of diamond crystals. He suggested further that the orientation change observed by Evans and Sauter (1961) was due to the by-products of the reaction, rather than the increase in temperature.

However, during the present work the change in the etch-pit orientation is observed even at 600°C to 650°C, in the case of synthetic diamonds as well as natural diamonds. Since only the larger and deeper etch-pits (figures 9.18, 9.29 and 9.30) changed orientation, it was concluded that this change only occurs at the sites of fast etching.

Because the orientation change was found to be independent of time and relatively independent of temperature, it was supposed that the by-products at the sites of fast etching are themselves responsible

for the change in the etch pit orientation. This hypothesis was substantiated by agitating the etch-system and encouraging the by-products to escape. It was observed that, by so doing, the change in etch-pit orientation is partially inhibited.

Similar etch experiments were made on the polished cubic faces of natural diamonds and the naturally smooth cubic faces of the cubo-octahedral micro-diamonds from the Premier Mine. All these cubic faces invariably exhibited the above phenomenon. This would indicate that the etch-pits on the cubic faces of diamonds are in negative orientation to start with at low temperatures (about 500°C with KNO_3) and as the temperature of etching is increased the etch-pits which are the sites of fast etching start changing their orientation through 45°. Since this happened in the case of all the cubic faces studied, it would appear to be a general property of the cubic faces of diamond, whether synthetic or natural or sectioned and polished faces.

Having decided that the change of orientation of the etch-pits at the sites of fast etching is an intrinsic property of all the cubic planes, the

question arises as to what these by-products may be.

Rudenko and Kulakova et al. (1965), during their experiments with alkali metal hydroxides and carbonates, suggested that these salts just act as catalysts. They found that diamond etches by atmospheric oxygen and carbon dioxide is the oxidation product of the reaction.

Karklina and Mastakovets (1969) during their etch studies with various sodium and potassium salts and hydroxides, found that the etching rate depended strongly on the volume of air available& carbon dioxide will be the by-product of the reaction.

Sappox and Boehm (1968) during their infrared studies on diamond powder, and Murphy and Ritter (1970) during their electron microscopic studies, observed that oxygen is chemisorbed even at room temperature. As the amount of chemisorbed gas increases, ultimately carbon dioxide is formed at temperature about $400^{\circ}C$ - $500^{\circ}C$. According to Murphy and Ritter carbon dioxide starts attacking diamonds even at $650^{\circ}C$.

Thus it is well-established that carbon dioxide will be a by-product of etching diamond in potassium nitrate and this may be in turn responsible for the

change of orientation of the etch pits at the sites of fast etching where it is produced in appreciable amounts.

13.4 The Cubo-Octahedral Natural Crystals

Depending upon the ambient conditions the form of the synthetic diamonds varies from octahedral to cubo-octahedral and to cubic (Litvin and Butuzove 1969). Similar crystals were found amongst the micro-diamonds. from the Premier Mine of South Africa. The cubic as well as octahedral faces of these crystals were often found to be mainly smooth (figures 10.1, 10.2, 10.6 and 10.10). The topographical studies made optically showed that the faces have definitely undergone minor etching in nature. The real nature of the apparently smooth cubic faces shows up at higher magnification of the electron-microscope. Though the faces appear smooth at low magnification, they show etch pitting at higher magnifications (figures 10.25, 10.28, 10.29 and 10.30). These features are different from the features on the faces of natural cubes.

The cubic truncations do not necessarily occur at all the corners of the octahedra and also their size is exceedingly small compared to the {111}

faces on the crystals, indicating that these faces are the result of a natural dissolution. On the other hand if they were formed in nature due to different temperature and pressure conditions, as is the case with synthetic diamonds, then their truncation at only a few corners cannot be explained. This gives a further indication of the 100 faces being the outcome of dissolution in nature.

Different planes are susceptible to differing extents to different etchants, as shown by Orem (1957) who observed that when a sphere of aluminium is subjected to acid or alkali etchants, it acquires the shape of an octahedron or a cube respectively. Therefore it is quite possible that the crystal which initially grew as an octahedron, on subsequent dissolution transformed into a cubo-octahedral form.

After detailed optical and electron-optical studies, the crystals were studied by the method of etching. Crystals were etched at various temperatures from 500°C to 800°C, at an interval of 50°C approximately. At all these stages the various faces etched were photographed. As shown in figures 10.8 and 10.15 etching produces pits of the same nature and orientation as the pre-existing pits, indicating further that the

crystals have been subjected to natural dissolution.

Thus all the above evidence proves that the crystals have undergone natural dissolution and the cubic truncations at the corners are most likely the outcome of etching in nature.

Faces of natural cubes are unsuitable for precision etch studies, because of their extremely rough nature (figures 11.2 and 11.3). If etching is carried out on the polished cubic faces, it produces an anomalous pattern and mars the real pattern making it more complicated. Therefore these smooth natural cubic faces of the cubo-octahedral crystals were found most suitable for the precision etch studies and thus the detailed etch studies on natural smooth $\{100\}$ faces were performed during the present work.

The change of orientation of the etch pits also takes place on these cubic faces, in exactly the same manner as observed with the synthetic crystals (figures 10.18 and 10.21). The bigger and deeper pits alone change their orientation through 45^{o} (figure 10.21), indicating that this orientation-change at the sites of fast etching is an inherent property of the cubic planes of diamonds.

13.5 Surface Studies of Natural Cubic Diamonds

As mentioned above the faces of natural cubes are very rough being deeply pitted (figures 11.2 and 11.3). This rough nature of these faces makes them unsuitable for precision optical studies, (Tolansky and Sunagawa 1960 c). Many features do not show because the facets on the surfaces reflect the light specularly, therefore the crystal surfaces were studied electron-optically during the present work. The electron-optical studies reveal the true nature of the surfaces. It was found that the pyramidal depressions are truly geometrical features; showing the right angled layered growth (figures 11.5, 11.13 and 11.14). The nature of these pyramidal cavities (quadrons) and the bent layers nearby quadrons, give support to the idea of a growth mechanism for the cubic faces as already suggested by Tolansky and Sunagawa (1960 c). The invariable pyramidal nature of the 'quadrons' and their differing sizes in the same region indicates that these cavities are the result of layered growth on the $\{100\}$ faces of diamond.

13.6 Electron Microscopic Studies on the Premier Mine Micro-Diamonds

Diamonds because of their chemical inertness

have not been studied much by the method of surface replication. During the course of detailed electron microscopic studies of Premier Mine micro-diamonds, during the present work, it was found that a few crystals exhibited some unusual features in addition to the commonly observed features.

Two such features studied during the present investigation are polygons and hook-like features. Polygons are cavities on the octahedral faces and have four, five or six-sides, all truly along crystallographic directions namely ⟨110⟩ . They occur along with trigons and may be described as trigons having their corners truncated. The polygons are invariably all flat-bottomed and of differing shapes and sizes (figures 12.6, 12.7 and 12.9) and may arise by the same mechanism producing trigons.

'Hook-like' features are also crystallographically oriented along ⟨112⟩ directions and may vary in shape and size. Hooks are however observed very rarely. They have been seen only on 4 crystals out of nearly a thousand crystals studied. These features are also seen on the octahedral faces alongside trigons and polygons (figures 12.20 and 12.24). The mechanism of formation of such features is not very clear. It is

likely that plane sheet growth at 60° to each other obstructed by some impurities gives rise to such features. These impurities may be in the form of liquid metal etc. at high pressure and temperature, the conditions under which diamond grows.

However, more detailed studies might give clues to the formation of these features.

Summarizing, it is concluded that diamonds (natural as well as synthetic) grow by the plane sheet mechanism, on the cubic as well as octahedral faces. When these growth layers are arrested or obstructed by some barriers, the various crystallographically oriented features displaying the symmetry of the face are formed.

REFERENCES

AIRY, (1831), Math. Tracts., 831.

AMELINCKX, S., (1951), Nature, Lond., 167, 939.

AMELINCKX, S., (1956), Phil. Mag., 1, 269.

AMELINCKX, S., (1964), "The Direct Observation of Dislocations" (Academic Press, New York), 20.

AMELINCKX, S., BONTINCK, W., DEKEYSER, W., (1957), Phil. Mag., 2, 48.

AMELINCKX, S., and STRUMANE, G., (1960), Brit. Jour. Phys., 31, 1359.

ANDERSON, P.A., (1932), Phys. Rev., 40, 596.

BARTOSHINSKII, Z.V., and MAKOROV, V.A., (1967), Ind. Diam. Rev., April, 160.

BERMAN, R., (1965), "Physical Properties of Diamond", Edited by R. Berman (Clarendon Press, Oxford).

BERTOCCI, U., HULETT, L.D., and JENKINS, L.H., (1963), J. Electrochem. Soc., 110, 1190.

BOCHKO, A.V., and DERYAGIN, B.V., (1969), Sov. Phys. Dok., 13, No. 8, 748.

BOULOUCH, (1893), J. Phys. Rad., 5, 789

BOVENKERK, H.P., BUNDY, H.P., HALL, H.T., STRONG, H.M., etc., (1959), Nature, Lond., 184, 1094.

BOVENKERK, H.P., (1961 a), "Progress in very high Pressure Research", (Wiley, New York).

BOVENKERK, H.P., (1961 b), Amer. Min., 46, 952.

BRADLEY, D.E., (1954), Brit. Jour. of Appl. Phys., 5, 65.

BRADLEY, D.E., (1959), Brit. Jour. of Appl. Phys., 10, 198.

BRAGG, W.H. and BRAGG, W.L., (1913), Proc. Roy. Soc., A 89, 277.

BRAGG, W.L., (1940), Proc. Phys. Soc. London, 54, (1940).

BUCKLEY, H.E., (1951), "Crystal Growth", (John Wiley & Sons, New York).

BUNDY, F.P., BOVENKERK, H.P., STRONG, H.M., etc. (1961), J. Chem. Phys. of Solids, 35, No. 2, 383.

BUNDY, F.P., (1963), J. Chem. Phys. of Solids, 38, 631.

BUNN, C.W., and EMMETT, H., (1949), Discussions Faraday Soc., No. 5, 124.

BUNN, C., (1964), "Crystals and their Role in Nature and Science" (Academic Press).

BURGESS, J.M., (1939), Koninkl. Ncl. Akad. Wetenschap., 42, 293.

BURGESS, J.M., (1940), Proc. Phys. Soc. London, 13, 52, 23.

BURTON, W.K., CABRERA, N., and FRANK, F.C., (1951), Phil. Trans. Roy. Soc. London, 243, 299.

CABRERA, N., (1957), "Semiconductor Surface Physics", Edited by R.H. Kingston (University of Pennsylvania).

CATICHA-ELLIS, S., and COCHRAN, W., (1958), Acta. Cryst., 11, 245.

CHAMPION, F.C., (1953), "Electrical Properties of Diamond", (Butterworth, London).

CLARK, C.D., DITCHBURN, R.W., and DYER, H.B., (1956), Proc. Roy. Soc., A 234, 363.

COWAN, G.R., DUNNINGTON, B.W., HOLZMANN, A.H., (1963), Patent Assigned to Dupont de Nemours Inc.

CROOKES, W., (1909), "Diamonds", London.

CURIE, P., (1885), Bull. Soc. Miner. France, 8, 145.

CUSTERS, J.F.H., (1952), Physica, 18, 489.

CUSTERS, J.F.H., (1955), Nature. Lond., 176, 173.

DE CARLI, P.S., and JAMIESON, J.C., (1961), Science, 133, 3467.

ECKERT, J.D., (1968), Ind. Diam. Rev. Feb. 75, Report No. ARL/P 22/67/3.

ELLIOT, R.J., (1960), Proc. Phys. Soc. Lond., 76, 787.

EMARA, S., and TOLANSKY, S., (1957), Proc. Roy. Soc., A 238, 289.

EVANS, T., and PHAAL, C., (1961),Fifth Carbon Conference.

EVANS, T., and PHAAL, C., (1962), Proc. Roy. Soc., A 270, 538.

EVANS, T., and SAUTER, D.H., (1961), Phil. Mag. 6, 429.

FABRY, (1922), Revue d'Optique, 1, 445.

FABRY and PEROT, (1897), Ann. de Chim. et de Phys., 12, 459.

FERSMANN, A., and GOLDSCHMIDT, V., (1911), "Der Diamant", (Heideberg:Winter).

FIZEAU, (1862), Compt. Rend., 54, 1237.

FORTY, A.J., (1954), Advan. Phys., (Phil. Mag. Suppl.), 3, 1.

FRANK, F.C., (1949), Dis. Faraday Soc., 5, 48.

FRANK, F.C., (1956), Proc. Roy. Soc., A 237, 168.

FRANK, F.C., (1967), Proc. Intern. Indust. Diamond Conf., Oxford, (1966), Diamond Information Bureau (1967).

FRANK, F.C., and LANG, A.R., (1959), Phil. Mag., 4, 383.

FRANK, F.C., PUTTICK, K.E., and WILKS, E.M., (1958), Phil. Mag., 3, 1262.

FRANK, F.C., and PUTTICK, K.E., (1958), Phil. Mag. 3, 1273.

FRENKEL, J., (1946), "Kinetic Theory of Liquid", J. Phys., U.S.S.R., 9, 392.

FRIEDEL, G., (1924), Bull. Soc. Fran. Min., 47, 60.

FRIEDEL, G., and RIBAUD, G., (1924), Bull. Soc. Fran. Min., 47, 94.

GEVERS, R., (1953), Nature, 171, 171.

GEVERS, R., AMELINCKX, S., DEKEYSER, W., (1952), Naturwissenschaften, 39, 443.

GIBBS, J.W., (1878), "Collected works Vol. I", Longmans, Green and Co., London (1928).

GILMAN, J.J., (1956), Trans. Am. Inst. Min. Met. Engrs., 206, 998.

GILMAN, J.J., and JOHNSTON, W.G., (1957), "Dislocations and Mechanical Properties of Crystals", (Wiley, New York).

GILMAN, J.J., JOHNSTON, W.G., and SEARS, G.W., (1958), J. Appl. Phys., 29, 747.

GLENDA HUGHES, E.E., WILLIAMS, B.R., and THOMAS, J.M., (1962), Trans. of Faraday Soc., 582, 2011.

GRIFFIN, L.J., (1950), Phil. Mag., 41, 196.

GIVARGIZOV, E.I., and SHEFTAL, N.N., (1966), Proc. Intern. Conf. on Crystal Growth, Boston (1966), Supplement to Phys. Chem. of Solids, 277.

HALL, H.T., (1956), Proc. Symposium on "High Temp. - A Tool for the future", Stamford, California, 161.

HALPERIN, A., (1954), Proc. Phy. Soc., 67, 538.

HALPERIN, A., (1958), Phil. Mag., 3, 1057.

HARI BABU, V., SIRDESHMUKH, D.B., and BANGIGIR, K.G., (1966), Phil. Mag., 14, 1078.

HARRISON, E.R., (1964), M. Sc. Thesis (London University).

HARRISON, E.R., and TOLANSKY, S., (1964), Proc. Roy. Soc., A 279, 490.

HOERNI, J.A., and WOOSTER, W.A., (1955), Acta. Cryst., 8, 187.

HOLMES, P.J., (1959), Acta. Met., 7, 283.

HONESS, A.P., (1927), "The Nature, Origin and Interpretation of Etch Figures on Crystals", (Wiley, New York).

HORN, F.H., (1952), Phil. Mag., 43, 1210.

HURLE, D.T.J., (1962), Prog. Material Sci., 10, 79.

JOSHI, M.S. and IHAYACHEN, M.A., (1967), Indian Jour. Pure and App. Phys., 7, 717.

KAISER, W.,and BOND, W.L., (1959), Phys. Rev., 115, 857.

KARKLINA, M.I. and MASTAKOVETS, Yu. P., (1969), Sov. Phys. Dokl., 13, No. 12, 1194.

KAY DESMOND, (1965), "Techniques for electron microscopy", (Blackwell Sc. Publications, Oxford).

KAYSER, J.F., (1944), Ind. Diam. Rev., 4, 2.

KOSSEL, W., (1927), "Theory of Crystal Growth", (Nachr. Ger. Wiss. Goettingem).

KRANITZ, M., and SEAL, M., (1962), Proc. of 5th Int. Con. on electron microscopy, Philedelphia, FF - 7.

KUCHARENKO, (1960), A monograph on Ural Diamonds.

KUKHARENKO, A., (1946), Dokl. Akad. Nauk. SSSR, 51, No. 8.

KVOHOV, K.G., (1959), Proc. Russ. Min. Soc., 88, 24.

LANG, A.R., (1964), Proc. Roy. Soc., A 278, 234.

LEMMELEIN, G.G., KLIYA, M.O. and CHERNOV, A.A., (1964), Sov. Phys. Crysta., 9, No. 2, 181.

LEVINSTEIN, H.J. and ROBINSON, W.H., (1962), J. Appl. Phys., 33, 3149.

LITVIN, Yu. A. and BUTUZOV, V.P., Soviet Phys. Doklady., 13, No. 8, 746.

LIVINGSTON, J.D., (1960), J. Appl. Phys., 31, 1071.

LOH, J.M., (1969), Mettalography, 2, 79.

LUZY, W., (1892), Ber. dtsch. Chem. Ges., 25, 2470.

MAHL, H., (1940a), Metallwirtsch, 19, 488.

MAHL, M., (1940b), Z. Techn. Phys., 21, 17.

MIER, H.A., (1903), Proc. Roy. Soc., 71, 439.

MIER, H.A., (1904), Phil. Trans. Roy. Soc., A 202, 459.

MILLEDGE, H.J. and MEYER, H.O.A., (1962), Nature Lond., 195, 171.

MILLER, R.F. and PUNGLIA, J., (1970), Ind. Diam. Rev., Oct., 202.

MOORE, M. and LANG. A.R., (1972), Phil. Mag., 25, 219.

MURPHY, R. and RITTER, G.J., (1970), Ind. Diam. Rev., 30, 354.

NEWKIRK, J.B., (1959), Tras. AIME., 215, 483.

OMAR, M., PANDYA, N.S. and TOLANSKY, S., (1954), Proc. Roy. Soc., A 225, 33.

OMAR, M. and KENAWI, M., (1957), Phil. Mag., 2, 859.

OREM, T.H., (1957), Research of Nation Bureau of Stds., 58, No. 3, 157.

OROWAN, E., (1934), Z. Physik., 89, 634.

PANDEYA, D.C., (1955), Ph.D. Thesis, (London University).

PANDEYA, D.C. and TOLANSKY, S., (1961), Proc. Phy. Soc., 78, 12.

PANDYA, N.S. and TOLANSKY, S., (1954), Proc. Roy. Soc., A 225, 40.

PATEL, A.R., (1961), Physica, 27, 1097.

PATEL, A.R., (1962), Physica, 28, 44.

PATEL, A.R., (1964), Physica, 30, 505.

PATEL, A.R. and AGARWAL, M.K., (1965), Amer. Min., 50, 124.

" " " " " (1966a), Ind. Diam. Rev., No. 307, 26, 240.

PATEL, A.R. and AGARWAL, M.K., (1966b), Ind. Diam. Rev., No. 307, 26, 335.

PATEL, A.R. and AGARWAL, M.K., (1967a), Ind. Diam. Rev., No. 325, 27, 524.

PATEL, A.R. and AGARWAL, M.K., (1967b), Ind. Diam. Rev., Nov., 482.

PATEL, A.R., AGARWAL, M.K., DESAI, C.C., (1966), Ind. Diam. Rev., Sept., 374.

PATEL, A.R. and BAHL, O.P., (1965), Carbon, 3, 181.

PATEL, A.R. and GOSWAMI, K.N., (1963), Brit. Jour. Appl. Phy., 14, 284.

PATEL, A.R. and GOSWAMI, K.N., (1964), Physica., 30, 965.

PATEL, A.R., GOSWAMI, K.N., and DESAI, C.C., (1964), Phil. Mag., 10, 931.

PATEL, A.R., GOSWAMI, K.N. and RAMANATHAN, S., (1963), Pro. Phy. Soc., 81, 1053.

PATEL, A.R. and PATEL, S.M., (1968a), Ind. Diam. Rev., 28, 272.

PATEL, A.R. and PATEL, S.M., (1968b), Brit. J. Appl. Phys. Ser. 2, 1, 1445.

PATEL, A.R. and PATEL, S.M., (1968c), Rev. Sci. Inst., 39, 409.

PATEL, A.R. and PATEL, S.M., (1969), Indian, J. of Pure and Applied Phy., 7, 690.

PATEL, A.R. and PATEL, T.C., (1971), Joul. Appl. Cryst., (June), 207.

PATEL, A.R. and RAMACHANDRAN, N., (1966), Ind. Diam. Rev., 26, 549.

PATEL, A.R. and RAMACHANDRAN, N., (1967a), J. Phys. Chem. Solids, 28, 1849.

PATEL, A.R. and RAMACHANDRAN, N., (1967b), J. Phys. Chem. Solids, 29, 190.

PATEL, A.R. and RAMACHANDRAN, N., (1968a), Ind. Diam. Rev., 28, 328.

PATEL, A.R. and RAMACHANDRAN, N., (1968b), Brit. J. Appl. Phy., 1, 505.

PATEL, A.R. and RAMANATHAN, S., (1962), Phil. Mag., 7, 1305.

PATEL, A.R. and RAMANATHAN, S., (1963), Physica., 29, 889.

PATEL, A.R. and RAMANATHAN, S., (1964), Physica., 30, 2003.

PATEL, A.R. and TOLANSKY, S., (1957a), Proc. Roy. Soc., A 243, 33.

PATEL, A.R. and TOLANSKY, S., (1957b), Proc. Roy. Soc., A 143, 41.

POLANYI, M., (1934), Z. Phyzik., 89, 660.

PHAAL, C., (1965a), Ind. Diam. Rev., 25, No. 300, 436.

" " (1965b), " " " 25, No. 301, 591.

RAAL, F.A., (1957), Amer. Min., 42, 354.

RAMACHANDRAN, G.N., (1946), Proc. India. Acad. Sci., A 24, 65.

RAMAN, C.V. and NILAKANTAN, P., (1940), Proc. India. Acad. Sci., A 11, 389.

RAMAN, C.V. and RAMASHESHAN, S., (1946), Proc. India. Acad. Sci., A 24, 1.

RAMAN, C.V. and RENDALL, G.R., (1944), Proc. India. Acad. Aci., A 19, 265.

RAMASHESHAN, S., Ibid, 122.

ROBERTSON, S., FOX, J.J. and MARTIN, A.E., (1934), Phil. Trans. Roy. Soc., A 232, 463.

RODENKO, A.P., KULAKOVA, I.I., (1965), Dokl. Akad. SSSR., 163, 778.

SAPPOX, R. and BOEHM, H.P., (1968), Carbon, 6, 573, (Pergamon Press).

SEAGER, A.F., (1953), Minerological, Mag., 30, No. 220, 1.

SEAL, M., (1961), Englehard Industries Inc. Tech. Bull. 3, 58.

SEAL, M., (1962a), Norelco Reporter, 9, No. 4, 88.

SEAL, M., (1962b), Proc. 1st Conf. on Diamonds in Industry, Paris, 313.

SEAL, M., (1962c), 1st Conf. on Diamonds in Industry, Paris, 361.

SEAL, M., (1962d), Englehard Industries Inc. Tech. Bull., 279, No. 3, 96.

SEAL, M., (1965), Amer. Min., 50, 105.

SEAL, M., (1966), Nature Lond., 212, 1528.

SEIGBAHN, (1932), M. Ak. Matem. Astro. Fysik., 23, 12.

SESTAK, B. and KADECKOVA, S., (1966), Phy. Status Solids, 16, 89.

SHAFRANOVSKY, I.I., (1940), Dokl. Akad. SSSR., 26, No. 7, Ibid, 31, No. 8.

SHOCKLEY, W. and READ, W.T., (1949), Phys. Rev., 75, 692.

SOBOLEV, E.V., LISOIVAN, V.I., (1968), Soviet Physics Doklady, 12, 665.

STRANSKI, I.N., (1928), "Crystal Growth", Z. Phys. Chem., 136, 259.

STRONG, H.M. and WENTORF, R.H., (1972), Die Naturwissenschaften, 59, 1.

SUITS, J.C. and LOW, J.R., (1957), Acta. Met., 5, 285.

SUTHERLAND, G.B.B.M., BLACKWELL, D.E. and SIMERAL, W.G., (1954), Nature Lond., 174, 901.

SUTTON, J.R., (1928), "The Diamond", (Murby, London).

TAYLOR, G.I., (1934), Proc. Roy. Soc. London, A 145, 362.

TAYLOR, W.H., (1947), Nature Lond., 159, 729.

THOMAS, J.M., GLENDA HUGHES, E.E. and WILLIAMS, B.R., (1963), Phil. Mag., 8, 1513.

TIWARI, N.N., (1964), Ph.D. Thesis (University of London).

TOLANSKY, S., (1946), Proc. Phy. Soc., 58, 654.

TOLANSKY, S., (1948), "Multiple-beam Interferometry of Surfaces and Films", (Clarendon Press, Oxford).

TOLANSKY, S., (1953a), Research, 6, 8.

TOLANSKY, S., (1953b), Industrial Diamond Rev., 13, 271.

TOLANSKY, S., (1952), Zeit. f. Electrochemic., 56, 263.

TOLANSKY, S., (1955), "An Introduction to Interferometry", (Longmans, Green & Co.).

TOLANSKY, S., (1955), "The Microstructures of Diamond Surfaces", (N.A.G. Press, London).

TOLANSKY, S., (1960), "Surface Microtopography", (Longmans, Green & Co., London).

TOLANSKY, S., (1961a), Proc. Roy. Soc., 263, 31.

TOLANSKY, S., (1961b), Nature, No. 4780, 190, 992.

TOLANSKY, S., (1962a), Proc. Roy. Soc., A 270, 443.

TOLANSKY, S., (1962b), Proc. 1st Inter. Conf. on Diamond in Industry, Paris, 343.

TOLANSKY, S., (1965), "Physical Properties of Diamond", Edited by R. Berman (Clarendon Press, Oxford).

TOLANSKY, S., (1966), Nature Lond., 211, 158.

TOLANSKY, S., (1968), "The Strategic Diamond", (Oliver and Boyed Ltd).

TOLANSKY, S., (1970), Proc. Int. Diamond Conf., Oxford.

TOLANSKY, S. and EMARA, S., (1958), Proc. Phy. Soc., B 58, 559.

TOLANSKY, S., HALPERIN, A. and EMARA, S., (1958), Phil. Mag., 3, 675.

TOLANSKY, S. and PANDEYA, D.C., (1958), Diam. Conf., Cambridge.

TOLANSKY, S. and PANDYA, N.S., (1954), Proc. Roy. Soc., 225, 40.

TOLANSKY, S. and PATEL, A.R., Phil. Mag., 2, 1003.

TOLANSKY, S. and OMAR, M., (1953a), Phil. Mag., 43, 808.

TOLANSKY, S. and OMAR, M., (1953b), Phil. Mag., 44, 514.

TOLANSKY, S. and RAWLE-COPE, M., (1968), Proc. Diamond Conf., Bristol.

TOLANSKY, S. and RAWLE-COPE, M., (1970), Diamond Conf., 1970.

TOLANSKY, S. and SUNAGAWA, I., (1959), Nature, 184, 1526.

TOLANSKY, S. and SUNAGAWA, I., (1960a), Ind. Diam. Rev., 20, 106.

TOLANSKY, S. and SUNAGAWA, I., (1960b), Nature Lond., 185, 203.

TOLANSKY, S. and SUNAGAWA, I., (1960c), Ind. Diam. Rev., 20, 7.

TOLANSKY, S. and WILCOCK, W.L., (1946), Nature Lond., No. 3992, 583.

TOLANSKY, S. and WILCOCK, W.L., (1947), Proc. Roy. Soc., A 191, 182.

TRUEB, L.A., (1968), J. Appl. Phys., 39, 4707.

VAN DER VEEN, A.L.W.E., (1913), Z. Kristallogr, 51, 545.

VARMA, C.K.R., (1967a), Phil. Mag., 16, 611.

VARMA, C.K.R., (1967b), Phil. Mag., 16, 621.

VARMA, C.K.R., (1967c), Phil. Mag., 16, 657.

VARMA, C.K.R., (1967d), Phil. Mag., 16, 959.

VARMA, C.K.R., (1970), J. Phy. Chem. Solids, 31, 890.

VERMA, A.R., (1951), Nature Lond., 167, 93.

VERMA, A.R., (1951), "Crystal Growth & Dislocations", (Butterworth, London).

VERMA, A.R. and KRISHNA, P., "Polymorphism and Polytypism in Crystals", (John Wiley & Sons).

VOGEL, F.L., PFANN, W.G., COREY, H.C. etc. (1959), Phys. Rev., 90, 489.

VOLMER, M.Z. Phys. Chem., 102, 267.

VOLMER, M. and SCHUTZE, (1931), Z. Phys. Chem., A 156, 1.

WENTORF, R.H., (1966), Ber. Bunsenges Phys. Chem., 70, 975.

WILCOCK, W.L., (1951), Ph.D. Thesis, Victoria University, Manchester.

WILKS, E.M., (1961), Phil. Mag., 6, 1089.

WILKS, E.M. and WILKS, J.I.D., (1971), Ind. Diam. Rev., June, 238.

WILLIAMS, A.F., (1932), "The Genesis of Diamond", (London: Benn).

WULFF, G., (1901), Z. Krist., 34, 449.

WYON, G. and LACOMBE, P., (1955), Report of Conf. "Defects in Solids", Bristol, (1955), 187.

ZAPFFE, C.A. and WORDEN, C.O., (1949), Acta. Cryst. Camb., 2, 383.

ZERNICKE, F., (1934), Physika, 1, 689.

ACKNOWLEDGEMENTS

I wish to express my gratitude to my supervisor, Professor S. Tolansky F.R.S., for his inspiring guidance and interest throughout the work and to Dr. R.F. Miller for his valuable help and advice in particular with respect to the electron microscope techniques.

My sincere thanks are due to Dr. A.F. Seager of the University of London and Professor T. Evans of the University of Reading for helpful suggestions and advice and also to Dr. C.K.R. Varma for useful discussions.

I thank the staff of the Physics Department of Royal Holloway College and in particular Mr. G. Cakebread and Mr. R.P. May for their cooperation and assistance.

Finally, I would like to thank Royal Holloway College for the award of Research Studentship.

A single stage replica technique for electron microscopy of microdiamond surfaces

BY **R F MILLER** AND **J S PUNGLIA**
DEPARTMENT OF PHYSICS ROYAL HOLLOWAY COLLEGE ENGLEFIELD GREEN SURREY UK

A single-stage replica technique has been developed for microdiamond surfaces of size below 100 microns, which overcomes some of the drawbacks of two-stage replication methods

It is normally difficult, if not impossible, to obtain a single-stage carbon replica from a clean diamond face, owing to the strong adhesion between the coating and the crystal surface. In order to make replicas of diamond or other mineral crystal surfaces, for examination by electron microscopy, it is usual either to employ an intermediate, soluble layer to contour the crystal surface[1] or to use some form of two-stage replica process[2]. These methods are generally satisfactory, but any additional step in the replica operation increases the likelihood of artefacts and loss of resolution and is therefore to be avoided if at all possible.

It was required to non-destructively examine the surfaces of natural and synthetic diamond particles of size 30 microns and less, by electron microscopy. The two-stage replica technique is normally employed for this type of specimen, by partially embedding the crystals in formvar, for example, and then replicating with cellulose acetate and carbon[3]. We have now found that direct replication with platinum-carbon is possible for diamond particles of this size by using the following method.

A piece of acetyl-cellulose film, 0·034 mm thick (Bioden R.F.A., Polaron Instruments Ltd), is moistened with methyl acetate and placed on a glass microscope slide. The microdiamonds are sprinkled on to the film and covered by another glass slide which is held in position by clips and kept at 80°C for 30 minutes. This partially embeds the crystals and prevents the film from curling during subsequent operations. The upper slide is removed and the film and diamonds are subjected to platinum-carbon evaporation *in vacuo* in the normal way. The plastic/crystallite/Pt-C composite is then manually stripped from its glass slide and placed, Pt-C downwards, on to another glass slide which has just been dipped into paraffin wax (M.P. 65°C). The whole is now placed in methyl acetate at room temperature to dissolve the plastic. The slide is then transferred to another dish of methyl acetate which is gradually brought to 50°C, at which temperature the wax rapidly dissolves and releases the Pt-C replica together with the crystals. At this stage the replica curls and flexes, releasing the crystallites which collect at the bottom of the dish. After repeated washings in fresh methyl acetate, the replica is transferred to an acetone bath and then to distilled water, where it floats on the surface and is stretched flat by surface tension. The replica may then be picked up and mounted for examination.

The technique becomes progressively less successful for crystals greater than 100 microns in size, owing to breakage of the replica at the crystal edges during the flexing process when the wax dissolves.

Examples of electron micrographs obtained from the surfaces of diamonds approximately 30 microns in overall size are given in Fig 1 to 4.

High resolution (< 100 Å) of surface detail is easily obtained for surfaces of various types found on grinding powders and on synthetic microdiamonds, and this technique is now being used in studies of the crystallographic and abrasion properties of such particles ◆

References

1. **Patel, A. R.** and **Patel, S. M.** Rapid method of preparing single-stage carbon replica for electron microscopy of some mineral crystals. *Rev Sci Instr* Vol 39, p 409, 1968.
2. **Eckert, J. D.** A replica technique for examining crystals and for retracing particles in grinding wheels. *Industr Diam Rev* Vol 28, No. 327, p 75, 1968.
3. **Trueb, L. F.** An electron microscope study of shock-synthesized diamond. *J Appl Phys* Vol 39, No. 10, p 4707, 1968.

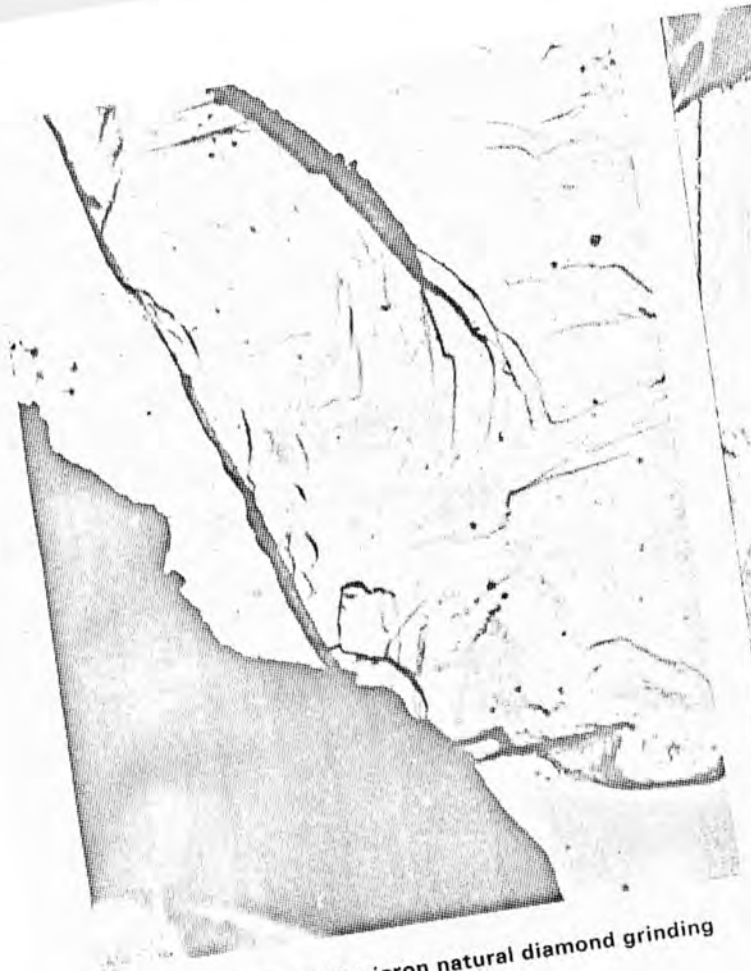

Fig 1 A particle of 30 micron natural diamond grinding powder (x 5000)

Fig 2 Multiple cleavage steps on 30 micron natural diamond (x 10,000)

Fig 3 Growth layers on 30 micron natural diamond (x 10,000)

Fig 4 Surface of 30 micron synthetic diamond (x 10,000)